Advances in Clinical and Experimental Medicine

MONTHLY ISSN 1899-5276 (PRINT) ISSN 2451-2680 (ONLINE) www.advances.umed.wroc.pl

2018, Vol. 27, No. 9 (September)

Impact Factor (IF) – 1.262
Ministry of Science and Higher Education – 15 pts.
Index Copernicus (ICV) – 155.19 pts.

Wroclaw Medical University

Advances
in Clinical and Experimental Medicine

ISSN 1899-5276 (PRINT) ISSN 2451-2680 (ONLINE) www.advances.umed.wroc.pl

MONTHLY 2018
Vol. 27, No. 9
(September)

Advances in Clinical and Experimental Medicine is a peer-reviewed open access journal published by Wroclaw Medical University. Its abbreviated title is Adv Clin Exp Med. Journal publishes original papers and reviews encompassing all aspects of medicine, including molecular biology, biochemistry, genetics, biotechnology, and other areas. It is published monthly, one volume per year.

Editorial Office
ul. Marcinkowskiego 2–6
50-368 Wrocław, Poland
Tel.: +48 71 784 12 05
E-mail: redakcja@umed.wroc.pl

Publisher
Wroclaw Medical University
Wybrzeże L. Pasteura 1
50-367 Wrocław, Poland

Online edition is the original version of the journal

Editorial Policy

Advances in Clinical and Experimental Medicine (Adv Clin Exp Med) is an independent multidisciplinary forum for exchange of scientific and clinical information, publishing original research and news encompassing all aspects of medicine, including molecular biology, biochemistry, genetics, biotechnology and other areas. During the review process, the Editorial Board conforms to the "Uniform Requirements for Manuscripts Submitted to Biomedical Journals: Writing and Editing for Biomedical Publication" approved by the International Committee of Medical Journal Editors (www.ICMJE.org/). The journal publishes (in English only) original papers and reviews. Short works considered original, novel and significant are given priority. Experimental studies must include a statement that the experimental protocol and informed consent procedure were in compliance with the Helsinki Convention and were approved by an ethics committee.

For all subscription related queries please contact our Editorial Office:

redakcja@umed.wroc.pl

For more information visit the journal's website:

www.advances.umed.wroc.pl

Pursuant to the ordinance no. 134/XV R/2017 of the Rector of Wroclaw Medical University (as of December 28, 2017) from January 1, 2018 authors are required to pay a fee amounting to 700 euros for each manuscript accepted for publication in the journal "Advances in Clinical and Experimental Medicine."

Indexed in: MEDLINE, Science Citation Index Expanded, Journal Citation Reports/Science Edition,

Scopus, EMBASE/Excerpta Medica, Ulrich's™ International Periodicals Directory, Index Copernicus

Typographic design: Monika Kolęda, Piotr Gil
DTP: Wydawnictwo UMW, TYPOGRAF
Cover: Monika Kolęda
Printing and binding: EXDRUK

Advances
in Clinical and Experimental Medicine

MONTHLY 2018, Vol. 27, No. 9 (September)

ISSN 1899-5276 (PRINT)
ISSN 2451-2680 (ONLINE)
www.advances.umed.wroc.pl

Contents

Original papers

Reviews

Osseointegration of zirconia implants with 3 varying surface textures and a titanium implant: A histological and micro-CT study

Paweł Kubasiewicz-Ross[A–D], Jakub Hadzik[C,D], Marzena Dominiak[D–F]

Department of Oral Surgery, Wroclaw Medical University, Poland

A – research concept and design; B – collection and/or assembly of data; C – data analysis and interpretation;
D – writing the article; E – critical revision of the article; F – final approval of the article

Advances in Clinical and Experimental Medicine, ISSN 1899-5276 (print), ISSN 2451-2680 (online) *Adv Clin Exp Med*. 2018;27(9):1173–1179

Address for correspondence
Paweł Kubasiewicz-Ross
E-mail: pawelkubasiewicz@wp.pl

Funding sources
None declared

Conflict of interest
None declared

Received on October 23, 2016
Reviewed on January 24, 2017
Accepted on March 1, 2017

Abstract

Background. Zirconium – a bioinert metal – in comparison with titanium implants, offers a variety of potential advantages for use in the esthetic area of dentistry due to its tooth-like color. Zirconium dental implants are considered to be an alternative method of treatment to conventional titanium dental implants for patients with a thin gingival biotype.

Objectives. This study was designed to study the bone tissue response to new zirconia implants with modified surfaces in comparison with commercially available titanium dental implants and commercially available zirconia implants.

Material and methods. The study was carried out on a group of 12 16-month-old minipigs. New zirconia implants with 3 different surfaces were used: M1 – blasted surface, M2 – etched surface and M3 – blasted and etched surface (Maxon Motor GmbH, Sexau, Germany) and compared to conventional titanium implants with an sandblasted and acid etched (SLA) surface (Straumann GmbH, Freiburg, Germany) and commercially available zirconia implants (Ziterion GmbH, Uffenheim, Germany). Histological and micro-computed tomopgraphy (micro-CT) evaluation was performed.

Results. In the micro-CT assessment, the average bone-implant contact (BIC) of the zirconia experimental implants was 41.44%. In particular, the BIC% for M1 was 39.72%, for M2 it was 43.97%, and for M3 – 40.63%; in the control group it was 49.63% and 27.77% for ceramic and titanium control implants, respectively. The intra-group analysis showed no statistically important differences between the BIC values for implants in any group. However, the analysis of BIC for different regions of the same implant showed statistically significant differences in all of the groups between the results of the threaded region and the neck and the apex.

Conclusions. The results of our study suggest that zirconia implants with modified surfaces display features of osseointegration similar to those of titanium implants. These results are promising in using zirconia implants for dental applications in the future.

Key words: dental implants, osseointegration, micro-computed tomography, histomorphometry, zirconia implant

DOI
10.17219/acem/69246

Introduction

Titanium implants are considered the gold standard of modern dental implantology. This is due to their long, traceable record of predictable clinical performance, excellent biocompatibility and mechanical properties, ability to osseointegrate, and to the fact that titanium implants are easy to produce.[1] However, titanium still bears several esthetic disadvantages, especially in the case of periodontia with a thin biotype in the esthetically-sensitive anterior area of the jaw. If a titanium implant is used in such a case, the mucosa in the neck area of the implant may become grayish, which consequently limits the success of the overall treatment. Titanium implants may also require additional surgical procedures concerning soft tissue augmentation, e.g., connective tissue grafting, which aims at widening and thickening keratinized tissue.[2] A less frequent, though possible, drawback is that titanium might be an allergen and may diffuse not only within the adjacent tissues – as is proven by the elevated concentrations found in the vicinity of oral implants and in regional lymph nodes – but also systemically.[3] As a possible alternative to titanium, ceramic materials have already been investigated and clinically used for years in the field of oral implantology.

Due to its good osseointegrative properties, the first ceramic material used in implantology was aluminum oxide.[4] In follow-up examinations after 10 years, the success of those implants was between 87% and 92.5%.[4,5] Systems based on aluminum oxide were used for immediate implantation in the cases of single tooth loss in the jaw, in the area of the incisors, canines, and premolars, i.e., in the areas where chewing forces are relatively weak. Even though implants were used in the above-mentioned clinical circumstances, there were cases of damage caused by chewing. Hence, because of inadequate mechanical strength, aluminum-oxide implants are no longer in use. Zirconium is another alternative material initiated by general medicine, mainly orthopedics.

A small number of complications, good chemical parameters, anticorrosion properties, mechanical strength, an elasticity module close to that of steel, and biocompatibility in particular made zirconium a perfect material for implants.[6]

Zirconium, a bioinert, non-resorbable metal, offers a variety of potential advantages over titanium implants for use in the esthetic area of dentistry due to its tooth-like color. Its surface texture can be modified and it does not show any chemical or physical bonding with plaque.[7] Furthermore, good scientific results in osseointegration comparable to titanium implants have been shown.[7]

Material and methods

Dental implants

The following newly-designed zirconia implants were used:

– ø4.0 × 10 mm ZrO_2 ceramic implant with blasted surface (Maxon Motor GmbH, Sexau, Germany) – M1;

– ø4.0 × 10 mm ZrO_2 ceramic implant with etched surface (Maxon Motor GmbH, Sexau, Germany) – M2;

– ø4.0 × 10 mm ZrO_2 ceramic implant with blasted and acid etched surface (Maxon Motor GmbH, Sexau, Germany) – M3.

For a control group, we decided to choose titanium implants with well-established osseointegration properties:

– ø4.1 × 10 mm Titanium standard implant SLA® (Straumann GmbH, Freiburg, Germany);

– ø4.0 × 10 mm ZrO_2 ceramic implant (Ziterion GmbH, Uffenheim, Germany).

Experimental design and surgical procedure

The study was performed on 12 16-month-old minipigs with an average weight of 50–60 kg. The study protocol was approved by the commission for animal studies.

The pigs underwent the removal of the permanent premolar teeth 2 months after the extraction of the deciduous premolar teeth in the jaw. Care was taken to avoid bone wall fractures. The extractions, implantations and euthanasia were performed under general anesthesia by intravenous application of pentobarbital (Vetbutal®, Biowet Puławy, Poland) at doses of 25 mg/kg along with the premedication ketamine (Ketamina 10%, Biowet Puławy, Poland) and local infiltration of 2% lignocaine with noradrenaline 1:200,000 (Polfa, Poland). Eight weeks after the extractions, a total of 60 implants were inserted in the 12 animals. Each pig was to receive 5 implants (1 per surface state and 2 reference implants) in the mandible (Fig. 1, 2). The position of the implants was statistically fully randomized. The implants were placed endosseously under continuous water cooling. After the insertion, the flap was repositioned using resorbable sutures (4/0 Monosyn®, B. Braun, Melsungen, Germany).

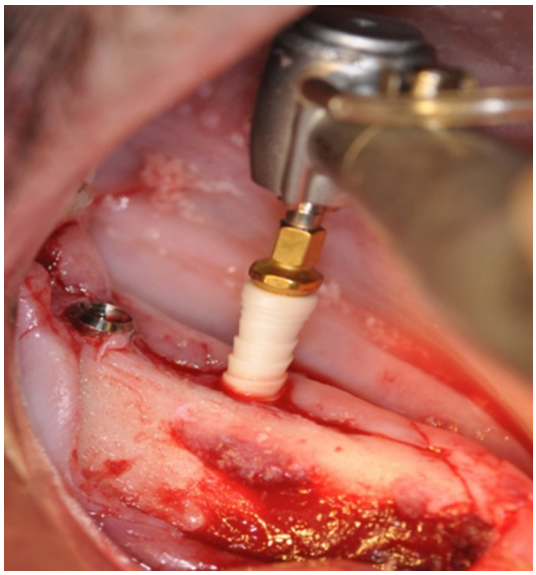

Fig. 1. Insertion of the ceramic implant

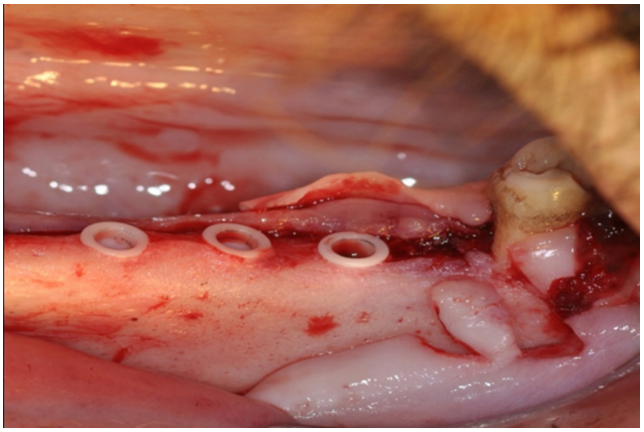

Fig. 2. Three ceramic implants inserted into the alveolar ridge

The animals were euthanized 12 weeks post-implantation using 50 mg/kg of pentobarbital (Morbital) and block biopsies of the implant sites were collected.

Micro-CT evaluation

In the micro-CT evaluation, the implant surfaces were divided into 3 regions of interest (ROI). The 1st one was the neck region, the 2nd was the thread area, and last one was the apex region of the implant. The bone-implant contact (BIC) was calculated separately for each ROI. The research was done with a SkyScan 1172 Micro-CT (Bruker, Kontich, Belgium). The exposure was performed with 50 kV of voltage and 10 W of power. The detection was done on a 12-bit CCD camera. The BIC was calculated using Adobe® PhotoShop® (San Jose, USA). At first, the total length of the vertical cross-section was achieved; next, the length of the cross-section of the implant in direct contact with the bone structure was calculated; and finally, the BIC was counted as a percentage of its proportions.

Histology

For histological examination, each bone-implant specimen was placed in 4% phosphate-buffered saline (PBS)-buffered formalin, dehydrated in a graded series of alcohol and embedded in methylmethacrylate (Technovit 9100 New®, Kulzer, Germany), as described previously.[8–11] For staining the bone-implant, specimens were cut using a diamond saw and ground to a thickness of approx. 100 µm with a grinding system (Exakt Apparatebau, Norderstedt, Germany) as described by Donath and Breuner.[12] The specimens were then stained with Masson–Goldner trichrome (Merck KGaA, Darmstadt, Germany). for differentiation between collagen and bone tissue, and a histomorphometric analysis was performed by light microscopy. A blind test was conducted at the same time, using identical staff, equipment and chemicals.

Statistical analysis

For all tested variables, the distribution type was checked. The Shapiro-Wilk test was applied with a significance level of $p = 0.05$. For measurable variables, arithmetic averages and standard deviations were calculated. Because none of the cases had a normal distribution, the analysis of variance (ANOVA) Kruskal-Wallis test was applied. At first, the calculation was performed for a significance level of $p < 0.05$; in the cases where $p < 0.05$, a pair-wise comparison was conducted and a new p-value for every significantly different pair was presented. The dependence between the results of radiological and histological evaluation was calculated with the application of Pearson's correlation coefficient and by calculating the ratio between both values. The analysis was performed with R-project (Auckland, New Zeland) and MedCalc (MedCalc Software, Ostend, Belgium).

Results

Postoperatively, all animals recovered quickly, returning to routine activities such as grooming, eating and drinking within 48 h. Regardless of the material used, there were no macroscopic or microscopic signs of cellular inflammation or implant rejection in any of the test groups.

Results of the micro-CT investigation

In the radiological assessment, the average BIC% of the zirconia experimental implants was 41.44%. In particular, the BIC% for M1 was 39.72%, for M2 it was 43.97% and for M3 – 40.63% (Fig. 3–5); in the control group it was 49.63% and 27.77% for the ceramic and titanium control implants, respectively (Fig. 6, 7). The distribution of BIC according to the ROI for particular groups is featured in Table 1.

The intra-group analysis showed no statistically significant differences between the BIC values for implants in any group, though the analysis of BIC for different ROIs of the same implant showed statistically significant differences in all of the groups between the results of the threaded region and the neck and the apex. In all groups apart from M1, statistically important differences were seen between the results of BIC for the neck and apex regions (Table 2). The intergroup analysis of the BIC results showed

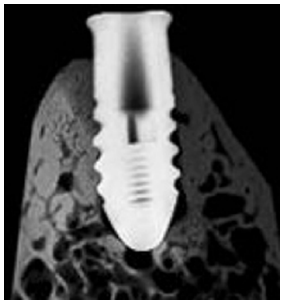

Fig. 3. Micro-CT scan of the M1 implant

Fig. 4. Micro-CT scan of the M2 implant

Fig. 5. Micro-CT scan of the M3 implant

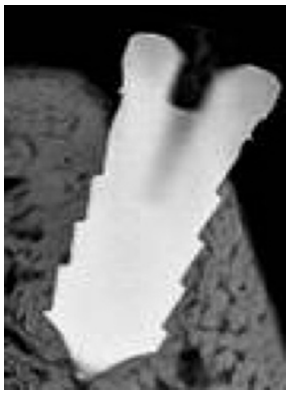

Fig. 6. Micro-CT scan of the zirconium control implant

Fig. 7. Micro-CT scan of the titanium control implant

significant differences for the threaded region between groups 1, 2 and 3 and group 5. There were no statistically significant differences between group 4 and the rest of the groups. In the apex region, statistically significant differences were seen between the ceramic control implants and others; additionally, differences were seen for M1/M2 and M1/titanium controls, but without statistical significance.

Results of the histological investigation

The mandibular bone texture showed typical spongious bone structures. Interconnecting areas of mineralization and osteoid formation between the host bone and the implant surface were detected for all surface states. The formation of woven bone was present within the implant threads of all tested and reference implants (Fig. 8). The bone structure almost completely covered the surface of dental implants, although areas of a well-vasculated medulla could be seen. In the regions mentioned, osteogenic cell lines were found. In most cases, the remodeling process was apparent, the old trabeculae were replaced with a new bone structure. No signs of inflammation were seen in any of the specimens. Test implants were present in the crestal implant area, a tightly surface-adapted connective tissue. The periosteal fibers were in direct contact with the surface and showed parallel fiber orientation. Bordering the connective tissue zone, the bone lamellae extended to the apical region and formed a close BIC. In contrast, using the reference ceramic implant, some resorption at the crestal bone level was observed and the bone appeared rounded down. In the test group, the different characteristics of the bone structure in the apex region could be seen upon histological examination. In the above-mentioned ROI, relatively thin bone trabeculae with highly vasculated medulla areas were noted (Fig. 9). Furthermore, fibrous connective tissue was quite commonly in direct contact with the implant surface. The number of samples with fibrous connective tissue is shown in Table 3. The BIC calculated in the histological analysis is shown in Table 4.

Table 1. The distribution of the bone-implant contact (BIC) according to the region of interest (ROI)

Group No.	Bone-implant contact in neck region [%]	Bone-implant contact in thread region [%]	Bone-implant contact in apex region [%]
M1	25.25	66.75	27.16
M2	23.83	72.91	35.16
M3	21.41	68.83	31.66
Control 1	5.41	77.91	65.58
Control 2	7.41	42.66	33.25

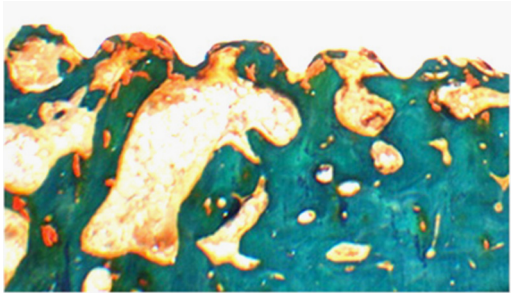

Fig. 8. The formation of woven bone presented within the implant threads

Table 2. Intragroup analysis of variance between the BIC parameters for different ROI in micro-CT examination

ROI	Implant group (n)	M1	M2	M3	Ceramic control	Titanium control
		significantly differed from	significantly differed from	significantly differed from	significantly differed from	significantly differed from
Apex	12	(thread) $p < 0.0001$	(neck) (thread) $p < 0.001$ for neck $p < 0.0001$ for thread	(neck) (thread) $p < 0.01$ for neck $p < 0.0001$ for thread	(neck) (thread) $p < 0.0001$ for both	(neck) (thread) $p < 0.0001$ for neck $p < 0.01$ for thread
Neck	12	(thread) $p < 0.0001$	(apex) (thread) $p < 0.001$ for apex $p < 0.0001$ for thread	(apex) (thread) $p < 0.01$ for apex $p < 0.0001$ for thread	(apex) (thread) $p < 0.0001$ for both	(apex) (thread) $p < 0.0001$ for both
Thread	12	(apex) (neck) $p < 0.0001$ for both	(apex) (neck) $p < 0.0001$ for both	(apex) (neck) $p < 0.0001$ for both	(apex) (neck) $p < 0.0001$ for both	(apex) (neck) $p < 0.0001$ for apex $p < 0.01$ for neck

Table 3. Number of samples with fibrous connective tissue

Implants	M1	M2	M3	Ceramic control	Titanium control
Number of samples with fibrous connective tissue, n (%)	4 (33)	6 (50)	3 (25)	7 (58)	4 (33)

Table 4. Average of BIC% according to histomorphometry

Implants	M1	M2	M3	Ceramic control	Titanium control
BIC%	46	61	56	58	64

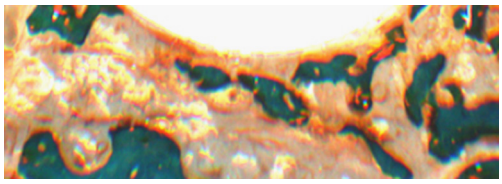

Fig. 9. The apical region of the ceramic implant

The intra-group analysis of the BIC results shows statistically significant differences between group 5 and groups 1 and 2. In the experimental group, the differences between the BIC results of group 1 and groups 2 and 3 were statistically significant (Table 5). Based on the results of the radiological and histological assessment of the BIC, the conclusion can be drawn that the most coherent result was achieved for zirconia implants.

Table 5. Intra-group analysis of variance in the achieved results of BIC%

Implant group	n	Different from
M1	12	(M2) (M3) (titanium control) (ceramic control) $p < 0.0001$ for M2; $p = 0.001$ for M3; $p < 0.0001$ for titanium control; $p < 0.0001$ for ceramic control
M2	12	(M1) $p < 0.0001$
M3	12	(M1) (titanium control) $p = 0.001$ for M1; $p = 0.02$ for titanium control
Titanium control	12	(M1) (M3) $p < 0.0001$ for M1; $p = 0.02$ for M3
Ceramic control	12	(M1) $p < 0.0001$

Discussion

The current definition of osseointegration describes it as the formation of a direct structural and functional conjunction between a dental implant and bone tissue without pathological soft tissue as a mediator.

Osseointegration methods can theoretically be classified into 2 basic types. The 1st group consists of methods where "the functionality of the implant anchorage" is the most important. These are biomechanical methods, where an experimental trial of pulling an implant out of the bone structure is used (Push and Pull Out Test, Removal Torque Test and Shear Strength Test). The disadvantage of these methods is the complexity of the procedures (which hinders repeatability), the need to transport bone tissue to a specialized laboratory and the fact that preparations are usually stabilized in formalin or other substance after sacrificing the laboratory animal, which may affect the results.[13,14]

The most commonly used and more reproducible methods of evaluating osseointegration quantitatively

is histomorphometry and micro-CT techniques. Micro-CT is emerging in the field of biomaterial research. Its biggest advantage is its ability to produce 3D images, since histological assessment is 2D. Taking the micro-CT, however, the final result can be interfaced by an artifact layer of various thickness (beam hardening), resulting in the miscalculation of the BIC.[15] This situation affects titanium implants more than zirconium ones.

Even though the BIC values are a kind of gold standard, the method of calculation varies fundamentally from study to study. Variations like the calculation of the "whole implant surface," the "mineralized bone between 2 threads"[16] and the "contact at the best 3 threads"[17] are often reported. Most studies, similar to the present work, use the option "from the first to the last bone contact", which allows for a comparison of different screw designs. Different software applications and algorithms are rarely made available to the reader and may lead to inaccurate results.

Sand-blasted and acid-etched titanium implants were considered a control group in our study. The histological parameters of osseointegration have been widely documented in the literature in tests on animal models. Buser et al. achieved BIC results of 78% for SLActive and 75% for SLA over 8 weeks of observation.[18] Schwarz et al., in tests on a dog model, proved the BIC value of SLA implants to be 55%.[19] SLA surface implants were also tested in a pig model and the BIC results showed a rise to 58.5% ±11.4% over 8 weeks of healing.[20]

In studies based on an animal model of beagles, a histomorphometric comparative assessment of titanium implant osseointegration with the SLA surface was also performed.[21] The extraction phase included premolars bilaterally. The healing period of unloaded implants was 2 weeks and the observation period lasted 4 weeks. The BIC values were different in the 2-week observations and amounted to 29% for SLActive surface and 24% for control SLA; after 4 weeks of healing, they both reached a value of 39%.

The issue of the histological assessment of zirconium implant osseointegration is still new. One should only consider those studies which include a larger sample of implantations, comply with statistical analysis guidelines and use methodology which includes an assessment of a titanium implant control group in the discussion.[18–20] In the earliest studies on zirconium implants, the BIC value in an 8-week observation of 156 zirconium implants was 86%.[22] This is the only report with such high osseointegration values. In other studies, the BIC value for such implants equaled 45% or 65%, values which are closer to our own studies.[23,24] In other studies performed on 28 zirconium implants over a 60-day observation period, the average BIC value was 56%.[25] In these studies, very unstable results were achieved, where the difference between the max and min BIC values was 32%. Scarano et al., in a 4-week observation of 20 implants, reported a BIC value of 68%.[26] With a longer, 60-day observation time, they placed 20 zirconia ceramic implants in the tibiae of 5 male rabbits. They found an average bone-implant contact of 68.4% ±2.4%. No gaps or fibrous tissue and no epithelial downgrowth were present at the interface. Wide marrow spaces were present, with some of them abutting on the implant surface. Aldini et al. achieved a BIC value of 55% ±27%.[27]

Whereas surface nanostructural features were not taken into consideration in the last 2 studies mentioned, Sennerby and Meredith published a precise analysis of the connection of zirconium implant surface roughness with the results of achieved BIC.[13] In the studies, the implants were divided into 3 groups depending on the degree of roughness. The studies were performed on a rabbit model, by applying the implants in the femoral and tibial area. The BIC results varied depending on the site of implantation. For implants applied to the femoral bone, seemingly more referential results were obtained – 46% for the 1st group, 60% for the 2nd and 70% for the 3rd – whereas the BIC for implants applied to the tibia bone were much lower: 19%, 31% and 22%, respectively. It seems, then, that the most preferential degree of zirconium implant surface roughness is different than in the case of titanium implants.

Depprich et al. designed a study to compare titanium implants of higher roughness with zirconium implants of lower roughness.[28] For this purpose, 24 screw-type zirconium implants with acid-etched surfaces were used and compared to 24 implants made of titanium – SLA implants. The implants were inserted into the tibiae of 12 mini-pigs. The histological results showed direct bone contact on the zirconium and titanium surfaces, which demonstrated that zirconium implants with modified surfaces result in osseointegration comparable to that of titanium implants.

In another study, the negative interaction of the bone tissue with zirconium implants after loading was shown.[29] In the study, 1-phase zirconium implants, which required immediate loading, were used alongside 2-phase unloaded ones. Despite generally good BIC parameters, marginal defects of the alveolar process after implant loading were observed. This study demonstrated that a 2-phase implantation method is preferred with zirconium implants.

In another study, a total of 18 zirconium implants and 18 titanium implants, identical in shape, with acid-etched and sand-blasted surfaces were tested on a mini-pig model. The observation period was 4, 8 and 12 weeks. The histological observation did not reveal any statistically significant differences between zirconium and titanium SLA implants for peri-implant bone density and BIC ratio. There were 2 exceptions: the mean peri-implant bone density and BIC values of the control implants were always higher than those of the tested zirconia implants. The conclusion was that no detectable difference in osseointegration could be observed between the 2 types of implants.[30]

Conclusions

The results from our study suggest that zirconia implants with modified surfaces display features of osseointegration similar to those of titanium implants. These results are promising in using zirconia implants for dental applications in the future.

Typical presence of relatively thin bone trabeculae with highly vasculated medulla (Masson-Goldner staining ×80).

References

1. Vishnu S, Kusum D. Advances in surface modification of dental implants from micron to nanotopography. *Int J Res Dent*. 2011;1:1–10.
2. Schwarz F, Mihatovic I, Shirakata Y, Becker J, Bosshardt D, Sculean A. Treatment of soft tissue recessions at titanium implants using a resorbable collagen matrix: A pilot study. *Clin Oral Implants Res*. 2014;25(1):110–115.
3. Evrard L, Waroquier D, Parent D. Allergies to dental metals. Titanium: A new allergen. *Rev Med Brux*. 2010;31(1):44–49.
4. De Wijs FL, Van Dongen RC, De Lange GL, De Putter C. Front tooth replacement with Tubingen (Frialit) implants. *J Oral Rehabil*. 1994;21: 11–26.
5. Schulte W, d'Hoedt B. 13 Jahre Tubinger Implantat aus Frialit-Weitere Ergebnisse. *Zeitschrift Zahnarzt Implant*. 1988;3:167–172.
6. Hisbergues M, Vendeville S, Vendeville P. Zirconia: Established facts and perspectives for a biomaterial in dental implantology. *J Biomed Mater Res*. 2009;88(2):519–529.
7. Gahlert M, Gudehus T, Eichhorn S, Steinhauser E, Kniha H, Erhardt W. Biomechanical and histomorphometric comparison between zirconia implants with varying surface textures and a titanium implant in the maxilla of miniature pigs. *Clin Oral Implants Res*. 2007; 18(5):662–668.
8. Allegrini S Jr, Allegrini MR, Yoshimoto M, et al. Soft tissue integration in the neck area of titanium implants: An animal trial. *J Physiol Pharmacol*. 2008;59(Suppl 5):117–132.
9. Gedrange T, Mai R, Mack F, et al. Evaluation of shape and size changes of bone and remodelled bone substitute after different fixation methods. *J Physiol Pharmacol*. 2008;59(Suppl 5):87–94.
10. Mai R, Lux R, Proff P, et al. O-phospho-L-serine: A modulator of bone healing in calcium-phosphate cements. *Biomed Tech*. 2008;53(5): 229–233.
11. Kunert-Keil Ch, Gedrange T, Mai R, et al. Morphological evaluation of bone defect regeneration after treatment with two different forms of bone substitution materials on the basis of BONITmatrix. *J Physiol Pharmacol*. 2009;60(Suppl 8):57–60.
12. Donath K, Breuner G. A method for the study of undecalcified bones and teeth with attached soft tissues. The Säge-Schliff (sawing and grinding) technique. *J Oral Pathology*. 1982;11(4):318–326.
13. Sennerby L, Meredith N. Implant stability measurements using resonance frequency analysis: Biological and biomechanical aspects and clinical implications. *Periodontology 2000*. 2008;47:51–65.
14. Coelho PG, Granjeiro JM, Romanos GE, et al. Basic research methods and current trends of dental implant surfaces. *J Biomed Mater Res B Appl Biomater*. 2009;88:579–596.
15. Barrett JF, Keat N. Artifacts in CT: Recognition and avoidance. *Radiographics*. 2004;24:1679–1691.
16. Wennerberg A, Albrektsson T, Lausmaa J. Torque and histomorphometric evaluation of c.p. titanium screws blasted with 25- and 75-microns-sized-particles of Al_2O_3. *J Biomed Mater Res*. 1996;30:251–260.
17. Larsson C, Thomsen P, Aronsson BO, et al. Bone response to surface-modified titanium implants: Studies on the early tissue response to machined and electropolished implants with different oxide thicknesses. *Biomaterials*. 1996;17:605–616.
18. Buser D, Broggini N, Wieland M, et al. Enhanced bone apposition to a chemically modified SLA titanium surface. *J Dent Res*. 2004;83: 529–533.
19. Schwarz F, Herten M, Sager M, Wieland M, Dard M, Becker J. Histological and immunohistochemical analysis of initial and early osseous integration at chemically modified and conventional SLAs titanium implants: Preliminary results of a pilot study in dogs. *Clin Oral Implants Res*. 2007;18:481–488.
20. Gahlert M, Röhling S, Wieland M, Sprecher CM, Kniha H, Milz S. Osseointegration of zirconia and titanium implants: A histological and histomorphometrical study in the maxilla of pigs. *Clin Oral Implants Res*. 2009;20(11):1247–1253.
21. Bornstein MM, Valderrama P, Jones AA, Wilson TG, Seibl R, Cochran DL. Bone apposition around two different sandblasted and acid-etched titanium implant surfaces: A histomorphometric study in canine mandibles. *Clin Oral Implants Res*. 2008;19(3):233–241.
22. Hayashi K, Matsuguchi N, Uenoyama K, Sugioka Y. Re-evaluation of the biocompatibility of bioinert ceramics in vivo. *Biomaterials*. 1992;13:195–200.
23. Chang YS, Oka M, Nakamura T, Gu HO. Bone remodeling around implanted ceramics. *J Biomed Mater Res*. 1996;30:117–124.
24. Dubruille JH, Viguier E, Le Naour G, Dubruille MT, Auriol M, Le Charpentier Y. Evaluation of combinations of titanium, zirconia, and alumina implants with 2 bone fillers in the dog. *Int J Oral Maxillofac Implants*. 1999;14:271–277.
25. Stanic V, Aldini NN, Fini M, et al. Osteointegration of bioactive glass-coated zirconia in healthy bone: An in vivo evaluation. *Biomaterials*. 2002;23:3833–3841.
26. Scarano A, Di Carlo F, Quaranta M, Piattelli A. Bone response to zirconia ceramic implants: An experimental study in rabbits. *J Oral Implantol*. 2003;29:8–12.
27. Aldini NN, Fini M, Giavaresi G, et al. Osteointegration of bioactive glass-coated and uncoated zirconia in osteopenic bone: An in vivo experimental study. *J Biomed Mater Res*. 2004;68:264–272.
28. Depprich R, Zipprich H, Ommerborn M, et al. Osseointegration of zirconia implants: An SEM observation of the bone-implant interface. *Head Face Med*. 2008;4:25. https://doi.org/10.1186/1746-160X-4-25
29. Akagawa Y, Ichikawa Y, Nikai H, Tsuru H. Interface histology of unloaded and early loaded partially stabilized zirconia endosseous implant in initial bone healing. *J Prosthet Dent*. 1993;69(6):599–604.
30. Gahlert M, Roehling S, Sprecher CM, Kniha H, Milz S, Bormann K. In vivo performance of zirconia and titanium implants: A histomorphometric study in mini pig maxillae. *Clin Oral Implants Res*. 2012;23:281–286.

Migration of human mesenchymal stem cells stimulated with pulsed electric field and the dynamics of the cell surface glycosylation

Katarzyna Jezierska-Woźniak[1,A–D], Seweryn Lipiński[2,C,D], Margaret Huflejt[3,A,C,D], Łukasz Grabarczyk[3,B], Monika Barczewska[3,A,C], Aleksandra Habich[4,B], Joanna Wojtkiewicz[5,C], Wojciech Maksymowicz[3,A,F]

[1] Department of Neurology and Neurosurgery, Faculty of Medical Sciences, Laboratory for Regenerative Medicine, University of Warmia and Mazury in Olsztyn, Poland
[2] Department of Electric and Power Engineering, Electronics and Automatics, Faculty of Technical Sciences, University of Warmia and Mazury in Olsztyn, Poland
[3] Center of Innovative Research in Medical and Natural Sciences, Faculty of Medicine, University of Rzeszów, Poland
[4] Department of Pathophysiology, Faculty of Medical Sciences, University of Warmia and Mazury in Olsztyn, Poland

A – research concept and design; B – collection and/or assembly of data; C – data analysis and interpretation;
D – writing the article; E – critical revision of the article; F – final approval of the article

Advances in Clinical and Experimental Medicine, ISSN 1899-5276 (print), ISSN 2451-2680 (online) *Adv Clin Exp Med*. 2018;27(9):1181–1193

Address for correspondence
Katarzyna Jezierska-Woźniak
E-mail: Katarzyna.jezierska@uwm.edu.pl

Funding sources
The study was funded from the National Science Center (NCN); grant No. 2012/07/B/NZ4/01427.

Conflict of interest
None declared

Received on September 19, 2017
Reviewed on January 2, 2018
Accepted on May 8, 2018

Abstract

Background. The analysis of the stem cells' glycome dynamics at different stages of differentiation and migration makes possible the exploration of the cell surface glycans as markers of the stem cell functional status, and, in the future, compatibility between transplanted cell and host environment.

Objectives. The objective of our study was to develop novel techniques of investigating cell motility and to assess whether the electric field of the therapeutic spinal cord stimulation system used in vivo contributes to the migration of human mesenchymal stem cells (hMSCs) in vitro.

Material and methods. We have investigated the electrotaxis of bone marrow-derived MSCs using pulsed electric field (PEF) in the range of 16–80 mV/mm and the frequency of 130 Hz and 240 Hz. The PEF-related dynamics of the cell surface glycosylation was evaluated using 6 plant lectins recognizing individual glycans.

Results. Pulsed electric field at physiological levels (10 mV/mm; 130 Hz) did not influence cellular motility in vitro, which may correspond to the maintenance of the transplanted cells at the lesion site in vivo. An increase of the PEF intensity and the frequency exceeding physiological levels resulted in an increase in the cellular migration rate in vitro. Pulsed electric field elevated above physiological intensity and frequency (40–80 mV/mm; 240 Hz), but not at physiological levels, resulted in changes of the cell surface glycosylation.

Conclusions. We found the described approach convenient for investigations and for the in vitro modeling of the cellular systems intended for the regenerative cell transplantations in vivo. Probing cell surface glycomes may provide valuable biomarkers to assess the competence of transplanted cells.

Key words: translational medicine, mesenchymal stem cells migration, stem cells homing, pulsed electric field, stem cell glycosylation

DOI
10.17219/acem/90872

Introduction

Stem cell therapy encompasses new technologies and therapies aiming at replacing damaged cells with healthy ones. However, there are still several challenges that must be tackled before such therapies become successful. One of these challenges is the migration of transplanted cells, fundamental both to the development and maintenance of regenerated tissues as well as to the success of the cell-based therapies. Therefore, precise localization of these cells directly into the injury site and their adaptation to host tissues are crucial for the success of therapy.

Delivering transplanted cells precisely at the lesion site is still an unsolved problem of cell therapy. This process, termed homing, is a major road-block in stem cell therapy due to the poor integration of transplanted stem cells with targeted host tissue. This results in poor healing responses and lack of regeneration. The main reason for poor cell homing is likely due to the fact that only a small fraction of injected cells migrate to the damaged tissue and are able to act therapeutically.[1] It is also critical to demonstrate that MSCs do not have unwanted homing that could drive undesirable differentiation and growth.[2]

The cells migrate in response to gradients in chemical composition (chemotaxis), mechanical forces and electric fields (galvanotaxis or electrotaxis). Natural electric fields (EFs) are present in all developing and regenerating tissues. Furthermore, damaged tissues and wounds also generate naturally-occurring endogenous EFs essential in guiding cell migration.[3] Endogenous EFs have been identified and measured in various species, tissues and organs in vitro and in vivo.[4,5] It has been shown that many cell types respond to applied EFs in vitro at the field strengths comparable to the endogenous wound EFs in vivo. The bioelectricity plays an important role in moving cells in a specific direction. Rat osteoblasts, bovine chondrocytes and mouse endothelial progenitor cells migrate towards the cathode, while rabbit osteoclasts, human osteosarcoma cells, rabbit corneal endothelial cells, or human umbilical vein endothelial cells migrate in the opposite direction.[6–8] These different responses indicate that the effects of electric current are cell type- and species-dependent. Consequently, an applied electric field may be used as a cue to guide directional migration of stem cells in the cell-based therapies.[9]

The most common assays for the in vitro electrotaxis studies employ a cell culture dish attached to an electrotaxis apparatus.[5,10] Microfluidic devices allowing better control of the electric field and cell migration environments have been recently developed.[11] New solutions, providing advanced experimental tools for electrotaxis research, improving productivity and enabling studies of the more complex cell migration environments, have also been recently reported.[12–14] However, these experimental tools allow investigations of cellular motility only in laboratory conditions, making transfer of the favorable experimental findings to the clinical setting difficult.

One of the major macromolecular systems defining cell-cell and cell extracellular matrix interactions is the cell glycome consisting of a large variety of complex glycans covalently attached to the membrane proteins and lipids.[15] These glycoproteins and glycolipids are actively involved in, and often control, cell-cell signaling, immune response, would healing, microbial infections, and other events on the cellular and tissue levels. The dynamics of glycomic profile reflects changes in the cellular activities such as division, differentiation, motility, secretory functions, and malignant transformation. Cell glycosylation-targeting investigations would, therefore, be expected to streamline the discovery of novel biological factors of potential clinical significance in regenerative medicine.

The aim of this study was to develop a novel technique for cell motility investigations and to assess whether the system used for spinal cord stimulation is able to direct the migration of MSCs in vitro. We first used pulsed electric field (PEF) to observe the phenomena of MSCs electrotaxis. Using time-lapse video microscopy, we demonstrated and analyzed the direct migration of the MSCs in the PEF. Additionally, using 6 plant lectins, we also evaluated changes in the cell surface glycosylation resulting from the stimulation of cells with PEF.

Methods

Cell culture

We used adult human MSCs derived from the bone marrow remaining after the hip replacement. The experimental design has been approved by the Ethic Committee of University of Warmia and Mazury in Olsztyn, Poland. Written informed consent was obtained from each participant prior to the study enrollment. Mesenchymal stem cells were isolated from the bone marrow according to their adhesive properties to tissue culture plastic under sterile conditions. Briefly, a phosphate-buffered saline (PBS)-diluted cell fraction of bone marrow was layered over a Ficoll density gradient (1.077 g/mL; GE Healthcare, Chicago, USA), followed by centrifugation at 400 g at room temperature for 40 min. Nucleated cells were collected, diluted with 2 volumes of PBS (Sigma-Aldrich, St. Louis, USA), centrifuged twice at 100 g for 10 min, and finally resuspended in a culture medium. Cells were plated at a density of 1,500 cells/cm^2 in a T75 flask and serially passaged at sub-confluence every 5–7 days at the same initial density. Cells were maintained in the Dulbecco's Modified Eagle Medium (DMEM) growth medium supplemented with 10% (v/v) FBS (Sigma-Aldrich) and 1% (v/v) antibiotics 1% 10,000-U penicillin/streptomycin (P/S) (Sigma-Aldrich), at 37°C in an air-5 % CO_2 incubator. For the evaluation of the EF-dependent changes in the cell surface, glycan profiles cells were seeded on the thin glass slides and treated with the EF stimulation using parameters described below.

Electric field stimulation and time lapse image recording

Cells (1,500 cells/cm^2) were seeded and grown for at least 12 h in culture conditions as described above. To test the effect of EF and to ensure a constant flow of current, in case of an impendence drop, temperature change and other similar technical issues, a PEF was applied through bipolar electrode (St. Jude Medical Inc., Saint Paul, USA). Electric field intensities of 4 mA (16 mV/mm), 10 mA (40 mV/mm) and 20 mA (80 mV/mm) were used in the experiments, with exposure times of 3, 6 and 9 h. Stimulation frequencies were set at 130 Hz and 240 Hz, respectively to the field intensities. The pulse wave was set to 200 ms.

Time-lapse imaging was performed using an inverted microscope (JuLi FL; NanoEntek; Seoul, South Korea) to digitally record MSC migration. Images were acquired every 15 min. For long-term observations, the cell cultures as well as the PEF stimulation device were kept in the air-CO_2 incubator. At the end of the exposure period, cells were fixed in the PBS-buffered 4% formalin and then digitally photographed for quantification.

Evaluation of cells movement

Each migrating cell was traced using the position of the centroid of the plane figure, covering the area occupied by the cell in image obtained for each timeframe. A human operator generated an outline of each cell manually.

The centroid of the cell represents the cell's center of gravity, with coordinates as given in[16]:

$$X = \frac{1}{\sum_{i=1}^{M}\sum_{j=1}^{N} I(x_i,y_j)} \sum_{i=1}^{M}\sum_{y=1}^{N} x_i \cdot I(x_i,y_j)$$

$$Y = \frac{1}{\sum_{i=1}^{M}\sum_{j=1}^{N} I(x_i,y_j)} \sum_{i=1}^{M}\sum_{y=1}^{N} y_j \cdot I(x_i,y_j)$$

where:

M, N – image dimensions,

$I(x_i, y_i)$ – value of the pixel with xi, yi coordinates (in our case each image contains binary information and so $I(x_i, y_i)$ equals 1 when pixel of these coordinates represents area covered by the cell, otherwise it is equal to 0.

Using the center of gravity to localize the so-called "blob" (i.e., a figure of an irregular shape) in a binary image is a commonly used approach and can be successfully utilized in experimental applications.[18,19] Figure 1 shows the centroid obtained for a sample cell. Based on the locations of the cells in each time frame, the parameter of distance was calculated section-by-section and as the straight-line distance between the 1st and the last frame, to obtain information about the linearity of migration, which can be evaluated through the straightness factor, i.e., the ratio of the straight-line distance to the total distance. All measurements were made in triplicates.

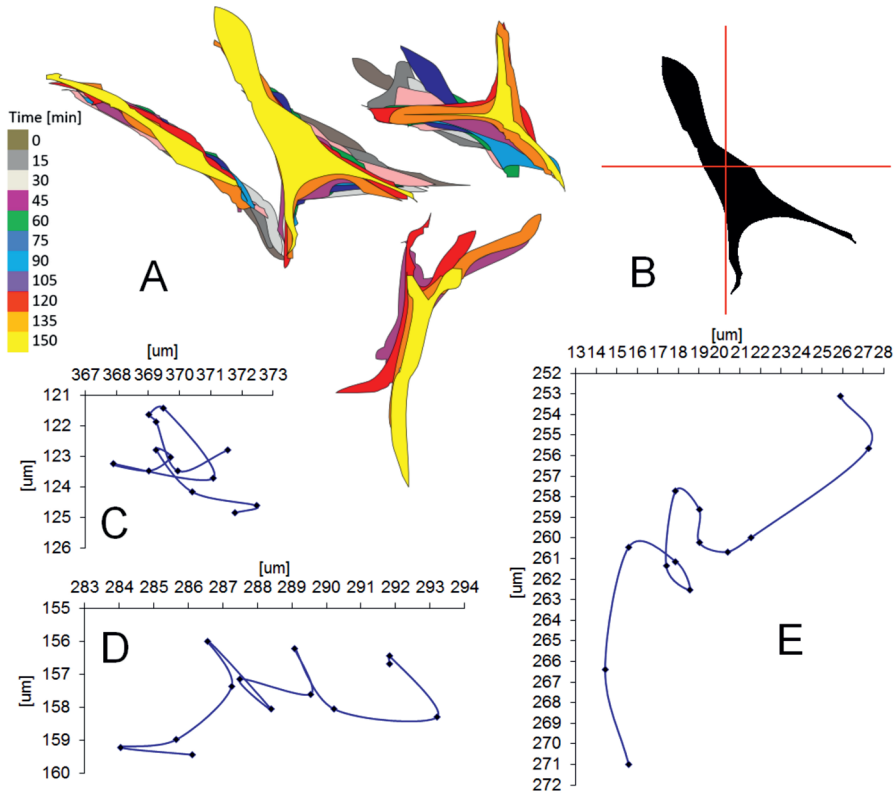

Fig. 1. A – manually outlined contours of 4 exemplary cells obtained by the time-lapse imaging; each color defines different time point; B – centroid of the exemplary cell indicated by the intersection of the red lines; C, D, E – migration pathways of 3 exemplary cells under different experimental conditions: C – 4 mA, 130 Hz; D – 10 mA, 130 Hz; E – 20 mA, 130 Hz.

Cell viability

Cell survival was assessed using a commercial assay The CellTiter 96 AQueous One Solution Cell Proliferation Assay (Promega, Madison, USA), according to the manufacturer's protocol.

Lectin binding

Following PEF treatment, cells were washed twice with PBS and fixed immediately for 15 min in the PBS-buffered 4% formalin. The carbohydrate phenotype was analyzed using 6 biotinylated lectins of plant origin: *Aleuria aurantia* (AAL), *Hippeastrum hybrid*, amaryllis (HHL), *Sambucus nigra* (SNA), Narcissus pseudonarcissus (NPL), wheat germ agglutinin (WGA), and concanavalin A (CON A)

Table 1. Lectins used in this study and their glycan-binding specificity

Lectin	Binding specificity
AAL (*Aleuria aurantia*)	α1,6 L-fucose
HHL (*Hippeastrum hybrid* – amaryllis)	α 1,3 and α1,6 mannose
SNA (*Sambucus nigra*)	Neu5Ac α2,6Gal or α2,6GalNAc
NPL (*Narcissus pseudonarcissus*)	α Man, (α1,6) galactomannans
WGA (wheat germ agglutinin)	(Neu5Ac) (Galβ4GlcNAc)$_{1\text{-}3,4}$ (GlcNAcβ4GlcNAc) $_{1\text{-}3,4}$
CON A (concanavalin A)	Terminal α Man, Man α3[Man α6] Man

(Table 1). All lectins were purchased from Vector Labs (San Diego, USA). Fixed cells were incubated with 2 μg/mL of each biotinylated lectin overnight, washed 3 times with PBS and incubated with FITC-streptavidin (Invitrogen) and Cy3-streptavidin (Invitrogen, Carlsbad, USA), in 1:2,000 dilution. Cellular nuclei were stained with the Hoechst 33258 dye (Sigma-Aldrich).

Results

Evaluation of cellular movement

The experiment was conducted in 2 steps. The 1st step aimed to determine whether the frequency of the pulsed electric field had an impact on the cell movement. As our preliminary results indicate, cellular motility increases with the value of the EF; therefore, we used 2 frequencies, 130 and 240 Hz, of the highest value of field intensity, i.e., 80 mV/mm, with 3 h observation time. We evaluated statistical differences in the total distance (i.e., distance measured section by section), as well as in the straight-line distance. The one-way analysis of variance (ANOVA) test, with a significance level (p-value) equal to 0.05, showed that there was no significant difference between any pair of data (pair of values). In conclusion, there was no reason to continue the experiment using various frequencies, so we chose 130 Hz for further evaluation of cellular movement.

In the 2nd step, we used PEFs with intensities equal to 4, 10 and 20 mA, and collected data for control group (0 mV/mm). For the data statistical analysis, we used Kruskal-Wallis H test (with 0.01 significance level), followed by multiple comparison test using post-hoc Fisher's least significant difference (LSD) test (with 0.05 significance level) in order to obtain pairwise comparison results. Matlab R2 013b Statistics (MathWorks, Natic, USA) and Machine Learning Toolbox were used for the purpose of all the abovedescribed statistical analysis. The results were as follows:

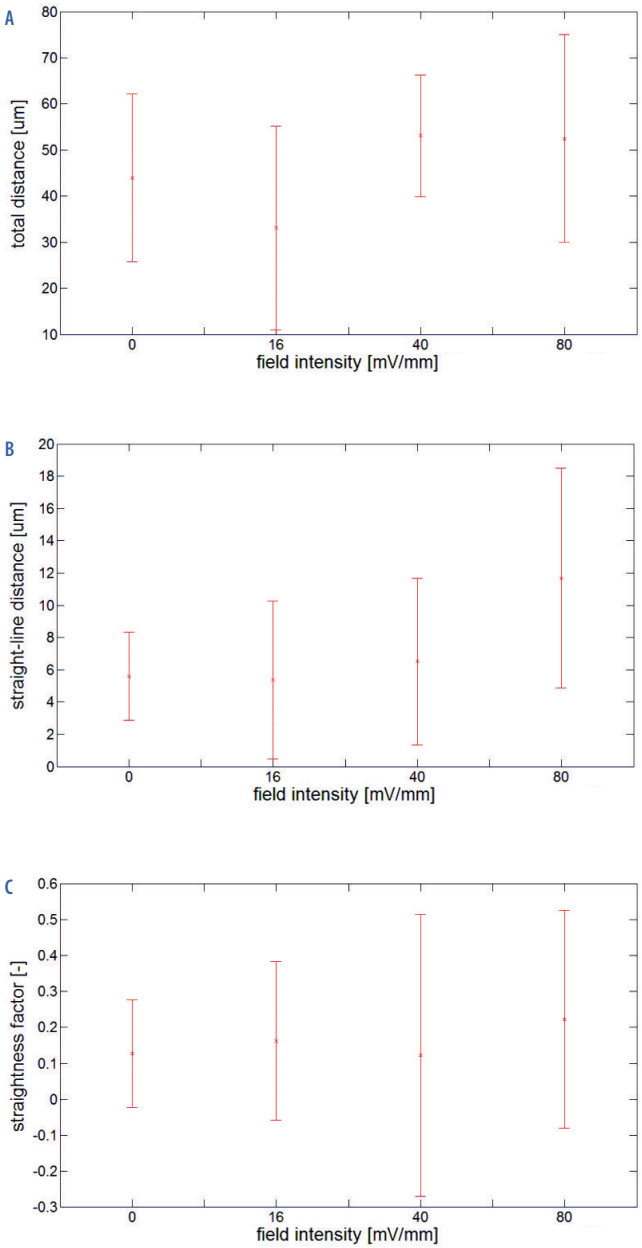

Fig. 2. Distance [μm] covered by 15 randomly selected mesenchymal stem cells (MSCs) during migration in pulsed electric field (0–20 mA; 130 Hz), measured in the time-lapse image

A – total distance; B – straight line distance; C – straightness factor.

• there were statistical differences between data on straight-line distance (Fig. 2A); between data on straight-line distance obtained for filed values equal to 4 and 10 mV/mm and data obtained for filed value equal to 20 mV/mm;

• there were statistical differences between data for straightness factor obtained for field values equal to 4 and 10 mV/mm and data obtained for field value equal to 20 mV/mm (Fig. 2B)

• there were no statistical differences between data on total distance (Fig. 2C); in other words, the test confirmed the null hypothesis that all 4 data samples (control group and 3 values of PEF intensity) come from the same distribution; in addition, there were no statistical differences between data on straight-line distance between control (0 mV/mm) and experimental data for field values equal to 4 and 10 mV/mm.

Presented figures depict cell images representative for given conditions.

Influence of pulsed electric field stimulation on the cell glyco-phenotype

We performed a comparative analysis of surface glycosylation in MSC population after PEF stimulation, using a panel of plant lectins shown in Table 1, known to bind certain structural oligosaccharides present in human cells. Staining with the fluorescein-labeled lectins has revealed the dynamics of terminal and internally linked α1,3 and α1,6 fucose, α1,3 and α1,6 mannose, α2,6 sialic acid, and terminal N-acetylglucosamine (GlcNAc), both on the cell surface and in intracellular localizations.

Cells from the control group untreated with the EF were positive for all analyzed lectins. Staining with *Hippeastrum hybrid* (HHL), *Sambucus nigra* (SNA), wheat germ agglutinin (WGA) and *Aleuria aurantia* (AAL) showed glycans located within endoplasmic reticulum and Golgi apparatus (ER/G). Concanavalin A (Con A) and *Narcissus pseudonarcissuss* (NPL) gave signals from both Golgi apparatus and from cytoplasm. We observed signals within different compartments of ER, both in the Golgi vesicles and around the nucleus. Signals closed to the nucleus varied depending on the direction of the EF. In certain EF conditions, signals appeared highly concentrated, forming a very characteristic cap on one side of the nucleus, called here "polarized ER" (ERp). Moreover, AAL, Con A, SNA and WGA were all highlighting multiple cell-cell contact points. Staining for Con A and WGA revealed specific points of cell attachment to the bottom of the culture dishes (glass, bottom substratum). Only in the case of these 2 lectins, the entire cell membrane was outlined by lectin signals in control cells, but following the EF stimulation, staining was reduced to only specific membrane foci, suggesting membrane rearrangements or fusion of newly-made membrane domains.

To compare the dynamic of complex glycans containing different types of mannose (Man) linkages, 3 mannose-binding lectins were used. High amounts of α-mannopyranosyl groups are present, as indicated by strong staining with Con A recognizing the internal branched Man core trisaccharide (Man α1,6[Man α1,3] Man) of N-linked glycans. HHL binds glycans with both (α1,3)- and (α1,6)-linked mannose structures, while NPL has a specificity towards α-linked mannose preferring polymannose structures containing (α1,6) linkages. The presence of poly-N-acetyllactosaminyl chains (LacNAc) was clearly demonstrated by the intense WGA staining and the presence of sialic acid in a (α2,6) linkage (Neu5Acα2,6) was shown by the SNA specific for Neu5Acα2,6Gal/GalNAc. The orange peel fungal lectin (*Aleuria aurantia* lectin – AAL) indicated α1,6-linked fucosyl groups occuring on the N,N'-diacetylchitobiosyl residues in N-linked glycoproteins.

The EF stimulation resulted in the re-distribution of glycans shown by all 6 lectins (Fig. 3) in both individual signal intensities and localizations. Table 2 presents key observations made during analyses of lectin staining patterns of glycan expression and localization.

Signals produced by AAL and SNA bindings behaved very similarly. Under exposure to high frequency (240 Hz) EF, target-glycans binding by AAL disappeared, there was no effect of current change on the AAL staining pattern, whereas an increase in the EF intensity resulted in the loss of SNA signal.

In the case of CON A, a very characteristic staining pattern corresponding to membrane shedding, as well as deposits of cell debris and cellular secretions of CON A-reactive materials were observed. In a few colonies, there were no CON-A-detectable cell-attachment sites away from the main cell population, but the cell-cell contact points were highlighted. This result could be explained by the different types of mannose linkages present in glycans in these locations.

Remodeling of cells surface glycosylation is also visualized by the HHL lectin. Initially visible clear ERp signal disappeared during the long exposure to the low field value and frequency, completely changing cellular localization by moving to the Golgi apparatus. The high frequency EF resulted in the loss of the HHL signal. We can hypothesize that the polarization of HHL-highlighted ER (ERp) demonstrated a polarization of the cell membrane components following cell motion direction.

Cell viability

To verify that MSCs were not damaged by applied PEFs, the viability of cells following a 3 h, 6 h and 9 h culture exposed to the PEF was compared with that of cells cultured for the same time under similar conditions but without PEF. The viability of cells following a 3 h, 6 h and 9 h culture of stimulation did not differ between groups ($p > 0.05$, one-way ANOVA). This suggests that the application of either low EF (130 Hz, 4 mA) or high EF (240 Hz, 20 mA) within a certain period of time did not result in any measurable damage to the cells.

Table 2. Description of the surface glycans profile changes caused by stimulation of pulsed electric field (PEF)

Field value: frequency/intensity/ time [h]	Lectin					
	AAL	CON A	HHL	NPL	SNA	WGA
Control/3 Control/6 Control/9	ER/G, cell -substrate contacts +++	ER/G, ERp, cell membrane, cell -substrate contacts	ERp	ER/G, ERp – mixed population	ER/G, ERp – mixed population	ER/G, ERp, cell membrane domains, cell-cell contacts
130/4/3	ER/G, cell-substrate +++, cell-cell contacts	no change	no change	no change	no change	no change
130/4/6	ER/G, cell substrate +	ER/G, ERp in single cells, cell-substrate	ER/G	no change	no change	no change
130/4/9	ER/G, ERp, cell substrate +	ER/G, ERp, cell membrane domains, cell-substrate	ER/G	no change	ER/G and ERp – mixed population, lost expression in single cells	no change
130/20/3	ER/G, ERp less, cell-cell contact points in single cells	ER/G, ERp, cells with no expression, cell membrane domains, cell-substrate in individual cells	no change	decreased of expression in ER/G	no signal	ER/G, cell membrane domains
130/20/6 130/20/9	no change	no change	no change	no change	no signal	no change
240/4/3 240/4/6 240/4/9 240/20/3 240/20/6 240/20/9	no signal	ER/G, ERp, heterogenous expression patterns, membrane sheading and deposits containing glyco-molecules reach in Con A-reactive mannose	no change	no change	no signal	no change

+++ – robust signal in all locations; ER – endoplasmic reticulum; G – Golgi apparatus; ERp – polarized endoplasmic reticulum; AAL – *Aleuria aurantia*; CON A – concanavalin A; HHL – *Hippeastrum hybrid* (amaryllis); NPL – *Narcissus pseudonarcissus*; SNA – *Sambucus nigra*; WGA – wheat germ agglutinin; ER/G – endoplasmic reticulum/Golgi apparatus.

Discussion

Aiming at a better understanding of human bone marrow-derived MSCs migration and at the development of new techniques to follow the stem cells motility, we analyzed the migration of MSCs in the absence of directional stimuli and in the presence of a PEF ranging from a low physiological level to the higher than physiological levels, using spinal cord stimulation system. For the first time we have also identified changes in the cell surface glycosylation resulting from it being stimulated with the PEF.

Most of the data on the in vitro electrotaxis has been obtained by exposing the cells to a direct electrical current. In these experiments, metal electrodes directly inserted into the medium, agar or in-house made salt bridges were used.[10,20–23] Effects of alternating electrical current stimulation combined with the direct EF current of very low frequencies have been reported for migration of keratinocytes.[24]

Despite the successful use of these experimental tools, it is challenging to effectively address more advanced scientific questions and meet higher technical requirements for the rapidly growing electrotaxis research, as well as to measure the applicability of these protocols in clinical trials. To our knowledge, this is the first work showing the effect of a PEF on the directed migration of MSCs after the application of a dedicated system already used in clinical practice.

We performed the stimulation of the MSCs using low and high current and low and high frequencies. In our previous studies, we have shown that cellular motility increases with the increase of the EF.[19] In this study we have also analyzed the effect of the frequency of the EF on cell motility. We used 2 frequencies, 130 Hz and 240 Hz, with the highest value of field intensity, i.e., 80 mV/mm, with 3 h observation time to assess the degree of migration. We evaluated statistical differences in the total distance (i.e., distance measured section by section), as well as in the straight-line distance. The one-way ANOVA test, with the significance level (p-value) equal to 0.01, showed that there was no significant difference between any pair of analysed data. This is in agreement with the results obtained by Jahanshahi et al. for electrical stimulation of the progenitor cells in the motor cortex. Furthermore, the frequency range does not seem to play any major role in the effectiveness of the electrical stimulation on proliferation.[25]

We then analyzed 3 parameters of cell migration, such as total distance, distance in straight line and factor

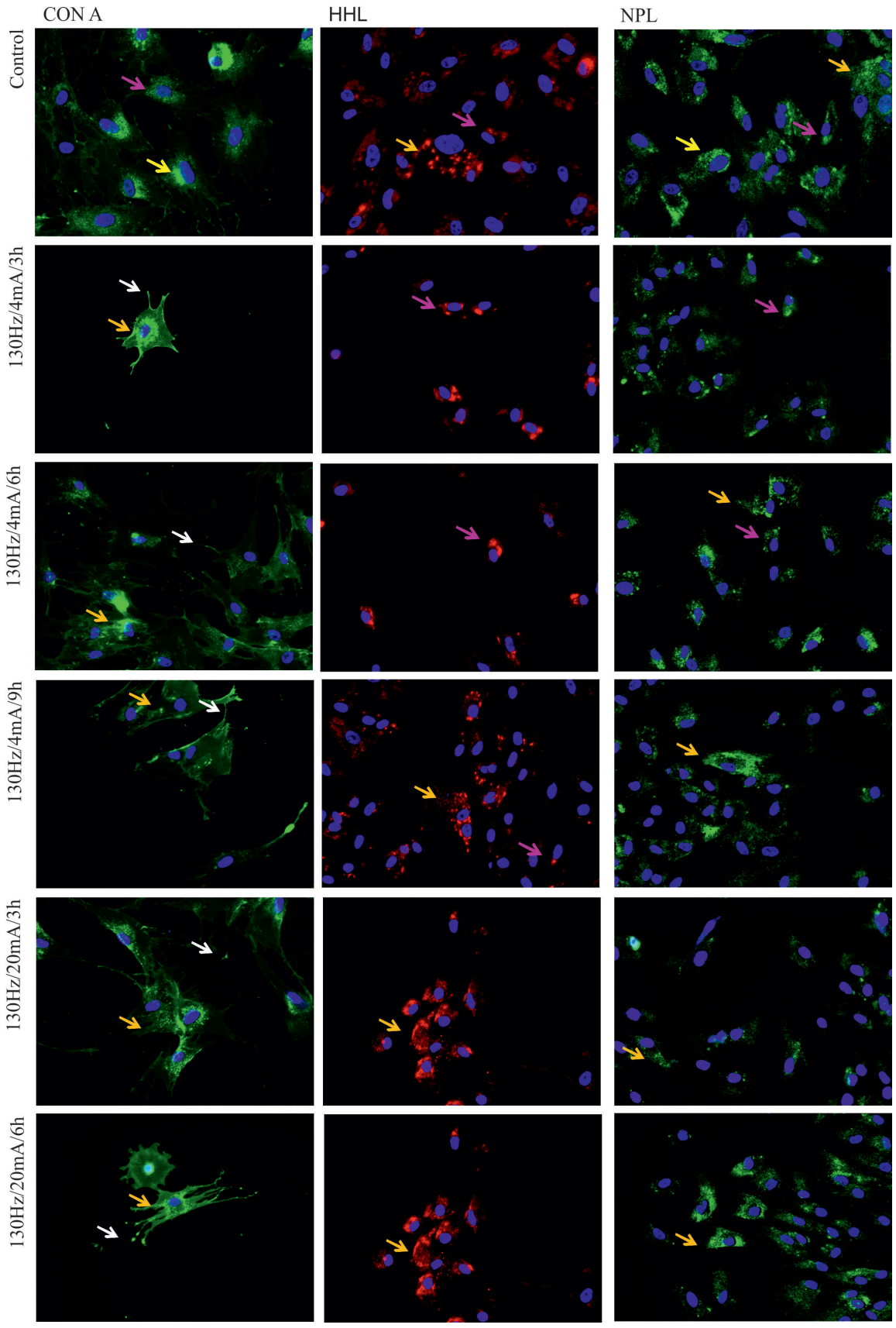

Fig. 3. Staining of selected glycans using fluorescence-labeled plant lectins in mesenchymal stem cells (MSCs) following stimulation in pulsed electric field (PEF), in conditions indicated on a left site of each row. Fluorescence labels: fluorescein-labeled streptavidin (green); Cy3-streptavidin (red); Hoechst nuclear stain (blue); 2 µg/mL. Scale bar: 10 µm.

Arrows indicate: ER – endoplasmic reticulum (bright yellow); G – Golgi apparatus (orange); ERp – endoplasmic reticulum polarized (pink); cell-cell and cell-substrate contact points (white).

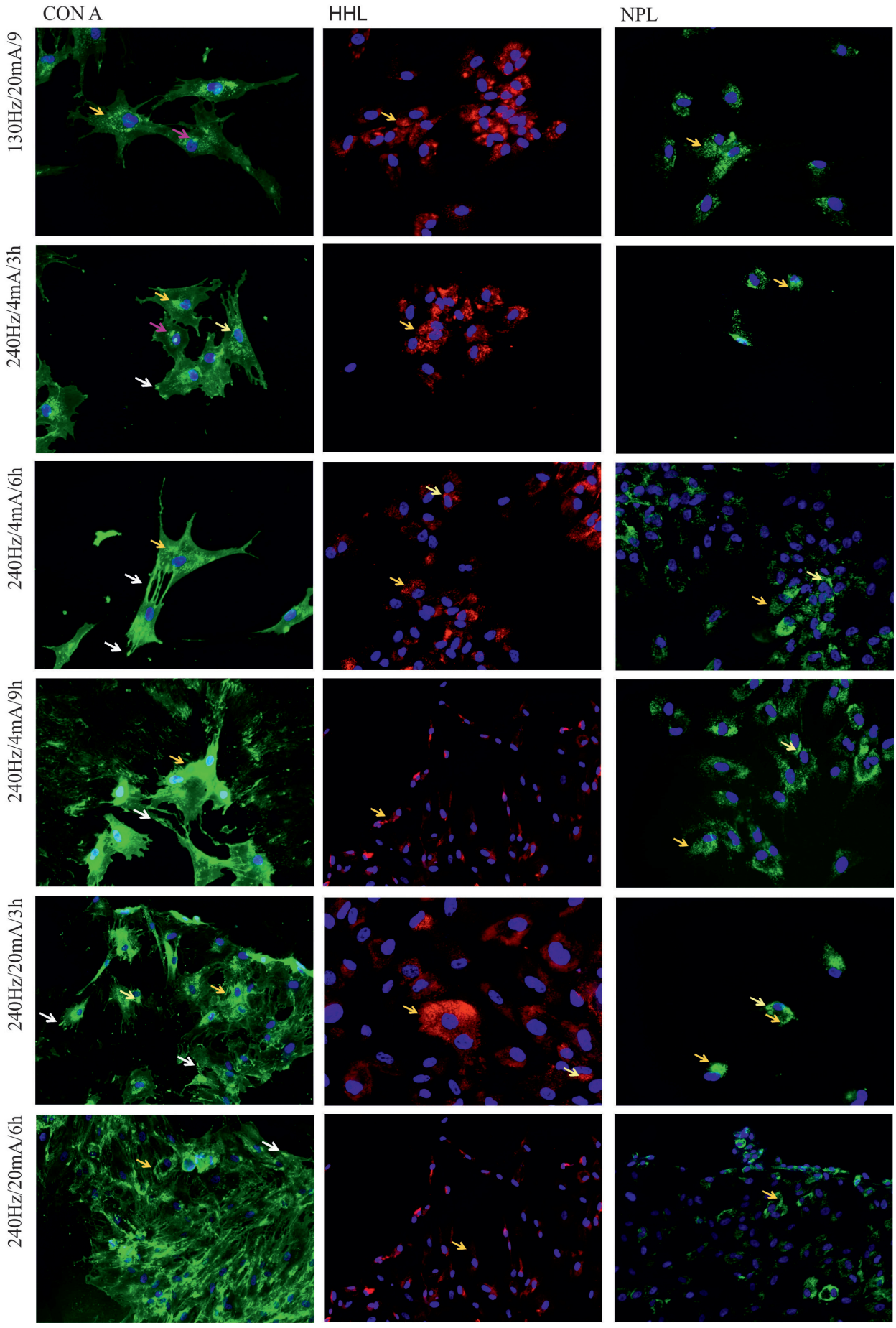
CON A
HHL
NPL
130Hz/20mA/9
240Hz/4mA/3h
240Hz/4mA/6h
240Hz/4mA/9h
240Hz/20mA/3h
240Hz/20mA/6h

Fig. 3. Cont.

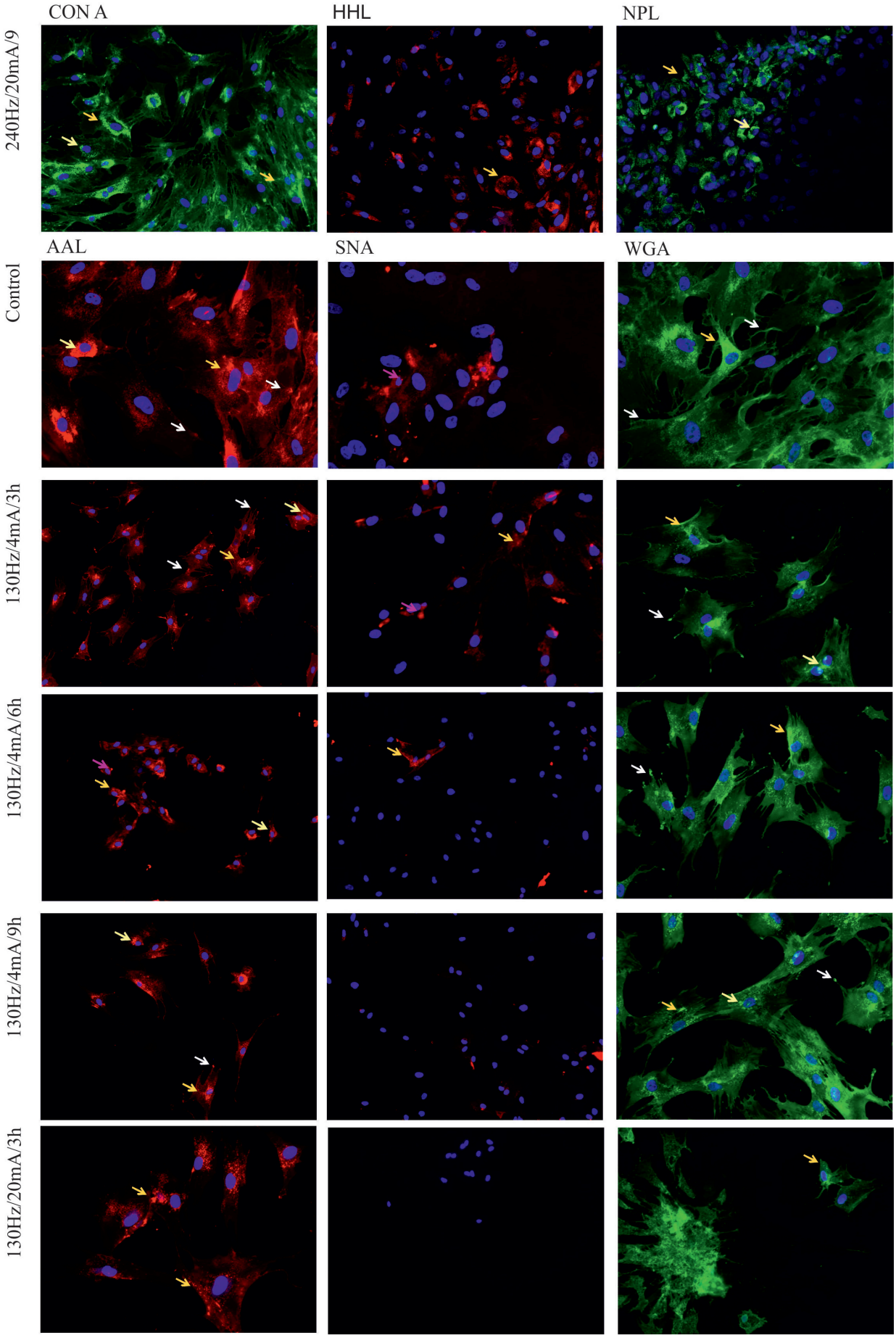
CON A
HHL
NPL
240Hz/20mA/9
AAL
SNA
WGA
Control
130Hz/4mA/3h
130Hz/4mA/6h
130Hz/4mA/9h
130Hz/20mA/3h

Fig. 3. Cont.

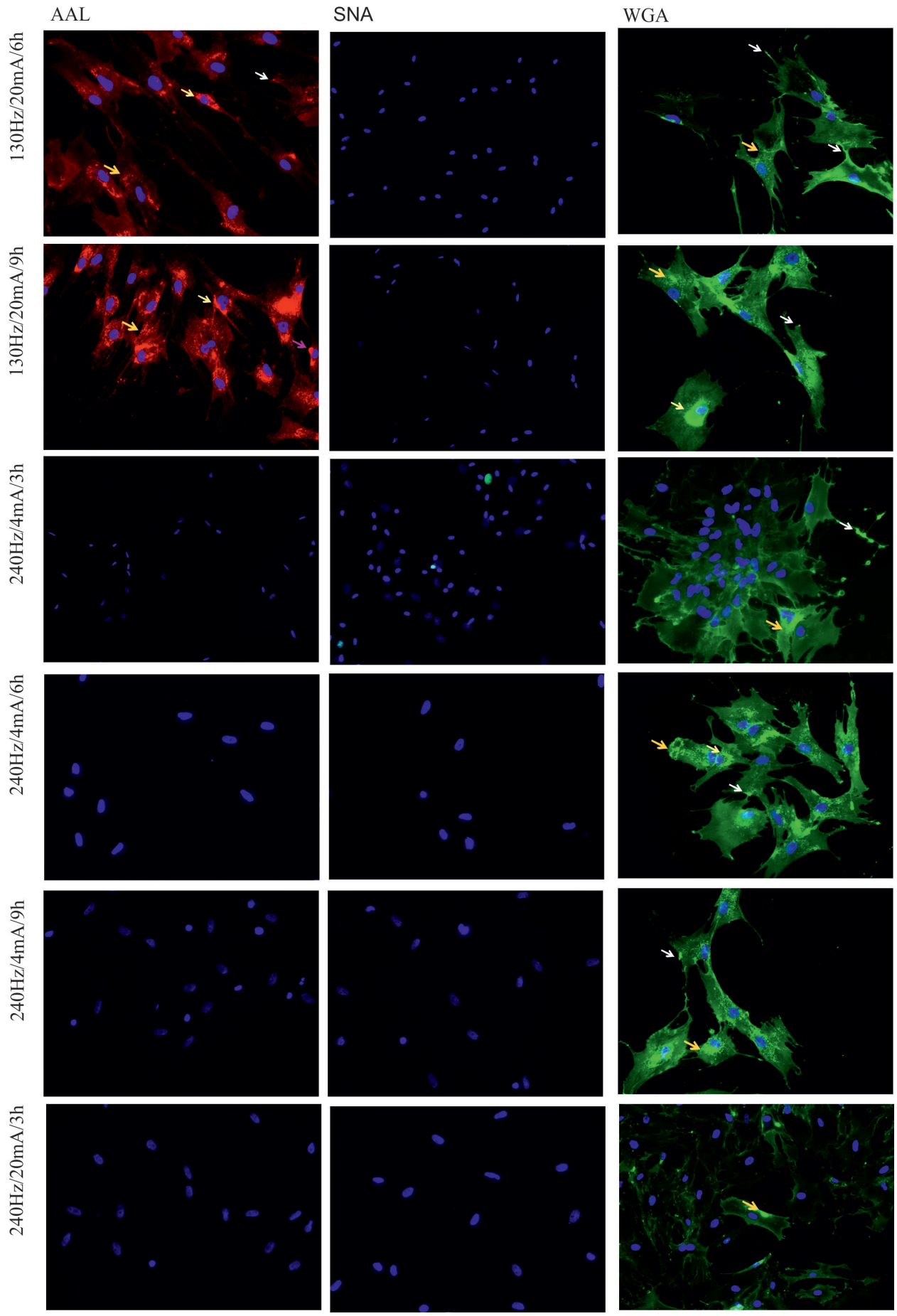
AAL
SNA
WGA
130Hz/20mA/6h
130Hz/20mA/9h
240Hz/4mA/3h
240Hz/4mA/6h
240Hz/4mA/9h
240Hz/20mA/3h

Fig. 3. Cont.

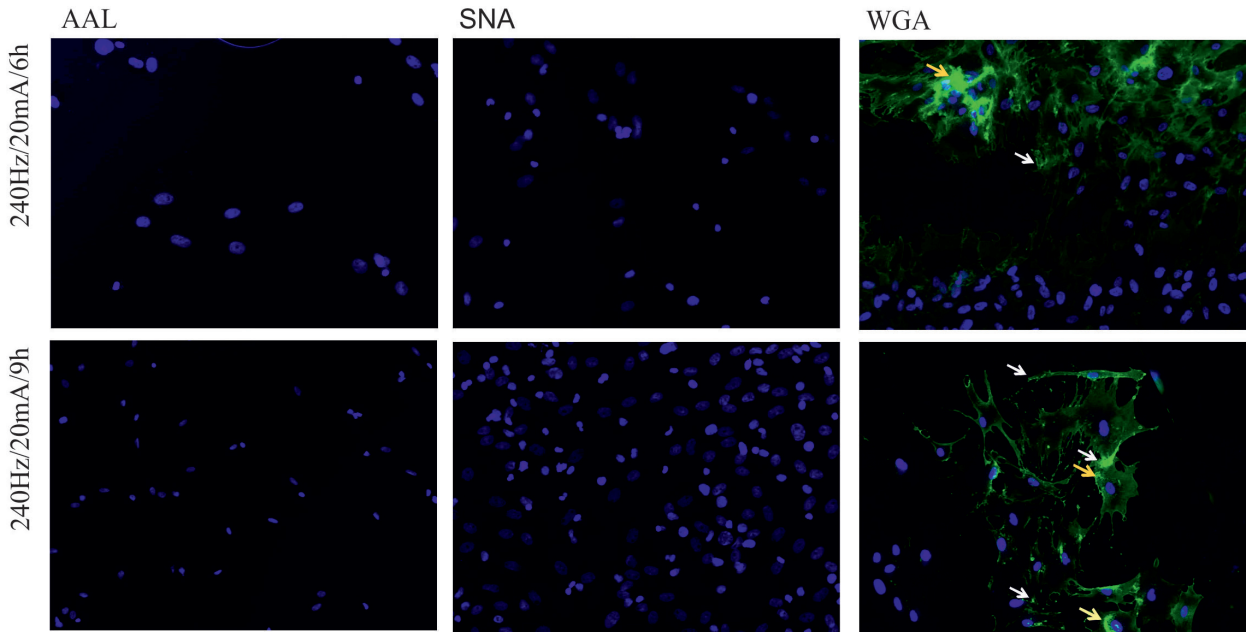

Fig. 3. Cont.

of straightness, as well as changes in the profile of cell surface glycans using 6 plant lectins of the specific glycan-binding properties. The most desirable results, i.e., those in which cells cover the longest possible track in one defined direction, were obtained for the field strength of 20 mA. Under these conditions, the cells migrated for the longest distance and had the highest parameter of straightness.

There are many advantages of using a low current for EF stimulation in cells migration studies, where most importantly, excessive heat and unwanted effects on different cell types in the 3D tissue settings are prevented.[3,7] Zhao et al. have shown that the directional migration occurred at a low threshold and with a physiological EF of ~25 mV/mm, while increasing the EF-enhanced MSC migratory response.[23] The authors concluded that these conditions selectively directed the migration of MSCs while potentially avoiding effects on endothelial cells and their progenitors.

The understanding of biochemical and biophysical changes occurring in cells during migration is rapidly growing. Biochemical studies include genetic manipulation of chemokines and their receptors such as CXCL12/CXCR-4, as well as stimulation of matrix metalloprotease secretion, enhancing chemotaxis and migration of stem cells.[26,27] Studies investigating the effects of the EF on cell migration show profound changes in the membrane electrical state due to the electrostatic membrane surface charge and altered electrodynamic ion fluxes through the membrane channels, resulting in cell membrane permeability changes followed by alterations of cytoskeleton structure.[12,28,29] There is also a growing number of reports documenting profile changes of membrane receptors, i.e., epidermal growth factor receptor (EGFR), Ca2 ions, and changes in expressions of cytoplasmic signaling proteins such as extracellular signal-regulated kinase (ERK), p38 mitogen-activated kinase (MAPK), cellular sarcoma gene family kinases (Src), protein kinase B (PKB) serine/threonine-specific protein kinase (Akt), and phosphatidylinositol-3 kinase (PI3K).[30,31]

The ability to recognize distinct carbohydrate determinants turned certain plant lectins into very valuable tools in blood typing, in evaluating cell differentiation processes, as cell separation and characterization agents, as markers used in microarrays, in immunological studies, and in studies of cell-cell recognition and cell signaling processes.[32–36] The importance of glycans in cell therapy has been known since 1988, when Hardy and Tavassoli showed that the carbohydrate moieties present on the stromal cells were important in homing stem cells bearing the corresponding lectin-like molecules and membrane lectins on a stem cell surface with a specificity for galactose and/or mannose-bearing glycoconjugates involved in the successful engraftment of hemopoietic progenitor cells in their specific stromal microenvironment.[37] Similarly, Hinge et al. showed that the mannose-containing carbohydrate moieties present on the hematopoietic stem and progenitor cells were recognized by mannose-binding lectins and played an importantrole in the HSPC-protecting effect of these lectins.[38] The protective effect of mannose-binding lectins has also been demonstrated by Li et al., where the effect of a mannose-binding lectin, NTL, purified from Narcissus tazetta var. chinensis, prolonged the maintenance and expansion of cord blood CD34+ cells. The results of this study indicate that the effect of NTL on the long-term preservation and expansion of early stem/multilineage progenitor cells might be useful in cell therapy strategies for DC34+ cells intended for transplantation.[39]

Much effort has gone into understanding the mechanisms of glycosylation and glycan modification within the ER and the Golgi apparatus. Enzymes involved in this

process are well-studied, which helped to define various functional compartments of the ER-Golgi pathway. We observed signals within different compartments of ER, both in the Golgi vesicles and around the nucleus. Signal closed to the nucleus varied depending on the direction of the EF. In certain EF conditions, signal appeared highly concentrated, forming a very characteristic cap on one side of the nucleus, and called here "polarized ER" (ERp). Similar observation was made by Pu and Zhao.[20]

In summary, our result show that: (i) EF value affects the rate of cell migration in contrast to the EF frequency; (ii) the rate of migration increases with the EF intensity above physiological levels, whereas EF at physiological levels did not affect cell motility, which may be important for the maintenance of the transplanted cells at the lesion site; (iii) EF above physiological levels resulted in changes of the cell surface glycans, whereas physiological EF levels did not change the cell glyco-phenotype as indicated by the lectins used in this study. Since the complex glycosylation of glycolipids and glycoproteins on cell surfaces forms a sophisticated architectural 3D-structure, creating the largest cell-surface and cell-substrate adhesion area, changes in this 3D-structure will have a large impact on all properties of cellular adhesion and motility.[40] The significance and novelty of our approach is based on (i): the recognition of the importance of the dynamics and regulatory function of structural cell surface glycosylation, and (ii) creating (formulating) a novel approach to studies of stem cell membrane glycosylation-based dynamics using a set of lectins binding cell surface carbohydrates.

The success of the stem cell transplantation depends on the effective and functional integration of transplanted cells into the patient's body and into the specific environment of extracellular matrix (ECM) produced and secreted by surrounding native cells. Based on the date results with the targeted cell migration, we used the low value EF remaining within the patient's tolerance range, which is a crucial factor in the cell therapy. Our results show that the application of well-tolerated stimulation parameters should allow securing the transplanted cells at the lesion site, without affecting the phenotype-surface glycans, thus providing a graft that is likely more compatible with the host environment.

If the goal of the stem cell-based therapy is to deliver cells to the lesion site and keep them there, it seems reasonable to reevaluate the concept of transplanted cells' homing. Perhaps it is better to choose stimulation/neuromodulation parameters that do not trigger cells to move, but instead keep the cells at the lesion site and prevent their migration to other tissues. Therefore, using the dedicated system for spinal cord stimulation/neuromodulation may provide us with a readily available tool for improving the effectiveness of stem cell therapy.

The use of plant lectins marking specific types of complex glycans allowed us to follow the reprograming of the cell surface glycosylation in response to certain PEF. Here, the specific changes in the cell surface glycans were observed only in cells showing directional movements under treatment with PEF above the physiological level, but in other conditions, such changes may indicate the unwanted migratory potential of cells intended for restorative transplantation.

Conclusions

The analysis of the stem cells' glycome dynamics at different stages of differentiation and migration makes possible the exploration of the cell surface glycans as markers of the stem cell functional status, and, in the future, compatibility between transplanted cell and host environment. Recently, substantial research effort focuses on changes in glycan profiles during differentiation of germ cells or induced pluripotent cells (iPS). There is a growing need for a better understanding of stem cell functional roles in the self-renewal and differentiation in vivo, as well as through niche interactions and signaling modulation. Since the complex cell surface glycans play a critical role in cell differentiation and migration, we should be aware that the information about glycan dynamics and its regulation may be extensively utilized and likely contribute to the optimizations of the stem cell preparations for future therapeutic applications. For instance, collective information about the type of transplanted stem cells and the more detailed characterization of their cell surface glycomes using more extensive lectin panel recognizing different 3D glycosylation patterns, can be correlated with the success rate of the transplant and used to optimize protocols for preparations of the therapeutic biomaterial of high quality and efficacy. We believe that our results obtained here using a panel of only 6 lectins provide proof of principle, and are an important step in the characterization of stem cells for restorative grafting.

References

1. Okano H, Sawamoto K. Neural stem cells: Involvement in adult neurogenesis and CNS repair. *Philos Trans R Soc Lond B Biol Sci.* 2008;363:2111–2122.
2. Breitbach M, Bostani T, Roell W, et al. Potential risks of bone marrow cell transplantation into infarcted hearts. *Blood.* 2007;110(4): 1362–1369.
3. McCaig CD, Rajnicek AM, Song B, Zhao M. Controlling cell behavior electrically: Current views and future potential. *Physiol Rev.* 2005;85:943–978.
4. Barker AT, Jaffe LF, Vanable Jr JW. The glabrous epidermis of cavies contains a powerful battery. *Am J Physiol.* 1982;242:R358–R366.
5. Zhao M, Song B, Pu J, et al. X Electrical signals control wound healing through phosphatidylinositol-3-OH kinase-gamma and PTEN. *Nature.* 1982;442:457–460.
6. Ozkucur N, Monsees TK, Perike S, Do HQ, Funk RH. Local calcium elevation and cell elongation initiate guided motility in electrically stimulated osteoblast-like cells. *PLoS One.* 2009;4:e6131.
7. Zhao Z, Qin L, Reid B, Pu J, Hara T, Zhao M. Directing migration of endothelial progenitor cells with applied DC electric fields. *Stem Cell Res.* 2011;8:38–48.

8. Zhao M, Bai H, Wang E, Forrester JV, McCaig CD. Electrical stimulation directly induces preangiogenic responses in vascular endothelial cells by signaling through VEGF receptors. *J Cell Sci.* 2004;117:397–405.
9. McCaig CD, Zhao M. Physiological electrical fields modify cell behavior. *Bioessays*. 1997;19:819–826.
10. Sato MJ, Ueda M, Takagi H, Watanabe TM, Yanagida T. Input-output relationship in galvanotactic response of Dictyostelium cells. *Biosystems*. 2007;88:261.
11. Li J, Zhu L, Zhang M, Lin F. Microfluidic device for studying cell migration in single or co-existing chemical gradients and electric fields. *Biomicrofluidics*. 2012;6(2):24121–2412113.
12. Huang C, Cheng J, Yen M, Young T. Electrotaxis of lung cancer cells in a multiple-electricfield chip. *Biosens Bioelectron.* 2009;24:3510.
13. Huang J, Hu X, Lu L, Ye Z, Zhang Q, Luo Z. Electrical regulation of Schwann cells using conductive polypyrrole/chitosan polymers. *J Biomed Mater Res*. 2009;93:164–174.
14. Rezai P, Salam S, Selvaganapathy PR, Gupta BP. Electrical sorting of Caenorhabditis elegans. *Lab Chip.* 2012;12:1831.
15. Alley WR Jr, Mann BF, Novotny MV. High-sensitivity analytical approaches for the structural characterization of glycoproteins. *Chem Rev*. 2013;113(4):2668–2732.
16. Malina W, Smiatacz M. *Methods of Digital Image Processing*. Warszawa, Poland: Academic Publishing House – Exit; 2005:159–176.
17. Batchelor B, Waltz F. *Interactive Image Processing for Machine Vision*. London, UK: Springer-Verlag; 2012:17–45.
18. Zieliński KW, Strzelecki M. *Computer Analysis of Biomedical Image*. Warszawa, Poland: Scientific Publishing House – PWN; 2002:170–178.
19. Jezierska-Woźniak K, Wojtkiewicz J, Grabarczyk Ł, Habich A, Lipiński S, Maksymowicz W. The effect of pulsed electric field on mesenchymal stem cell direct migration. *IFMBE Proceedings*. 2016;53:159–162.
20. Pu J, Zhao M. Golgi polarization in a strong electric field. *J Cell Sci*. 2005;118:1117–1128.
21. Li J, Lin F. Microfluidic devices for studying chemotaxis and electrotaxis. *Trends Cell Biol.* 2011;21:489.
22. Huang Y-J, Samorajski J, Kreimer R, Searson PC. The influence of electric fields and confinement on cell motility. *PLoS One*. 2013;8:1–9.
23. Zhao Z, Watt C, Karystinou A, et al. Directed migration of human bone marrow mesenchymal stem cells in a physiological direct current electric field. *Eur Cell Mater.* 2011;29(22):344–358.
24. Hart FX, Laird M, Riding A, Pullar CE. Keratinocyte galvanotaxis in combined DC and AC electric fields supports an electromechanical transduction sensing mechanism. *Bioelectromagnetics*. 2013;34:85–94.
25. Jahanshahi A, Schonfeld L, Janssen ML, et al. Electrical stimulation of the motor cortex enhances progenitor cell migration in the adult rat brain. *Exp Brain Res.* 2013;231(2):165–177.
26. Fong EL, Chan CK, Goodman SB. Stem cell homing in musculoskeletal injury. *Biomaterials*. 2011;32:395–409.
27. Miller RJ, Banisadr G, Bhattachary BJ. CXCR4 signaling in the regulation of stem cell migration and development. *J Neuroimmunol*. 2008;198:31–38.
28. Puc M, Corovic S, Flisar K, Petkovsek M, Nastran J, Miklavcic D. Techniques of signal generation required for electropermeabilization. Survey of electropermeabilization devices. *Bioelectrochemistry*. 2004; 64:113–124.
29. Kojima J, Shinohara H, Ikariyama Y, Aizawa M, Nagaike K, Morioka S. Electrically promoted protein production by mammalian cells cultured on the electrode surface. *Biotechnol Bioeng*. 1992;39:27–32.
30. Fang KS, Ionides E, Oster G, Nuccitelli R, Isseroff RR. Epidermal growth factor receptor relocalization and kinase activity are necessary for directional migration of keratinocytes in DC electric fields. *J Cell Sci*. 1999;112:1967–1978.
31. Huang L, Cormie P, Messerli MA, Robinson KR. The involvement of Ca2+ and integrins in directional responses of zebrafish keratocytes to electric fields. *J Cell Physiol.* 2009;219:162–172.
32. Wu D, Ma X, Lin F. DC electric fields direct breast cancer cell migration, induce EGFR polarization, and increase the intracellular level of calcium ions. *Cell Biochem Biophys*. 2013;67;1115–1125.
33. Yura H, Kanatani Y, Ishihara M, et al. Selection of hematopoietic stem cells with a combination of galactose-bound vinyl polymer and soybean agglutinin, a galactose-specific lectin. *Transfusion*. 2008;48: 561–566.
34. Naeem A, Saleemuddin M, Khan RH. Glycoprotein targeting and other applications of lectins in biotechnology. *Curr Protein Pept Sci*. 2007;8:261–271.
35. Tao SC, Li Y, Zhou J, Qian J, Schnaar RL, Zhang Y, et al. Lectin microarrays identify cell-specific and functionally significant cell surface glycan markers. *Glycobiology.* 2008;18:761–769.
36. Kullolli M, Hancock WS, Hincapie M. Preparation of a high-performance multi-lectin affinity chromatography (HP-M-LAC) adsorbent for the analysis of human plasma glycoproteins. *J Sep Sci.* 2008;31: 2733–2739.
37. Hardy CL, Tavassoli M. Homing of hemopoietic stem cells to hemopoietic stroma. *Adv Exp Med Biol.* 1988;241:129–133.
38. Hinge AS, Limaye LS, Surolia A, Kale VP. In vitro protection of umbilical cord blood-derived primitive hematopoietic stem progenitor cell pool by mannose-specific lectins via antioxidant mechanisms. *Transfusion.* 2010;50(8):1815–1826.
39. Li K, Ooi VE, Chuen CK, et al. The plant mannose-binding lectin NTL preserves cord blood haematopoietic stem/progenitor cells in long-term culture and enhances their ex vivo expansion. *Br J Haematol.* 2008;140(1):90–98.
40. Amano M, Yamaguchi M, Takegawa Y, et al. Threshold in stage-specific embryonic glycotypes uncovered by a full portrait of dynamic N-glycan expression during cell differentiation. *Mol Cell Proteomics*. 2010;9:523–537.

Effect of metformin in the prognosis of patients with small-cell lung cancer combined with diabetes mellitus

Hongyang Lu[1,2,A,B,D], Fajun Xie[2,B], Zhiyu Huang[2,B], Jing Qin[2,C,E], Na Han[2,B], Weimin Mao[1,A,F]

[1] Zhejiang Key Laboratory of Diagnosis and Treatment Technology on Thoracic Oncology (Lung and Esophagus), Zhejiang Cancer Hospital, Hangzhou, China
[2] Department of Thoracic Medical Oncology, Zhejiang Cancer Hospital, Hangzhou, China

A – research concept and design; B – collection and/or assembly of data; C – data analysis and interpretation;
D – writing the article; E – critical revision of the article; F – final approval of the article

Advances in Clinical and Experimental Medicine, ISSN 1899-5276 (print), ISSN 2451-2680 (online) *Adv Clin Exp Med*. 2018;27(9):1195–1199

Address for correspondence
Weimin Mao
E-mail: weiminmao@163.com

Funding sources
This work was supported by the Zhejiang Province Medical Science Fund Project of China (No. 2015ZHA006), and the 1022 Talent Training Program of Zhejiang Cancer Hospital.

Conflict of interest
None declared

Received on April 13, 2016
Reviewed on June 17, 2016
Accepted on February 16, 2017

Abstract

Background. The prognosis for small-cell lung cancer (SCLC) is very poor, so a new therapeutic strategy and new drugs are imperative.

Objectives. The aim of this study was to examine the effect of metformin on the prognosis of patients with SCLC combined with diabetes mellitus (DM).

Material and methods. From 2005 to 2013, 32 patients (4 female and 28 male) with SCLC combined with DM were included in this retrospective study at the Zhejiang Cancer Hospital, Hangzhou, China. All patients were diagnosed with SCLC by pathological analysis and had received more than 4 cycles of chemotherapy. Metformin was used in 12 patients. Seventeen patients had limited-stage disease (LD) and 15 patients had extensive-stage disease (ED). Patients with LD SCLC were administered thoracic radiotherapy. The follow-up deadline was January 27, 2016. At that point, 4 patients were alive, 21 patients had died, and 7 patients did not participate in follow-up examinations.

Results. In patients with SCLC combined with DM using metformin, a complete response (CR) was observed in 4 patients, a partial response (PR) in 6 patients, a stable disease (SD) in 1 patient, and a progressive disease (PD) in 1 patient, whereas in patients who did not use metformin, CR was observed in 2 patients, PR in 15 patients, SD in 2 patients, and PD in 1 patient ($p = 0.384$). There was no difference in the median survival time (MST) between patients using metformin and those who did not (12 vs 13 months; $p = 0.784$). There was a trend toward prolonged MST in patients with LD SCLC using metformin compared with those who did not use metformin (58 vs 29 months; $p = 0.084$). There was no difference due to the use of metformin observed in MST of patients with ED SCLC (12 vs 13 months; $p = 0.396$).

Conclusions. Metformin use may have a prognostic benefit in patients with SCLC combined with DM. This combination is promising and further clinical trials are required.

Key words: small-cell lung cancer, diabetes mellitus, metformin, prognosis

DOI
10.17219/acem/69021

Lung cancer is the leading cause of cancer-related mortality and the most common malignancy in the world.[1] The data from the National Central Cancer Registry of China indicated that an estimated 4,292,000 new patients with cancer and 2,814,000 cancer-related deaths would occur in China in 2015, and that lung cancer is the leading cause of cancer death.[2] Lung cancer includes small-cell lung cancer (SCLC) and non-small cell lung cancer (NSCLC). The proportion of SCLC among all histological types of lung cancer decreased from 17.26 in 1986 to 12.95 in 2002.[3] The prognosis of SCLC is very poor, and a new therapeutic strategy and new drugs are imperative.

Metformin is the preferred drug for starting treatment of diabetes mellitus (DM), and it has been reported to have a potential anticancer effect on some solid tumors, such as lung, hepatocellular, and melanoma.[4–6] Metformin might be used in combination with tyrosine kinase inhibitors (TKIs) in patients with NSCLC, harboring mutations in epidermal growth factor receptor to overcome resistance to TKI and to prolong the survival time of patients.[7] Metformin and gefitinib are synergistic in LKB1 wild-type NSCLC cells,[8] and metformin has the ability to partially block the M2-like polarization of macrophages through the adenosine monophosphate-activated protein kinase α1 pathway, which plays an important role in metformin-inhibited metastasis of Lewis lung cancer.[9] Metformin as a monotherapy reduces the metabolic viability of SCLC in the NCI-H460 cell line. Combining metformin with cisplatin or etoposide produced a synergistic effect and is more effective than the use of cisplatin or etoposide as a monotherapy in the NCI-H460 cell line.[10] At the time of diagnosis of SCLC, DM did not have prognostic importance for the survival of patients.[11] Metformin use may be associated with a good prognosis in patients with lung cancer combined with DM, but the effect was modest. However, it could achieve benefits in a selective sub-group of patients with lung cancer, especially in patients with SCLC from Asia.[12]

This study aimed to further elucidate the effect of metformin treatment in combination with chemotherapy in patients with SCLC combined with DM. A total of 32 patients with SCLC combined with DM were included in this study. The clinical parameters and survival data were collected and analyzed.

Material and methods

Patient characteristics

From 2005 to 2013, 32 patients (4 female and 28 male) with SCLC combined with DM were included in this retrospective study at the Zhejiang Cancer Hospital, China. All patients were diagnosed with SCLC by pathological analysis based on the standard criteria defined by the World Health Organization classification and they had received more than 4 cycles of chemotherapy. The stages of the Veterans Administration Lung Study Group (VALSG) included limited-stage disease (LD) in 17 patients and extensive-stage disease (ED) in 15 patients. Fifteen patients with LD SCLC received thoracic radiotherapy. The mean age of patients was 62 years (range: 48–75 years). Five patients were non-smokers, 2 patients were light smokers, 25 patients were heavy smokers, and there were 0 moderate smokers. The median value for smoking history was 40 pack-years. Metformin was used in 12 patients. There were no significant differences in age, smoking history, or disease stage between the patients with SCLC using metformin and those not using metformin ($p > 0.05$), whereas there was a difference in sex ($p = 0.015$) (Table 1). There were no significant differences in age, sex, smoking history, or disease stage between the patients using metformin and those not using metformin in either subgroup of patients – with LD and ED SCLC ($p > 0.05$) (Tables 2, 3).

Table 1. Clinical features of patients with SCLC using metformin or not

Characteristics	Metformin	Without metformin	p-value
Number of patients (n = 32)	12	20	–
Age (median)	60 (48–73)	62.5 (51–75)	0.29
Sex (female/male)	0/12	4/16	0.015
Smoking history (median pack-years)	35 (4–120)	40 (0–120)	0.27
Stage (LD/ED)	6/6	11/9	0.784

SCLC – small-cell lung cancer; LD – limited-stage disease; ED – extensive-stage disease.

Table 2. Clinical features of patients with LD SCLC using metformin or not

Characteristics	Metformin	Without metformin	p-value
Number of patients (n = 17)	6	11	–
Age (median)	60 (54–65)	60.5 (48–73)	0.79
Sex (female/male)	0/6	3/8	0.159
Smoking history (median pack-years)	45 (4–60)	40 (0–70)	0.37

LD SCLC – limited-stage disease small-cell lung cancer.

Table 3. Clinical features of patients with ED SCLC using metformin or not

Characteristics	Metformin	Without metformin	p-value
Number of patients (n = 15)	6	9	–
Age (median)	62.5 (48–73)	68 (52–75)	0.22
Sex (female/male)	0/6	1/8	0.398
Smoking history (median pack-years)	45 (20–120)	40 (0–120)	0.52

ED SCLC – extensive-stage disease small-cell lung cancer.

Follow-up

The follow-up deadline was January 27, 2016. At that point, 4 patients were alive, 21 patients had died, and 7 patients did not participate in follow-up examinations. The survival time was calculated from the date of pathological diagnosis.

Statistical analysis

The data was analyzed using the statistical package for the social sciences software v. 15.0. Overall data was screened using the χ^2 test, and survival time was calculated using Kaplan–Meier software with a statistical significance of $p < 0.05$.

Results

In patients with SCLC combined with DM using metformin, a complete response (CR) was observed in 4 patients, a partial response (PR) in 6 patients, a stable disease (SD) in 1 patient, and a progressive disease (PD) in 1 patient, whereas in patients not using metformin, CR was observed in 2 patients, PR in 15 patients, SD in 2 patients, and PD in 1 patient (p = 0.384). There was no significant difference in the median survival time (MST) between patients using metformin and those not using metformin (12 vs 13 months; p = 0.784) (Fig. 1). In patients with LD SCLC combined with DM using metformin, CR was observed in 4 patients, PR in 2 patients, SD in 0 patients, and PD in 0 patients, whereas in patients not using metformin, CR was observed in 2 patients, a PR in 8 patients, SD in 1 patient, and PD in 0 patients (p = 0.125). There was a trend toward prolonged MST in patients with LD SCLC using metformin compared to those not using metformin (58 vs 29 months; p = 0.084) (Fig. 2). In patients with ED SCLC

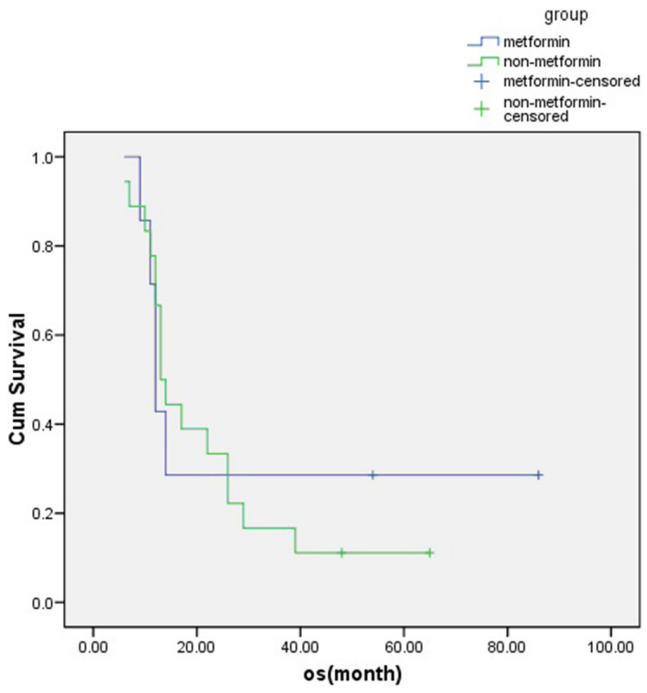

Fig. 1. The survival time of patients with SCLC combined with DM using metformin or not (n = 32)

SCLC – small-cell lung cancer; DM – diabetes mellitus.

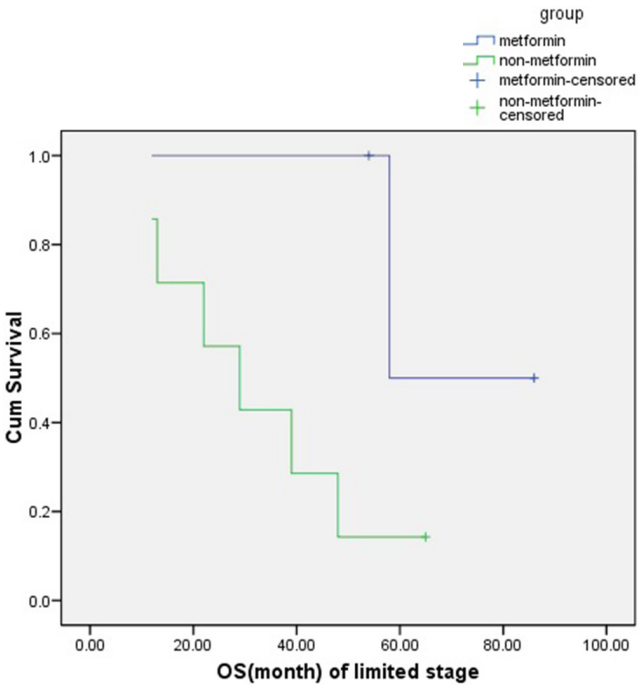

Fig. 2. The survival time of patients with LD SCLC combined with DM using metformin or not (n = 17)

LD SCLC – limited-stage disease small-cell lung cancer; DM – diabetes mellitus.

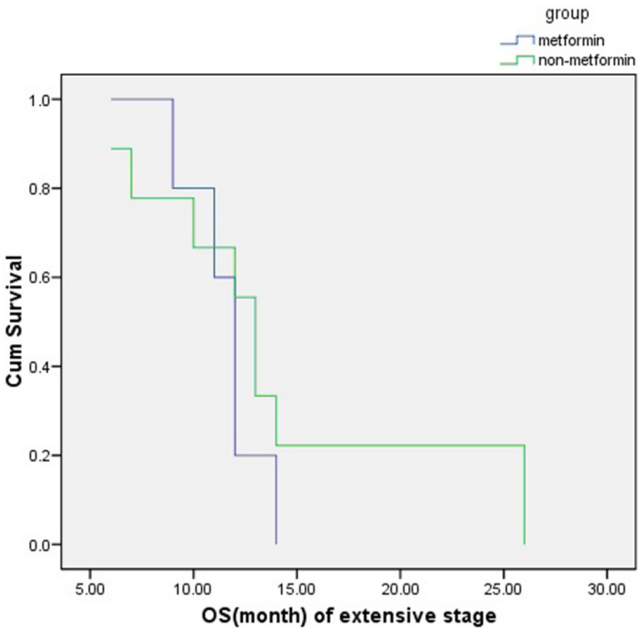

Fig. 3. The survival time of patients with ED SCLC combined with DM using metformin or not (n = 15)

ED SCLC – extensive-stage disease small-cell lung cancer; DM – diabetes mellitus.

combined with DM using metformin, CR was observed in 0 patients, PR in 4 patients, SD in 1 patient, and PD in 1 patient, whereas in patients not using metformin, CR was observed in 0 patients, PR in 7 patients, SD in 2 patients, and PD in 1 patient (p = 0.446). There was no difference in MST between patients with ED SCLC using metformin and those not using metformin (12 vs 13 months; p = 0.396) (Fig. 3).

Discussion

Patients with SCLC are commonly classified as LD or ED by the VALSG staging system. Chemotherapy is the cornerstone of the treatment; however, 4 to 6 cycles of chemotherapy are needed for patients with ED or LD SCLC. The standard clinical practice in LD SCLC is to combine chemotherapy and thoracic radiotherapy (TRT). In this study, all patients had received more than 4 cycles of chemotherapy, and patients with LD SCLC additionally received TRT. A response to combination chemotherapy can be achieved by 80–90% of patients with LD SCLC and their MST is 15–20 months, with or without TRT.[13–14] Of all the patients with ED SCLC, 60–80% respond to chemotherapy and their MST is 8–12 months.[15–17] The most commonly used initial combination chemotherapy regimens are etoposide combined with cisplatin (EP) and etoposide combined with carboplatin (EC). Several studies have shown a similar effect with chemotherapy regimens of irinotecan combined with cisplatin and irinotecan combined with carboplatin in ED SCLC compared to EP or EC.[15–17] Despite trends toward a modest improvement in survival of SCLC, the prognosis is extremely poor. Certain newly-targeted agents offer a promise of improved outcomes, but no targeted drugs have been recommended by the National Comprehensive Cancer Network guideline for SCLC.[18] It is imperative to seek new drugs to improve the survival time of patients. The use of metformin improved the long-term outcome of patients with SCLC combined with DM, which might be considered a potential useful prognostic indicator and anticancer drug.[19] There are few studies about the effect of metformin use in patients with SCLC combined with DM, and it needs to be further evaluated and confirmed, especially in China.

Disease stage and sex were identified as important prognostic factors, but not DM.[11,20] There is a significant difference in sex between the patients who used metformin and those who did not, whereas there was no significant difference between the patients with LD SCLC or ED SCLC who used metformin and those who did not. There were no significant differences in age, disease stage, or smoking history between patients using metformin and those not using it. Wheatley-Price et al. reported that data from over 1,700 patients with SCLC in randomized chemotherapy trials confirmed that women survive slightly longer than men.[20] The results have shown that there was no significant difference in MST between all patients with SCLC, using metformin and not. Due to the higher number of female patients with SCLC not using metformin, there may be no difference in MST between the groups. There was a trend toward prolonged MST in patients with LD SCLC using metformin compared to those not using it, and there was no significant difference in sex. Metformin use may have a prognosis benefit in patients with SCLC combined with DM based on the results of this study and that of Kong et al.[19] Considering the limited number of patients in this study, however, the results need to be validated on a larger sample of patients, probably in a multicenter prospective study. More studies need to be carried out in order to clarify the mechanism of the synergistic effect of metformin and chemotherapy/radiotherapy, though this combination is promising.

References

1. Siegel R, Naishadham D, Jemal A. Cancer statistics, 2013. *CA Cancer J Clin*. 2013;63:11–30.
2. Chen W, Zheng R, Baade PD, et al. Cancer statistics in China, 2015. *CA Cancer J Clin*. 2016. doi: 10.3322/caac.21338
3. Govindan R, Page N, Morgensztern D, et al. Changing epidemiology of small-cell lung cancer in the United States over the last 30 years: Analysis of the surveillance, epidemiologic, and end results database. *J Clin Oncol*. 2006;24:4539–4544.
4. Leone A, Di Gennaro E, Bruzzese F, Avallone A, Budillon A. New perspective for an old antidiabetic drug: Metformin as anticancer agent. *Cancer Treat Res*. 2014;159:355–376.
5. Guo Z, Cao M, You A, et al. Metformin inhibits the pro-metastatic effect of sorafenib in hepatocellular carcinoma by upregulating the expression of TIP30. *Cancer Sci*. 2016. doi: 10.1111/cas.12885
6. Liang G, Ding M, Lu H, et al. Metformin upregulates E-cadherin and inhibits B16F10 cell motility, invasion and migration. *Oncol Lett*. 2015;10:1527–1532.
7. Li L, Han R, Xiao H, et al. Metformin sensitizes EGFR-TKI-resistant human lung cancer cells in vitro and in vivo through inhibition of IL-6 signaling and EMT reversal. *Clin Cancer Res*. 2014;20:2714–2726.
8. Morgillo F, Sasso FC, Della Corte CM, et al. Synergistic effects of metformin treatment in combination with gefitinib, a selective EGFR tyrosine kinase inhibitor, in LKB1 wild-type NSCLC cell lines. *Clin Cancer Res*. 2013;19:3508–3519.
9. Ding L, Liang G, Yao Z, et al. Metformin prevents cancer metastasis by inhibiting M2-like polarization of tumor associated macrophages. *Oncotarget*. 2015;6:36441–36455.
10. Teixeira SF, Guimarães Idos S, Madeira KP, Daltoé RD, Silva IV, Rangel LB. Metformin synergistically enhances antiproliferative effects of cisplatin and etoposide in NCI-H460 human lung cancer cells. *J Bras Pneumol*. 2013;39:644–649.
11. Inal A, Kaplan MA, Kucukoner M, et al. Is diabetes mellitus a prognostic factor for survival in patients with small cell lung cancer? *Asian Pac J Cancer Prev*. 2012;13:1491–1494.
12. Tian RH, Zhang YG, Wu Z, Liu X, Yang JW, Ji HL. Effects of metformin on survival outcomes of lung cancer patients with type 2 diabetes mellitus: A meta-analysis. *Clin Transl Oncol*. Epub 2015 Oct 12.
13. Takada M, Fukuoka M, Kawahara M, et al. Phase III study of concurrent versus sequential thoracic radiotherapy in combination with cisplatin and etoposide for limited-stage small-cell lung cancer: Results of the Japan Clinical Oncology Group Study 9104. *J Clin Oncol*. 2002;20:3054–3060.
14. Sun JM, Ahn YC, Choi EK, et al. Phase III trial of concurrent thoracic radiotherapy with either first- or third-cycle chemotherapy for limited-disease small-cell lung cancer. *Ann Oncol*. 2013;24:2088–2092.
15. Zatloukal P, Cardenal F, Szczesna A, et al. A multicenter international randomized phase III study comparing cisplatin in combination with irinotecan or etoposide in previously untreated small-cell lung cancer patients with extensive disease. *Ann Oncol*. 2010;21:1810–1816.

16. Lara PN Jr, Natale R, Crowley J, et al. Phase III trial of irinotecan/cisplatin compared with etoposide/cisplatin in extensive-stage small-cell lung cancer: Clinical and pharmacogenomic results from SWOG S0124. *J Clin Oncol*. 2009;27:2530–2535.
17. Hermes A, Bergman B, Bremnes R, et al. Irinotecan plus carboplatin versus oral etoposide plus carboplatin in extensive small-cell lung cancer: A randomized phase III trial. *J Clin Oncol*. 2008;26:4261–4267.
18. Lu HY, Wang XJ, Mao WM. Targeted therapies in small cell lung cancer (Review). *Oncol Lett*. 2013;5:3–11.
19. Kong F, Gao F, Liu H, et al. Metformin use improves the survival of diabetic combined small-cell lung cancer patients. *Tumour Biol*. 2015;36:8101–8106.
20. Wheatley-Price P, Ma C, Ashcroft LF, et al. The strength of female sex as a prognostic factor in small-cell lung cancer: A pooled analysis of chemotherapy trials from the Manchester Lung Group and Medical Research Council Clinical Trials Unit. *Ann Oncol*. 2010;21:232–237.

Frequency of isolation and drug susceptibility of bacterial strains isolated from child oncohematological patients 2011–2014: A single center study

Beata Kowalska-Krochmal[1,A–F], Radosław Chaber[2,3,A,C–F], Katarzyna Jermakow[4,B,C], Magdalena Hurkacz[5,C], Elżbieta Piątkowska[1,B], Grażyna Gościniak[4,B,C], Grażyna Wróbel[2,B,C,E,F]

[1] Department of Pharmaceutical Microbiology and Parasitology, Wroclaw Medical University, Poland
[2] Chair and Clinic of Pediatric Hematology, Oncology and Bone Marrow Transplantation, Wroclaw Medical University, Poland
[3] Department of Pediatric Oncology and Hematology, Faculty of Medicine, University of Rzeszów, Poland
[4] Chair and Department of Microbiology, Wroclaw Medical University, Poland
[5] Chair and Department of Clinical Pharmacology, Wroclaw Medical University, Poland

A – research concept and design; B – collection and/or assembly of data; C – data analysis and interpretation; D – writing the article; E – critical revision of the article; F – final approval of the article

Advances in Clinical and Experimental Medicine, ISSN 1899-5276 (print), ISSN 2451-2680 (online) *Adv Clin Exp Med*. 2018;27(9):1201–1209

Address for correspondence
Beata Kowalska-Krochmal
E-mail: beata.kowalska-krochmal@umed.wroc.pl

Funding sources
None declared

Conflict of interest
None declared

Received on November 16, 2016
Reviewed on January 28, 2017
Accepted on February 15, 2017

Abstract

Background. Infections in pediatric patients with oncohematological diseases pose a huge therapeutic and diagnostic problem.

Objectives. The aim of the study was to investigate the etiology of bacteremia and the antibiotic susceptibility of pathogenic and colonizing bacterial strains in pediatric oncohematological patients.

Material and methods. In the period 2011–2014, 17,209 positive test results, including 1,129 positive blood cultures, were subjected to a detailed analysis. The assessment of drug susceptibility was conducted in accordance with the CLSI (American), EUCAST (European), and KORLD (Polish) recommendations.

Results. A high percentage (86–91%) of negative blood culture results was demonstrated. A predominance of Gram-positive bacteria was seen in all years (60–70%) in contrast to Gram-negative strains (30–40%). Coagulase-negative staphylococci (CNS) were the strains most frequently isolated from blood (41–47%) among all bacterial strains. Susceptibility to linezolid and vancomycin was 96–100%, and to teicoplanin 82–96%. Methicyllin-resistant coagulase-negative *Staphylococcus* (MRCNS) were isolated in 77–86%. All *Staphylococcus aureus* (*S. aureus*) strains were susceptible to glycopeptides and linezolid, while *Enterococcus* spp. was susceptible to linezolid. Apart from the year 2014, no methicillin-resistant *S. aureus* (MRSA) were isolated. Enterobacteriaceae (EN) were the most susceptible to imipenem and meropenem (91–100%) as well as to amikacin (77–93%). From 2013 to 2014, non-fermentative rods (NF) isolated from blood were less susceptible to imipenem and meropenem (71% and 67–71%, respectively) than to other antibiotics. It has been shown that strains isolated from blood have a statistically significantly different susceptibility to antibiotics (CNS and EN are less and NF is more susceptible) than those existing as colonizing flora.

Conclusions. Our results show that choosing appropriate antibiotics for treating infection in children with oncohematological diseases based on antibiograms for colonizing flora may be difficult because they may not take into account the more resistant strains. According to the antibiotic susceptibility of the strains isolated from blood in our center, the most viable active empirical and carbapenem-saving therapy could be conducted with piperacillin/tazobactam or cefepime.

Key words: antibiotic susceptibility, blood infections, oncohematological children

DOI
10.17219/acem/69003

Introduction

Infections in neutropenic patients in the course of cancer treatment and treatment of some hematological diseases constitute a significant factor which worsens the patients' condition and in some cases poses a direct threat to their life. The choice of antibiotic for treatment is difficult because it is nearly always empirical, owing to the time needed to wait for the results of microbiological tests. The spread of multi-drug-resistant pathogens additionally aggravates the already difficult decision-making process regarding antibiotic treatment.[1] The assessment of the suitability of antibiotic therapy is also complicated by the fact that there are often problems with the identification of etiological factors despite the use of microbiological diagnostics.[2–6] According to numerous reports, the negative test results of samples taken from seriously ill patients with clinically diagnosed infections unfortunately occur frequently, and account for as much as 80% of all samples in the case of blood cultures.[2–4] Thus, for neutropenic patients with negative microbiological results of diagnostically relevant materials such as blood, it is important to identify the colonizing flora. Knowledge of the particular flora's drug resistance profile may be significant in enhancing the effectiveness of the therapy.[1] In the case of neutropenic patients, there is a high risk of translocating endogenous flora from physiological sites to sterile areas. The aim of this paper was to present the local frequency of isolation and drug susceptibility of strains isolated in the period 2011–2014 from the blood of neutropenic children and to compare the susceptibility of blood isolates with the results for the colonizing flora and for strains isolated from all materials together. The aim of this study was also to specify the optimal options for empirical therapy in our center, based on the results of the susceptibility of blood-borne strains, and to estimate the suitability of antibiogram tests for colonizing flora in selecting the most probable active antibiotics to treat infections in children with hematological diseases who had negative test results of diagnostically relevant samples.

Material and methods

The analysis included the results of microbiological tests of patients hospitalized in the oncohematological wards of the Chair and Clinic of Pediatric Oncology, Hematology, and Bone Marrow Transplantation in Wrocław from 2011 to 2014. Children subjected to bone marrow stem cell transplantation were excluded from the study. The majority of the children studied had acute leukemia (60%) with a predominance of acute lymphoblastic leukemia and lymphomas, particularly non-Hodgkin's lymphoma (15–20%). Other markings were performed in patients with solid tumors, among which neuroblastoma, rhabdomyosarcoma, and Ewing's sarcoma prevailed. The samples for microbial diagnosis included in this research were collected in cases of suspected infections. In total, microbiological tests were conducted on 50,407 various clinical samples, including 11,468 in 2011, 12,234 in 2012, 13,762 in 2013, and 12,943 in 2014. The largest proportion of analyzed materials in the years 2011, 2012, 2013, and 2014 were as follows: feces samples (24%, 21%, 23%, and 23%, respectively), samples from the upper respiratory tract (24%, 23%, 23%, and 23%, respectively), blood (22%, 21%, 18%, and 20%, respectively) and urine (16%, 15%, 15%, and 16%, respectively). The samples included in the research were collected in cases of suspected infections only. Microbiological diagnostics was performed at the Specialist Microbiological Laboratory of the Wroclaw Medical University Foundation. The blood cultures were processed in a Bactec 9120 (BD) using BD Bactec Peds Plus/F or BD Bactec Plus Aerobic/F and BD BactecPlus Anaerobic/F (Becton Dickinson Life Science-Diagnostic Systems). At least 2 blood samples were collected from each patient. The strains were identified using a manual system – BBL Crystal (BD) – or an automatic system – VITEK 2 (bioMerieux S.A., Marcy L'Etoile, France). The assessment of drug susceptibility and resistance mechanisms was performed in accordance with the recommendations in force during the given year, of either the Clinical and Laboratory Standards Institute (CLSI) (for the period January 1, 2011 to April 30, 2011) or of the European Committee on Antimicrobial Susceptibility Testing (EUCAST) (May 1, 2011–December 31, 2014), as well as the recommendations of the National Reference Center for Antibiotic Resistance and Surveillance (KORLD).[7–9] Depending on the above-mentioned recommendations, susceptibility was tested by means of the disc diffusion method, the automatic VITEK system, and the quantitative method, using bands saturated with an antibiotic within the concentration gradient (E-tests, bioMerieux S.A., Marcy L'Etoile, France). We analyzed the positive test results of the various studied materials from 2011 to 2014 and measured the frequency of isolation of individual types of bacteria broken down into Gram-positive and Gram-negative strains. Also, drug susceptibility testing was carried out for the strains isolated in 2014 from all materials together and for only colonizing bacterial strains isolated primarily from stools and from the upper respiratory tract. A detailed assessment of the type of isolated bacteria and their susceptibility to antimicrobial agents was also conducted for the strains isolated from positive blood cultures, taking into account the dynamics of changes from year to year. In cases of repeated isolations from a single patient of the same bacteria with the same susceptibility profile, the relevant susceptibility analysis included the result for a single strain only. Coagulase-negative staphylococci were regarded as the etiological factor of bacteremia when they was isolated from at least 2 blood samples. The data was statistically analyzed with the use of STATISTICA 12.0 packages (StatSoft), in particular the significance test for the difference between 2 indices of structure (Significant Difference Test). Values of $p < 0.05$ were regarded as statistically significant.

Results

Positive microbiological test results constituted a small percentage of the total number of samples collected from patients, with the majority being negative (Table 1). A particularly high percentage of negative results was obtained from blood cultures (from 86% in 2011 to as much as 91% in 2014). The number of strains from various positive samples cultured in 2011 was 1,629; in 2012, there were 2,286; in 2013 there were 2,225; and in 2014 there were 1,831 strains. Gram-positive bacteria were the predominant type in all 4 years (Table 2). A statistically significant increase in the frequency of isolation of Gram-positive bacteria was found in 2012 and 2013 compared to 2011. Coagulase-negative *Staphylococcus* (CNS) was decidedly the predominant group of bacteria. Gram-negative bacteria were isolated less frequently; the differences in the frequency of isolation in individual years were statistically significant only in 2012 ($p = 0.0173$). Among Gram-negative strains isolated from blood, the most frequent were *Klebsiella* spp. (6–11%) and *E. coli* (1–11%). Non-fermentative rods were isolated less frequently. The susceptibility test results of the strains isolated from blood (Table 3) show that regardless of the year, CNS strains were most susceptible to linezolid and vancomycin (96–100%) and to teicoplanin (82–96%), with MRCNS (methicillin-resistant CNS) accounting for 77–86%. They were least susceptible to macrolides and, additionally, a statistically significant drop in susceptibility to these drugs was observed, from 31% in 2011 to 4% in 2014 ($p = 0.0001$). The drug susceptibility of *S. aureus* and *Enterococcus* spp. is difficult to assess due to the low occurrence of this strain. However, it was found that all *S. aureus* strains were susceptible to glycopeptides, and linezolid and *Enterococcus* spp. were susceptible to linezolid. Additionally, 100% of the enterococci isolated in 2013 and 2014 were susceptible to glycopeptides. Apart from the year 2014 ($p = 0.0013$), MRSA strains (methicillin-resistant *S. aureus*) were not isolated. The susceptibility of Gram-negative bacilli isolated from blood is presented in Table 4. All of the Enterobacteriaceae strains (100%)

Table 1. The ratio of negative results of microbiological culture over 4 years

Year	Examined samples							
	all		blood		urine		from lower respiratory tract	
	n	negative results, n (%)	n	negative results, n (%)	n	negative results, n (%)	n	negative results, n (%)
2011	11,468	6666 (58)	2500	2146 (86)	986	508 (52)	49	10 (20)
2012	12,234	8372 (68)	2568	2268 (88)	1000	510 (51)	24	9 (38)
2013	13,762	8980 (65)	2526	2283 (90)	1095	602 (55)	33	8 (24)
2014	12,943	9180 (71)	2565	2333 (91)	1108	514 (46)	21	6 (29)

Table 2. Frequency of isolation of bacterial strains from blood

Year	2011		2012		2013		2014	
Bacterial strains	n	%	n	%	n	%	n	%
Gram-positive	167[A]	60	196[B]	70	155[C]	67	140[D]	63
CNS	113	41	132	47	107	47	105	47
Enterococcus spp.	28	10	15	5	10	4	6	3
S. aureus	3	1	19	7	5	2	16	7
Steptococcus orale gr.	16	6	12	4	11	5	12	5
other Gram-positive	7	2	18	6	22	9	1	<1
Gram-negative	112[E]	40	86[F]	30	78[G]	33	82[H]	37
Enterobacteriaceae	73	26	49	17	56	24	58	26
E. coli	17	6	30	11	15	6	21	9
Klebsiella spp.	30	11	4	1	16	7	16	7
Enterobacter spp.	10	4	15	5	9	4	15	7
other Enterobacteriaceae	16	5	0	0	16	7	6	3
Non-fermentative rods	39	14	37	13	22	9	24	11
Acinetobacter spp.	10	4	25	9	8	3	4	2
Pseudomonas aeruginosa	14	5	10	4	14	6	12	5
other non-fermentative rods	15	5	2	<1	0	0	8	4
Total	279	100	282	100	233	100	222	100

CNS – coagulase-negative *Staphylococcus*; n – number of isolated strains; $p < 0.05$ ($^{B/A}$ $p = 0.009$, $^{C/A}$ $p = 0.0145$, $^{F/E}$ $p = 0.0173$); $p > 0.05$ ($^{D/A}$, $^{G/E}$, $^{H/E}$).

Table 3. Drug susceptibility patterns of Gram-positive bacterial strains isolated from blood from children in the oncohematological ward

Gram-positive bacterial strains	2011[A]		2012		2013		2014[B]		p B/A
	n	%	n	%	n	%	n	%	
Coagulase-negative *Staphycococcus*									
Cefoxitin	93	23	94	18	97	14	87	18	ns
Erythromycin	36	31	79	24	94	9	72	4	0.0001
Clindamycin	35	63	77	47	91	52	72	36	0.0089
Gentamicin	81	44	94	43	97	52	87	53	ns
Co-trimoxazole	91	23	91	13	97	20	86	19	ns
Doxycycline	77	65	89	76	96	71	86	58	ns
Vancomycin	91	100	94	100	95	96	85	100	ns
Teicoplanin	93	87	93	82	93	95	85	96	0.024
Linezolid	91	100	93	98	95	96	87	100	ns
S. aureus									
Cefoxitin	3	100	10	100	4	100	12	92	0.0013
Erythromycin	3	67	9	56	4	100	10	80	ns
Clindamycin	3	67	9	67	4	100	10	90	ns
Gentamicin	3	67	10	90	4	100	12	92	ns
Co-trimoxazole	3	100	10	80	4	100	11	100	ns
Doxycycline	2	100	10	90	4	100	12	100	ns
Vancomycin	3	100	10	100	4	100	12	100	ns
Teicoplanin	3	100	9	100	4	100	11	100	ns
Linezolid	3	100	10	100	4	100	12	100	ns
Enterococcus spp.									
Ampicillin	18	11	11	64	6	16	6	0	ns
Gentamicin high concent	10	70	11	73	8	88	6	33	ns
Streptomycin high concent	11	82	11	45	8	50	6	33	0.0456
Vancomycin	17	82	11	55	8	100	6	100	ns
Teicoplanin	18	100	11	64	8	100	6	100	ns
Linezolid	18	100	11	100	8	100	6	100	ns

p B/A - significance test result for the difference in antibiotic susceptibility between 2014 (B) and 2011 (A); n – number examined; % – percent of susceptibility; ns – not statistically significant.

were susceptible to imipenem and meropenem, apart from the year 2014 (with 9% resistant strains) ($p > 0.05$). Susceptibility to ertapenem was lower and it stood at 80% in 2014 ($p > 0.05$). Apart from carbapenems, intestinal rods were most susceptible to amikacin (77–93%). The non-fermentative rods isolated in 2013 and 2014 were less susceptible to imipenem and meropenem, at 71% for both antibiotics in 2013, and 67% and 71%, respectively, in 2014. The decrease in susceptibility to carbapenems was statistically significant in 2014 ($p = 0.0307$).

The study also included a comparison of the drug susceptibility of strains isolated from blood with those reported as a colonizing flora and with bacterial strains isolated from all the materials together. It was found that compared to the total number of investigated strains and to those isolated as colonizing flora, CNS isolated from blood were nearly twice as frequently resistant ($p < 0.05$) to cefoxitin (MRCNS). The same strains were also statistically significantly more susceptible to gentamicin in comparison to colonizing bacteria (Fig. 1). Furthermore, Enterobacteriaceae isolated from blood were more frequently resistant to antimicrobials than the other 2 compared groups. They were especially statistically significantly resistant to carbapenems and ceftazidime (Fig. 2). Different data were obtained for Gram-negative non-fermenters (NF), a statistically significant higher percentage of which was susceptible to half of the analyzed antibiotics (piperacillin/tazobactam, ceftazidime, cefepime, doripenem, gentamicin, and ciprofloxacin) among blood isolates in comparison with the colonizing strains (Fig. 3). Gram-negative non-fermenters were more resistant only to imipenem, but the differences were not statistically significant ($p = 0.0721$). Table 5 presents the frequency of isolation of bacteria with specified resistance phenotypes. These data also confirm that the blood-borne staphylococci, enterococci, and Enterobacteriaceae were resistant to methicillin and to high concentrations of aminoglycosides and that they produced extended-spectrum beta-lactamases (ESBL) more often than the bacteria isolated from all materials.

Table 4. Drug susceptibility patterns of Gram-negative bacterial strains isolated from blood from children in the oncohematological ward

Gram-negative bacterial strains	2011[A]		2012		2013		2014[B]		p B/A
	n	%	n	%	n	%	n	%	
Enterobacteriaceae									
Piperacillin/tazobactam	35	69	27	70	48	85	45	62	ns
Cefotaxime	35	71	27	81	48	79	44	55	ns
Ceftazidime	35	71	27	85	48	79	44	55	ns
Cefepime	32	75	27	89	48	85	45	67	ns
Aztreonam	32	69	27	89	48	81	39	51	ns
Imipenem	36	100	27	100	48	100	45	91	ns
Meropenem	36	100	27	100	48	100	45	91	ns
Doripenem	35	94	27	100	48	100	42	90	ns
Ertapenem	35	91	27	100	48	100	45	80	ns
Gentamicin	36	64	27	74	48	77	45	62	ns
Amikacin	36	83	27	93	48	79	45	77	ns
Tobramycin	22	47	20	70	48	71	45	68	ns
Co-trimoxazole	35	37	27	26	48	56	45	18	ns
Ciprofloxacin	32	50	27	59	48	79	45	60	ns
Colistin	6	100	0	0	0	0	17	100	ns
Non-fermentative rods									
Piperacillin/tazobactam	8	100	6	100	14	71	13	85	ns
Ceftazidime	8	75	7	86	14	86	14	93	ns
Cefepime	4	100	7	86	13	100	14	93	ns
Aztreonam	7	86	5	40	15	33	7	29	0.0309
Imipenem	14	100	10	70	21	71	14	71	0.0307
Meropenem	14	100	10	80	21`	67	14	71	0.0307
Doripenem	11	100	10	80	21	71	12	100	ns
Gentamicin	14	86	10	70	21	100	14	100	ns
Amikacin	14	86	10	70	21	90	14	93	ns
Tobramycin	12	83	10	70	21	86	14	100	ns
Ciprofloxacin	13	85	10	60	21	86	14	100	ns
Colistin	3	100	3	100	4	25	7	100	ns

p B/A - significance test result for the difference in antibiotic susceptibility between 2014 (B) and 2011 (A); n – number examined; % – percent of susceptibility; ns – not statistically significant.

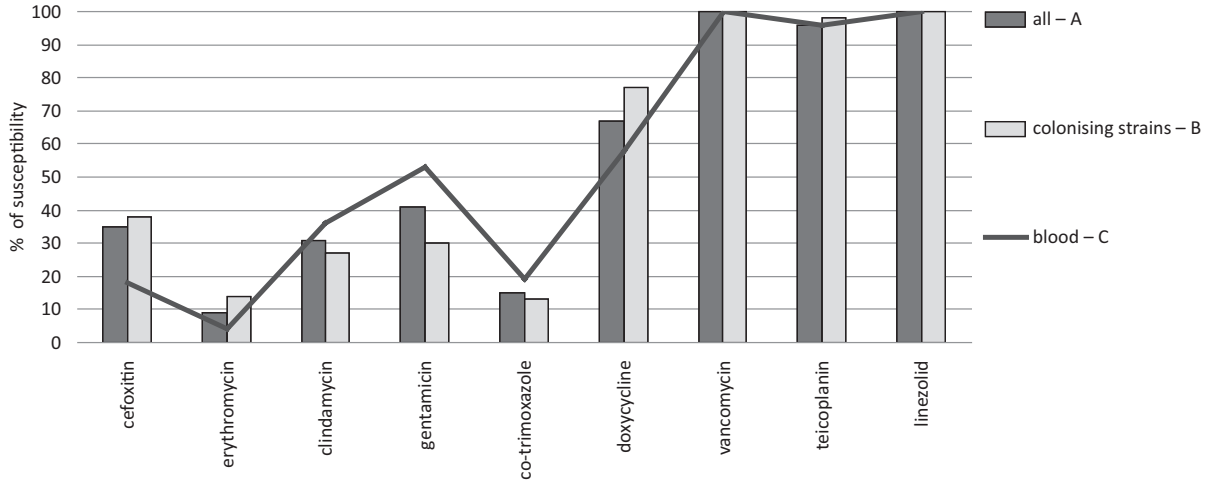

Fig. 1. Comparison of antibiotic susceptibility (%) of CNS strains isolated from blood, from all materials and for colonising strains in 2014

C/A $p < 0.05$ for cefoxitin ($p = 0.0024$); C/A for other antibiotics $p > 0.05$; C/B $p < 0.05$ for cefoxitin ($p = 0.007$), erythromycin ($p = 0.0434$), gentamicin ($p = 0.0037$), doxycycline ($p = 0.0093$); C/B for other antibiotics $p > 0.05$.

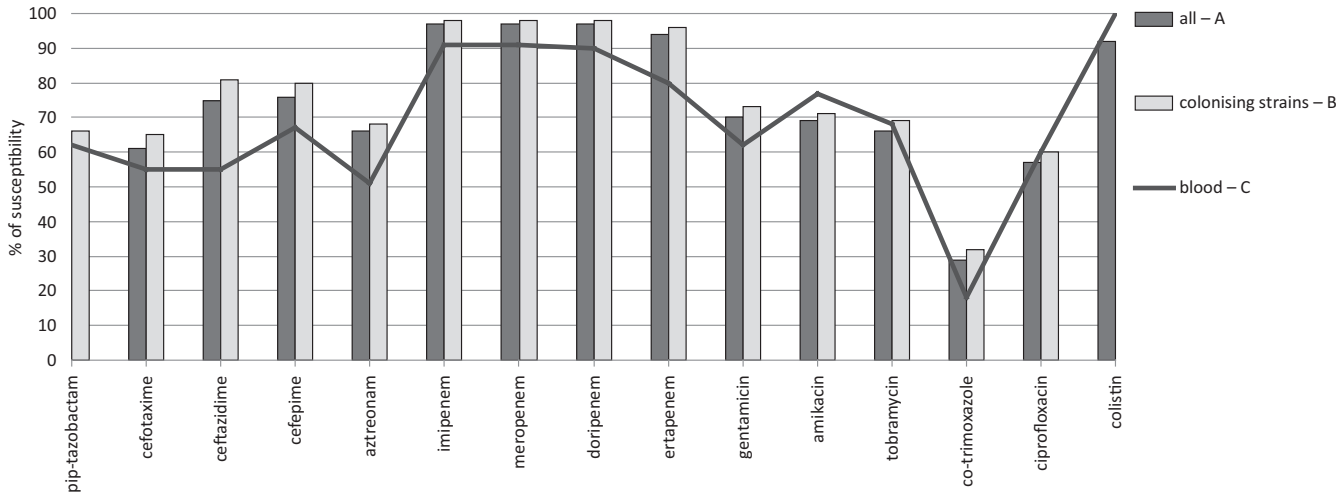

Fig. 2. Comparison of antibiotic susceptibility (%) of Enterobacteriaceae strains isolated from blood, from all materials and for colonising strains in 2014

C/A $p < 0.05$ for ceftazidime ($p = 0.021$), imipenem ($p = 0.0162$), meropenem ($p = 0.0164$), doripenem ($p = 0.0086$), ertapenem ($p = 0.0001$), for other C/A $p > 0.05$; C/B $p < 0.05$ for ceftazidime ($p = 0$), cefepime ($p = 0.0272$), aztreonam ($p = 0.0276$), imipenem ($p = 0.0006$), meropenem ($p = 0.0041$), doripenem ($p = 0.0005$), ertapenem ($p = 0$), co-trimoxazole ($p = 0.0439$), for other C/B $p > 0.05$.

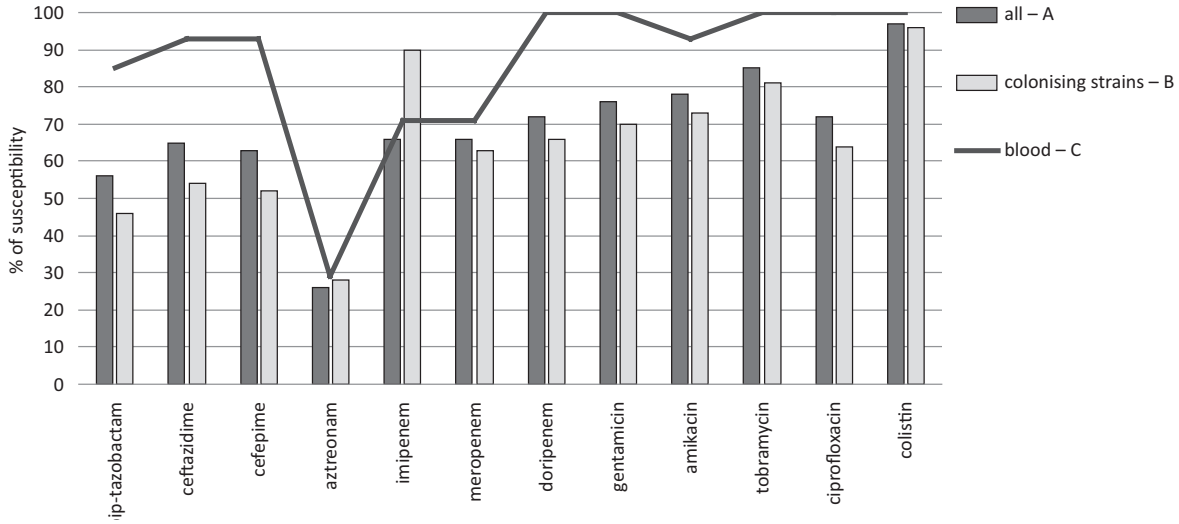

Fig. 3. Comparison of antibiotic susceptibility (%) of non-fermentative rods isolated from blood, from all materials and for colonising strains in 2014

C/A $p < 0.05$ for ceftazidime ($p = 0.0398$), cefepime ($p = 0.0317$), doripenem ($p = 0.0341$), gentamicin ($p = 0.0422$), for other C/A $p > 0.05$; C/B $p < 0.05$ for piperacillin/tazobactam ($p = 0.0129$), ceftazidime ($p = 0.0087$), cefepime ($p = 0.0061$), doripenem ($p = 0.0162$), gentamicin ($p = 0.0173$), ciprofloxacin ($p = 0.0082$), for other C/B $p > 0.05$.

Discussion

Blood is the most valuable material for the purposes of microbiological diagnosis of infections in hematological patients. It plays a significant role not only in the diagnosis of sepsis, but also in organ infections, where the bacteria enter the bloodstream in the majority of cases. At the same time, it becomes challenging to determine the location of the infection due to neutropenia and the lack of evident clinical symptoms. Unfortunately, blood is also one of the most difficult materials to culture microorganisms in, especially in patients who previously received antibiotic prophylaxis.[1,10] Numerous studies confirm the difficulties encountered in blood diagnostics and suggest that positive results of blood cultures may be obtained in only 11–30% of cases.[10–14] During our own studies conducted over a period of 4 years, we had an average of 11% of positive blood cultures. Such a small percentage of positive cultures may be due to a number of factors, including blood collection coinciding with antibiotic treatment and non-compliance with the procedures concerning blood collection for culture.[5] It also shows the need to actively monitor microbiological diagnostic procedures, especially of mistakes relating to collecting blood for culture from oncohematological pediatric patients. Another reason for the reduced frequency of isolating bacteria from blood is the fact that microbiological tests are performed in all febrile neutropenic patients. Although bacterial infections are responsible for a large number of febrile episodes in this group of patients, in some of them their cause is different, for example, a neoplastic disease, chemotherapy, blood product transfusion, or a viral or fungal infection. The low

Table 5. Mechanism of resistance of strains identified in 2014

Phenotyp of resistance	Frequency of isolation									
	all materials		blood		urine		from lower respiratory tract		colonising flora*	
	N	n/%	N	n/%	N	n/%	N	n/%	N	n/%
Gram-positive										
Staphylococcus spp.										
MRSA	35	2/6	16	2/13	1	0	0	0	18	0
MRCNS	451	293/65	87	71/82	109	84/77	2	0	187	144/62
Enterococcus spp.										
HLAR	1512	941/62	6	4/67	235	20/9	2	0	1265	917/72
VRE or GRE	1501	283/19	6	0	235	20/9	2	0	1265	263/19
Gram-negative										
Enterobacteriaceae										
ESBL	1080	195/18	45	19/42	149	32/22	3	3/100	878	141/16
MBL	1080	6/<1	45	0	149	1/<1	3	0	878	5/<1
P. aeruginosa										
MBL	30	7/23	12	0	3	0	2	0	22	7/32

* mainly strains from stools and the upper respiratory tract; N – number of examined strains; n – number of strains with a particular mechanism of resistance; % – percent of resistance; MRSA – methicillin-resistant *Staphylococcus aureus*; MRCNS – methicillin-resistant coagulase-negative *Staphylococcus;* HLAR – high-level aminoglycoside resistance; VRE – vancomycin-resistant *Enterococcus*, GRE – glycopeptide-resistant *Enterococcus;* ESBL – extended spectrum beta-lactamases; MBL – metallo-beta-lactamases.

detection rates of bacteria in blood as well as the risk of a fast-developing infection from a previous colonization are 2 reasons why in oncohematological neutropenic patients, colonizing bacteria from stools or from the upper respiratory tract are more frequently diagnosed microbiologically than in other patients. The results of the above tests are valuable as they allow us to monitor multi-resistance.[1,15] In the case of oncohematological patients, knowledge about the resistance profile of the colonizing flora can be used in the selection of an adequate antibiotic therapy at the time of onset of the infection and before test results become available.[5,16] Additionally, it can serve as valuable information for Nosocomial Infection Surveillance Teams, which, in the case of isolating alert pathogens, can initiate efforts to prevent the relevant strains from spreading further. Multi-resistance increases the virulence potential of pathogens and is the reason why such strains are more frequently found in invasive infections. This process also reduces the chances for effective treatment.[1] This claim was confirmed by the results of our research, where both MRCNS strains and ESBL-positive Enterobacteriaceae and *Enterococcus* with the HLAR phenotype were more frequently isolated from blood than from other materials. On the other hand, the fact that CNS strains and Enterobacteriaceae isolated from blood showed a higher resistance to antibiotics than the colonizing flora may indicate an exogenous origin of the bacterial strains; however, this supposition cannot be proven due to a lack of genetic studies. Future introduction of genetic studies which would examine the similarities between strains isolated from the blood and colonizing flora could help assess the usefulness of monitoring the susceptibility of colonizing flora when selecting effective treatment options at the time of infection. In accordance with the data presented by Mikulska et al., the percentage of strains isolated from the blood of hematological pediatric patients was smaller than in our research, which for MRSA was from 0 to 26%, for MRCNS was 38–39%, and for ESBL was 18%.[17] According to Mikulska et al., the significantly higher percentage of resistant strains found in our study (the 82% of MRCNS and the 42% of ESBL, in particular) is more characteristic of adult patients.[17] However, data presented by other authors, including Al-Mulla et al. from Qatar confirm a high percentage of MRCNS strains (from 78% to 100%).[18] Similar data were reported by Lv et al. from China showing 73–100% of MRCNS strains.[19] In general, literature data most often show the prevalence of Gram-positive over Gram-negative bacteria among blood isolates,[17,20–23] which is in line with the results of our own research conducted from 2011 to 2014 (63–70% vs 30–40%). The previous study from 2001–2002 from the same clinic showed a greater number of Gram-negative than Gram-positive bacteria (56% vs 44%) isolated from blood.[20] Currently, there are reports indicating the predominance of Gram-negative microorganisms.[11,12,17,24] Mikulska et al. noted a predominance of Enterobacteriaceae in 5 out of the 12 analyzed research studies.[17] On the basis of reports from various centers, she also noted the growing role of *Enterococcus* spp. and Enterobacteriaceae and the decreasing role of *P. aeruginosa*. No similar tendency was observed in our study. On the contrary, the percentage of isolation of enterococci in 2014 declined by 7% in comparison with 2011 and no differences were found in the consecutive years of the study with respect to other types of bacteria. Despite the fact that CNS strains are predominant among blood isolates, they do not pose such a threat to patients' lives as

Enterobacteriaceae or non-fermenters. They have at their disposal not only a huge arsenal of various virulence factors, but also the ability to develop resistance to the majority of antibiotics.[24] In accordance with American recommendations regarding the protocol in cases of neutropenic fever in oncological pediatric patients and/or patients subjected to transplantations of hematopoietic stem cells, given the high risk of infectious complications, initial empirical therapy should account for the administration of an antibiotic active against Gram-negative bacilli, including *P. aeruginosa.*[5] Among the antibiotics recommended in monotherapy are piperacillin/tazobactam, ticarcillin/clavulanic acid, cefepim, ceftazidime and meropenem, or imipenem.[5] The choice of an antibiotic is better when it is based on knowledge of the local epidemiological situation. Thus, it seems that – in line with our microbiological analysis of local epidemiological situation – our pediatric ward might use piperacillin/tazobactam or cefepime (which additionally would be a carbapenem-saving strategy) for the initial therapy. For patients suffering from acute myeloid leukemia with no symptoms of infection but with a high risk of infection complications, oral chemoprophylaxis with the use of fluoroquinolone may be the recommended option.[1] Although fluoroquinolones have been reported as an important option in the prevention of infection, there are a number of controversies associated with this group.[1,25,26] On the one hand, there are reports confirming the role of antibiotic prophylaxis in reducing the risk of infection with Gram-negative bacilli; on the other hand, growing levels of resistance to fluoroquinolones have unfortunately been reported.[25–28] However, in our research no negative changes in the susceptibility to ciprofloxacin were observed among the Gram-negative bacilli isolated from blood. Nevertheless, in comparison with the results of studies conducted from 2001 to 2002 at the same center, there has been a visible increase (by 20%) in resistance to fluoroquinolones.[20] The susceptibility of Gram-negative bacilli to other antibiotics was varied. In 2014, apart from carbapenems and colistin, Enterobacteriaceae strains remained most susceptible to amikacin (77%), but there has been an increase in resistance to this antibiotic as well. Fewer strains were susceptible to gentamicin and tobramycin. However, in 2014 there were as many as 21% more strains susceptible to tobramycin than in 2011. In their study of pediatric patients, Aslan et al. reported that only 7.7% of *E. coli* were susceptible to amikacin and 69.2% were susceptible to gentamicin, while Lv et al. reported 91.7% and 16.7%, respectively.[19,29] In our own research, tobramycin was 100% active in vitro against non-fermenters and, additionally, 7% more active than amikacin. Thus, it may serve as an alternative to amikacin, which is generally used in combined therapy, especially against such strains as *P. aeruginosa.* Lv et al. reported that more strains were susceptible to gentamicin than to amikacin among *P. aeruginosa.*[19] In general, however, susceptibility to individual aminoglycoside agents is very diversified across the centers conducting the studies, which was clearly demonstrated by Trecarichi and Tumbarello.[30]

In summary, our study included only one center, so the achieved results and conclusions may have some limitations and may reflect only local trends. Over the 4 years of our research, a growing drug resistance was observed among the Enterobacteriaceae bacilli, with no such trend among non-fermenters. However, in the case of the latter ones, many more strains have been observed to be resistant to carbapenems than to other studied antibiotics. The problem of growing drug resistance among nosocomial strains is also reflected by the isolation from blood of a methicillin-resistant *S. aureus* strain for the 1st time in 2014. The results of the sensitivity of Gram-negative bacteria from blood indicate that, apart from carbapenems, the strains were most susceptible to piperacillin/tazobactam, cefepime, and aminoglycosides. In our Wrocław center, it has also been shown that CNS and Enterobacteriaceae strains isolated from blood were statistically significantly less susceptible to antibiotics than colonizing flora.

Conclusions

Our results show that the choice of appropriate antibiotics for the treatment of infections in children from the studied hematological ward based on antibiograms for colonizing flora may be difficult because there is a risk that the antibiograms do not take into account the more resistant strains. According to the antibiotic susceptibility of the examined strains isolated from blood, the most probable active empirical and carbapenem-saving therapy could be conducted with piperacillin/tazobactam or cefepime.

References

1. Gustinetti G, Mikulska M. Bloodstream infections in neutropenic cancer patients: A practical update. *Virulence*. 2016;7(3):280–297. doi: 10.1080/21505594.2016.1156821
2. Skovbjerg S, Welinder-Olsson C, Kondori N, et al. Optimization of the detection of microbes in blood from immunocompromised patients with haematological malignancies. *Clin Microbiol Infect*. 2009;15(7): 680–683.
3. Xu J, Moore JE, Millar BC, et al. Improved laboratory diagnosis of bacterial and fungal infections in patients with hematological malignancies using PCR and ribosomal RNA sequence analysis. *Leuk Lymphoma*. 2004;45:1637–1641.
4. Mancini N, Clerici D, Diotti R, et al. Molecular diagnosis of sepsis in neutropenic patients with haematological malignancies. *J Med Microbiol*. 2008;57:601–604.
5. Lehrnbecher T, Phillips R, Alexander S, et al. Guideline for the management of fever and neutropenia in children with cancer and/or undergoing hematopoietic stem-cell transplantation. *J Clin Oncol*. 2012;30(35):4427–4438.
6. Oliver JD. Recent findings on the viable but nonculturable state in pathogenic bacteria. *FEMS Microbiol Rev*. 2010;34(4):415–425. doi: 10.1111/j.1574-6976.2009.00200
7. Clinical and Laboratory Standards Institute. Performance Standards for Antimicrobial Susceptibility Testing. CLSI ; Twenty-First Informational Supplement. CLSI document M100-S21. Clinical and Laboratory Standards Institute, Wayne, PA, 2011.

8. The European Committee on Antimicrobial Susceptibility Testing – EUCAST. Clinical breakpoints v. 1.3, v.2, v.3.1, v.4. http://www.eucast.org/ast_of_bacteria/previous_versions_of_documents/. Accessed January 6, 2014.
9. Krajowy Ośrodek Referencyjny ds. Lekowrażliwości Drobnoustrojów – KORLD. http://www.korld.edu.pl/spec_rekomendacje.php. Accessed April 10, 2013.
10. Gaytán-Martínez J, Mateos-García E, Sánchez-Cortés E, González-Llaven J, Casanova-Cardiel LJ, Fuentes-Allen JL. Microbiological findings in febrile neutropenia. *Arch Med Res*. 2000;31:388–392.
11. Asturias EJ, Corral JE, Quezada J. Evaluation of six risk factors for the development of bacteremia in children with cancer and febrile neutropenia. *Curr Oncol*. 2010;17(2):59–63.
12. Greenberg D, Moser A, Yagupsky P, et al. Microbiological spectrum and susceptibility patterns of pathogens causing bacteraemia in paediatric febrile neutropenic oncology patients: comparison between two consecutive time periods with use of different antibiotic treatment protocols. *Int J Antimicrob Agents*. 2005;25:469–473.
13. Duncan C, Chisholm JC, Freeman S, Riley U, Sharland M, Pritchard-Jones K. A prospective study of admissions for febrile neutropenia in secondary paediatric units in South East England. *Pediatr Blood Cancer*. 2007;49:678–681.
14. Koivula I, Hämäläinen S, Jantunen E, et al. Elevated procalcitonin predicts Gram-negative sepsis in haematological patients with febrile neutropenia. *Scand J Infect Dis*. 2011;43(6–7):471–478. doi: 10.3109/00365548.2011.554855
15. Carlet J. The gut is the epicentre of antibiotic resistance. *Antimicrob Resist Infect Control*. 2012;1(1):1–7.
16. Szmyd K, Wróbel G, Węcławek-Tompol J, Wójcik D, Dobaczewski G, Chybicka A. Czynniki ryzyka wystąpienia zakażenia krwi u dzieci z upośledzoną odpornością. *Adv Clin Exp Med*. 2004;13(4):575–580.
17. Mikulska M, Viscoli C, Orasch C, et al. Aetiology and resistance in bacteraemias among adult and paediatric haematology and cancer patients. *J Infect*. 2014;68(4):321–331.
18. Al-Mulla NA, Taj-Aldeen SJ, El Shafie S, Janahi M, Al-Nasser AA, Chandra P. Bacterial bloodstream infections and antimicrobial susceptibility pattern in pediatric hematology/oncology patients after anticancer chemotherapy. *Infect Drug Resist*. 2014;7:289–299.
19. Lv H, Ning BT, Wu XY, et al. Clinical features of bloodstream infection in children with haematological malignancies. *Hong Kong J Paediatr*. 2013;18(1):12–18.
20. Kowalska-Krochmal B, Dolna I, Ruczkowska J, et al. Częstość izolacji i wrażliwość na antybiotyki bakterii od dzieci z oddziału hematologii (Wrocław, 1999–2000 vs 2001–2002). *Adv Clin Exp Med*. 2004;13(2):215–226.
21. Castagnola E, Rossi MR, Cesaro S, et al. Incidence of bacteremias and invasive mycoses in children with acute non-lymphoblastic leukemia: Results from a multi-center Italian study. *Pediatr Blood Cancer*. 2010;55:1103–1107.
22. Simon A, Ammann RA, Bode U, et al. Healthcare-associated infections in pediatric cancer patients: Results of a prospective surveillance study from university hospitals in Germany and Switzerland. *BMC Infect Dis*. 2008;8:70–79.
23. Nørgaard M. Risk of infections in adult patients with haematological malignancies. *Open Infect Dis J*. 2012;6(1):46–51.
24. Gedik H, Şimşek F, Yıldırmak T, et al. Which multidrug resitant bacteria are emerging in patients with hematological malignancies?: One-Year Report. *Indian J Hematol Blood Transfus*. 2015;31(1):51–56.
25. Villafuerte-Gutierrez P, Villalon L, Losa JE, Henriquez-Camacho C. Treatment of febrile neutropenia and prophylaxis in hematologic malignancies: A critical review and update. *Adv Hematol*. 2014. http://dx.doi.org/10.1155/2014/986938
26. Freifeld AG, Bow EJ, Sepkowitz KA, et al. Clinical practice guideline for the use of antimicrobial agents in neutropenic patients with cancer: 2010 Update by the Infectious Diseases Society of America. *Clin Infect Dis*. 2011;52:427–431.
27. Bucaneve G, Micozzi A, Menichetti F, et al. Levofloxacin to prevent bacterial infection in patients with cancer and neutropenia. *N Engl J Med*. 2005;353:977–987.
28. Kern WV, Klose K, Jellen-Ritter AS, et al. Fluoroquinolone resistance of *Escherichia coli* at a cancer center: Epidemiologic evolution effects of discontinuing prophylactic fluoroquinolone use in neutropenic patients with leukemia. *Eur J Clin Microbiol Infect Dis*. 2005;24:111–118.
29. Aslan S, Citak EC, Yis R, Degirmenci S, Arman D. Bacterial spectrum and antimicrobial susceptibility pattern of bloodstream infections in children with febrile neutropenia: Experience of single center in southeast of Turkey. *Indian J Microbiol*. 2012;52(2):203–208.
30. Trecarichi EM, Tumbarello M. Antimicrobial-resistant Gram-negative bacteria in febrile neutropenic patients with cancer: Current epidemiology and clinical impact. *Curr Opin Infect Dis*. 2014;27(2):200–210.

Perioperative standards for the treatment of coagulation disorders and usage of blood products in patients undergoing liver transplantation used in the Clinic for Transplant Surgery in Wrocław

Marceli K. Łukaszewski[1,A–E], Paweł Chudoba[2,A,C,E], Agnieszka Lepiesza[2,B], Marcin Rychter[2,B], Piotr Szyber[2,E,F]

[1] Department of Anesthesiology and Intensive Therapy, Wroclaw Medical University, Poland
[2] Department of Vascular, General and Transplantation Surgery, Wroclaw Medical University, Poland

A – research concept and design; B – collection and/or assembly of data; C – data analysis and interpretation;
D – writing the article; E – critical revision of the article; F – final approval of the article

Advances in Clinical and Experimental Medicine, ISSN 1899-5276 (print), ISSN 2451-2680 (online) *Adv Clin Exp Med*. 2018;27(9):1211–1215

Address for correspondence
Marceli K. Łukaszewski
E-mail: marceliluk@gmail.com

Funding sources
None declared

Conflict of interest
None declared

Received on May 17, 2016
Reviewed on June 6, 2016
Accepted on March 9, 2017

Abstract

Background. Coagulation system disorders in liver transplantation (ltx) patients are considered a serious issue. Liver cirrhosis leads to decreased synthesis of clotting factors and decreased elimination of waste products, including coagulation proteins. Platelet sequestration and dysfunction in an enlarged spleen additionally worsen these conditions. The resulting state, the most common pathology of the coagulation system, involves the reduction of clotting potential and hyperfibrinolysis.

Objectives. Tackling the problem of impaired hemostasis is a dynamic process. Throughout the whole procedure, consisting of the preanhepatic, the anhepatic and the neohepatic phases, consecutive pathomechanisms disrupt the very balance that anesthesia aims to preserve.

Material and methods. Rotational thromboelastometry (ROTEM), having been introduced in the Clinic of Anesthesiology and Intensive Therapy, Wroclaw Medical University, Poland, enables the efficient and early diagnosis of clotting disorders. An additional major problem which occurs during ltx, namely blood loss, could be solved using a cell separator.

Results. In this study, we present the standards introduced to the Transplantology Department of the Vascular Surgery Clinic, Wroclaw Medical University, Poland, that describe blood treatment during ltx procedures.

Conclusions. We conclude that thromboelastometric examination and the use of a cell separator have significantly increased the safety of ltx procedures at our clinic. The introduction of thromboelastometry (TEM) and the implementation of the cell separator recovery method have enabled us to perform the dangerous and complicated surgical procedure of ltx in a much more stable and much safer manner than in the past.

Key words: point of care, thromboelastometry, cell separator, liver transplantation

DOI
10.17219/acem/69398

Introduction

Liver cirrhosis is a disease which leads to disruptions in the functioning of many organs and systems. Liver dysfunction leads to impaired metabolic and endocrine pathways in the body, causes disorders in blood coagulation, and impairs the cardiovascular, renal and pulmonary systems. In the coagulation system specifically, cirrhosis manifests itself through decreased synthesis and an impaired removal of functional proteins.[1]

The reduced synthesis of fibrinolytic inhibitors and a simultaneous extenuation of reticuloendothelial clearance leads to increased fibrinolysis, which is especially amplified in the anhepatic phase of liver transplantation (ltx). Portal hypertension and blood drainage through the spleen promote platelet sequestration and induce thrombocytopenia and an abnormal functioning of platelets.

During surgery, the abovementioned disorders are exacerbated by a loss of blood. Supplementation of blood with neutral fluids leads to dilutional coagulopathy. Heparinoids released during the neohepatic phase promote the activation of fibrinolysis. In addition to an increased risk of bleeding, inadequate treatment of coagulopathy in many cases leads to disseminated intravascular coagulation in the newly created vascular anastomoses and in the clamped inferior vena cava.[1,2]

Objectives

The aim of perioperative therapy is to stabilize the clotting system as a safeguard against diathesis and bleeding as well as to prevent excessive clotting, especially in the vasculature of the newly transplanted liver.

Hemostasis for ltx patients consists of normothermia, a normal blood pH, a normal Ca^{2+} level, and normal blood count (recommended hemoglobin level: 8–10 g%).

The treatment of coagulation disorders is aimed at the creation of a balance between the pro- and anticoagulation systems. Homeostasis in the clotting system is often achieved when the coagulation parameters are below standard. Interference in an imbalanced system and excessive replacement of one of the clotting factors lead to further disruptions in the unstable balance and may eventually result in hemorrhagic diathesis or thrombosis.[2–5]

Dealing with the issue of impaired hemostasis is a dynamic process. Throughout the whole surgery, consisting of the pre-, an- and neohepatic phases, the resulting pathomechanisms disrupt the balance that anesthesia aims to preserve.

New hemostasis assessment methods: thromboelastometry (TEM), the concept of point-of-care, and the superiority of modern methods of coagulation system assessment over the previously used quantitative methods.

Point-of-care (POC) tests are performed near or bedside the patient. Traditionally these tests were performed in laboratory. Advanced technology enables quick obtainment of test results and rapid treatment decisions. The recent concept of treating coagulation system disorders during the procedure of ltx is based on a dynamic assessment of the coagulation system through viscometry. The most commonly used method is rotary thromboelastometry (ROTEM).

The immediate availability of diagnostic results allows an appropriate therapy to be established and the effectiveness of therapeutic interventions to be evaluated.[2,5–7] Treatment of coagulation dysfunction via TEM also identifies the occurrence of hyperfibrinolysis, which is recognized as the cause of late bleedings.

Currently, we have 2 agents that inhibit the activity of plasminogen: epsilon-aminocaproic acid (EACA) and tranexamic acid (Exacyl®). It is very difficult to assess and diagnose hemostasis based solely on TEM, both in terms of the coagulation cascade and fibrinolysis.

Decisions about diagnosis and treatment should be based on the appearance or disappearance of parenchymal bleeding.

Surgery is evaluated as safe and proper according to the amount of blood lost from the surgical field. The concept of general anesthesia for ltx is based on creating hemodynamic conditions which minimize blood loss from the surgical field (low central venous pressure [CVP] anesthesia).

It is acknowledged that with an increasing amount of transfused blood, the likelihood of complications and side effects also increases. This significantly worsens the patients' prognosis.[8,9] In order to reduce the number of transfusions, extravasated blood is recovered from the operating field by a cell separator.

Material and methods

The concept of prevention of intraoperative coagulation disorders is based on the assessment of the results of a coagulation system diagnosis, performed directly on the surgical patient in the operating room (POC).

Rotary thromboelastometry diagnosis based on POC provides the clinically relevant data necessary for the treatment of coagulation disorders as early as 10 min after obtaining measurements from the blood sample. Additionally, apart from standard laboratory tests, ROTEM evaluates fibrinolysis, coagulation dysfunction due to platelet disorders, and the influence of endogenous and exogenous heparinoids.

Thromboelastometry is performed in a fixed temporal and causal setting.

Anesthesia standards for a liver transplantation patient

Surgical ltx is performed under typical anesthetic procedures, such as monitoring of the following parameters:

1. the depth of anesthesia (BIS monitoring – of the bispectral index);

2. skeletal muscle relaxation (neuromuscular transmission monitor – TOF Guard;),
3. anesthetic gas concentrations in the respiratory mixture;
4. plethysmography.

Hemodynamic monitoring includes the following:

1. electrocardiography (ECG);
2. direct blood pressure measurement – the catheter is usually inserted into the radial artery;
3. CVP;
4. pulmonary artery pressure (the Swan-Ganz catheter) and hemodynamic tests performed with the thermodilution technique;
5. hourly diuresis monitoring;
6. core body temperature.

Vascular access includes peripheral cannulation established in the catchment area of the superior vena cava (upper limb), a central line access and a high flow catheter (minimum cross-section: 12 F) inserted through the internal jugular or the subclavian vein, and a vascular sheet (7.5–8 F) for introducing the Swan-Ganz catheter (7 F).

Blood is recovered from the operating field using a Dideco Electa cell separator (Sorin Group, Milan, Italy).

Anesthetics include Diprivan®, sufentanil, triacrium, and desflurane.

Substances can be administered in the form of standard, fractionated doses and continuous infusions: tranexamic acid, calcium chloratum, insulin, norepineohrine, vasopressin, epinephrine, and dobutamine.

Solutions of 0.9% NaCl, 20% glucose and human albumin are typically used, in addition to concentrated red blood cells (PRBC), platelet concentrate, blood coagulation factors, fresh frozen plasma (FFP), cryoprecipitate, fibrinogen, prothrombin complex concentrate, and factor VIIa.

The hemodynamic treatment of patients undergoing ltx complies with the standards of restrictive infusion therapy (low CVP anesthesia), yet does not differ from the standards of ensuring proper oxygen delivery to the tissues (DO_2) and maintaining proper visceral flow and a urine output of at least 0.5 mL/kg/h.

The treatment and maintenance of hemostasis are based on the results of TEM performed by a ROTEM delta device (Tem Innovations GmbH, Munich, Germany). This diagnostic method describes the process of coagulation in the whole blood (we get preliminary results 10 min after a blood sample) and enables fast therapeutic intervention. Decision-making about the treatment of coagulation disorders is always based on clinical observation and assessment is made by the operator.

Standard treatment of coagulation disorders applied in the Department of Vascular, General and Transplantation Surgery, Wroclaw Medical University, Poland, is based on the Compendium of Recommendations from the Society of Essener Runde algorithm and European guidelines for the management of bleeding and coagulopathy.[2,5,10]

Examination protocol

Standard measurements include the assessment of intrinsic and extrinsic clotting pathways by means of ROTEM (INTEM and EXTEM assays), the differentiating activity of fibrinogen and thrombocytes (FIBTEM assay), and the patients' response to anti-fibrinolytic treatment (APTEM assay).

The thromboelastometric graph shows time periods and amplitudes which correspond to the components of the coagulation cascade (section CT – coagulation time, ά – angle alpha, CFT – clot formation time, A – amplitude, MCF – maximum cloth firmness, and CL – clot lysis) (Fig. 1).

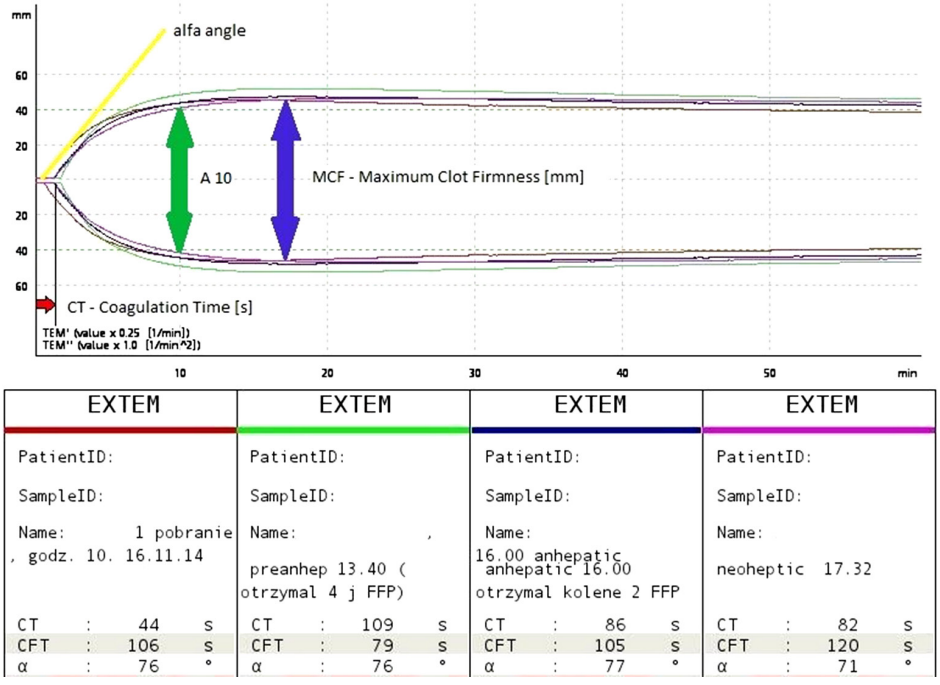

Fig. 1. The example of thromboelastometric examinations (EXTEM) during phases of LTx

The first initial examination is performed immediately after the admission of the patient to the operation theatre. It provides an initial assessment of coagulation disorders and a reference to the implemented therapy. Further tests are carried out 60 min into the procedure, during the preanhepatic phase, at the early anhepatic phase, and at every 30 min of the neohepatic phase. Subsequently, they are also carried out 5–10 min after reperfusion and, finally, 30 min after the beginning of the neohepatic phase.[2] Standard tests (EXTEM, INTEM, FIBTEM, and APTEM) are extended by the HAPTEM test in case of suspected heparin pollution of the blood cell separator (the fast track procedure in case of massive bleeding).

Additionally, after each intervention aimed at the correction of blood clotting, a treatment control test is performed. Clotting disorders reported by the surgeon, usually referred to as parenchymal bleeding, are handled in accordance with the recommendations of the Essener Runde algorithm for ROTEM. For example, parenchymal intraoperative bleeding requires the administration of fibrinogen when MCF (EX) <45 mm and MCF (FIB) <15 mm, the administration of platelets when MCV (EX) <45 mm and MCF (FIB) >15 mm, the substitution of prothrombin complex factors when CT (EXT) >80 s, and the substitution of FFP factors when CT (INT) >280 s. Anti-fibrinolytic treatment is managed using tranexamic acid when ML (EX) >15%, with an initial dose of 2 g (25 mg/kg) followed by a continuous infusion of 10 mg/kg/h and ROTEM tests.[1]

During surgery, the blood extravasated from the operating field is sucked out by a cell separator. After it proceeds through the phases of collecting, filtering and rinsing, a significant portion of the red blood cells is recovered (cell suspension in saline solution with hematocrit [Ht] 50–70%). The red blood cell suspension in saline solution is transfused to the patients' circulation immediately after each rinsing. The device estimates the amount of blood leakage, thereby making it possible to calculate the adequate amount of plasma needed to properly compensate for total blood loss. We maintain a standard hemoglobin level of 8–10 g/dL.

Results

Since the introduction of viscometry based on POC as a clotting system diagnostic method in 2015–2016 and the standard for erythrocyte recovery from the surgical field using a blood cell separator, 12 orthoscopic ltx have been performed. The results are presented in Table 1.

The observations presented in the table show that the main factor of coagulation supplemented to ltx patients was fibrinogen. The dosages of fibrinogen were in the range of 3–10 g per procedure. Furthermore, all patients with confirmed hypofibrinogenemia were given Exacyl® as a standard measure in our department.

In our observations, in almost half of the patients undergoing ltx, the second-most supplemented substances were prothrombin complex factors and plasma, the latter mainly in the case of a deficiency in intrinsic path factors VIII, IX, XI, and XII, but not for a deficiency in prothrombin complex factors.

A cell separator was used in cases of suspected or increased blood loss, and was always ready for immediate use in case it was needed. As shown in the presented data, only 3 patients received an infusion for the blood lost from the surgical field, and there was no significant bleeding in the remaining cases.

Table 1. Intraoperative blood loss and the use of clotting factors during liver transplantation in the Department of Vascular, General and Transplantation Surgery, Wroclaw Medical University, Poland, 6/26/2015–4/4/2016

No. of a patient	Date	Separator [mL]	Re-transfusion [mL]	FFP (u-unit)	PC	PRBC (u-unit)	Fibrinogen	Prothrombin-complex	Factor VIIa	Exacyl®	Cryoprecipitate
1	6/26/2015	low	–	–	–	–	3 g	1,500 u	–	2 g	–
2	8/27/2015	2,390	1,109	–	–	–	7 g	1,000 u	–	2 g	–
3	9/20/2015	low	–	–	–	–	4 g	–	–	2 g	–
4	10/1/2015	low	–	2 u	–	2 u	4 g	–	–	2 g	–
5	11/5/2015	low	–	2 u	–	2 u	2 g	–	–	2 g	–
6	11/13/2015	800	300	–	–	2 u	8 g	–	–	2 g	–
7	12/21/2015	1,000	169	–	–	–	6 g	2,000 u	–	2 g	–
8	1/8/2016	low	–	2 u	–	2 u	6 g	–	–	2 g	–
9	1/30/2016	low	–	–	–	–	10 g	2,000 u	–	2 g	–
10	2/19/2016	low	–	2 u	–	2 u	6 g	1,000 u	–	2 g	–
11	3/17/2016	2,845	974	2 u	–	1 u	6 g	–	–	2 g	–
12	4/4/2016	low	–	–	–	–	4 g	–	–	2 g	–

FFP – fresh frozen plasma; PC – platelet concentrates; PRBC – concentrated red blood cells; 1 unit PRBC = 250 mL; 1 unit FFP = 250–300 mL; low cell separator not in use, lack of excessive bleeding.

Patients 2 and 11 in Table 1 experienced significant bleeding (Patient #2: 2400 mL and Patient #11: 3000 mL). The use of a cell separator and the recovery of almost 1000 mL of red blood cell suspension enabled ltx to be performed without any blood transfusion whatsoever in the case of Patient #2, and using only 1 additional unit (250 mL) of PCRB to Patient #11. These results directly show a significant decrease in the quantity of foreign blood transfusions when using a cell separator.

Conclusions

The concept of POC and the implementation of TEM are a generally acknowledged standard of modern ltx. The introduction of POC diagnostic standards and blood cell separators to common practice could – according to our team – reduces the number of blood transfusions and related complications, including transfusion-related acute lung injury (TRALI), infections and the immunization of the patient.

The use of TEM for the assessment of coagulation disorders allows the replenishment of selective deficiencies, restoring the balance of the coagulation system. This leads to a reduced number of previously, often only intuitively, prescribed transfusions of components such as plasma and platelets, simultaneously diminishing the risk of thrombotic embolism.

A very important achievement of applying these standards is the implementation of a coagulation system diagnostic method that quickly and conveniently describes the pathological mechanisms of coagulation observed in the surgical field and, at the same time, reflects the effectiveness of the implemented therapy or lack thereof.

Thanks to the standards introduced, we gained a quick diagnostic method that enables an appropriate choice of therapeutic strategy. As soon as 10 min after the beginning of the procedure and filling of the sample cuvettes, we are able to obtain preliminary results of the activation of the extrinsic and intrinsic coagulation cascade pathways and parameters evaluating the consolidation of the forming clot.

The introduction of TEM and the implementation of the cell separator recovery method have allowed us to perform the dangerous and complicated surgical procedure of ltx in a much more stable and much safer way than in the past.

References

1. Møller S, Henriksen HJ, Bendtsen F. Extrahepatic complications to cirrhosis and portal hypertension: Haemodynamic and homeostatic aspects. *World J Gastroenterol*. 2014;20(42):15499–15517.
2. Görlinger K. Coagulation management during liver transplantation [in German]. *Hamostaseologie.* 2006;26(Suppl 1):64–75.
3. Hartog A, Mills G. Anaesthesia for hepatic resection surgery. *Continuing Education in Anaesthesia, Critical Care & Pain.* 2009;9(1):1–5.
4. Feltracco P, Brezzi ML, Barbieri S. Blood loss, predictors of bleeding, transfusion practice and strategies of blood cell salvaging during liver transplantation. *World J Hepatol*. 2013;5(1):1–15
5. Lier H, Vorweg M, Hanke A, Görlinger K. Thromboelastometry guided therapy of severe bleeding. Essener Runde Algorithm. *Hemostaseologie*. 2013;33(1):51–61.
6. Ganter MT, Hofer CK. Coagulation monitoring: Current techniques and clinical use of viscoelastic point-of-care coagulation devices. *Anesth Analg*. 2008;106(5):1366–1375.
7. Krzanicki D, Sugavanam A. Mallett S. Intraoperative hypercoagulability during liver transplantation as demonstrated by thromboelastography. *Liver Transpl*. 2013;19(8):852–861.
8. Roullet S, Pillot J, Freyburger G, et al. Rotation thromboelastometry detect thrombocytopenia and hypofibrinogenaemia during orthotopic liver transplantation. *Br J Anaesth*. 2010;104(4):422–428.
9. Romero FA, Razonable RR. Infections in liver recipients. *World J Hepatol*. 2011;3(4):83–92.
10. Spahn DR, Bouillon B, Cerny V, et al. Management of bleeding and coagulopathy following major trauma: An updated European guideline. *Crit Care*. 2013;17(2):R76.

Labor in pregnancies with small for gestational age suspected fetuses

Damian Warzecha[A–D], Eliza Kobryń[A–D], Marta Bagińska[B–D], Dorota Bomba-Opoń[A,E,F]

1st Department of Obstetrics and Gynecology, Medical University of Warsaw, Poland

A – research concept and design; B – collection and/or assembly of data; C – data analysis and interpretation;
D – writing the article; E – critical revision of the article; F – final approval of the article

Advances in Clinical and Experimental Medicine, ISSN 1899-5276 (print), ISSN 2451-2680 (online) *Adv Clin Exp Med*. 2018;27(9):1217–1224

Address for correspondence
Dorota Bomba-Opoń
E-mail: dorota.bomba-opon@wum.edu.pl

Funding sources
None declared

Conflict of interest
None declared

Received on December 16, 2016
Reviewed on February 5, 2017
Accepted on March 7, 2017

Abstract

Background. Fetal growth restriction (FGR) is an unclearly defined condition described as a fetal weight which is too low in relation to gestational age. It is recognized in 10–15% of singleton pregnancies and can lead to severe complications, including stillbirth. To reduce the adverse fetal and neonatal outcomes, many medical interventions are being introduced by obstetricians. These, like all medical procedures, may induce further complications, such as preterm labor and its consequences.

Objectives. The aim of this study was to assess in terms of perinatal and neonatal outcomes such management procedures as expectant monitoring, induction or elective cesarean section (ECS) in pregnancies where the fetus is suspected of being small for gestational age (SGA). There was also the goal of determining the specificity of ultrasound examination in the recognition of SGA.

Material and methods. The single-center retrospective study was carried out among 146 patients who were prenatally suspected of having SGA pregnancies and who delivered in our hospital. Small for gestational age was defined as estimated fetal weight (EFW) in the 10th percentile or below. The output cohort was divided into 2 subgroups: group A – with antenatally confirmed hypotrophy, and group B – without antenatally confirmed hypotrophy.

Results. Out of 146 newborns suspected of being SGA, 65 had a birth weight in the 10th percentile or below, and the estimated positive predictive value of ultrasound examination amounted to 44.5%. Underweight mothers correlated with 5 times higher rates of SGA overdiagnosis. Serious neonatal complications, such as neonatal deaths, respiratory or cardiovascular dysfunctions, and admission to the neonatal intensive care unit (NICU), occurred significantly more often in confirmed SGA cases (46% vs 19% in group B, with a p-value of 0.0066, 0.0253, 0.0027, and 0.0253, respectively). The highest rate of ECS concerned patients from group A (44.6% vs 30.9% in unconfirmed samples; $p = 0.04$), while expectant management was more often associated with neonatal death and admission to the NICU than with elective procedures (18.2% vs 7.4% and 36.4% vs 27.8%, respectively).

Conclusions. Customized charts used during ultrasound examination, which evaluate additional parameters such as body mass index (BMI), may decrease the overdiagnosis of SGA.

Key words: small for gestational age, body mass index, fetal hypotrophy, labor induction, elective procedures

DOI
10.17219/acem/69347

Introduction

Fetal growth restriction (FGR) is a condition unclearly defined as a fetal weight which is too low in relation to gestational age. Different kinds of FGR appear in 5–10% of all pregnancies.[1] This multitude of forms is due to different definitions based on diverse diagnostic criteria. Fetal hypotrophy is synonymous with a small fetus which did not fully realize its growth potential. Other disorders, such as "small for gestational age" (SGA) and "intrauterine growth restriction" (IUGR) are diagnosed by ultrasound examination during the 2nd and 3rd trimester of pregnancy. Small for gestational age is defined as estimated fetal weight (EFW) below the 10th percentile in ultrasound examination using a software program which calculates the fetal weight on the basis of particular parameters.[2] The definition of IUGR is the same as SGA, but there is an additional requirement to evaluate impaired Doppler flows in the umbilical artery or in the medium cerebral artery.

All types of FGR are associated with severe complications, which are a challenge and a substantial problem for contemporary perinatology. The causes of SGA can be constitutional determinants or various pathological factors, but typically a combination of several of them leads to fetal hypotrophy.[3] Fetal growth restriction is associated with an increased risk of adverse perinatal outcomes, especially stillbirth, preterm delivery, intrauterine hypoxia, cerebral palsy, and other complications in late childhood, as well as lower IQ scores in young adults.[4,5] Thus, every patient with suspected fetal hypotrophy should be monitored under professional obstetric care.

The problem becomes more complex when regarding the opinions of scientific committees about the standards of management in patients with suspected SGA fetuses. A lack of medical interventions with proven effectiveness, which could stop or reverse the development of FGR, render appropriate perinatal care to be the only therapeutic option. However, there is no unanimity among European and American societies concerning the time and method of delivery. According to the guidelines set forth by the Royal College of Obstetricians and Gynecologists, the essential parameters deciding about the best management are umbilical Dopplers. In fetuses with inappropriate umbilical artery flows (absent or reversed end-diastolic velocity), the committee recommends delivery by cesarean section, while induced labor may be offered to those with normal umbilical artery Doppler flows (with level B evidence).[6] Canadians suggest that if a pregnancy lasts longer than 37 weeks, the obstetrician should consider the choice between expectant management with close fetal/maternal surveillance and delivery. When undertaking clinical interventions, such as cesarean section, ultrasound assessment is a useful tool in evaluating fetal viability.[7]

On the other hand, the American College of Obstetricians and Gynecologists cites the results from trials such as the Growth Restriction Intervention Trial (GRIT) and the Disproportionate Intrauterine Growth Intervention Trial At Term (DIGITAT), which proved no benefit or harm caused by immediate delivery.[8]

According to the Polish Gynecological Society's guidelines, induced labor is recommended in such cases.[9] There is research proving that SGA recognized antenatally implicates more frequent obstetric interventions, without a significant positive impact on early neonatal outcomes.[10]

Objectives

The study aimed to assess different kinds of management (expectant monitoring, induction or elective cesarean section – ECS) in pregnancies with suspected SGA fetuses in the context of perinatal outcomes and neonatal complications. The other purpose was to determine the specificity of ultrasound examination in recognizing SGA.

Material and methods

This retrospective single-center study was carried out in the 1st Department of Obstetrics and Gynecology at the Medical University of Warsaw, Poland. Data regarding the baseline characteristics of patients and the course of gestation was obtained from archival medical documentation of hospitalizations during the last pregnancy. The inclusion criteria were women in singleton pregnancies suspected of fetal hypotrophy or SGA who delivered in the 25th–41st week of gestation between January 1, 2013 and December 31, 2014. The exclusion criteria were insufficient or incomplete medical history (usually associated with missing ultrasound scans), women in multiple pregnancies and fetuses with chromosomal abnormalities. The study group consisted of 146 patients, according to the abovementioned criteria.

The authors also evaluated the following complications during pregnancy: gestational hypertension, preeclampsia, diabetes, oligohydramnios (defined as an amniotic fluid index – AFI <5 cm after summing up the measurements of the largest fluid pockets from each of the 4 uterine quadrants), and obesity (body mass index – BMI ≥30 kg/m^2).[11–13] Other parameters, such as maternal age, parity and smoking during pregnancy, were also taken into consideration. The authors also carefully took into account complications in previous pregnancies – especially stillbirth, IUGR and preeclampsia.

The study group comprised 146 women in singleton pregnancies with suspected SGA. Small for gestational age was defined as a fetus with EFW below the 10th percentile for adequate gestational age, using standard population-based centile charts. Estimated fetal weight was assessed through ultrasound examination during the 3rd trimester, based on the following biometric measurements: bi-parietal diameter (BPD), head circumference

(HC), abdominal circumference (AC), and femur length (FL), using the Hadlock-1 formula (BPD + HC + AC + FL) developed by Professor Kypros Nicolaides. Many research studies have proven the utility of this formula with a high positive correlation between EFW and actual birth weight.[14,15] Also, in comparison with other available patterns, it seems to have the highest predictive value.[16] The authors took into account only the outcome of the recent ultrasound examination which confirmed SGA. Each ultrasound examination was carried out at the hospital ultrasonography station, using high-quality ultrasound systems with a curvilinear array real-time system and a 3.5 or 5.0 MHz transducer.

From the cohort of 146 patients with suspected SGA fetuses, the authors retrospectively selected a group of patients with hypotrophy of the fetuses confirmed after delivery, hereafter called group A. Neonatal hypotrophy was defined as a newborn's birth weight below the 10th percentile for the appropriate week of delivery, sex and population. Patients with false positive diagnosis of SGA, unconfirmed after delivery, were classified as group B.

Both groups were compared between each other with regard to the average duration of gestation, the percentage of preterm births, the mother's age, BMI, and parity – and in the cases of multiparous women, the time since the previous pregnancy. All patients were of Caucasian ethnicity.

Patients from the study group were evaluated for the mode of delivery, medical procedures undertaken during pregnancy and perinatal complications. The authors assessed whether women from the study group had indications for induced labor or ECS, and what influence these procedures had on the maternal and neonatal outcomes. Adverse neonatal outcomes were defined as death before hospital discharge, a 5-minute Apgar score <7 and admission to the neonatal intensive care unit (NICU). In perinatal complications, the authors also evaluated the length of stay at the NICU or the neonatal ward, respiratory disorders, sepsis, hypoglycemia, and intraventricular hemorrhage.

The outcomes were analyzed with regard to double cut-off thresholds for both the study group and the control group: <10th–3rd percentile and <3rd percentile.

Statistical analysis was performed with the Mann–Whitney U test for qualitative values and the Fisher's exact test in the case of quantitative references. P-values <0.05 were considered significant. For a statistical evaluation of the results obtained, the authors used the Statistical Analysis Statement program (SAS/STAT® v. 14.1 Software, SAS Institute Inc., Cary, USA).

Results

Sixty-five newborns suspected of being SGA antenatally by ultrasound examination had a birth weight below the 10th percentile, which represents 44.5% of the sample size. Eighty-one patients (55.5%) were not confirmed as SGA after delivery (later defined as group B). The accordingly positive predictive value of ultrasound examination in the recognition of SGA was estimated at 44.5%. Within group A, the mean age of the mothers equaled 32.5 years (±5.05) and was significantly higher than the mean age within group B, which was 29.5 years (±5.69) (p = 0.0015). The percentage of primiparous women was lower among patients whose newborns were diagnosed as SGA after birth, but without statistical significance (62% vs 74% in group B; p = 1.0). When it comes to multiparous women, the time elapsed since their last pregnancy was similar in both groups (1.74 ±4.89 years vs 1.72 ±2.83 years in groups A and B, respectively; p = 0.3496).

The average duration of pregnancy was lower among patients from the 1st group and equaled 34.9 ±3.80 weeks, in comparison to 36.9 ±2.55 weeks in the 2nd one (p = 0.0317).

Among all mothers, 58.9% delivered between the 37th and the 41st week of pregnancy, 40.4% before the 37th week and 0.7% of the pregnancies lasted over 41 weeks. Late-preterm deliveries (between the 34th and the 36th week) made up 23.3% of all pregnancies, while early-preterm (before the 34th week) constituted 17.1% of the sample size. The full characteristics of patients are presented in Table 1.

The average BMI value at the beginning of the pregnancy was 23.38 ±4.38 kg/m^2 in patients with SGA confirmed after delivery, while in group B, the mean BMI was 21.97 ±4.26 kg/m^2. A retrospective analysis evaluating BMI values in comparison with a positive predictive value of SGA recognition during antenatal ultrasound examination was also conducted. Patients from the study group were divided into 3 subgroups depending on BMI values, namely: <18.5 kg/m^2, between 18.5 kg/m^2 and 25 kg/m^2, and >25 kg/m^2 (Table 2). Maternal underweight (BMI <18.5 kg/m^2) correlated with only an 11% positive predictive value of SGA recognition in ultrasound

Table 1. Baseline characteristics of groups

Parameter	Group A	Group B	p-value
Sample size	65	81	–
Percentage of the study group	44.5%	55.5%	–
The mothers' mean age [years]	32.5 ±5.05	29.5 ±5.69	0.0015*
Percentage of primiparous women	62%	74%	1.000
Mean time since last pregnancy [years]	1.74 ±4.89	1.72 ±2.83	0.3496
Mean duration of pregnancy [weeks]	34.9 ±3.80	36.9 ±2.55	0.0317*
Average BMI [kg/m^2]	23.38 ±4.38	21.97 ±4.26	0.0208*

Group A – group with a confirmed diagnosis of small for gestational age (SGA) after delivery; group B – group without a confirmed diagnosis of SGA after delivery; BMI – body mass index; * statistically significant.

Table 2. Percentage of confirmed SGA diagnoses after birth according to the patients' BMI before pregnancy

BMI [kg/m²] before pregnancy	Percentage of confirmed diagnoses of SGA after delivery
≤18.49	11%
18.5–24.99	49%
≥25	46%

BMI – body mass index; SGA – small for gestational age.

examination (p = 0.0051). The results obtained show that up to 89% of pregnancies were overdiagnosed and that in that group, the standard methods of SGA recognition are less efficient. The percentage of confirmed SGA fetuses after birth was similar in women with normal weight (BMI of between 18.5 kg/m^2 and 25 kg/m^2) and those who were obese before pregnancy (BMI >25 kg/m^2), and it amounted to 49% and 46%, respectively.

Body mass index evaluated in the last trimester of pregnancy had no significant influence on the detection of SGA babies.

Among all patients, 59 gestations were complicated, with preterm delivery. In that group, 42.4% of samples (25) were classified as early preterm (defined as labor between the 22nd and the 34th week of gestation), while 57.6% (34) were late preterm deliveries (between weeks 35 and 37). With a view to generating more precise results, we decided to isolate a group of severe hypotrophy with EFW below the 3rd percentile. In the 1st group, 84% of newborns were classified below the 3rd percentile after birth and 16% of them were between the 3rd and 9.9th percentile. In the case of late preterm delivery, the percentage of newborns below the 3rd percentile was lower than in the previous group and amounted to 53%, while 47% of them gained in birth weight from the 3rd to the 9.9th percentile.

Patients who underwent iatrogenic procedures comprised 86.3% of all pregnancies (126). Up to 43% (54) of those pregnancies were ended by ECS and 57% (72) by induced labor. Induced deliveries ended with ECS in 23.6% of cases. Of all deliveries, 13.7% (20) began spontaneously, where 65% (13) were managed by vaginal delivery and 35% (7) required cesarean section. The most frequently isolated medical indication for induced labor was fetal hypotrophy (about 50%). In 37.5% of all patients, the suspicion of SGA occurred together with several other indications, such as post-term pregnancy, oligohydramnios, gestational diabetes mellitus, pregnancy-induced hypertension, and abnormalities in a non-stress test. Only 12.5% of all cases were associated with indications other than fetus hypotrophy, e.g., preeclampsia or preterm rupture of membranes.

The most severe complication – intrauterine death – occurred in 2 cases in group A (3% of the sample), while it was not reported among group B. The risk of intrauterine death did not significantly correlate with any pathologies during the course of pregnancy, including IUGR (p = 0.196). In each case, the prenatal diagnosis of SGA was confirmed after delivery with a neonatal birth weight below the 1st percentile (418 g and 880 g). Both of those pregnancies ended with vaginal delivery, the 1st one spontaneously in the 27th week, while the 2nd one ended after induction and steroid therapy in the 31st week of pregnancy due to the threat of asphyxia.

In total, 78 pregnancies ended with cesarean section – in 69% as an elective procedure, in 22% after an unsuccessful induction and in 9% following a spontaneously begun delivery. Most of them were associated with the following indications: imminent fetal asphyxia, fetal hypotrophy, abnormal outcome of a non-stress test, failed induction, and breech position or preeclampsia.

The Apgar score, the simplest and most reliable method of evaluation, was performed to assess the general condition of newborn babies suspected of being SGA. We observed significantly worse perinatal outcomes in the group with confirmed severe hypotrophy (below the 3rd percentile). Of those newborns, 17.6% scored <7 points and 8.8% scored <3 points in the Apgar score in the 1st minute, while only 4.5% of the infants between the 3rd and 9.9th percentile in weight scored <7 points (p = 0.0213).

For 13 newborns from the output cohort, medical documentation was unavailable, which is why the following outcomes regard a smaller sample size than before, 59 samples with confirmed hypotrophy (group A) and 74 without confirmation after delivery (group B).

Serious complications in the early neonatal period, e.g., respiratory disorders, cardiovascular insufficiency, intraventricular hemorrhage, or neonatal deaths, occurred in 34% (45) of all newborns whose medical history was available, and separating that data, in 46% and 19% of samples from groups A and B, respectively.

Elective cesarean section was performed in 68.4% of patients from group A and in 63.2% of group B patients, respectively; induced labor was executed in 10.5% of patients from group A and in 21.1% from group B.

Newborns with confirmed hypotrophy were more often admitted to the NICU after birth (32.2% vs 23%; p =0.0253) and significantly more frequently suffered from cardiovascular insufficiency (18.6% vs 2.7%; p = 0.0027). Moreover, children from group A more often required invasive procedures, such as synchronized intermittent mandatory ventilation (SIMV) (18.6% vs 5.4%; p = 0.0253). We reported 6 neonatal deaths after delivery in group A (10.2%), while that complication was not observed among any neonates with an unconfirmed diagnosis of SGA (p = 0.0066). More details concerning severe neonatal complications are presented in Table 3.

The complications which occurred in the remaining newborns, such as intraventricular hemorrhage, early infections and hypoglycemia, did not demonstrate any statistically significant correlations. The average duration of hospitalization was similar in both groups (8.67 ±9.81 days vs 7.86 ±8.80 days; p = 0.2365).

Table 3. Percentage of neonatal complications among the studied groups

Complication	Total	Group A	Group B	p-value
Neonatal deaths	4.5%	10.2%	0.0%	0.0066*
NICU hospitalization	27.1%	32.2%	23.0%	0.0253*
Respiratory dysfunction: CPAP SIMV	 7.5% 11.3%	 5.0% 18.6%	 9.5% 5.4%	 0.0511 0.0253*
Cardiovascular insufficiency	9.8%	18.6%	2.7%	0.0027*
Intraventricular hemorrhage	14.3%	18.6%	10.1%	0.2211
Hypoglycemia	19.5%	11.9%	25.7%	0.0508
Infection	23.3%	27.1%	20.3%	0.4113
Average hospitalization time [days]	8.13 ±9.22	8.67 ±9.81	7.86 ±8.80	0.2365

Group A – group with a confirmed diagnosis of small for gestational age (SGA) after delivery; group B – group without a confirmed diagnosis of SGA after delivery; NICU – neonatal intensive care unit; CPAP – continuous positive airway pressure; SIMV – synchronized intermittent mandatory ventilation; * statistically significant.

Table 4. Correlation between neonatal complications and methods of management

Variable	Group A	Group B	p-value
Total amount	65	81	comparison between both groups
Induced labor – NICU hospitalization – newborn deaths	38.5% (25) 8.0% (2) 4.0% (1)	58.0% (47) 8.5% (4) 0%	0.0208* 0.6726 0.4452
Elective C-section – NICU hospitalization – newborn deaths	44.6% (29) 44.8% (13) 10.3% (3)	30.9% (25) 48.0% (12) –	0.0400* 0.5083 0.0860
Spontaneous vaginal delivery – NICU hospitalization – newborn deaths	16.9% (11) 36.4% (4) 18.2% (2)	11.1% (9) 33.3% (3) 0%	0.3408 0.7003 0.1965
Elective delivery (induced labor + C-section) – NICU hospitalization – newborn deaths	83.1% (54) 27.8% (15) 7.4% (4)	88.9% (72) 22.2% (16) 0%	0.3408 0.6861 0.0373*

Group A – group with a confirmed diagnosis of small for gestational age (SGA) after delivery; group B – group with an unconfirmed diagnosis of SGA after delivery; NICU – neonatal intensive care unit; C-section – cesarean section; * statistically significant.

Hospitalization at the NICU was required in 8% and 8.5% of newborns after induced labor (p = 0.6726), in 45% and 48% of those delivered by ECS (p = 0.5083), and in 36% and 33% of children after spontaneous vaginal birth (p = 0.7) in groups A and B, respectively.

In accordance with the method of management (Table 4), we found the highest rate of ECS among patients with confirmed hypotrophy after delivery (44.6% vs 30.9% in the unconfirmed group; p = 0.04). That mode of delivery was also most frequent among mothers from group A. The percentage of induced labor cases was the highest in patients with unverified SGA and equaled 58% vs 38.5% in group A (p = 0.0208). Both groups are characterized by a similar percentage of elective procedures (induction and cesarean section altogether), measured at 83.1% (A) and 88.9% (B) with a p-value of 0.3408. A decidedly less frequently reported method of delivery in the studied group was spontaneous vaginal delivery, without a significant difference between groups A and B (16.9% vs 11.1%; p = 0.3408).

Expectant management in both groups led to worse perinatal outcomes than elective procedures performed to prevent fetal complications.

From a different perspective, dividing the groups into severe (below the 3rd percentile) and mild (3rd–9.9th percentile) hypotrophy, serious complications occurred in 62% and 38% of newborn babies, respectively (Fig. 1).

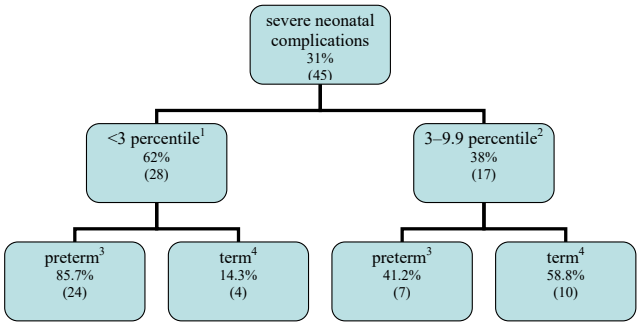

Fig. 1. Percentage of severe neonatal complications classified depending on the percentile of newborn weight and time of birth

1 – newborns birth weight under 3rd percentile; 2 – newborns birth weight between 3rd to 9.9 percentile; 3 – percentage of severe neonatal complications among preterm births; 4 – percentage of severe neonatal complications among at term births.

Discussion

In this study, the estimated positive predictive value of ultrasound examination in the recognition of SGA during late pregnancy was 44.5%. This data is similar to the findings from a large population-based study on French pregnant women, where 1/2 of all infants suspected of FGR were not confirmed after delivery.[17]

To the best of our knowledge, there are limited studies which ex post facto evaluate the correlation between different variables and their influence on making a correct or false positive diagnosis of SGA. The available clinical data is very limited and precludes any reliable conclusion in that area.

According to our study, mothers with SGA babies confirmed after delivery were significantly older than those with the false positive diagnosis (mean age of 32.5 years in group A; p = 0.0015). Early motherhood is considered a risk factor for lower birth weight in newborns, while advanced age seems to increase the frequency of SGA only in primiparous women.[18,19]

Apart from that, a longer duration of pregnancy and advanced gestational age at the time of delivery (36.9 ±2.55 weeks vs 34.9 ±3.80 weeks in confirmed cases) correlate with a higher incidence of incorrect antenatal diagnoses (p = 0.0317).

Interesting conclusions can be drawn when it comes to the comparison of the positive predictive value of ultrasound examination with the mothers' BMI values at the beginning of pregnancy.

Underweight mothers (BMI <18.5 kg/m^2) correlate with nearly 5 times more frequent overdiagnosis of SGA in comparison to BMI values between 18.5 kg/m^2 and 25 kg/m^2, and >25 kg/m^2 (11% of correct diagnoses vs 49% and 46% in the remaining groups, respectively; p = 0.0051). In that group, only 11% of the fetuses suspected antenatally of being SGA were confirmed as hypotrophic fetuses after birth. Lower maternal initial BMI values seem to be associated with impaired EFW assessment. The phenomenon described above may be related to the influence of certain constitutive factors.

There is substantial evidence in the literature which proves that petite women, especially those underweight before pregnancy, give birth to smaller babies.[20] On the other hand, a recently published vast meta-analysis provides evidence that short maternal stature and chronic malnutrition, especially in developing countries, contribute to a higher incidence of SGA.[21] It is hard to draw clear conclusions if that diagnosis is connected to inter-subject variability or the damaging influence of exogenous factors.

More often, the overdiagnosis of SGA babies in women with lower BMI before pregnancy seems to confirm that most of those cases are likely associated with genetic factors rather than pathological intrauterine growth retardation. Such hypotheses were also presented by previous researchers, who concluded that a generational transmission of SGA is possible.[22]

In this situation, it is worth considering the usefulness of customized charts during ultrasound examination in pregnant women, rather than standard population-based ones.[23] It has been proven that for SGA suspected antenatally, using customized growth potential is able to identify substantially more pregnancies at risk for adverse outcomes than the currently used national standard for fetal growth.[24] Recently, the authors of a multi-center project called INTERGROWTH-21st, which included 13,108 pregnant women, created fetal growth curves with regard to 5 basic ultrasound measurements. The utility of those charts was positively evaluated in different populations and it may offer precise assessment of intrauterine fetal growth before the customized charts become available.[25]

Such factors as the mother's age, the duration of pregnancy, parity, or the time elapsed since the previous delivery seem not to correlate with a true or false positive diagnosis of SGA.

The most severe complication in the course of pregnancy – intrauterine death – occurred 2 times in group A, while it was not reported among patients from group B. However, the risk of intrauterine death was not significantly correlated with any pathologies during the course of pregnancy, including IUGR (p = 0.196), though this may result from the small sample size.

Aware of fetal complications, obstetricians decide to induce labor, while this procedure is not without consequences.

The multi-center randomized trial, DIGITAT, comparing both types of managements (induction and expectant monitoring), provided similar efficacy regarding perinatal outcomes. Despite this, the researchers found that induced labor seems to be a more rational method of management which reduces the risk of stillbirth and newborn morbidity.[26]

In this study, the estimated percentage of ECSs among true-positives amounted to 44.6% and was twice as high as that from the previously described study on the French population (44.6% vs 23.8%), while the ECSs in false-positives were carried out with similar frequency (30.9% vs 28.4% in the French study).[17]

Stricter indications for elective procedures and more appropriate recognition of FGR could prevent the side effects of unnecessary medical interventions in the future.

In the context of the final neonatal outcomes, the current study shows that expectant management can increase the percentage of neonatal complications; the best indicators of that are the number of neonates hospitalized in the NICU and neonatal deaths. Elective delivery – labor induction or ECS – despite the risk of these invasive procedures, could minimize adverse neonatal outcomes in patients with suspected fetal hypotrophy.

In contrast, previous longitudinal studies on pregnant women with suspected FGR suggest that a higher incidence of obstetric interventions does not entail demonstrable positive effects upon short-term neonatal outcomes.[27] Moreover, induction of labor seems to be associated with

a higher rate of adverse neonatal outcomes.[28,29] Evidence on the best management strategy for at term IUGR, when it comes to perinatal outcomes, is still lacking.[30]

This difficult decision between elective procedure and expectant management should always be taken by an experienced obstetrician, with careful consideration of the advantages and disadvantages of both methods. It is hard to draw an explicit conclusion about which form of management could be better, and in each case, all conditions should be individually assessed.

There are several limitations of this study that should be considered along with the results.

First of all, the selected study group is from a single-center study, conducted in a tertiary medical center unit. At baseline, most patients underwent more than 1 diagnosis, which makes it hard to compare them to the standard population.

On the other hand, the cohort of patients with confirmed SGA after delivery accounted for only 65 cases. In such limited study group, it is hard to draw unmistakable correlations between different factors and their influence on the occurrence of SGA. More research on a larger group of patients with confirmed SGA is required.

Secondly, as mentioned before, the measurements which were the basis for diagnosing SGA were taken by several ultrasonography technicians. Aberrations caused by human error cannot be excluded, and they may impact the reproducibility of the results between sequential ultrasound examinations.

The assessment of SGA was set only based on EFW below the 10th percentile. On the other hand, there are some studies which prove that evaluating artery flow with fetal biometry aids in identifying the babies at risk of IUGR. Such a procedure may decrease the number of antenatal false positive diagnoses of SGA in the future.

Conclusions

Creating customized percentile charts which could be correlated with other additional parameters, such as the patient's BMI, may decrease the overdiagnosis of SGA when using ultrasound imaging in the future. Stricter indications for the induction of labor would prevent unnecessary medical procedures and their side effects. However, expectant management leads to worse perinatal outcomes, defined as a higher rate of neonate death or required NICU treatment, than elective procedures.

With the goal of better neonatal outcomes, it seems more rational to choose elective management in patients suspected of being SGA, indeed, if that diagnosis is characterized by sufficient reliability.

References

1. Thompson JL, Kuller JA, Rhee EH. Antenatal surveillance of fetal growth restriction. *Obstet Gynecol Surv*. 2012;67(9):554–565. doi: 10.1097/OGX.0b013e31826a5c6f
2. Dashe JS, McIntire DD, Lucas MJ, Lenovo KJ. Effects of symmetric and asymmetric fetal growth on pregnancy outcomes. *Obstet Gynecol*. 2000;96(3):321–327.
3. De Jong CLD, Francis A, van Geijn HP, Gardosi J. Fetal growth rate and adverse perinatal events. *Ultrasound Obstet Gynecol*. 1999;13:86–89.
4. Løhaugen GC, Østgård HF, Andreassen S, et al. Small for gestational age and intrauterine growth restriction decreases cognitive function in young adults. *J Pediatr*. 2013;163(2):447–453.
5. Østgård HF, Skranes J, Martinussen M, et al. Neuropsychological deficits in young adults born small-for-gestational age (SGA) at term. *J Int Neuropsychol Soc*. 2014;20(3):313–323.
6. Royal College of Obstetricians and Gynaecologists (RCOG). The investigation and management of the small-for-gestational-age fetus. London, UK: Royal College of Obstetricians and Gynaecologists (RCOG); 2013:34 (Green-top Guideline No. 31).
7. Lausman A, Kingdom J; Maternal Fetal Medicine Committee. Intrauterine growth restriction: Screening, diagnosis, and management. *J Obstet Gynaecol Can*. 2013;35(8):741–748.
8. American College of Obstetricians and Gynecologists (ACOG). ACOG Practice bulletin No. 134: fetal growth restriction. *Obstet Gynecol*. 2013;121(5):1122–1133.
9. Rekomendacje zespołu ekspertów Polskiego Towarzystwa Ginekologicznego dotyczące opieki okołoporodowej i prowadzenia porodu. *Ginekol Pol*. 2009;80:548–557.
10. Ohel G, Ruach M. Perinatal outcome of idiopathic small for gestational age pregnancies at term: The effect of antenatal diagnosis. *Int J Gynaecol Obstet*. 1996;55(1):29–32.
11. Phelan JP, Smith CV, Broussard P, Small M. Amniotic fluid volume assessment with the four-quadrant technique at 36–42 weeks' gestation. *J Reprod Med*. 1987;32:540–542.
12. Shanks A, Tuuli M, Schaecher C, Odibo AO, Rampersad R. Assessing the optimal definition of oligohydramnios associated with adverse neonatal outcomes. *J Ultrasound Med*. 2011;30:303–307.
13. Ogden CL, Carroll MD, Fryar CD, Flegal KM. Prevalence of obesity among adults and youth: United States, 2011–2014. NCHS. Data brief, no 219. Hyattsville, MD: National Center for Health Statistics; 2015. https://www.cdc.gov/nchs/data/databriefs/db219.pdf. Accessed January 10, 2016.
14. Basha AS, Abu-Khader IB, Qutishat RM, Amarin ZO. Accuracy of sonographic fetal weight estimation within 14 days of delivery in a Jordanian population using Hadlock formula 1. *Med Princ Pract*. 2012;21(4):366–369.
15. Geerts L, Widmer T. Which is the most accurate formula to estimate fetal weight in women with severe preterm preeclampsia? *J Matern Fetal Neonatal Med*. 2011;24(2):271–279.
16. Esinler D, Bircan O, Esin S, et al. Finding the best formula to predict the fetal weight: Comparison of 18 formulas. *Gynecol Obstet Invest*. 2015;80(2):78–84.
17. Monier I, Blondel B, Ego A, Kaminiski M, Goffinet F, Zeitlin J. Poor effectiveness of antenatal detection of fetal growth restriction and consequences for obstetric management and neonatal outcomes: A French national study. *BJOG*. 2015;122(4):518–527.
18. Cooper LG, Leland NL, Alexander G. Effect of maternal age on birth outcomes among young adolescents. *Soc Biol*. 1995;42(1–2):22–35.
19. Schimmel MS, Bromiker R, Hammerman C, et al. The effects of maternal age and parity on maternal and neonatal outcome. *Arch Gynecol Obstet*. 2015;291(4):793–798.
20. Belogolovkin V, Alio AP, Mbah AK, Clayton HB, Wathington D, Salihu HM. Patterns and success of fetal programming among women with low and extremely low pre-pregnancy BMI. *Arch Gynecol Obstet*. 2009;280(4):579–584.
21. Kozuki N, Katz J, Lee AC, et al.; Child Health Epidemiology Reference Group Small-for-Gestational-Age/Preterm Birth Working Group. Short maternal stature increases risk of small-for-gestational-age and preterm births in low- and middle-income countries: Individual participant data meta-analysis and population attributable fraction. *J Nutr*. 2015;145(11):2542–2550.

22. Castrillio SM, Rankin KM, David RJ, Collins JW. Small-for-gestational age and preterm birth across generations: A population-based study of Illinois births. *Matern Child Health J*. 2014;18(10):2456–2464.
23. Stirnemann JJ, Benoist G, Salomon LJ, Bernard JP, Ville Y. Optimal risk assessment of small-for-gestational-age fetuses using 31–34-week biometry in a low-risk population. *Ultrasound Obstet Gynecol*. 2014; 43(3):311–316.
24. Odibo AO, Francis A, Cahill AG, Macones GA, Crane JP, Gardosi J. Association between pregnancy complications and small-for-gestational-age birth weight defined by customized fetal growth standard versus a population-based standard. *J Matern Fetal Neonatal Med*. 2011;24(3):411–417.
25. Papageorghiou AT, Ohuma EO, Altman DG, et al.; International Fetal and Newborn Growth Consortium for the 21st Century (INTERGROWTH-21st). International standards for fetal growth based on serial ultrasound measurements: The fetal growth longitudinal study of the INTERGROWTH-21st project. *Lancet*. 2014;384(9946):869–879.
26. Boers KE, Bijlenga D, Mol BWJ, et al. Disproportionate Intrauterine Growth Intervention Trial At Term: DIGITAT. *BMC Pregnancy Childbirth*. 2007;7:12. doi: 10.1186/1471-2393-7-12
27. Ohel G, Ruach M. Perinatal outcome of idiopathic small for gestational age pregnancies at term: The effect of antenatal diagnosis. *Int J Gynaecol Obstet*. 1996;55(1):29–32.
28. Kramer MS, Demissie K, Yang H, Platt HR, Sauve R, Liston R. The contribution of mild and moderate preterm birth to infant mortality. *J Am Podiatr Med Assoc*. 2000;284(7):843–849.
29. Tomashek KM, Shapiro-Mendoza CK, Davidoff MJ, Petrini JR. Differences in mortality between late-preterm and term singleton infants in the United States, 1995–2002. *J Pediatr*. 2007;151(5):450–456.
30. Boers KE, van der Post JA, Mol BW, van Lith JM, Scherjon SA. Labour and neonatal outcome in small for gestational age babies delivered beyond 36+0 weeks: A retrospective cohort study. *J Pregnancy*. 2011. doi: 10.1155/2011/293516

Disturbances in intraventricular conduction in children with end-stage renal disease on peritoneal dialysis: A pilot study

Krystyna Laszki-Szczachor[1,B–E], Danuta Zwolińska[2,E,F], Małgorzata Sobieszczańska[1,A,D–F], Michał Tabin[1,B], Dorota Polak-Jonkisz[2,A,B,D,F]

[1] Department of Pathophysiology, Wroclaw Medical University, Poland
[2] Department of Pediatric Nephrology, Wroclaw Medical University, Poland

A – research concept and design; B – collection and/or assembly of data; C – data analysis and interpretation; D – writing the article; E – critical revision of the article; F – final approval of the article

Advances in Clinical and Experimental Medicine, ISSN 1899-5276 (print), ISSN 2451-2680 (online) *Adv Clin Exp Med.* 2018;27(9):1225–1231

Address for correspondence
Małgorzata Sobieszczańska
E-mail: malgorzata.sobieszczanska@umed.wroc.pl

Funding sources
None declared

Conflict of interest
None declared

Received on August 20, 2016
Reviewed on November 7, 2016
Accepted on March 2, 2017

Abstract

Background. The progression of chronic kidney disease is accompanied by multi-organ disorders, among which cardiovascular diseases have the status of a serious clinical problem. The body surface potential mapping (BSPM) technique is a non-invasive method which enables the detection of pathological changes in the bioelectrical activity of the heart.

Objectives. The aim of this study was to identify possible disturbances in the intraventricular conduction system in peritoneally dialyzed children.

Material and methods. Cardiac examination consisted of 12-lead electrocardiography, echocardiography and BSPM. The evaluation of disturbances in the cardio-electrical field was performed by comparing the qualitative and quantitative features of the heart potentials on the isopotential map.

Results. Data was collected from 10 children treated with automatic peritoneal dialysis (APD) (mean age: 13.6 ±2.3 years) and 26 healthy children. The maps of dialyzed children showed a shift in positive isopotentials toward the left lower part of the thorax, while negative values were observed in its left upper part. A distribution of lines on the isopotential maps revealed disturbances in the stimulation spread within the heart ventricles, especially within the anterior fascicle of the left bundle branch of His.

Conclusions. Intraventricular conduction disturbances were observed in the left bundle branch of His in the peritoneally dialyzed children. The body surface potential mapping was a more sensitive method in identifying the early stage of conduction disturbances within the heart ventricles than 12-lead electrocardiography. Further research involving a larger population of dialyzed children is planned.

Key words: children, peritoneal dialysis, isopotential maps, body surface potential mapping

DOI
10.17219/acem/69255

Introduction

Patients with chronic kidney diseases (CKD) are at a high risk of cardiovascular diseases, including arrhythmia, cardiomyopathy, valve disorders, and sudden cardiac death. Cardiovascular complications become more probable with CKD progression, and are identified in 1/3 of the examined dialyzed patients.[1,2]

Parekh et al. reported that mortality risk in children with CKD is 10-fold higher than in the general child population, and Foley et al. stated that the mortality rate increased by even 500–1000 times.[3–5] Therefore, the American Heart Association classified CKD children as the "highest risk" group.[6]

Numerous uremia complications in CKD children are responsible for cardiac problems, including structural changes in the myocardium and restructuring of the coronary vessels. Alterations within the intraventricular conduction system cause delayed ventricular depolarization with subsequent hemodynamic dyssynchrony and left ventricle systolic-diastolic dysfunction.

Early diagnosis of cardiovascular impairments in CKD children seems extremely beneficial, as it may offer a preventive management program which reduces the risk of morbidity and mortality from cardiovascular disorders.[7] Non-invasive cardiac diagnostic techniques include body surface potential mapping (BSPM), a computerized method which enables an analysis of the cardio-electrical field activity using 3 types of maps: isopotential, isointegral and isochrones.[8]

Isopotential maps were used in this study, allowing the identification of initial disorders in electrical stimulation spreading through the intraventricular conduction system. Isopotential maps display the points on the thorax of equal value of heart electrical potentials connected by isolines. The identification of possible abnormalities in the cardio-electrical field of an examined patient is done by comparing the values of heart potentials at corresponding points on the reference map, enhanced by the visual evaluation of the distribution of isopotential lines.

The aim of the study was to determine the possible changes in the heart intraventricular system in children with CKD at stage 5 treated with peritoneal dialysis (PD).

To the best of our knowledge, there have been no reports so far on the identification of intraventricular heart conduction system disturbances with isopotential maps in PD children.

The present study was approved by the Research Ethics Committee of Wroclaw Medical University, Poland (No. KB – 229/2007).

Material and methods

Biochemical tests

In all patients, serum concentrations of the following substances were assayed: inorganic phosphate (P_i), total calcium (t-Ca), sodium (Na), urea, creatinine (cr), intact parathormone (iPTH), C-reactive protein (CRP), and albumin.

Serum P_i, Na and t-Ca levels were tested by the direct potentiometry method, using ionoselective ISE electrodes, by a Konelab automatic analyzer (bioMérieux, Marcy l'Etoile, France), with the following normal ranges: t-Ca: 8.80–10.80 mg/dL; P_i: 4.5–5.52 mg/dL; and Na: 135–146 mmol/L. Serum creatinine was measured by the Jaffe method (normal range: 0.3–1.0 mg/dL) and urea was determined by the enzymatic-colorimetric method (normal range: 10.00–45.00 mg/dL). Intact parathormone was assayed by the immunoenzymatic method (enzyme-linked immunosorbent assay – ELISA; Roche Diagnostics, Warszawa, Polska) (normal value: 11.00–67.00 pg/mL). We used method for the serum albumin determination with bromocresol green solution (normal range: 3.4–4.2 g/dL).

End-stage renal disease (ESRD) children were kept on a phosphate-poor diet (phosphate intake <500–800 mg/day) and were treated with compounds which bind phosphate in the intestine (calcium carbonate <35–200 mg/kg/day) in order to maintain a serum phosphate concentration of 4.5–5.52 mg/dL. Dietary calcium intake was defined as 500–600 mg of elemental calcium per day to keep a serum calcium concentration of 8.8–10.8 mg/dL.

Measurements of blood pressure were taken after the completion of nocturnal dialysis, according to the obligatory recommendations (the Fourth Report on the diagnosis, evaluation and treatment of high blood pressure in children and adolescents from the National High Blood Pressure Education Program Working Group on High Blood Pressure in Children and Adolescents).[9] The obtained RR results were assessed basing on percentile charts in relation to gender, age and body height.

Blood samples were drawn from peripheral veins of the patients after an overnight fast. The collected samples were clotted for 30 min and centrifuged at 4°C for 10 min. The serum was stored at –20°C until assayed.

The results of the biochemical analysis are presented in Table 1.

ECG and ECHO

Standard 12-lead electrocardiography (ECG) examination was performed twice in each examined child and the results were interpreted according to the commonly accepted criteria.[10]

In all of the patients on automatic peritoneal dialysis (APD), a transthoracic echocardiographic examination (ECHO) was carried out on the same day as BSPM using

Table 1. The results of the biochemical analysis in the study groups

Index group		Urea [mg/dL]	cr [mg/dL]	t-Ca [mg/dL]	P_i [mg/dL]	Na [mmol/L]	iPTH [pg/mL]	Albumins [g/dL]
I (PD patients) n = 10		95.32 ±7.12	6.71 ±1.00	9.35 ±1.35	5.89 ±0.33	138.77 ±3.19	556.44 ±399.14	4.02 ±0.28
II (controls) n = 26		29.11 ±9.45	0.73 ±0.08	10.03 ±1.11	4.78 ±0.9	140.44 ±2.92	26.3 ±8.98	4.1 ±0.11
p-value	M-W	p < 0.001	p < 0.001	NS	p < 0.001	NS	p < 0.001	NS
	Student's t test	p < 0.001	p < 0.001	NS	p < 0.001	NS	p < 0.001	NS

PD – peritoneal dialysis; cr – creatinine; t-Ca – total calcium; P_i – inorganic phosphate; Na – sodium; iPTH – intact parathormone; M-W – Mann-Whitney test; NS – nonsignificant.

a Hewlett Packard Sonos 1000 device (Hewlett Packard, Palo Alto, USA), and according to the guidelines of the American Society of Echocardiography.[11]

Body surface potential mapping

Changes in the bioelectrical field were monitored by the body surface potential mapping (BSPM) method with the use of an HPM 7100 system (Fukuda-Denshi Co., Tokyo, Japan), recording ECG signals simultaneously from 87 leads. Standardized, disposable electrodes were placed on the patient's body, distributed across 13 self-adhesive strips, with 7 electrodes on each strip placed along the axillary lines (Fig. 1). Such a cylindrical configuration of the electrodes enables the recording of electrocardiographic signals from the entire thoracic surface.[12]

Isopotential maps were plotted for the QRS ventricular complex by linking the points which show the potentials of the same value with a solid line (i.e., isolines). The identification of disorders in the stimulation spreading across

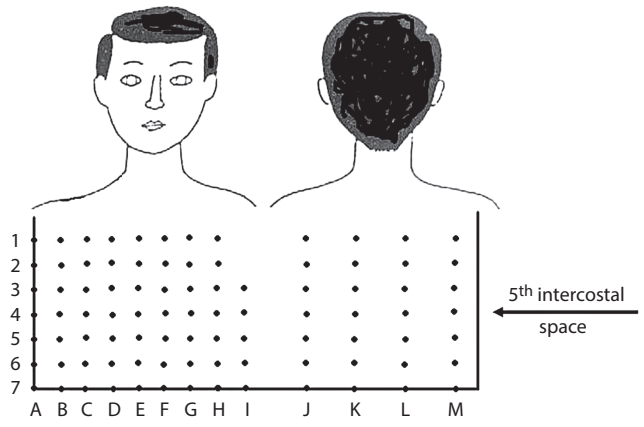

Fig. 1. The layout of electrodes on a patient's body

the intraventricular conduction system was carried out by comparing the potential values at certain points of the patient's map with the potential values at corresponding points on the reference map (averaged for healthy persons from the control group).

All of the parents of the examined children and adolescent minors enrolled in the study gave their informed consent to their child's participation in the procedures. The investigation protocol was approved by the local ethics committee and was compliant with the Declaration of Helsinki.

Statistical analysis

The data was presented as arithmetic means with standard deviation (x ±SD). The statistical significance of the null hypothesis for the equality of means expected for particular characteristics in groups I and II was verified by the Mann-Whitney nonparametric test. A p-value of <0.05 was considered statistically significant.

Results

The study group (group I) was comprised of 10 children with end-stage renal disease (ESRD) (4 boys and 6 girls; mean age: 13.6 ±2.31 years) treated with APD. The control group (group II) consisted of 26 age-matched healthy children (12 boys and 14 girls) with no clinical renal or cardiac symptoms, and arterial blood pressure, 12-lead ECG, ECHO, and BSPM examination results within norms.

The causes of CKD in the studied group included chronic glomerulonephritis (6 patients), chronic pyelonephritis (3 patients) and congenital malformations of the urinary system (1 patient).

The APD duration varied in the studied patients from 6 months to 1.7 years (mean duration: 1.17 ±0.33 years). The Kt/V index was 2.11 ±0.05. The standard prescription of APD (HomeChoice Pro; Baxter Healthcare, Warszawa, Poland) included dwell changes of 9–12 h, with 800–1000 mL/m^2 body surface area (BSA) of 1.36% glucose PD4 (Baxter Healthcare) per dwell per fill volume. Two patients had a routine APD prescription. Three patients had PD with Physioneal on alternate days; in those patients, ventricular activation time (VAT) maps were taken on the days without Physioneal. Five patients had APD cycles with 1.36% PD at night and, additionally, up to 2 continuous ambulatory peritoneal dialysis (CAPD) changes during the daytime with 2.27% glucose. Glucose concentrations were dependent on the fluid amounts to be removed in order to maintain a clinically euvolemic state. Three children

with APD were anuric. Seven other patients with residual renal function had a urine output of 721 ±133 mL/day.

The pharmacotherapy which was administered included hypotensive agents, erythropoietin, analogs of vitamin D, vitamin C, folic acid, and iron supplements.

Six of the ESRD patients were treated with antihypertensive drugs (calcium channel blockers, angiotensin-converting enzyme inhibitors [ACEI], and beta-blocker agents). Three patients were treated with monotherapy (calcium channel blockers or ACEI) and the remaining 3 with combined therapy (calcium channel blockers with beta blockers or calcium channel blockers with ACEI).

The analysis of the distribution of isopotential lines was first performed in the control group of healthy subjects using the mean map plotted for that group (Fig. 2). In healthy subjects, isolines build up a hat-like shape on the mean map, spreading out fairly uniformly to the left and right side of the thorax. It is clearly evident that the subendocardial layer at the lower left surface of the interventricular septum and a part of the free wall of the left ventricle are the earliest stimulated parts of the heart.

In the subsequent phase of depolarization, the front of the stimulation wave moves from the left side toward the right side of the septum surface. Further on, synchronic

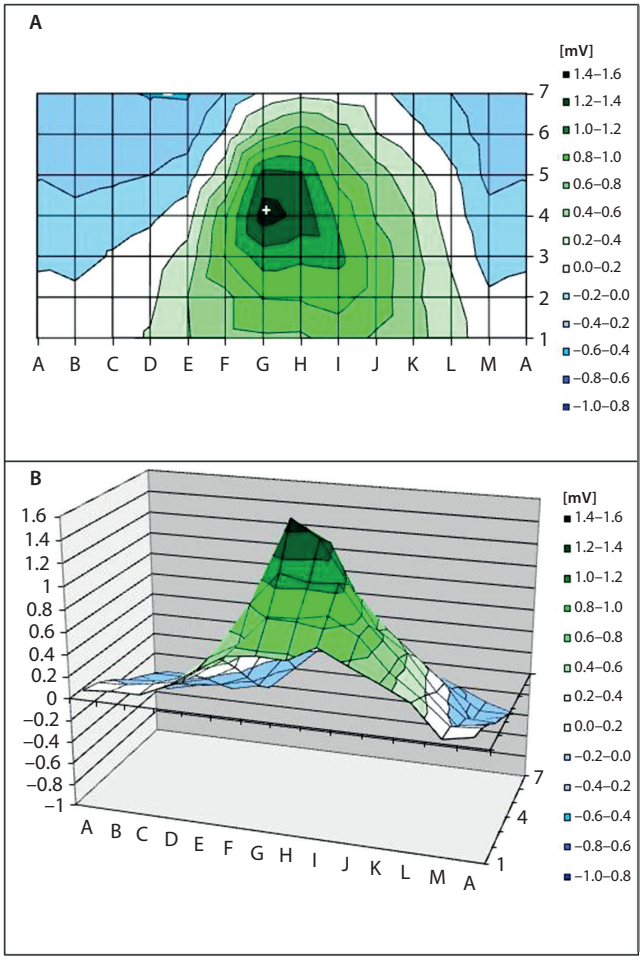

Fig. 2. Averaged isopotential map of healthy children

A – 2-dimensional; B – 3-dimensional.

stimulation of the myocardium occurs, spreading out through both branches of the bundle of His.

The maximum positive potential accumulates at the G4 electrode (1.5 mV), located in the middle of the midclavicular line in the left anterior part of the thorax. In electrocardiographic records, this area is characterized by the largest R waves in the QRS complex.

The stimulation wave spreads uniformly to the right and to the left side, which is depicted by the isolines that symmetrically fall on either side, i.e., to the right and to the left with decreasing values of the positive potentials.

Another phase of depolarization is identified on the epicardial surface of the right ventricle, including its para-apical and medial parts. Because of the larger thickness of the left ventricle, it arrives at the epicardial part a bit later.

The picture of the final phase of the spreading stimulation wave presents an upward direction of the isolines (negative potential values), visible on the mean map both on the right side of the thorax and on the shoulders.

The smallest registered potentials are seen mainly in the upper right part of the thorax, including the E7 and D7 electrodes (–0.42 mV and –0.41 mV, respectively) at the sternal line and the right parasternal line, and in the upper part of the shoulders in the right posterior axillary line (from –0.4 mV to –0.32 mV). Electrocardiographic records in this area present mainly QS complexes (without the R wave).

The distribution of isopotential lines described on the mean map for young healthy subjects is a mapped representation of the normal stimulation spread through the heart.

In turn, the distribution of isolines on the mean map plotted for the ESRD patients treated with PD (Fig. 3) only resembles the course of isolines on the map of healthy subjects in certain regions. In the PD patients, the isolines for positive potential values are initially distributed within an area similar to the one for normal subjects. However, by the left upper part of the thorax, the isolines already begin a shift toward the left lower part the thorax. The middle of the bundles, made up of positive and negative points linking the lines, is visible at the F4 electrode (the range of potential values is from –0.04 mV to 0.02 mV).

In the subsequent time interval, the patients' mean map reveals an accumulation of lines at the region between the E4, F4 electrodes along the sternal and the parasternal lines up to the G5, H5 electrodes along the midclavicular line and the left anterior axillary line.

The direction of movement of positive potential isolines clearly indicates a block in the intraventricular conduction route within the anterior fascicle of the left branch of the bundle of His. Potential values are lower than those on the map for the control group. A maximum value (+1.13 mV) stabilizes at the H3 electrode at the left anterior axillary line.

Weakening positive potentials indicate a problem with the stimulation wave spreading throughout a blocked area,

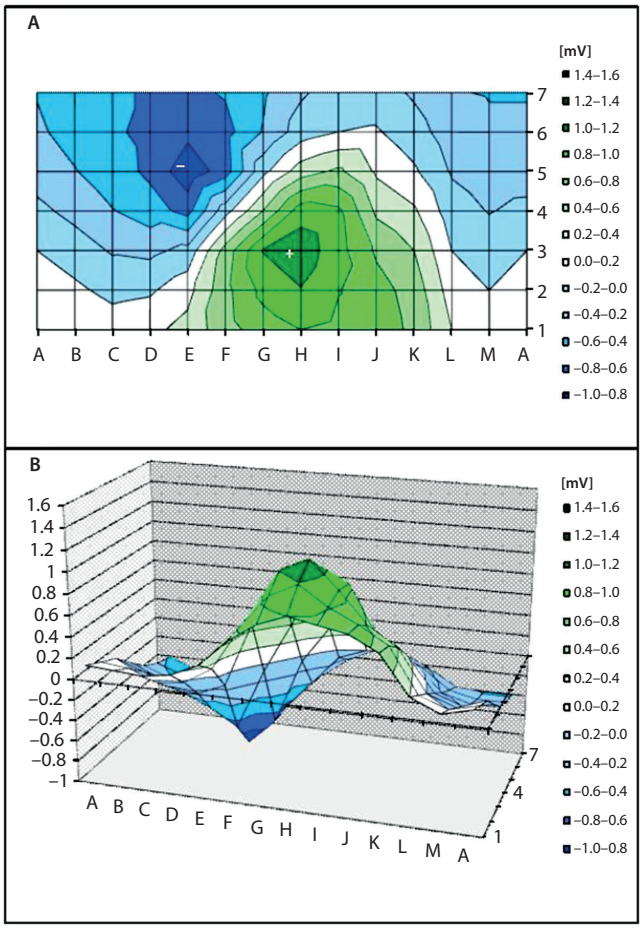

Fig. 3. Averaged isopotential map of peritoneally dialyzed children

A – 2-dimensional; B – 3-dimensional.

in which case the front of the wave tries to find any possible bypass routes. In consequence of the block at the anterior left fascicle of the bundle of His, the free wall of the posterior ventricle is stimulated with some delay via the route through the posterior bundle.

The final part of the depolarization process is observed in the right upper part of the thorax and depicted on the map with isolines of negative values. The minimum value (–0.95 mV), also lower than in the control group, is visible at the E5 electrode in the sternal line, in the anterior part of the thorax.

The above-presented pattern of isoline distribution, which may be observed on isopotential maps of all the studied patients, is characteristic of an anterior bundle block in the left branch of the bundle of His (left anterior fascicle block [LAFB]).

No such changes were observed on standard ECG tracings, though they may simply have been beyond the 12-lead ECG capture capacity.

Regarding ECHO examination, no signs of left ventricular hypertrophy were found in the examined patients on APD, as neither left ventricular mass (LVM) nor left ventricular mass index (LVMi) exceeded the 95th percentile, following the standards recommended by Khoury et al.[13] The ECHO results also showed fairly normal left ventricle systolic function, as determined by ejection fraction (EF) and shortening fraction (FS).

Discussion

In 1998, the National Kidney Foundation Task Force on Cardiovascular Disease announced an epidemic of cardiovascular disease in patients with ESRD.[14] During the subsequent years of continued observation, high mortality rates were recorded for cardiac reasons (cardiac death) not only in adult patients but also in children on renal replacement therapy. It was additionally established that the incidence of cardiac disorders did not depend on the type of dialysis therapy (hemodialysis – HD or PD), while kidney transplantation did support the normalization of cardiovascular changes, despite the administration of aggressive pharmacotherapy.[15,16] Following the data of the United States Renal Data System (USRDS) (2011), in patients with successful kidney transplantation, cardiac disorders are the second most common cause of death after infections.[6]

The application of multi-electrode ECG recording in the BSPM system has opened a new possibility for the early diagnosis of changes in the depolarization wave spreading across the heart of dialyzed patients. This process may be measured through the magnitude of potentials and through the specificity of isoline distribution on isopotential maps.

In the present study, the analysis of the isopotential maps in the examined group of peritoneally dialyzed children demonstrated a certain similarity with the control group regarding the initial phase of ventricular depolarization. This means that the stimulation process in the heart began at the same locations and time points as in healthy children. However, significant differences were observed in the further course of the stimulation process. In ESRD children on APD, a combined leftward and downward shift of the isolines began by the left upper part of the thorax, which is a clear illustration of an electrical impulse passage block in the anterior fascicle of the left branch of the bundle of His. The picture of suppressed positive potential of the electrical impulse, as observed on the isopotential maps, is direct evidence for pathological spreading of the stimulation wave within the blocked area, confirmed by the attempts of the wave front to find another, more convenient bypass.

It was clearly demonstrated in the group of peritoneally dialyzed children that the free wall of the left ventricle is stimulated with some delay through the posterior bundle of His, which results from the anterior left bundle branch block.

The pathogenesis of cardiovascular changes in children and adolescents with CKD is multifactorial, where disorders related to the primary disease and the type of therapy applied are of major significance. All these components lead to degenerative changes in cardiomyocytes, affecting

the vascular architecture and causing strains and remodeling of the left ventricle as well as calcification in the entire myocardium.

The effects of these degenerative processes include conduction disorders in the intraventricular conduction system.[1,5,7,15,16]

Parathormone (PTH) is one of the major causative factors responsible for cardiac pathologies in this population of patients. This uremic toxin is – starting in the earliest stages of CKD – significantly responsible for metabolic disorders. Following many authors, one should perceive PTH as a direct cause of impaired processes in the systolic-diastolic function of the heart in patients with CKD.[17–19]

It should be considered fairly symptomatic that high iPTH levels (also observed in our patients) support mitochondrial damage in cardiomyocytes, which in turn disturbs the energy processes in these cells.[1,12,20] Moreover, PTH shares some responsibility for the excessive influx of calcium ions into the cells, leading to suppressed or even cut-off conduction of the electrical impulse among the cardiac cells. It may therefore be assumed that the decrease of the positive electrical potential observed on the isopotential maps of dialyzed children is a manifestation of disorders in the generation and spreading of the electrical stimulation signal within the cardiac ventricles, where the anterior left fascicle block causes a delay in the stimulation of the free wall of the left ventricle.

Chronic kidney disease is characterized by the retention of inorganic phosphorus, which is assumed to play a key role in the pathogenesis of disorders, such as renal osteodystrophy or circulation diseases. Unfortunately, despite the administered therapies with agents which bind phosphates in the intestines, even such agents as calcimimetics, high serum phosphate levels are observed in approx. 30% of dialyzed patients. As is known, high P levels bind with increased serum PTH concentrations resulting from deficits of vitamin D_3 and, in consequence, are associated with blood vessel calcification and elevated morbidity and mortality rates.[21,22] Both inorganic phosphates and their esters are significant regulators of calcification processes in cells of the smooth muscles and cardiac valves.[13,22,23] The process of cardiac calcification was identified in 2003 as a risk factor for cardiovascular disease. Cardiac calcification is thought to be strongly correlated with a predisposition to the formation of atherosclerotic coronary plaque. On the other hand, coronary artery calcification is significantly accelerated in patients with CKD, being inversely proportional to the glomerular filtration rate.[24,25] Moreover, it has also been reported that the intensification of coronary calcification in CKD patients is higher than in non-CKD patients with diagnosed ischemic heart disease and, furthermore, that this factor can be regarded as an independent predictor of mortality in patients with CKD.[26]

It seems that in the ESRD children taking part in our study, hyperphosphatemia also contributes to the observed disorders of the spreading of electrical stimulation, compromising the conduction of the electrical impulse in a uremic heart. It should therefore be assumed that the increased concentrations of serum P observed in our patients was partly responsible for the delayed spread of the stimulation wave in the heart, as observed on the isopotential maps.

As Wang reported, there is growing evidence that the significant disorders of calcium metabolism, which support the calcification of blood vessels, may be a much stronger trigger of cardiac changes than hyperphosphatemia in patients with CKD.[23] Both low and high Ca concentrations in the serum of the patients in this population may be responsible for the development of cardiovascular disorders. Moreover, Ca, which is a signaling molecule in the process of electrical impulse transfer, may significantly contribute to disorders in spreading such an impulse across the conduction system of a uremic heart. In the studied group of children, Ca concentrations in serum did not present any statistically significant changes compared with the group of healthy children.

Following literature data from 2012, hypoalbuminemia, which is concomitant to CKD, is one of the most frequent disorders in these patients, while the mechanism is a result of both the primary disease and the applied renal displacement therapy.[8,17,27] According to Mitsnefes, hypoalbuminemia contributes to the development of cardiovascular disease in half of the dialyzed patients.[20]

Margetts et al. stated that the occurrence of hypoalbuminemia might be explained by primary cardiac insufficiency or vascular permeability, which disturb both the extracellular fluid balance and the peritoneal membrane transport status.[28] In our group of patients, we observed only statistically insignificantly decreased serum concentrations of albumins, compared with the healthy children. Thus, hypoalbuminemia could not have influenced the transmission of electrical stimulation in the intraventricular system of the heart.

It is quite likely that other uremic toxins may also play a significant role in the pathogenesis of cardiovascular changes in patients with ESRD; however, with our current knowledge we cannot identify any specific cardiotoxic substances.[29]

Histopathological changes in a uremic heart also seem significant for the proper functioning of the heart conduction system. Diffuse interstitial fibrosis and the loss of cardiomyocytes, including microvascular disease, lead to some instability in myocardial metabolism. In effect, functional disorders of the heart are observed, creating conditions which may support disturbances in the flow of electrical impulses.

Summing up, the method of BSPM presented in the study allows the identification of early changes in the intraventricular conduction system of the heart in children on PD. Body surface potential mapping, due to its non-invasive character, is a highly desirable technique, applied in order to evaluate changes in the functioning of the heart, especially in young populations. Cardiac monitoring of patients

with CKD with this method is very helpful in the prognosis of cardiac episodes, while the identification of disturbed conductivity in the left branch of the bundle of His in uremic patients demands special attention of medical staff.[30,31]

The rather small study group was an obvious limitation of this pilot study. It may, in some way, be justified by the objective fact that the number of children with end-stage renal failure is not large, compared with adult patients. Moreover, because of legal and formal regulations, we were only able to evaluate the children hospitalized in our hospital.

Conclusions

In peritoneally dialyzed children, intraventricular conductivity disorders were observed in the left branch of the bundle of His, as confirmed by changes seen on isopotential maps.

Body surface potential mapping is a more precise diagnostic method than standard ECG, allowing for the early identification of changes not evident on ECG recordings.

Further research involving a larger population of children with end-stage renal failure and on PD is planned in order to verify and strengthen the evidence for the preliminary findings of this study.

References

1. Chavers BM, Li S, Collins AJ, Herzog CA. Cardiovascular disease in pediatric chronic dialysis patients. *Kidney Int*. 2002;62:648–653.
2. Parekh RS. Expect the unexpected: Sudden cardiac death in dialysis patients. *Clin J Am Soc Nephro*. 2012;7:8–11.
3. Parekh RS, Carroll CE, Wolfe RA, Port FK. Cardiovascular mortality in children and young adults with end-stage kidney disease. *J Pediatr*. 2002;141:191–197.
4. Almeida FA, Machado FC, Moura JA Jr, Guimarães AC. Global and cardiovascular mortality and risk factors in patients under hemodialysis treatment. *Arq Bras Cardiol*. 2010;94:187–192,201–206,190–195.
5. Foley RN, Parfrey PS, Sarnak MJ. Clinical epidemiology of cardiovascular disease in chronic renal disease. *Am J Kidney Dis*. 1998;32 (Suppl 3):S112–S119.
6. US Renal Data System. *USRDS 2011 Annual Data Report: Atlas of Chronic Kidney Disease and End-Stage Renal Disease in the United States*. Bethesda, MD: National Institutes of Health, National Institute of Diabetes and Digestive and Kidney Diseases; 2011. https://www.usrds.org/atlas11.aspx. Accessed December 15, 2015.
7. Groothoff J, Liien M, Kar N, Wolff E, Davin J. Cardiovascular disease as a late complication of end-stage renal disease in children. *Pediatr Nephrol*. 2005;20:374–379.
8. Laszki-Szczachor K, Polak-Jonkisz D, Zwolińska D, Rusiecki L, Janocha A, Sobieszczańska M. Heart ventricular activation in VAT difference maps from children with chronic kidney disease. *Pediatr Nephrol*. 2012;27:251–259.
9. The Fourth Report on the diagnosis, evaluation and treatment of high blood pressure in children and adolescents. National High Blood Pressure Education Program Working Group on High Blood Pressure in Children and Adolescents. *Pediatrics*. 2004;114:555–576.
10. Wagner G. *Marriott's Practical Electrocardiography*. 10th ed. Philadelphia, PA: Lippincott Williams and Wilkins; 2001.
11. Spencer KT, Kimura BJ, Korcarz CE, Pellikka PA, Rahko PS, Siegel RJ. Focused cardiac ultrasound: Recommendations from the American Society of Echocardiography. *J Am Soc Echocardiogr*. 2013;26:567–581.
12. *Heart Potential Mapping System*. Tokyo: Fukuda Denshi Co., Ltd. Bulletin; 1990.
13. Khoury PR, Mitsnefes MS, Daniels SR, Kimball TR. Age specific reference intervals for indexed left ventricular mass index in children. *J Am Soc Echocardiogr*. 2009;22:709–714.
14. Levey AS, Beto JA, Coronado BE, National Kidney Foundation Task Force on Cardiovascular Disease. Controlling the epidemic of cardiovascular disease in chronic renal disease: What do we know? What do we need to learn? Where do we go from here? *Am J Kidney Dis*. 1998;32:853–906.
15. Van Biesen W, Verbeke F, Vanholder R. Cardiovascular disease in haemodialysis and peritoneal dialysis: Arguments pro peritoneal dialysis. *Nephrol Dial Transplant*. 2007;22:53–58.
16. Pego C, Rodrigues A, Ronco C. Role of peritoneal dialysis as a chronic renal replacement therapy in cardiorenal patients. *Contrib Nephrol*. 2012;178:182–188.
17. Robinson RF, Nahata MC, Sparks E, et al. Abnormal left ventricular mass and aortic distensibility in pediatric dialysis patients. *Ped Nephrol*. 2005;20:64–68.
18. Mitsnefes MM, Kimball TR, Kartal J, et al. Cardiac and vascular adaptation in pediatric patients with chronic kidney disease: Role of calcium-phosphorus metabolism. *J Am Soc Nephrol*. 2005;16:2796–2803.
19. Wanic-Kossowska M, Lehmann P, Czekalski S. Left ventricular systolic and diastolic dysfunction in patients with chronic renal failure treated with hemodialysis. *Pol Arch Med Wewn*. 2003;109:365–373.
20. Mitsnefes MM. Cardiovascular disease in children with chronic kidney disease. *J Am Soc Nephrol*. 2012;23:578–585.
21. Cozzolino M, Stucchi A, Rizzo MA, et al. Phosphate control in peritoneal dialysis. *Contrib Nephrol*. 2012;178:116–123.
22. Mozos I. Laboratory markers of ventricular arrhythmia risk in renal failure. Hyperphosphatemia: Treatment options. *Biomed Res Int*. 2014. http://dx.doi.org/10.1155/2014/509204
23. Wang AY. Calcium balance and negative impact of calcium load in peritoneal dialysis patients. *Perit Dial Int*. 2014;34:345–352.
24. Russo D, Palmiero G, De Blasio AP, Balletta MM, Andreucci VE. Coronary artery calcification in patients with CRF not undergoing dialysis. *Am J Kidney Dis*. 2004;44:1024–1030.
25. Fox CS, Larson MG, Keyes MJ, et al. Kidney function is inversely associated with coronary artery calcification in men and women free of cardiovascular disease: The framing ham heart study. *Kidney Int*. 2004;66:2017–2021.
26. Iyer H, Abraham G, Reddy YN, et al. Risk factors of chronic kidney disease influencing cardiac calcification. *Saudi J Kidney Dis Transpl*. 2013;24:1189–1194.
27. Bosch A, Ulmer HE, Keller HE, Bonzel KE, Schärer K. Electrocardiographic monitoring in children with chronic renal failure. *Pediatr Nephrol*. 1990;42:140–144.
28. Margetts PJ, McMullin JP, Rabbat CG, Churchill DN. Peritoneal membrane transport and hypoalbuminemia: Cause or effect? *Perit Dial Int*. 2000;20:14–18.
29. Segall L, Covic A. Cardiovascular disease in haemodialysis and peritoneal dialysis: Arguments for haemodialysis. *Nephrol Dial Transplant*. 2007;22:59–63.
30. Devereux RB, Alonso DR, Lutas EM, et al. Echoradiographic assessment of left ventricular hypertrophy: Comparison to necropsy findings. *Am J Cardiol*. 1986;57:450–458.
31. Scharer K, Schmidt KG, Soergel M. Cardiac function and structure in patients with chronic renal failure. *Pediatr Nephrol*. 1999;13:951–965.

Fetal *HLA-G* alleles and their effect on miscarriage

Altuğ Koç[1,A–F], Özgür Kırbıyık[1,B,D,E], Yaşar B. Kutbay[1,B,D,E], Berk Özyılmaz[1,B,D,E], Taha R. Özdemir[1,B,D,E], Özge Özer Kaya[1,B–E], Gözde Kubat[2,C], Zeynep Peker Koç[3,A,D]

[1] Genetic Diagnosis Center, Tepecik Training and Research Hospital, Health Sciences University, Izmir, Turkey
[2] Foreign Trade Department, Kazan Vocational School, Başkent University, Ankara, Turkey
[3] Allergy and Immunology Clinic, Dr. Suat Seren Chest Diseases and Surgery Training and Research Hospital, Health Sciences University, Izmir, Turkey

A – research concept and design; B – collection and/or assembly of data; C – data analysis and interpretation;
D – writing the article; E – critical revision of the article; F – final approval of the article

Advances in Clinical and Experimental Medicine, ISSN 1899-5276 (print), ISSN 2451-2680 (online) *Adv Clin Exp Med*. 2018;27(9):1233–1237

Address for correspondence
Altuğ Koç
E-mail: draltug@gmail.com

Funding sources
Financial contribution from Intron Saglik Company.

Conflict of interest
None declared

Acknowledgements
We would like to thank Intron Saglik Company for their kind financial contribution, ATQ Biotechnology Ltd. for their HLA-G typing and analysis support, and Dr. Ediz Yesilkaya for data analysis and interpretation.

Received on December 18, 2016
Reviewed on February 11, 2017
Accepted on March 22, 2017

Abstract

Background. Immunosuppression at the feto-maternal interface is crucial for a successful pregnancy outcome. Human leukocyte antigen-G (*HLA-G*) seems to be a major contributor to fetal tolerance. The *HLA-G* expression is seen in cytotrophoblasts and in maternal blood. Fetal *HLA-G* acts on decidual antigen-presenting cells (APCs), natural killers (NKs) and T cells. Recent findings revealed that defects in placentation and their consequences are associated with maternal *HLA-G* variants and their expression levels.

Objectives. The objective of this article is to investigate the relationship between fetal *HLA-G* alleles and miscarriage, which has not been investigated to date.

Material and methods. The present study includes 204 recurrent miscarriage (RM) cases who were admitted to our clinic between 2012 and 2016. Twenty-eight miscarriage products without maternal cell contamination and any known pathology were analyzed by *HLA-G* typing. In addition, 3' untranslated region (UTR) 14-base pair (bp) insertion/deletion polymorphism was also investigated by Sanger sequencing.

Results. For our population, the most frequent *HLA-G* type was G*01:01, both in the study group (30.3%) and in the control group (47%). The study revealed that the G*01:04 allele was significantly associated with miscarriage ($p = 0.007$). The 3' UTR 14bp deletion was more frequent in the miscarriage group, but there was no significant correlation.

Conclusions. *HLA-G* alleles seem to be related with miscarriage and should be considered in RM cases.

Key words: miscarriage, human leukocyte antigen-G, G*01:04, 3' untranslated region polymorphism

DOI
10.17219/acem/69692

Introduction

Human leukocyte antigen-G (*HLA-G*) is an atypical HLA (Class Ib) molecule and is mainly expressed in immune-privileged sites of the body. There are accumulating reports on the possible involvement of *HLA-G* in cancer, transplantation, allergies, and autoimmune disorders.[1–3] The role of *HLA-G* in the maintenance of maternal tolerance and in reproduction has been also widely studied.[4] Up to 50% of the endometrium of a pregnant uterus (decidua) is composed of maternal immune cells.[5] The mother is expected to generate graft-attacking antibodies and a cytotoxic T lymphocyte response to foreign paternal HLA or other antigens expressed by the fetal cells.[1] Ensuring immune tolerance to the semi-allogenic fetus is achieved by the immune modulation of decidual natural killer (NK) cells, antigen presenting cells (APCs), including dendritic cells and macrophages (innate immune system), and by regulatory T cells (adaptive immune system). Shallow fetal trophoblast invasion is likely related to a partial breakdown of maternal–fetal immune tolerance and may underlie recurrent miscarriage (RM) and preeclampsia.[5,6]

Trophoblasts strictly regulate their expression of HLA genes. HLA Class Ia (A, B and C) are not expressed by trophoblasts to prevent a maternal immune response – the exception is the mild expression of *HLA-C*. A special set of HLA Class (Ib: E, F and G) is presented on the fetal cells, which are thought to have an inhibitory effect on the maternal immune system.[1] These molecules share structural similarities with Class Ia antigens, but also have some distinct features. In contrast to Ia antigens, Class Ib antigens are not ubiquitous. Their expressions are organ-specific and conditional. Atypical Class Ib antigens have a low number of alleles and have both soluble and membrane-bound forms. On the other hand, typical Class Ia antigens are highly polymorphic and only have membrane-bound forms.[7]

The expression of *HLA-G* was first described in the placenta as the conventional *β2m*-linked, membrane-bound form. However, studies reveal that *HLA-G* has 7 splice variants, including 4 membrane-bound (*HLA-G1* to *-G4*) and 3 soluble isoforms (*HLA-G5* to *-G7*). Furthermore, membrane-bound *HLA-G1* can be shed and released as soluble *HLA-G1*. About 50 *HLA-G* alleles and 16 proteins have been reported to date.[8]

HLA-G has 7 introns and 8 exons. Exon 1 is related to a signal peptide. Exons 2, 3 and 4 encode the extracellular domains: α1, α2 and α3, respectively. Intron 4 contains a stop sequence and yields soluble *G5* and *G6* isoforms. The transmembrane domain is encoded by exon 5. Exons 6 and 7 encode the intracellular domain.

The polymorphisms of *HLA-G* have also been widely studied.[1,4,8–12] The *HLA-G* gene has 14-base pair (bp) insertion/deletion (ins/del) polymorphism in 3' untranslated region (UTR), which influences messenger RNA (mRNA) size and stability.[1] An inserted 14bp sequence probably acts as a cryptic splice site and causes a 92bp deletion in 3' UTR. As a result, *HLA-G* mRNA stability is increased.[1,8]

Recent studies have focused on the functions of *HLA-G* isoforms,[3] *HLA-G* dimers and β2-microglobulin (β2m) association.[13,14] The disulfide-linked homodimer of β2m-associated *HLA-G* is found to be the major fraction expressed by trophoblast cells.[15] *LIRB1* has been proposed as the principal ligand for the *HLA-G* dimer, which is expressed on decidual APCs, NKs and T lymphocytes. Interactions with *LIRB2*, *CD160*, *KIR2DL4*, and other receptors have also been reported.[15–17]

HLA-G alleles have been investigated in women with a history of miscarriage and in their partners, but not in conceptus material to date. One of the reasons for that is the difficulty in obtaining maternal-cell-free fetal tissues and the increased failure rates for cell culture and polymerase chain reaction (PCR). In addition to these factors, many of the miscarriage samples contain chromosomal anomalies which should be excluded from the study groups. The determination of parental *HLA-G* alleles, as in the current literature, just leads to indirect estimations about the fetal *HLA-G* status. Definite fetal *HLA-G* genotyping should be the preferred approach instead of parental genotyping, because *HLA-G* is expressed by fetal trophoblasts.[15] In this study, we aimed to find an association between fetal *HLA-G* type, *HLA-G* 3' UTR 14bp ins/del polymorphism and miscarriage, and to determine the most common *HLA-G* alleles in our population.[18]

Material and methods

Study and control groups

The study group consisted of 28 cases out of 204 patients referred to our center between 2012 and 2016 who had at least 2 miscarriages (range: 2–4). All of the mothers were investigated for hereditary thrombophilia. Miscarriage samples were karyotyped and analyzed by quantitative fluorescent polymerase chain reaction (QF-PCR) for aneuploidies of chromosomes 13, 15, 16, 18, 21, and 22, and sex chromosomes. The short tandem repeat (STR) markers of a QF-PCR kit were also used to detect maternal cell contamination. At least 10 informative STR markers were needed to exclude maternal cell contamination. The samples with 46,XY karyotype or 46,XX karyotype with no maternal contamination were included. Miscarriage materials with chromosomal anomalies, culture failure or PCR failure were excluded. The mothers with thrombophilic mutations, a history of in vitro fertilization (IVF) or any known obstetric reason for miscarriage, such as uterine malformations, antiphospholipid syndrome or hormone disorders, were also excluded. Fetuses with anencephaly, increased nuchal translucency, anhydramnios, early rupture of membranes, or other major malformations on fetal ultrasonography were excluded. The mean age

of mothers was 30.3 years and the majority of pregnancy losses occurred during the 1st trimester (gestational weeks 5–15). Twenty-one healthy individuals representing successful deliveries were used as controls for *HLA-G* types determined by the sequencing of exons 2, 3 and 4. For 3' UTR polymorphism, 101 healthy individuals were used as controls. The project received the permission of the local Tepecik Training and Research Hospital ethics committee.

Routine genetic workup of miscarriage

The routine genetic investigation of miscarriage cases included a conventional cytogenetic analysis of the miscarriage sample by GTG banding (550 bands) and a QF-PCR analysis with 26 STR markers (Compact v3 QF-PCR; Devyser, Stockholm, Sweden). Hereditary thrombophilia mutations (Factor V Leiden and Factor II G20210A) were investigated by real-time PCR (FV R2 [H1299R] QLP 3.0; Prothrombin QLP 3.0, Iontek, Istanbul, Turkey) from maternal blood.

HLA-G typing

Exons 2, 3 and 4 were sequenced for *HLA-G* typing. Commercial primer/oligonucleotide sets dedicated for high-resolution HLA sequencing-based typing (SBT) for the identification of HLA alleles were used according to the manufacturer's protocols (SBTexcellerator® HLA Kits; GenDx, Utrecht, the Netherlands).

HLA-G 3' UTR 14bp ins/del polymorphism (rs371194629)

The polymorphism was investigated by Sanger sequencing. The PCR primers were F: 5'-TGT GAA ACA GCT GCC CTG TGT-3' and R: 5'-GTC TTC CAT TTA TTT TGT-3'. The PCR conditions were as follows: the first denaturation was at 95°C for 10 min; 35 cycles of denaturation at 95°C for 30 s, annealing at 60°C for 45 s, and elongation at 72°C for 45 s; and the last elongation was at 72°C for 7 min. The PCR products were purified as follows: 5 µL of PCR products were treated with 2 µL of ExoSAP-IT enzyme (USB; Affymetrix, Santa Clara, USA) at 37°C for 30 min and at 85°C for 15 min. Sequence PCR (cycle sequencing) was done using a reverse PCR primer (5 pmol) and a BigDye® Terminator v. 3.1 Cycle Sequencing Kit (Lifetechnologies, Waltham, USA). The sequence PCR conditions were as follows: at 96°C for 10 s, at 50°C for 5 s and at 60°C for 4 min; the cycle was repeated 25 times. The products of sequence PCR were purified (the 2nd purification) by spin colon (ZR DNA Sequencing Clean-up Kit™, Zymo Research, Irvine, USA). Sanger sequencing was performed by capillary electrophoresis after 5 min of denaturation (3500 Genetic Analyzer; Lifetechnologies). The obtained sequences were analyzed using SeqScape® software v. 3.0 (Applied Biosystems by Life Technologies, Carlsbad, USA).

Statistical analysis

Allelic and genotypic frequencies were determined from the observed genotype counts, and the expectations of the Hardy-Weinberg equilibrium were evaluated by χ^2 analysis. The χ^2 test was used for comparisons between allelic and genotypic frequencies. Statistical analysis was done using SPSS v. 13 statistical software (SPSS Inc., Chicago, USA). A p-value <0.05 was considered statistically significant.

Results

In all groups, there were 10 *HLA-G* types, coded for 4 distinct proteins, and their combinations gave rise to 8 distinct genotypes. The most frequent *HLA-G* type was G*01:01 both in the study group (30.3%) and in the control group (47%). The findings are summarized in Table 1. G*01:01/*01:01 was the most frequent genotype for the study and control groups: its frequency was 35.7% in the study group and 48% among the controls. The genotypes G*01:04/*01:04, G*01:03/*01:04 and G*01:03/*01:06 were found only in the study group, and the G*01:06/*01:06 genotype was found only in the control group (Table 2). There was a significant association between the *HLA-G* allele G*01:04 and miscarriage (p = 0.007).

Table 1. Comparison of study and control groups' *HLA-G* types

HLA-G types*	Frequencies in miscarriage samples, % (n)	Frequencies in control samples, % (n)	p-value
01:01	30.3 (17/56)	47 (19/42)	0.189
01:01:01	12.5 (7/56)	17.5 (7/42)	
01:01:02	7.1 (4/56)	5 (2/42)	
01:01:03	3.5 (2/56)	2.5 (1/42)	
01:01:12	1.7 (1/56)	–	
01:06	7.15 (4/56)	22.5 (9/42)	0.176
01:03	7.15 (4/56)	5 (2/42)	0.299
01:04:01	12.5 (7/56)	5 (2/42)	0.007**
01:04:04	12.5 (7/56)	–	
01:04	5.3 (3/56)	–	

The study group consisted of 28 miscarriage samples (56 alleles) and the control group included 21 blood samples (42 alleles) from healthy individuals. There were 10 *HLA-G* types that code 4 proteins. * The *HLA-G* types with the same initial 2 digits have the same amino acid (aa) sequence, e.g., 01:04:01 and 01:04:04 code for the same specific protein; ** statistically significant.
For HLA nomenclature, see http://hla.alleles.org/nomenclature/naming.html.

The results of 3' UTR polymorphism are presented in Table 3. The frequency distribution of alleles was in Hardy-Weinberg equilibrium. In the miscarriage samples, the most frequent allele was the 14bp deletion (57%) and the most frequent genotype was homozygous deletion (39%). Homozygous deletion was approx. 2 times more frequent

in the miscarriage group than in the controls. In the control group, the most frequent allele was the allele with insertion (54%), and heterozygosity was the most frequent genotype (53%).

Table 2. Comparison of *HLA-G* genotype frequencies in study and control groups

HLA-G genotypes**	Frequencies in miscarriage samples, % (n)	Frequencies in control samples, % (n)	p-value
*01:01/*01:01	35.7 (10/28)	48 (10/21)	0.128
*01:01/*01:04	25 (7/28)	9.5 (2/21)	
*01:04/*01:04	14.3 (4/28)	–	
*01:01/*01:06	10.7 (3/28)	23.5 (5/21)	
*01:03/*01:04	7.1 (2/28)	–	
*01:01/*01:03	3.6 (1/28)	9.5 (2/21)	
*01:03/*01:06	3.6 (1/28)	–	
*01:06/*01:06	–	9.5 (2/21)	

The study group consisted of 28 miscarriage samples and the control group included 21 blood samples from healthy individuals. There were 8 *HLA-G* genotypes. * The same genotype name was used for genotypes specific to the same protein, e.g., G*01:04:01/*01:04:04 was shown as *01:04/*01:04.

Table 3. Frequency distribution of the 3' UTR 14bp ins/del polymorphism (rs371194629) in miscarriage and control samples

Alleles	Frequencies in miscarriage samples, % (n)	Frequencies in control samples, % (n)	p-value
Insertion	43 (24/56)	54 (108/202)	0.301
Deletion	57 (32/56)	46 (94/202)	0.082
Genotypes			
Heterozygous	36 (10/28)	53 (54/101)	0.215
Homozygous insertion	25 (7/28)	27 (27/101)	
Homozygous deletion	39 (11/28)	20 (20/101)	

The study group consisted of 28 miscarriage samples (56 alleles) and the control group included 101 blood samples (202 alleles) from healthy adults.

Discussion

The β2m-associated/free *HLA-G* dimers are shown to be expressed from trophoblasts.[13,14] *HLA-G* stimulates trophoblastic invasion.[3] In addition to this, it is one of the major tolerogenic molecules in pregnancy.[1,2] The *HLA-G* expression is studied in preeclampsia, recurrent miscarriage and IVF.[8] The results indicated an association between an *HLA-G* expression pattern and a risk of RM as well as other disorders.[7]

We proposed that the fetal *HLA-G* alleles may underlie miscarriage and that the condition may recur, so we could find the miscarriage-prone *HLA-G* alleles in the conceptus material of mothers with a history of miscarriage. Healthy adults were used as controls and they were assumed not to carry miscarriage-prone alleles. We investigated samples of 204 miscarriage cases that had at least 1 previous miscarriage. Triploidy (9 cases), trisomy 15 (8 cases), trisomy 16 (6 cases), and 45,X (5 cases) were the leading causes of miscarriage in our series, and all cases with genetic pathology were excluded from the study. Twenty-eight out of 204 samples from distinct mothers constituted our study group.

There were 10 *HLA-G* types coded for 4 specific proteins (Table 1) and 8 genotypes were determined in all groups (Table 2). The G*01:04 allele was found in a homozygous state in 4 cases of the study group (14.3%) and in none of the controls. There was a significant correlation between the fetal *HLA-G* allele G*01:04 and miscarriage ($p = 0.007$). As an interesting point, all the samples with the G*01:04 allele also had the 14bp deletion allele. The G*01:04 allele may be linked with the 14bp deletion and had to be investigated in our population.

Ober et al. showed that a variation in the parental *HLA-G* promoter influences miscarriage rates. They hypothesized that the transmission of a high-risk allele from either parent to the fetus would be associated with fetal loss.[10] Maternal homozygosity for 14bp insertion polymorphism has been proposed to predispose to miscarriage.[11] We found that the allele with the 3' UTR 14bp deletion polymorphism was the most frequent allele in the study group (57%). The homozygous genotype of the same allele was about 2 times more common in the study group than in the controls (39% vs 20%). The *HLA-G* allele with insertion was the most frequent (54%) in the control group (Table 3). The 14bp deletion of 3' UTR seems to be related with miscarriage, but the restricted number of study group subjects ($n = 28$) unfortunately prevented any statistical association to be revealed.

In conclusion, fetal G*01:04 *HLA-G* type and the 3' UTR 14bp deletion polymorphism may underlie miscarriages, and investigations of *HLA-G* alleles with a larger sample of miscarriage products and related immune components (such as *LIRB1* and NKs) may contribute to a better understanding of the miscarriage process.

References

1. Hunt JS, Petroff MG, McIntire RH, Ober C. HLA-G and immune tolerance in pregnancy. *FASEB J*. 2005;19:681–693.
2. Favier B, HoWangYin K-Y, Wu Y, et al. Tolerogenic function of dimeric forms of HLA-G recombinant proteins: A comparative study in vivo. *PLoS One* 6(7): e21011. https://doi.org/10.1371/journal.pone.0021011
3. Guo Y, Lee CL, So KH, et al. Soluble human leukocyte antigen-g5 activates extracellular signal-regulated protein kinase signaling and stimulates trophoblast invasion. *PLoS One*. 2013;8(10):e76023. doi: 10.1371/journal.pone.0076023
4. Larsen MH, Bzorek M, Pass MB, et al. Human leukocyte antigen-G in the male reproductive system and in seminal plasma. *Mol Hum Reprod*. 2011;17(12):727–738.
5. Hsu P, Nanan RKH. Innate and adaptive immune interactions at the fetal-maternal interface in healthy human pregnancy and pre-eclampsia. *Front Immunol*. 2014;28:125.

6. Zhao L, Purandare B, Zhang J, Hantash BM. β2-Microglobulin-free HLA-G activates natural killer cells by increasing cytotoxicity and pro-inflammatory cytokine production. *Hum Immunol*. 2013;74:417–424.
7. Mosaferi E, Majidi J, Mohammadian M. HLA-G expression pattern: Reliable assessment for pregnancy outcome prediction. *Adv Pharm Bull*. 2013;3:443–446.
8. Dahl M, Djurisic S, Hviid TV. The many faces of human leukocyte antigen-G: Relevance to the fate of pregnancy. *J Immunol Res*. 2014; 591489. doi: 10.1155/2014/591489
9. Warner CM, Tyas DA, Goldstein C, Comiskev M, Cohen J, Brenner CA. Genotyping: The HLA system and embryo development. *Reprod Biomed Online*. 2002;4:133–139.
10. Ober C, Aldrich CL, Chervoneva I, et al. Variation in the HLA-G promoter region influences miscarriage rates. *Am J Hum Genet*. 2003;72: 1425–1435.
11. Christiansen OB, Kolte AM, Dahl M, et al. Maternal homozygocity for a 14 base pair insertion in 3′ UTR of the HLA-G gene and carriage of HLA class II alleles restricting HY immunity predispose to unexplained secondary recurrent miscarriage and low birth weight in children born to these patients. *Hum Immunol*. 2012;73:699–705.
12. Jassem RM, Shani WS, Loisel DA, Sharief M, Billstrand C, Ober C. HLA-G polymorphisms and soluble HLA-G protein levels in women with recurrent pregnancy loss from Basrah province in Iraq. *Hum Immunol*. 2012;73:811–817.
13. Apps R, Gardner L, Sharkey AM, Holmes N, Moffett A. A homodimeric complex of *HLA-G* on normal trophoblast cells modulates antigen-presenting cells via LILRB1. *Eur J Immunol*. 2007;37:1924–1937.
14. Morales PJ, Pace JL, Platt JS, Langat DK, Hunt JS. Synthesis of beta (2)-microglobulin-free, disulphide-linked HLA-G5 homodimers in human placental villous cytotrophoblast cells. *Immunology*. 2007; 122:179–188.
15. Kuroki K, Maenaka K. Immune modulation of HLA-G dimer in maternal-fetal interface. *Eur J Immunol*. 2007;37:1727–1729.
16. Clements CS, Kjer-Nielsen L, Kostenko L, et al. Crystal structure of *HLA-G*: A nonclassical MHC class I molecule expressed at the fetal-maternal interface. *Proc Natl Acad Sci*. 2005;102:3360–3365.
17. Yan WH, Fan LA. Residues Met76 and Gln79 in HLA-G alpha1 domain involve in KIR2DL4 recognition. *Cell Res*. 2005;15:176–182.
18. Kuroshli Z, Gourabi H, Bazrgar M, Sanati MH, Bahraminejad E, Anisi K. *HLA-G* allele and haplotype frequencies in a healthy population of Iran. *Iran J Allergy Asthma Immunol*. 2014;13:207–213.

Phosphorus is an independent risk factor for the progression of diabetic nephropathy

Haiyan Xiang[A–D], Haitao Zhang[A,E], Minlin Zhou[C], Song Jiang[C], Lihua Zhang[B], Dacheng Chen[C], Zhihong Liu[E]

National Clinical Research Center of Kidney Diseases, Jinling Hospital, Nanjing University School of Medicine, China

A – research concept and design; B – collection and/or assembly of data; C – data analysis and interpretation; D – writing the article; E – critical revision of the article; F – final approval of the article

Advances in Clinical and Experimental Medicine, ISSN 1899-5276 (print), ISSN 2451-2680 (online) *Adv Clin Exp Med*. 2018;27(9):1239–1245

Address for correspondence
Haitao Zhang
E-mail: htzhang136@163.com

Funding sources
None declared

Conflict of interest
None declared

Acknowledgements
All samples were collected from the Renal Biobank of National Clinical Research Center of Kidney Diseases. This work was supported by the National Key Technology R&D Program (2013BAI09B04, 2015BAI12B05), the Jiangsu Provincial clinical science and technology project (BL2012007) and the Innovation Capability Development Project of Jiangsu Province (BM2015004).

Received on November 15, 2016
Reviewed on April 1, 2017
Accepted on April 2, 2017

Abstract

Background. Serum phosphorus is thought to be an important risk factor for the progression of chronic kidney disease (CKD). However, the association of serum phosphorus with disease progression in patients with different causes of kidney diseases remains to be elucidated.

Objectives. The aim of this study was to estimate the effect of serum phosphorus on disease progression in 2 cohorts of CKD with different causes.

Material and methods. A total of 591 patients with diabetic nephropathy and 957 patients with IgA nephropathy from the National Clinical Research Center of Kidney Diseases, Nanjing, China, with biopsy-proven kidney disease, stage 1–4 CKD and a follow-up of at least 1 year were recruited. We evaluated the relationship between the baseline phosphorus category and the disease progression in the 2 cohorts.

Results. Multivariate Cox regression analyses indicated that the risk of the endpoint event was 1.68-fold higher (95% confidence interval (CI): 0.95–2.91) in IgA nephropathy patients and 2.88-fold higher (95% CI: 1.12–5.04) in diabetic nephropathy patients with the highest quartile of serum phosphorus compared with the risk of those with the lowest quartile.

Conclusions. The association of serum phosphorus with the progression of CKD may vary in specific CKD patient subgroups. Serum phosphorus is independently associated with the progression of kidney disease in patients with diabetic nephropathy.

Key words: risk factors, chronic kidney disease, phosphorus, IgA nephropathy, diabetic nephropathy

DOI
10.17219/acem/70094

Introduction

Chronic kidney disease (CKD) has become a major worldwide public health issue due to its increasing prevalence, poor outcomes and high cost of treatment for kidney failure.[1] Early diagnosis and proper management of CKD and its risk factors are crucial for slowing the progression of the disease. In addition to the common risk factors of CKD progression, a growing body of evidence has suggested a link between serum phosphorous and the progression of CKD.[2]

Hyperphosphatemia is associated with an increased rate of hyperparathyroidism, mineral and bone disorder (MBD), vascular calcifications, cardiovascular events and mortality, and it has been demonstrated to be an independent risk factor for the progression of CKD.[2,3] However, some studies have failed to reveal such a relationship between serum phosphorous and the progression of CKD.[4] Notably, most of the existing data concerning the relationship between serum phosphorus and the prognosis of CKD did not include a sufficiently long follow-up period, and comparisons between different underlying kidney diseases have remained unclear. Some studies have shown differences in phosphorus metabolism in patients with diabetic nephropathy vs non-diabetic nephropathy;however, the relationship between serum phosphorus and CKD progression is unclear.[5,6]

We studied 2 cohorts that were treated at our center from August 2003, including patients with biopsy-positive IgA nephropathy and diabetic nephropathy with stage 1–4 CKD.[7,8] We investigated the association of higher serum phosphorus with disease progression in patients with different causes of kidney disease.

Material and methods

Patients and data collection

All the samples and data were collected from the Renal Biobank of the National Clinical Research Center of Kidney Diseases, Nanjing, China. The study protocols were approved by the Ethical Committee of Jinling Hospital, Nanjing, China. Two cohorts of diabetic nephropathy and IgA nephropathy with stage 1–4 CKD according to the 2012 Kidney Disease: Improving Global Outcomes (KDIGO) clinical practice guidelines for CKD from the renal division of Nanjing Jinling Hospital were enrolled from August 2003 to October 2014.[9] All patients were biopsy-diagnosed and regularly followed up at our facility. The diagnostic criteria for diabetic nephropathy and IgA nephropathy were described in 2 previous studies.[7,8] The exclusion criteria included patients with the following characteristics: 1. an estimated glomerular filtration rate (eGFR) of <15 mL/min/1.73 m^2, receiving dialysis or kidney transplant; 2. age of <18 years; 3. followed for less than 1 year; 4. with incomplete medical records. Baseline clinical and laboratory parameters were collected, including general characteristics (e.g., age, gender, primary disease, history of diabetes mellitus and hypertension) and medication history (e.g., angiotensin-converting enzyme inhibitors – ACEIs, angiotensin II receptor blockers – ARBs, sodium bicarbonate, calcium, activated vitamin D, steroids, diuretics, or lipid-lowering drugs). All participants provided 12-h-fasting blood samples for laboratory tests (serum calcium and phosphorus, intact parathyroid hormones (iPTH), blood glucose, total cholesterol, triglycerides, high-density lipoprotein cholesterol, low-density lipoprotein cholesterol, urea, creatinine, uric acid, albumin, routine urinalysis, and urine sediment) and 24-h urine samples for a proteinuria test. Two BP measurements were taken using a mercury sphygmomanometer after 5 min of rest, and the average was used in the analyses. Hypertension was defined as a systolic blood pressure (BP) of ≥140 mm Hg, a diastolic BP of ≥90 mm Hg and/or the use of antihypertensive medications; body mass index (BMI) was calculated based on weight and height (weight [kg]/height [m^2]).

We estimated eGFR using the Chronic Kidney Disease Epidemiology Collaboration (CKD-EPI) 2009 creatinine equation.[10]

Patients received regular follow-up care 2–4 times per year in the outpatient ward and the information collected at each visit was recorded. During the follow-up period, we maintained the patient's BP in the normal range; glycated hemoglobin (HbA_{1c}) was maintained at about 6.5% in patients with diabetes. End points were validated by at least 2 physicians. The endpoint events included the following: a sustained doubling of creatinine, an eGFR of <15 mL/min/1.73 m^2, and dialysis for more than 3 months or transplantation.

Statistical analysis

All data was analyzed using the statistical software SPSS 19.0 (SPSS Inc., Chicago, USA) and Stata/SE software v. 12 (Stata Corp, College Station, USA). Normally distributed variables are expressed as mean ±SD and non-parametric variables are expressed as medians (ranges or interquartile ranges). Differences between the 2 groups were analyzed by Student's t-test (normally distributed, homogeneity of variance), the Welch-Satterthwaite t-test (normally distributed, heterogeneity of variance), or the Wilcoxon rank sum test (non-normally distributed). Differences between more than 2 groups were analyzed by analysis of variance (ANOVA) for continuous variables. Categorical variables are expressed as percentages and were compared using the Pearson's χ^2 test. All p-values were 2-tailed, and values <0.05 were considered statistically significant. Patients were grouped into 4 strands based on the quartile of serum phosphorus at baseline. Time-to-event survival analysis using Cox proportional hazard modeling was performed to evaluate the relationship between serum phosphorus and the endpoint event.

Results

General clinical and laboratory data at baseline is shown in Tables 1 and 2. A total of 591 patients were diagnosed with diabetic nephropathy. The median follow-up period was 40 months, and the average eGFR was 73.3 ±30.6 mL/min/1.73 m^2. IgA nephropathy was diagnosed in 957 patients; additionally, the median follow-up period for this group was 83 months, and the average eGFR was 84.7 ±32.9 mL/min/1.73 m^2. Patients with diabetic nephropathy were older, had a higher level of serum phosphorus and a higher incidence of hypertension.

At baseline, participants with higher serum phosphorus levels tended to have higher proteinuria, higher cholesterol, higher uric acid, lower eGFRs, and lower albumin. Additionally, participants with higher serum phosphorus in IgA nephropathy had higher triglyceride levels, and patients with diabetic nephropathy had a higher incidence of hypertension.

During the follow-up period, 208 participants (35.2%) with diabetic nephropathy and 166 patients (17.3%) with IgA nephropathy reached the endpoint. The incidence rates of reaching endpoint were 25 (95% confidence interval (CI): 18, 32) and 88 (95% CI: 70, 102) per 1,000 person-years for patients with IgA nephropathy and diabetic nephropathy, respectively. Patients were grouped into 4 strands based on the quartile of serum phosphorus at baseline. In the highest phosphorus quartile group, 26.8% of IgA nephropathy patients and 57.7% of diabetic nephropathy patients reached the endpoint; these were significantly higher percentages than those of patients in the lowest quartile group. Participants in the higher serum phosphorus quartile groups had a higher cumulative incidence of endpoint events (log-rank $p < 0.001$; Fig. 1).

In diabetic nephropathy patients, univariate Cox regression revealed that the risk of experiencing an endpoint event was 5.99 times higher (95% CI: 3.51–10.23; $p < 0.001$) in patients in the highest phosphorus quartile group than in patients in the lowest quartile group. After adjusting for age, gender, the presence of hypertension, albumin, total cholesterol, triglycerides, high-density lipoprotein cholesterol, low-density lipoprotein cholesterol, urea, calcium, uric acid, BMI, iPTH, proteinuria, and eGFR, multivariate Cox regression indicated that the risk of reaching an endpoint event was 2.88 times higher (95% CI: 1.12–5.04; $p = 0.024$) in the highest quartile group.

In IgA nephropathy patients, univariate Cox regression indicated that the risk of an endpoint event was 2.78 times higher (95% CI: 1.75–4.43; $p < 0.001$) for patients in the

Table 1. Baseline characteristics of patients with IgA nephropathy by quartiles of serum phosphorus

Parameter	Phosphorus category				p-value
	quartile 1	quartile 2	quartile 3	quartile 4	
	n = 239 (25.0%)	n = 217 (22.7%)	n = 262 (27.3%)	n = 239 (25.0%)	
Serum phosphorus [mmol/L]	0.9 ±0.1	1.1 ±0.1	1.2 ±0.1	1.4 ±0.1	<0.001
Age [years]	38.8 ±9.2	37.2 ±9.3	35.3 ±9.0	34.2 ±9.7	<0.001
Male, n (%)	160 (66.9)	106 (48.8)	134 (51.1)	134 (56.1)	0.065
Hypertension, n (%)	106 (44.4)	96 (44.2)	104 (39.7)	119 (49.8)	0.134
BMI [kg/m^2]	24.7 ±3.5	24.8 ±2.7	24.2 ±3.6	23.9 ±3.1	0.092
eGFR [mL/min/1.73 m^2]	85.5 ±30.5	88.5 ±30.3	86.5 ±33.7	78.5 ±35.8	0.007
eGFR stage, n (%)					
≥90	120 (25.6)	117 (25.0)	132 (28.2)	99 (21.2)	0.142
60–89	55 (25.5)	49 (22.7)	65 (30.1)	47 (21.7)	0.089
45–59	33 (26.2)	27 (21.4)	25 (19.8)	41 (32.6)	<0.001
30–44	24 (26.4)	18 (19.8)	20 (21.9)	29 (31.9)	<0.001
15–29	7 (12.5)	6 (10.7)	20 (35.7)	23 (41.1)	<0.001
Creatinine [mg/dL]	1.1 ±0.5	1.1 ±0.5	1.2 ±0.6	1.3 ±0.7	<0.001
Urea nitrogen [mg/dL]	16.1 ±5.8	16.6 ±6.9	17.2 ±8.5	20.7 ±12.1	<0.001
Uric acid [µmol/L]	376.7 ±101.6	365.5 ±107.6	392.7 ±115.1	407.3 ±118.6	<0.001
Albumin [g/L]	41.2 ±5.2	41.1 ±5.1	40.1 ±5.3	38.7 ±6.3	<0.001
Total cholesterol [mmol/L]	4.9 ±1.4	4.7 ±1.2	4.9 ±1.3	5.3 ±1.9	0.002
Triglyceride [mmol/L]	2.0 ±1.5	1.6 ±0.9	1.7 ±1.1	1.8 ±1.5	0.003
Calcium [mmol/L]	2.2 ±0.1	2.2 ±0.2	2.2 ±0.2	2.2 ±0.1	0.964
Proteinuria [g/24 h]	1.1 ±0.9	1.2 ±1.1	1.2 ±1.1	1.5 ±1.2	<0.001
Fasting blood glucose [mmol/L]	5.1 ±1.3	5.3 ±1.5	4.9 ±1.8	5.2 ±1.6	0.526
LDL-cholesterol [mmol/L]	3.5 ±1.8	3.8 ±1.5	3.2 ±1.3	3.5 ±1.2	0.213
HDL-cholesterol [mmol/L]	1.0 ±0.8	0.9 ±0.5	1.1 ±0.9	1.1 ±0.8	0.329
iPTH [pg/mL]	42.9 ±32.8	54.3 ±32.2	88.1 ±64.5	190.9 ±103.6	<0.001

BMI – body mass index; eGFR – estimated glomerular filtration rate; LDL – low density lipoprotein; HDL – high density lipoprotein; iPTH – intact parathyroid hormone.

Table 2. Baseline characteristics of patients with diabetic nephropathy by quartiles of phosphorus

Parameter	Phosphorus category				p-value
	quartile 1	quartile 2	quartile 3	quartile 4	
	n = 145 (24.5%)	n = 141 (23.9%)	n = 156 (26.4%)	n = 149 (25.2%)	
Serum phosphorus [mmol/L]	1.0 ±0.1	1.2 ±0.1	1.3 ±0.1	1.5 ±0.2	<0.001
Age [years]	50.0 ±8.3	50.5 ±8.9	48.9 ±9.0	48.3 ±10.5	0.192
Male, n (%)	98 (67.5)	96 (68.1)	98 (62.8)	88 (59.0)	0.073
Hypertension, n (%)	101 (69.7)	112 (79.4)	124 (79.5)	127 (85.2)	0.012
BMI [kg/m^2]	26.1 ±3.5	25.9 ±3.7	25.2 ±3.5	25.1 ±3.3	0.059
eGFR [mL/min/1.73 m^2]	84.2 ±24.1	80.6 ±30.3	69.5 ±29.9	59.7 ±28.5	<0.001
eGFR stage, n (%)					
≥90	71 (33.5)	65 (30.7)	50 (23.5)	26 (12.3)	<0.001
60–89	42 (28.2)	37 (24.8)	35 (23.5)	35 (23.5)	<0.001
45–59	15 (15.6)	16 (16.7)	31 (32.3)	34 (35.4)	<0.001
30–44	14 (15.2)	17 (18.2)	27 (29.0)	35 (37.6)	<0.001
15–29	3 (7.3)	6 (14.6)	13 (31.7)	19 (46.3)	<0.001
Creatinine [mg/dL]	1.1 ±0.4	1.1 ±0.5	1.3 ±0.6	1.5 ±0.6	<0.001
Urea nitrogen [mg/dL]	18.7 ±6.5	20.7 ±8.6	22.6 ±8.8	29.0 ±11.8	<0.001
Uric acid [µmol/L]	350.5 ±98.1	372.3 ±96.0	381.9 ±99.8	401.8 ±101.8	<0.001
Albumin [g/L]	44.0 ±5.7	41.7 ±7.6	38.7 ±7.3	37.0 ±7.1	<0.001
Total cholesterol [mmol/L]	4.9 ±1.2	5.5 ±2.2	5.7 ±1.9	6.0 ±1.8	0.003
Triglyceride [mmol/L]	2.2 ±0.9	2.3 ±1.3	2.0 ±1.1	2.0 ±1.1	0.389
Calcium [mmol/L]	0.8 ±0.4	0.9 ±0.5	0.9 ±0.5	0.9 ±0.6	0.207
Proteinuria [g/24 h]	1.8 ±1.3	2.3 ±1.7	2.5 ±1.5	2.8 ±1.9	<0.001
Fasting blood glucose [mmol/L]	7.2 ±1.6	7.3 ±1.3	6.9 ±1.8	7.1 ±2.2	0.264
LDL-cholesterol [mmol/L]	3.4 ±1.9	3.7 ±1.7	3.5 ±1.3	3.8 ±1.6	0.286
HDL-cholesterol [mmol/L]	1.1 ±0.3	0.9 ±0.3	1.1 ±0.5	1.0 ±0.6	0.516
HbA_{1c} [%]	7.2 ±1.8	7.3 ±1.5	7.3 ±1.6	7.4 ±1.2	0.132
iPTH [pg/mL]	50.9 ±23.8	65.7 ±22.5	96.1 ±52.3	205.9 ±95.6	<0.001

BMI – body mass index; eGFR – estimated glomerular filtration rate; LDL – low density lipoprotein; HDL – high density lipoprotein; HbA1c – hemoglobin A1c; iPTH – intact parathyroid hormone.

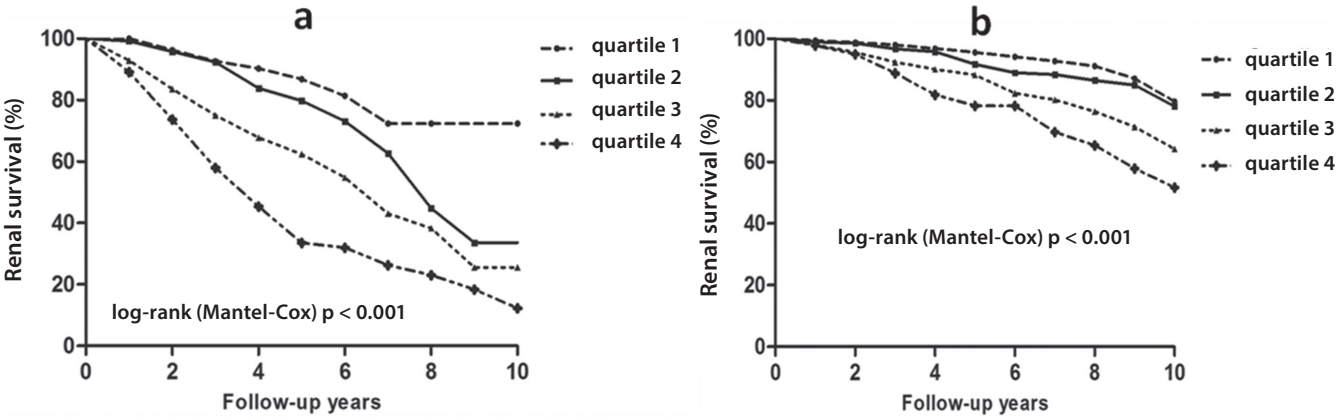

Fig. 1. Renal survival curves according to the quartile of serum phosphorus in the subgroups of CKD patients

A – diabetic nephropathy; B – IgA nephropathy.

highest phosphorus quartile group than for patients in the lowest quartile group. After adjusting for risk factors, the risk of reaching an endpoint was attenuated such that statistical significance was lost (HR 1.68; 95% CI: 0.95–2.91; p = 0.086) (Table 3).

Subgroup multivariate Cox analysis was performed for patients with an eGFR of more or less than 60 mL/min/1.73 m^2. In diabetic nephropathy patients, the highest quartile of phosphorous level predicted a greater risk of the endpoint (HR 5.37, (95% CI: 1.61–12.26; p = 0.009)) in the eGFR ≥ 60 mL/min/1.73 m^2 group, as shown in Fig. 2 A. Multivariate Cox regression showed no correlation between serum phosphorus and the progression of kidney disease in IgA nephropathy, as shown in Fig. 2 B.

Table 3. Cox regression of prognosis associated with baseline serum phosphorus in diabetic nephropathy and IgA nephropathy

Serum phosphorus	Diabetic nephropathy		IgA nephropathy	
	HR (95% CI)	p-value	HR (95% CI)	p-value
Unadjusted				
Quartile 1 (ref)	1		1	
Quartile 2	2.47 (1.37, 4.45)	0.003	1.05 (0.61, 1.81)	0.85
Quartile 3	4.17 (2.42, 7.17)	<0.001	1.87 (1.16, 3.01)	0.01
Quartile 4	5.99 (3.51, 10.23)	<0.001	2.78 (1.75, 4.43)	<0.001
Multivariate adjusted				
Quartile 1 (ref)	1		1	
Quartile 2	1.81 (0.82, 4.02)	0.143	0.95 (0.59, 1.76)	0.638
Quartile 3	2.14 (1.02, 4.47)	0.044	1.52 (0.85, 2.72)	0.098
Quartile 4	2.88 (1.12, 5.04)	0.024	1.68 (0.95, 2.91)	0.082

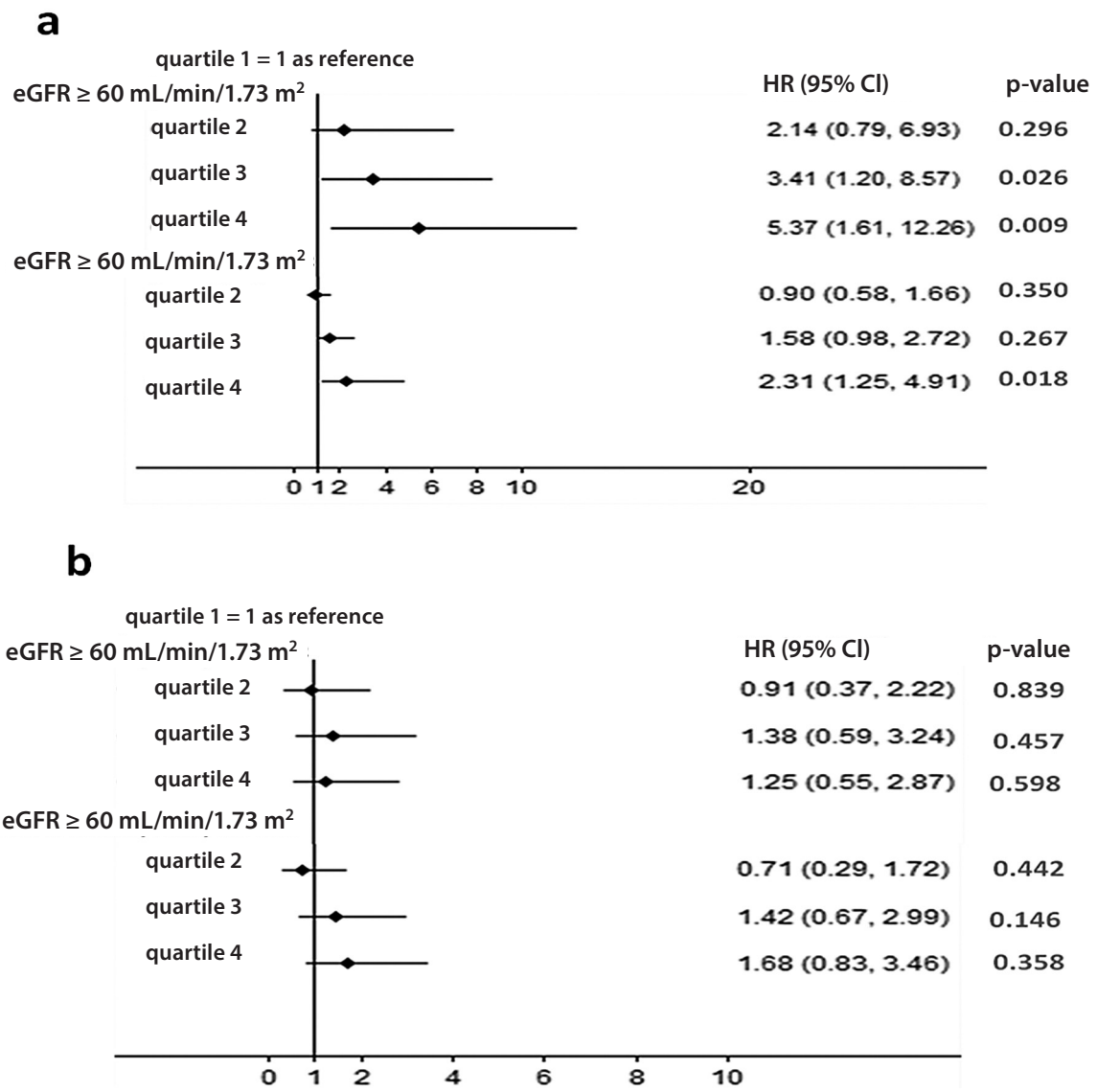

Fig. 2. Subgroup analysis of the association between serum phosphorus and disease progression

A – diabetic nephropathy; B – IgA nephropathy.

Discussion

Hyperphosphatemia is a major complication of CKD and is negatively correlated with residual renal function and prognosis. The proper management of serum phosphorus is critical at all stages of CKD.[11] Hyperphosphatemia has been reported to be associated with an increased risk of disease progression, end stage renal disease (ESRD) and a rapid deterioration of residual renal function.[12–15] However, Mehrotra et al. failed to find an association of serum phosphorus with CKD progression and ESRD in the Kidney Early Evaluation Program (KEEP) study.[4] Because the median follow-up period of this study was only 2.3 years, further research covering a much longer period is needed to confirm this conclusion.

The leading causes of CKD are chronic glomerulonephritis and diabetic nephropathy, and IgA nephropathy is the most common cause of chronic glomerulonephritis. Prognosis varies between different subgroups of CKD, among which diabetic nephropathy patients exhibit the most rapid progression.[16,17] Thus, the etiologies of CKD should be considered when assessing the progression of CKD due to the notable differences in the progression of diabetic nephropathy compared with that of other diseases. The current study indicated that patients with IgA nephropathy had a more promising prognosis than patients with diabetic nephropathy. The risk factors for end-stage renal disease (ESRD) differed between the 2 cohorts in our previous studies, but the relationship between phosphorus and prognosis was not mentioned.[7,8]

Previous studies revealed a significant difference in the diagnosis of mineral and bone disorder in diabetic patients compared with non-diabetic patients. Derangements of mineral metabolism began to occur earlier in patients with diabetes; in stage 1–2 CKD patients with diabetic nephropathy, elevated serum phosphorus and fibroblast growth factor 23 (FGF-23) levels and decreased calcium and vitamin D levels were detected.[6,18,19] The current study demonstrated that the prevalence of hyperphosphatemia was higher among diabetic nephropathy patients compared with patients with IgA nephropathy in every stage of CKD, consistent with previous reports. Previous studies confirmed that diabetic nephropathy patients had lower urinary phosphate excretion and higher serum phosphate levels than non-diabetic nephropathy patients, and that increased FGF-23 and decreased vitamin D levels occurred earlier in diabetic nephropathy patients than in non-diabetic patients.[16,17,20] Therefore, the prevalence of hyperphosphatemia is higher among patients with diabetic nephropathy compared with non-diabetic nephropathy.[6]

Many studies have explored the association between serum phosphorus and CKD progression. Bellasi et al. showed higher predictive values of phosphorus for disease progression in diabetic nephropathy than non-diabetic nephropathy.[21] Fliser et al. found that FGF-23 was an independent risk factor for disease progression in the moderate and advanced stages of CKD in non-diabetic patients, while serum phosphorus had no predictive value (HR 1.09; p = 0.063).[22] Such a discrepancy may be attributed to patient ethnicity and differing etiologies of CKD. The current study demonstrated that the association of serum phosphorus with CKD progression varied in different patient subgroups. Serum phosphorus was an independent risk factor for CKD progression in patients with diabetic nephropathy but was not an independent risk factor in patients with IgA nephropathy, indicating that serum phosphorus has a higher predictive value in patients with diabetic nephropathy than in patients with non-diabetic nephropathy.

The association of serum phosphorus with the progression of kidney disease in specific CKD patient subgroups remains to be elucidated. Animal models have demonstrated that hyperphosphatemia can lead to deteriorated renal function and renal structural alterations.[23] Consumption of a high-phosphorus diet has been shown to accelerate the deterioration of renal function, and a low-phosphorus diet can delay the progression of CKD.[24,25] Hyperphosphatemia can injure podocytes and compromise the glomerular filtration barrier by affecting pituitary-specific positive transcription factor 1 (Pit-1), resulting in glomerular sclerosis.[26] In non-dialysis CKD patients, serum phosphorus was associated with increased levels of inflammatory cytokines and C-reactive protein.[27] An increased phosphorus load results in systemic vascular endothelial injury and promotes the deposition of calcium and phosphorus in the renal tubule and the renal interstitial area, leading to tubular atrophy, interstitial fibrosis and a further decline in renal function.[28] Thus, serum phosphorus is linked to adverse effects on renal function and prognosis in diabetic nephropathy, independent of other traditional risk factors, which may result from hormone imbalances regulated by phosphorous and the early presence of hyperphosphatemia. Increased phosphorus could further accelerate renal tubular dysfunction, inflammation, glomerular sclerosis, and renal function deterioration, but the exact mechanism remains to be identified.

It is widely recognized that phosphorus starts to accumulate in stage 3b of CKD and begins to rise until eGFR decreases to <40 mL/min/1.73 m^2.[29] However, the adverse health effects of hyperphosphatemia and/or an overload of phosphorus do not appear to be limited to the advanced stages of CKD.[2,3] Previous reports have demonstrated in the early stages of CKD that serum phosphorus begins to accumulate and that elevations in serum phosphorus are associated with the risk of CKD progression.[21] This study demonstrated that in the eGFR ≥ 60 mL/min/1.73 m^2 group of patients with diabetic nephropathy, the highest quartile of phosphorous level predicted a greater risk of the endpoint. The result is also only found in diabetic nephropathy but not in IgA nephropathy.

The current study preliminarily analyzed the association of serum phosphorus with prognosis in specific CKD

patient subgroups. Patients were monitored for an extended period of time. However, this study has several limitations that require discussion. Firstly, because this was a retrospective study, the influence of different treatment options – which would inevitably have had an impact on prognosis – was not investigated. Secondly, because few patients had repeated measurements of serum phosphorus, we used single baseline serum phosphorus measurements in analyses. Thirdly, factors that regulate calcium and phosphorus metabolism – including FGF-23 and vitamin D – were not detected, though they may be important mediators of the relationship between serum phosphorus and CKD progression.

Conclusions

The association of serum phosphorus with the progression of kidney disease may vary in specific CKD patient subgroups. Serum phosphorus is an independent risk factor for the progression of CKD in patients with diabetic nephropathy, even in the early stages of CKD. Thus, levels of serum phosphorus should be detected and well-controlled in the early stages of diabetic nephropathy in order to slow the progression of the disease.

References

1. Eckardt KU, Coresh J, Devuyst O, et al. Evolving importance of kidney disease: From subspecialty to global health burden. *Lancet*. 2013; 382(9887):158–169.
2. Da J, Xie X, Wolf M, et al. Serum phosphorus and progression of CKD and mortality: A meta-analysis of cohort studies. *Am J Kidney Dis*. 2015;66(2):258–265.
3. O'Seaghdha CM, Hwang SJ, Muntner P, et al. Serum phosphorus predicts incident chronic kidney disease and end-stage renal disease. *Nephrol Dial Transplant*. 2011;26(9):2885–2890.
4. Mehrotra R, Peralta CA, Chen SC, et al. No independent association of serum phosphorus with risk for death or progression to end-stage renal disease in a large screen for chronic kidney disease. *Kidney Int*. 2013;84(5):989–997.
5. Schwarz S, Trivedi BK, Kalantar-Zadeh K, Kovesdy CP. Association of disorders in mineral metabolism with progression of chronic kidney disease. *Clin J Am Soc Nephrol*. 2006;1(4):825–831.
6. Wahl P, Xie H, Scialla J, et al. Earlier onset and greater severity of disordered mineral metabolism in diabetic patients with chronic kidney disease. *Diabetes Care*. 2012;35(5):994–1001.
7. Le W, Liang S, Hu Y, et al. Long-term renal survival and related risk factors in patients with IgA nephropathy: Results from a cohort of 1155 cases in a Chinese adult population. *Nephrol Dial Transplant*. 2012;27(4):1479–1485.
8. An Y, Xu F, Le W, et al. Renal histologic changes and the outcome in patients with diabetic nephropathy. *Nephrol Dial Transplant*. 2015; 30(2):257–266.
9. Stevens PE, Levin A; Kidney Disease: Improving Global Outcomes Chronic Kidney Disease Guideline Development Work Group Members. Evaluation and management of chronic kidney disease: Synopsis of the kidney disease: Improving global outcomes 2012 clinical practice guideline. *Ann Intern Med*. 2013;158(11):825–830.
10. Levey AS, Stevens LA, Schmid CH, et al. A new equation to estimate glomerular filtration rate. *Ann Intern Med*. 2009;150(9):604–612.
11. Slatopolsky E, Moe S. 50 years of research and discovery in chronic kidney disease and mineral & bone disorder: The central role of phosphate. *Kidney Int*. 2011;79(S121):S1–S2.
12. Norris KC, Greene T, Kopple J, et al. Baseline predictors of renal disease progression in the African American study of hypertension and kidney disease. *J Am Soc Nephrol*. 2006;17(10):2928–2936.
13. Scialla JJ, Astor BC, Isakova T, Xie H, Appel LJ, Wolf M. Mineral metabolites and CKD progression in African Americans. *J Am Soc Nephrol*. 2013;24(1):125–135.
14. Chue CD, Edwards NC, Davis LJ, Steeds RP, Townend JN, Ferro CJ. Serum phosphate but not pulse wave velocity predicts decline in renal function in patients with early chronic kidney disease. *Nephrol Dial Transplant*. 2011;26(8):2576–2582.
15. Block GA, Ix JH, Ketteler M, et al. Phosphate homeostasis in CKD: Report of a scientific symposium sponsored by the National Kidney Foundation. *Am J Kidney Dis*. 2013;62(3):457–473.
16. Haynes R, Staplin N, Emberson J, et al. Evaluating the contribution of the cause of kidney disease to prognosis in CKD: Results from the study of heart and renal protection (SHARP). *Am J Kidney Dis*. 2014;64(1):40–48.
17. Ekart R, Ferjuc A, Furman B, Gerjevič Š, Bevc S, Hojs R. Chronic kidney disease progression to end stage renal disease: A single center experience of the role of the underlying kidney disease. *Ther Apher Dial*. 2013;17(4):363–367.
18. Tanaka H, Hamano T, Fujii N, et al. The impact of diabetes mellitus on vitamin D metabolism in predialysis patients. *Bone*. 2009;45(5): 949–955.
19. Mehrotra R. Disordered mineral metabolism and vascular calcification in nondialyzed chronic kidney disease patients. *J Ren Nutr*. 2006;16(2):100–118.
20. Chen H, Li X, Yue R, Ren X, Zhang X, Ni A. The effects of diabetes mellitus and diabetic nephropathy on bone and mineral metabolism in T2DM patients. *Diabetes Res Clin Pract*. 2013;100(2):272–276.
21. Bellasi A, Mandreoli M, Baldrati L, et al. Chronic kidney disease progression and outcome according to serum phosphorus in mild-to-moderate kidney dysfunction. *Clin J Am Soc Nephrol*. 2011;6(4):883–891.
22. Fliser D, Kollerits B, Neyer U, et al. Fibroblast growth Factor 23 (FGF23) predicts progression of chronic kidney disease: The Mild to Moderate Kidney Disease (MMKD) study. *J Am Soc Nephrol*. 2007;18(9):2600–2608.
23. Neves KR, Graciolli FG, dos Reis LM, Pasqualucci CA, Moysés RM, Jorgetti V. Adverse effects of hyperphosphatemia on myocardial hypertrophy, renal function, and bone in rats with renal failure. *Kidney Int*. 2004;66(6):2237–2244.
24. Newsome B, Ix JH, Tighiouart H, et al. Effect of protein restriction on serum and urine phosphate in the Modification of Diet in Renal Disease (MDRD) study. *Am J Kidney Dis*. 2013;61(6):1045–1046.
25. Isakova T, Barchi-Chung A, Enfield G, et al. Effects of dietary phosphate restriction and phosphate binders on FGF23 levels in CKD. *Clin J Am Soc Nephrol*. 2013;8(6):1009–1018.
26. Navarro-González JF, Mora-Fernández C, Muros M, Herrera H, García J. Mineral metabolism and inflammation in chronic kidney disease patients: A cross-sectional study. *Clin J Am Soc Nephrol*. 2009;4(10): 1646–1654.
27. Nadkarni GN, Uribarri J. Phosphorus and the kidney: What is known and what is needed. *Adv Nutr*. 2014;5(1):98–103.
28. Kanbay M, Goldsmith D, Akcay A, Covic A. Phosphate – the silent stealthy cardiorenal culprit in all stages of chronic kidney disease: A systematic review. *Blood Purif*. 2009;27(2):220–230.
29. Levin A, Bakris GL, Molitch M, et al. Prevalence of abnormal serum vitamin D, PTH, calcium, and phosphorus in patients with chronic kidney disease: Results of the study to evaluate early kidney disease. *Kidney Int*. 2007;71(1):31–38.

Denture adhesives' effect on retention of prostheses in patients with xerostomia

Zdzisław A. Bogucki[A–F]

Department of Dental Prosthetics, Wroclaw Medical University, Poland

A – research concept and design; B – collection and/or assembly of data; C – data analysis and interpretation;
D – writing the article; E – critical revision of the article; F – final approval of the article

Advances in Clinical and Experimental Medicine, ISSN 1899-5276 (print), ISSN 2451-2680 (online) *Adv Clin Exp Med*. 2018;27(9):1247–1252

Address for correspondence
Zdzisław A. Bogucki
E-mail: zdzislaw.bogucki@umed.wroc.pl

Funding sources
None declared

Conflict of interest
None declared

Received on June 11, 2016
Reviewed on February 8, 2017
Accepted on February 21, 2017

Abstract

Background. Patients with xerostomia have difficulties using dentures. Application of denture adhesives (DAs) can improve the stabilization of prostheses.

Objectives. The aim of the study was to determine the retention capability of complete maxillary dentures in patients with xerostomia, determined with and without the use of prosthetic DAs.

Material and methods. This study evaluated the retention force of prostheses in a group of 60 patients diagnosed with xerostomia. Completely edentulous patients were classified into groups and all used the same kind of DAs during the study. The evaluation was performed 1, 3 and 6 h after application.

Results. All patients had poor retention of maxillary dentures without DAs. Maxillary denture retention was much better when DAs were used. The majority of the DAs used were most effective in terms of retention after 1 h. Denture adhesives in the form of glue had the best retention in this study of patients with xerostomia.

Conclusions. The results of the present study revealed the impact of DAs on average retention forces in complete maxillary denture patients with xerostomia. Patients affected by a reduced secretion of saliva have difficulties using prosthetics. In some cases, such use becomes impossible because of a complete lack of retention. The application of DAs could be a solution in these cases. Denture adhesives in glue form had the best retention during the study for patients with xerostomia.

Key words: denture adhesives, patients with xerostomia, retention of prostheses

DOI
10.17219/acem/69078

Introduction

Two of the conditions determining the success of prosthetic treatment are good retention and stability. The retention of prostheses is influenced by a number of factors, in particular, cohesion, adhesion, atmospheric pressure, capillary force, and the viscosity of saliva. The mutual interaction of these factors contributes to the force which holds prostheses. However, the current view is that the most essential components are capillary force and the density of the liquid layer. The 2 primary factors are the surface tension of the liquid layer (between the prosthesis and the mucous membrane) and the friction which occurs during the flow of liquid in capillary spaces, on both mating surfaces between the liquid and the prosthesis. One condition for the occurrence of these forces is a layer of saliva in the space between the prosthesis and the oral mucous membrane.[1–3]

Patients affected by reduced saliva secretion have difficulties using a complete maxillary dentures. In some cases, these devices cannot be used because of a complete lack of stability and retention caused by a lack of saliva. A solution in these cases is to apply denture adhesives (DAs), which facilitate the maintenance of prostheses. There is quite limited research targeting the effectiveness of DAs in patients with xerostomia, although this affects a relatively large group of individuals. Especially among geriatric patients, there are evident symptoms of dryness of the mouth and dentures adaptation can be difficult.[4–6]

Xerostomia may appear as a single illness – initially caused by a salivary gland dysfunction – or as one of the symptoms of a systemic disease. Another reason for the almost entire disappearance of saliva secretion may be the physiological processes of aging causing changes in the saliva secreting function. In elderly patients, involution of the oral mucous membrane and the related salivary glands appears. Decreased saliva production usually develops between the ages of 50 and 70 years (in most cases, in females during and after menopause). Many authors show no relationship between aging and a reduced secretion of saliva, but we must remember that involution degenerates and atrophies the whole body, including the salivary glands. The dynamics of this process are different. This is due to many factors, both external and internal. Age as a factor does not affect the secretion of saliva. However, it is important to note that aging itself is not the only reason for the appearance of xerostomia symptoms, but that other systemic diseases and some types of medication can cause it as well. Xerostomia is a subjective complaint of dry mouth, whereas hyposalivation is an objective decrease in salivary flow. The subjective oral dryness can be assessed by questionnaire (e.g., with the use of Fox's test), by clinical examination (e.g., the Challacombe score) and by measurement of the salivary flow rate (sialometry diagnosing salivary dysfunction). Sometimes, cases of xerostomia have been described in patients with a normal salivary flow rate.

Xerostomia vera is diagnosed on the basis of a clinical examination and standard sialometry tests. The most commonly used tests measure the unstimulated salivary flow rate (u-SFR), the stimulated salivary flow rate (s-SFR), the level of endocrine secretion of the parotid glands (PAR), and the secretion of the palatal salivary glands (PAL). The normal values of u-SFR and s-SFR are 0.3–0.6 mL/min and 1–2 mL/min, respectively; u-SFR values <0.1 mL/min and s-SFR values <0.2–0.5 mL/min indicate a reduction in the function of the salivary glands.[7]

In the literature, there are very few studies of DA effectiveness in patients with xerostomia, although this affects a relatively large proportion of them.[7,8]

The aim of this study was to estimate the retention capability of prosthetic DAs in complete maxillary denture patients with previously diagnosed xerostomia.

Material and methods

The study consisted of 60 patients with previously diagnosed xerostomia: 52 women and 8 men aged 63–77 years. The inclusion criteria were complete maxillary edentulism and partial or complete mandibular edentulism. Patients with previously diagnosed xerostomia were referred to the Department of Prosthodontics at the Wroclaw Medical University, Poland. An interview with the patients was done to determine the frequency of dryness of the mouth. Prior to qualifying for the study, decreased salivary flow was confirmed. During subsequent visits, 3 tests were carried out to assess salivary secretion during 1 min in total rest (u-SFR).

The DAs used in the study included the following:

1. Adhesive seals: Secure® (Johnson & Johnson, New Brunswick, USA) (based on agar). Lot No.: 4L027. Weight of one seal: 250 mg.
2. Adhesive seals: Protefix® (Queisser Pharma, Flensburg, Germany) (71 g viscose–cellulose and 29 g alginate sodium). Lot No.: OA5269010. Weight of one seal: 570 mg.
3. Adhesive powder: Protefix® (Queisser Pharma, Flensburg, Germany) (alginate sodium, menthol and sodium chlorophyll in cupric salts). Lot No.: 029091. Weight of one seal: 30 g.
4. Glue for dentures: Fittydent® (Fittydent International GmbH, Vienna, Austria) (sodium carboxymethylcellulose, polyvinyl acetate, denatured alcohol, petrolatum, hydroxypropylcellulose). Lot No.: 280605. Contents: 40 g.
5. Glue: Blend-a-dent Extra Stark® (Wick Pharma, Greensboro, USA) (poly maleic acid methoxyethylen –2.7:1, 302 mg Calcium-Zinc Salt, 192 mg carmellose natrium). Lot No.: 81311. Contents: 40 mL.
6. Adhesive cream: Corega Fix&Fest® (Block Drug Company Inc., Jersey City, USA) (copolimerisat methylvinylether maleic acid, sodium magnesium zinc salt, carboxymethylcellulose sodium salt). Lot No.: 01164A. Contents: 40 mL.

Sixty denture wearers with healthy oral tissues were referred to the Wroclaw Medical University, Department

of Prosthodontics, for construction of maxillary and mandibular dentures. They were the subjects of this study. The experimental protocol was approved by the Ethical Review Committee of the University. The patients received conventional complete maxillary and mandibular dentures and the treatment followed a standardized protocol.

This study evaluated the retention force of prostheses in a group of 60 patients diagnosed with xerostomia. In the 1st stage of the study, there were new additions to the prosthetic devices: acrylic complete maxillary dentures and partial or complete mandibular dentures. After a 3-week period for initial adaptation, the new prostheses were assessed for their stability and retention.

In order measure the force required to pry the complete maxillary denture from the denture base, a dynamometer was used. Measurement of force was performed using an FG-5000 Digital dynamometer with an RS 232 interface from LUTRON (Coopersburg, USA) (units of measurement: grams [g]/ounces [oz], resolution: 1 g/0.05 oz, minimum reading: 3 g/0.15 oz, accuracy: 0.2% + 1 digit). It assessed the size of the force in grams and the spread of screws placed between the 2nd premolar and the 1st molar of the complete maxillary denture. This corresponded to the prosthesis as the site of application of the force. The force was applied until the retention was broken between the prosthesis and the denture base. Before initiating, the appropriate tests determined whether the mucous membranes were affected, i.e., not inflamed, irritated or abraded. Measurements of the retention were carried out first without the use of DAs, the dentures were rinsed with distilled water, and then DA was used, after 3 h and after 6 h. The patients were divided into 6 groups according to the type of DA. Twenty patients used 2 different kinds of adhesive seals, 10 patients used adhesive powder, 20 patients used 2 different types of adhesive glue, and 10 patients used adhesive locking. The adhesives were applied according to the manufacturers' instructions. Before measuring the force, the head of the patient was fixed in the same position. Reference points were cranial landmarks and the horizontal positioning of the occlusal surface.

Statistical analysis

Analysis of the variability of measurements for benchmarks depending on the application of DAs and materials was done using analysis of variance (ANOVA).

Measurements for benchmarks between groups (materials) were compared with Tukey's test least significant difference (LSD) (post hoc test).

Results

The average results of dynamometric testing of the retention forces of complete upper prostheses without adhesives in all groups were as follows: Secure seals – 1187 g, Protefix seals – 1150 g, Blend-a-dent glue – 1070 g, Protefix powder – 1145 g, Fittydent glue – 1301 g, and Corega cream – 1370 g.

After applying the adhesives, the maximum results of dynamometric testing of the retention forces of complete upper prostheses in the particulars groups were as follows: Secure seals – 2590 g (3 h after application), Protefix seals – 1812 g (1 h after application), Blend-a-dent glue – 3459 g (1 h after application), Protefix powder – 2162 g (1 h after application), Fittydent glue – 3360 g (1 h after application), and Corega cream – 3182 g (1 h after application).

The results of measurements of the retention force of complete maxillary dentures in patients with DAs, with and without the use of DAs, are shown in Table 1.

The average values of dynamometrically measured retention in the study groups are shown in Fig. 1. A comparison of the dynamometric measurements testing retention capability between groups (materials) is shown in Table 2.

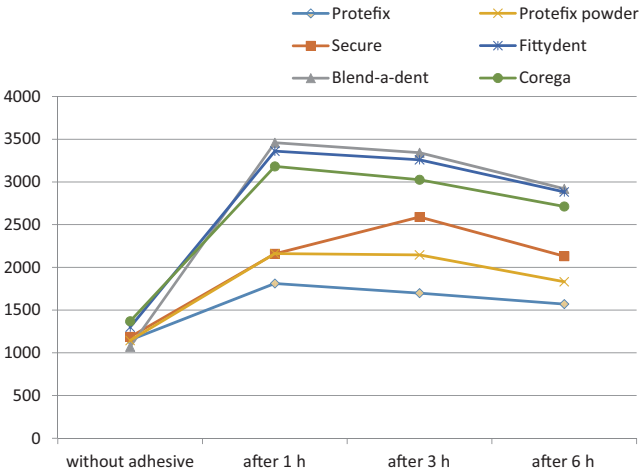

Fig. 1. Average dynamometrically measured values of retention in the analyzed groups

Discussion

In the literature, there are very few research reports of the effectiveness of DAs after application, especially in patients with xerostomia. They often consist of a survey evaluating the subjective opinion of the patients or exploring the magnitude of the incisal bite force.[8,9]

In recent years, Oliveira da Rosa et al. presented "Current trends and future perspectives in the development of denture adhesives: An overview based on technological process monitoring and systematic review". The aim of that paper was to systematically review the articles and patents with regard to DAs in order to obtain a scientific

Table 1. The results of dynamometric testing of retention effectiveness of complete upper prostheses after applying adhesives

Adhesives/ Application→	Average measurement of dynamometer [g]			
	without adhesive in groups	1 h after application	3 h after application	6 h after application
Secure seals	1187	2159	2590	2131
Difference*	–	972	1403	944
Protefix seals	1150	1812	1699	1571
Difference*	–	662	549	421
Blend-a-dent glue	1070	3459	3342	2920
Difference*	–	2389	2372	1850
Protefix powder	1145	2162	2146	1832
Difference*	–	1017	1001	687
Fittydent glue	1301	3360	3259	2883
Difference*	–	2059	1958	1582
Corega cream	1370	3182	3026	2713
Difference*	–	1812	1656	1343

* refers to the difference in prosthesis retention with adhesive material and without.

Table 2. A comparison of dynamometric measurements of the retention effectiveness between groups (materials). The values of the probabilities p marked in bold differ statistically significantly ($p < 0.05$)

Patient and group	Without adhesive	1 h after application	3 h after application	6 h after application	Total
1 : 2	0.574	**0.000**	**0.000**	**0.000**	**0.000**
1 : 3	0.523	0.957	**0.000**	**0.000**	**0.000**
1 : 4	0.087	**0.000**	**0.000**	**0.000**	**0.000**
1 : 5	0.082	**0.000**	**0.000**	**0.000**	**0.000**
1 : 6	**0.007**	**0.000**	**0.000**	**0.000**	**0.000**
2 : 3	0.939	**0.000**	**0.000**	**0.000**	**0.000**
2 : 4	**0.025**	**0.000**	**0.000**	**0.000**	**0.000**
2 : 5	0.232	**0.000**	**0.000**	**0.000**	**0.000**
2 : 6	**0.001**	**0.000**	**0.000**	**0.000**	**0.000**
3 : 4	**0.021**	**0.000**	**0.000**	**0.000**	**0.000**
3 : 5	0.263	**0.000**	**0.000**	**0.000**	**0.000**
3 : 6	**0.001**	**0.000**	**0.000**	**0.000**	**0.000**
4 : 5	**0.001**	0.081	0.210	0.221	0.950
4 : 6	0.296	**0.002**	**0.001**	**0.000**	**0.005**
5 : 6	**0.000**	**0.000**	**0.000**	**0.000**	**0.006**

1 – Secure; 2 – Protefix seals; 3 – Protefix powder; 4 – Fittydent; 5 – Blend-a-dent; 6 – Corega.

and technological overview of this material. A search for studies published between 1960 and 2014 was conducted in seven databases: Medline (PubMed), Web of Science, Lilacs, Ibecs, the Cochrane Library, Scielo, and Scopus. Additionally, the following patent databases were screened: USPTO, EPO, JPO, INPI, the Derwent Innovations Index, Patentscope, and Questel Orbit. Data was tabulated and analyzed with Microsoft Office Excel 2013 (Microsoft, Redmond, USA) and Questel Orbit (Questel, Paris, France). A total of 54 articles and 78 patents were included in the analysis. The largest number of patents (n = 19) were filed by Procter and Gamble (Cincinnati, USA). Furthermore, in vivo studies were the most prevalent (n = 30) and the types of adhesive most frequently studied were creams or powders (n = 14). It was possible to identify the current scientific and technological development of DAs, in which patents filed in many underdeveloped countries were mostly foreign-owned. Moreover, recent advances in such materials have been related more to presentation than to the additional effects of DAs.[10]

Kumar and Thombare conducted an in vivo study which was similar to our research. They published a comparative analysis of the effect of various DAs available on the market, studying the retentive ability of maxillary dentures. For measurement of retention, 5 patients who fulfilled the criteria described above and experienced minimal

retention were selected for the study. It was planned to fabricate 5 denture bases for each patient, making a total of 25 denture bases. A specially designed apparatus, based on the principle stated by Skinner, was created and used to measure the values of denture retention for each base with and without DAs. In this study, 4 DAs, readily available and commonly used by patients, were evaluated for their effect on enhancing the quality of denture retention. The retention values obtained with adhesives are more than twice than those of dentures alone. The paste form established its superiority over powdered DAs and provided double the retention values of powdered adhesives. The values of retention recorded in this study are in agreement with our observations, although they refer to different materials and to healthy patients without xerostomia.[11]

In 2009, Pradies et al. presented a clinical study comparing the efficacy of 2 DAs in complete denture patients. The aim of their study was to compare the efficacy of 2 denture adhesives in edentulous patients wearing complete maxillary and mandibular dentures. Twenty-four edentulous patients were treated with complete dentures following a standardized protocol. Resistance to dislodgement of both dentures was measured in simulated functional movements by means of a gnathometer and a dynamometer. These outcome measurements were assessed first without the adhesive and then after 2 successive 2-week periods of using a randomly assigned denture adhesive in a crossover experimental design. The adhesives used were a standard one (Kukident Classic) and a new adhesive with a similar formulation but different physical characteristics (Kukident Pro). The dynamometer results showed highly significant differences between the maxillary and mandibular dentures in both the non-adhesive group and in the 2 adhesive groups ($p \leq 0.0001$). Similarly, highly significant differences were found when any of the adhesive groups were compared to the non-adhesive group ($p = 0.0001$). The patient's subjective evaluation was very favorable for both adhesives. The study confirmed the predicted and expected improvement in the stability and retention of well-fitting, complete dentures with the adjunctive use of adhesives. The observed and recorded improvements of the new adhesive compared to the traditional one were not statistically significant.[12]

Similar research was conducted by Polyzois et al. The purpose of this study was to investigate the effect of 4 commercially available DAs on the incisal and premolar dislodgement forces of maxillary complete dentures by using an electronic and disposable gnathodynamometer and to analyze the measured incisal forces for differences. This study was conducted with 12 complete maxillary denture wearers. Four commercially available DAs (Super Corega®, Corega Ultra®, Super Corega Powder®, and Fittydent Cationic®) were investigated. The testing protocol and sequence included baseline measurements from an electronic and disposable gnathodynamometer without adhesives (control) for previous and new dentures, followed by replications of measurements with the 4 adhesives. The highest dislodgement forces were recorded in 2 sites between the central incisors and the left 2nd premolars. To estimate the effect of the different adhesives on the dislodgement forces, the data were analyzed by 2-way and 3-way ANOVA, and to estimate the similarity of the 2 devices, Bland–Altman and Mountain plots were used. The ANOVAs indicated significant differences between adhesives ($p < 0.05$), denture types ($p < 0.05$) and biting sites ($p < 0.05$) with both devices. The Bland–Altman and Mountain plots indicated little similarity between the 2 devices. It was concluded that DAs increase the denture dislodgement forces, but with differences among them. The 2 devices do not highly agree with each other, but each one alone is useful in estimating dislodgement forces in clinical practice and research.[13]

In our study, the analysis of our results showed a difference in retention force depending on the use of DA. This applies to the entire group tested and to all the materials used. Differences in the average force in many cases are more than 2-fold. The most significant difference can be noted in the group of denture glues. The average value of the retention force without the adhesives was 1070 g and 1301 g. After the application of denture glue, in various periods of time the force was: 3459 g and 3360 g. Typically, the most powerful retention for these adhesives occurred in the 1st hour after application and fell gradually. The difference was 2389 g and 2059 g. The maximum retention force for both of the tested DAs was similar. For the cream adhesives dynamics of force distribution was similar. However, the retention force after DA application and use was not as significant as with the use of glue; it amounted to 1370 g without any preparation and 3182 g in the 1st hour. The difference in average force gradually decreased and reached 1343 g after 6 h. Dynamometric testing indicated increased retention forces of complete maxillary prostheses after applying powdered DAs compared to retention without the use of adhesives. In the evaluated group of patients, the original average strength of retention was 1145 g and after applying the adhesives it increased to 2162 g. This value gradually decreased and after 6 h it fell to 1832 g. There were also differences in retention force when it comes to the group of patients using adhesive seals. The average values varied between 1150 g without preparation to 2590 g after application. For the glue the maximum retention force occurred at the time of application. For the other two materials: creams, and powders, after 3 h.

Also, the difference in the retention strength for creams and powders was smaller than in the group of other tested adhesives. The comparison of the average values of retention force in complete maxillary dentures in patients with xerostomia showed a difference of 2388 g between the highest value recorded in the 1st hour after using glue adhesives and the measurements without DAs. The statistical analysis of the clinical trials in the test group of patients

with xerostomia using the studied adhesives demonstrated statistically significant differences ($p < 0.05$).

Synthetic materials presently dominate the DA market. The most popular and successful products are mixtures of salts of fast-acting (carboxymethylcellulose or CMC) and slow-acting (polyvinyl methyl ether maleate or Gantrez) polymers. In the presence of water, CMC hydrates and displays quick-onset ionic adherence to both dentures and the mucous epithelium. The original fluid increases its viscosity and the CMC increases in volume, thereby eliminating voids between the prosthesis and the basal seat. These 2 actions markedly enhance the interfacial forces acting on the denture. Polyvinylpyrolidone (povidone) is another, less commonly used agent that reacts like CMC. Over a longer time period than necessary for the onset of hydration of CMC, Gantrez salts hydrate and increase in adherence and viscosity. The slow-acting Gantrez salts also display molecular cross-linking, resulting in a measurable increase in cohesive behavior. This effect is significantly more pronounced and longer-lasting in calcium zinc Gantrez formulas than in calcium sodium Gantrez. Eventually, all the polymers become fully soluble and washed out by saliva; this elimination is hastened by the presence of hot liquids. Denture adhesive distributed on the inside of the prosthesis must have a high degree of hydration for optimal effect. Thanks to the presence of carboxylic salt, CMC undergoes dissociation in the aquatic environment of the mouth. This is an instance of the ion adhesive force between the denture and the DAs and between the adhesives and the mucous membrane. The increased volume of DAs in the saliva and, as a result DAs, effectively fills voids between the palate and the denture foundation and increases the tension between these surfaces.[12,14]

Denture adhesives are composed of less soluble salts than CMC; salts of Poly(vinyl methyl ether) hydrazine (PVM/MA) are longer, free up more slowly, and increase viscosity and adhesion. They also have cross-bonds, which increase cohesive strength. Ultimately, all the polymers contained in DAs become totally soluble and are rinsed away by saliva. A diet rich in hot foods or drinks quickens DA dissolution and leaching. By improving stability and retention, patients have increased bite force, improved efficiency of chewing, a more evenly distributed load on the basal bone, and a beneficial effect on the respiratory track. Tests have shown that DAs significantly improved the retention of dentures. In patients affected by xerostomia and other factors impeding the achievement of proper stabilization and retention of dentures, DAs may be a solution for this difficult situation.[7]

The fact that patients can frequently use a badly adjusted prosthesis over a long period of time thanks to the liberal use of DAs is not irrelevant to the status of the basal bone. There is no scientific evidence to confirm this claim, though. Because DAs have a semi-liquid or liquid consistency, like saliva, they are not capable of interacting with saliva to exert a force which can increase the alveolar ridge resorption process. There is, however, an increased tolerance and adaptation to bad dentures which affect the basal bone. The use of DA to improve the retention of a broken or damaged prosthesis is absolutely contraindicated.

Conclusions

All patients had poor retention of their maxillary dentures without DAs.

The results of the present study revealed the impact of DAs on the average retention forces of complete maxillary dentures in patients with xerostomia.

The majority of DA used shoed the highest retention ability after 1 h.

Denture adhesives in the form of glue had the best retention capability during the study for the patients with xerostomia.

In the analysis of the statistical results of the clinical trials in the test group of patients with chronic xerostomia using the studied preparations, the differences were statistically significant ($p < 0.05$).

References

1. Christersson CE, Lindh L, Arnebrant T. Film-forming properties and viscosities of saliva substitutes and human whole saliva. *Eur J Oral Sci*. 2000;108(5):418–425.
2. Niedermeier WH, Kramer R. Salivary secretion and denture retention. *J Prosthet Dent*. 1992;67(2):211–216.
3. Chew CL. Retention of denture adhesives – an in vitro study. *J Oral Rehabil*. 1990;17(5):425–434.
4. Kulak Y, Özgan M, Arikan A. Subjective assessment by patients of the efficiency of two denture adhesive pastes. *J Prosthodont*. 2005;14(4): 248–252.
5. Turner M, Jahangiri L, Ship JA. Hyposalivation, xerostomia and the complete denture. *J Am Dent Assoc*. 2008;139(2):146–150.
6. Grasso JE, Gay T, Rendel J, et al. Effect of denture adhesive on retention of the mandibular and maxillary dentures during function. *J Clin Dent*. 2000;11(4):98–103.
7. Bogucki ZA. Clinical aspects of the use of dental adhesive materials in patients with chronic xerostomia. *Gerodontology*. 2013;30(2): 162–166.
8. Bogucki ZA, Napadlek P, Dabrowa T. A clinical evaluation denture adhesives used by patients with xerostomia. *Medicine (Baltimore)*. 2015;94(7):545–547.
9. de Baat C, van't Hof M, van Zeghbroeck L, Ozcan M, Kalk W. An international multicenter study on the effectiveness of a denture adhesive in maxillary dentures using disposable gnathometers. *Clin Oral Invest*. 2007;11(3):237–243.
10. Oliveira da Rosa WL, Simone Oliveira GD, Rosa CH, et al. Current trends and future perspectives in the development of denture adhesives: An overview based on technological monitoring process and systematic review. *J Biomed Sci*. 2016;4:1–4. doi: 10.4172/2254-609X.10003
11. Kumar MS, Thombare RU. A comparative analysis of the effect of various denture adhesives available in market on the retentive ability of the maxillary denture: An in vivo study. *J Indian Prosthodont Soc*. 2011;11(2):82–88.
12. Pradies G, Sanz I, Evans O, Martnez F, Sanz M. Clinical study comparing the efficacy of two denture adhesives in complete denture patients. *Int J Prosthodont*. 2009;22(4):361–367.
13. Polyzois G, Lagouvardos P, Frangou M. Efficacy of denture adhesives in maxillary dentures using gnathodynamometry: A comparative study. *Odontology*. 2011;99(2):155–161.
14. Rendell JK, Gay T, Grasso JE. The effect of denture adhesive on mandibular movement during chewing. *J Am Dent Assoc*. 2000;131(7): 981–986.

Anti-CCP antibodies and rheumatoid factor in systemic sclerosis: Prevalence and relationships with joint manifestations

Ewa Wielosz[A–F], Maria Majdan[A,C,E,F], Magdalena Dryglewska[B,C], Robert Zwolak[B,C,E]

Department of Rheumatology and Connective Tissue Diseases, Medical University of Lublin, Poland

A – research concept and design; B – collection and/or assembly of data; C – data analysis and interpretation;
D – writing the article; E – critical revision of the article; F – final approval of the article

Advances in Clinical and Experimental Medicine, ISSN 1899-5276 (print), ISSN 2451-2680 (online) *Adv Clin Exp Med*. 2018;27(9):1253–1257

Address for correspondence
Ewa Wielosz
E-mail: ewa.wielosz@wp.pl

Funding sources
None declared

Conflict of interest
None declared

Received on October 30, 2016
Reviewed on December 14, 2016
Accepted on March 28, 2017

Abstract

Background. It is known that anti-citrullinated protein (a-CCP) antibodies and rheumatoid factor (RF) can be present in systemic sclerosis (SSc) patients, particularly with joint involvement.

Objectives. The aim of the study was to assess the prevalence of a-CCP antibodies and immunoglobulin M class (IgM) RF, and the relationships between their presence and joint manifestations in patients with SSc.

Material and methods. The study included 100 European Caucasian SSc patients hospitalized consecutively in the Department of Rheumatology and Connective Tissue Diseases (Lublin, Poland). Anti-citrullinated protein antibodies and IgM RF were determined using a commercial enzyme-linked immunosorbent assay (ELISA) test.

Results. Anti-citrullinated protein antibodies were found in 10 out of 100 (10%) SSc patients and IgM RF in 71 out of 100 (71%) SSc patients. In the study, 90/100 (90%) SSc patients had joint manifestations (arthralgia or arthritis), 34/100 (34%) had arthritis and 6/100 (6%) had a systemic sclerosis-rheumatoid arthritis (SSc-RA) overlap syndrome. Significantly higher a-CCP antibody levels ($p = 0.012$), erythrocyte sedimentation rate (ESR) ($p = 0.029$) and C-reactive protein (CRP) levels ($p = 0.020$) were observed in the SSc group with arthritis. A significant correlation was found between the group with arthritis and the presence of a-CCP antibodies, and between the arthralgia group and the presence of IgM RF.

Conclusions. The prevalence of RF and a-CCP antibodies is relatively high in SSc, and joint involvement occurs frequently. There was a significantly higher prevalence of IgM RF in the group with joint manifestations. About 1/3 of SSc patients had symptoms of arthritis. Arthritis is connected with the presence of a-CCP antibodies, while arthralgia is connected with the presence of IgM RF.

Key words: systemic sclerosis, arthritis, rheumatoid factor, anti-citrullinated protein antibodies, arthralgia

DOI
10.17219/acem/69921

Introduction

Systemic sclerosis (SSc) is a multisystem disorder characterized by vascular damage, immune activation and fibroblast activation, changes which lead to a progressive thickening of the skin with structural and functional abnormalities of different organs. Musculoskeletal involvement is present in 24–97% of SSc patients.[1–3] A more common manifestation is arthralgia, whereas arthritis is rare.[4,5] Hand involvement is often the first clinical manifestation of SSc.[6,7] Symmetrical polyarthritis similar to rheumatoid arthritis (RA) can also be found in SSc, but it particularly characterizes a systemic sclerosis-rheumatoid arthritis (SSc-RA) overlap syndrome.[2,8–10] In some cases, arthritis in the course of SSc and SSc-RA overlap syndrome can be very difficult to distinguish. It is known that the main serological markers for diagnosing RA are anti-citrullinated protein (a-CCP) antibodies and rheumatoid factor (RF). These parameters can be present in SSc patients, particularly with joint involvement.[1,2,8] The aim of the study was to assess the prevalence of a-CCP antibodies and immunoglobulin M class (IgM) RF, and the relationships between their presence and joint manifestations in patients with SSc.

Material and methods

The study included 100 European Caucasian SSc patients (82 female and 18 male) hospitalized consecutively in the Department of Rheumatology and Connective Tissue Diseases (Lublin, Poland). The patients fulfilled the American College of Rheumatology (ACR) classification criteria of SSc (Table 1).[11] Serum samples were obtained from 100 patients and a joint examination was performed at the same time. Anti-citrullinated protein antibodies and IgM RF were determined using the enzyme-linked immunosorbent assay (ELISA) commercial test : EUROIMMUN for IgM RF (EUROIMMUN AG, Lübeck, Germany) and INOVA for a-CCP antibodies (INOVA Diagnostics, San Diego, USA). The test kit was used according to the manufacturer's suggested procedures. The samples were classified as negative for a-CCP antibodies at <20 units and negative for IgM RF at <30 RU/mL. Two markers of inflammation, erythrocyte sedimentation rate (ESR) and C-reactive protein (CRP), were also determined. The samples were classified as negative for ESR at <16 mm/h for women and at <11 mm/h for men, and at <10 mg/L for CRP. Joint involvement was assessed according to clinical manifestations, such as arthralgia or arthritis. Arthralgia was assessed by involving 2 or more peripheral joints characterized by tenderness. Non-erosive arthritis was determined by involving 2 or more peripheral joints characterized by tenderness and swelling or confirmed by ultrasonography (USG). Moreover, flexion contractures, tendon friction rubs (TFRs) and finger-to-palm distance in flexion (FTP) were assessed. Finger-to-palm distance in flexion was determined by measuring the minimal distance (mm) between the nail tip of the middle finger and the transverse palmar creases in both hands (normally no distance can be measured).[12] Rheumatoid arthritis was diagnosed according to the ACR criteria.[13] Anti-topoisomerase I (a-Scl-70) and anti-centromere antibodies (ACA) were determined using a commercial test, the EUROLINE Systemic Sclerosis Profile (EUROIMMUN AG, Lübeck, Germany).

All calculations were performed with STATISTICA v. 10.0 software (StatSoft, Kraków, Poland). Data was analyzed using the non-parametric χ^2 test for comparisons between the groups. Quantitative data was assessed using the Mann-Whitney U test, whereas qualitative data was determined by the Yule correlation. Probability value $p < 0.05$ was considered statistically significant.

Table 1. Characteristics of the SSc study group

Characteristics	Patients' data
Number of patients	100
SSc subtype	dcSSc – 50
	lcSSc – 50
Age [years]	52.68 ±13.85 (range 18–81)
Duration of disease [years]	6.46 ±6.05 (range 0.1–23)
ACA	19/100 (19%)
Anti-Scl-70	46/100 (46%)
Overlap syndrome	21/100 (21%)
SSc/RA	6/100 (6%)
SSc/SS	8/100 (8%)
SSc/DM/PM	7/100 (7%)

SSc – systemic sclerosis; dcSSc – diffuse cutaneous SSc; lcSSc – limited cutaneous SSc; ACA – anti-centromere antibodies; anti-Scl-70 – anti-topoisomerase I antibodies; RA – rheumatoid arthritis; SS – Sjögren's syndrome; DM/PM – dermatomyositis/polymyositis.
Data is presented as mean ± standard deviation (SD), number and percentage.

Results

According to our observations, 90 out of the 100 (90%) SSc patients had arthralgia, 34 (34%) SSc patients had arthritis and 24 (24%) SSc patients developed flexion contractures. Finger-to-palm distance in flexion was decreased in 26 out of 100 (26%) SSc patients, while 5 (5%) SSc patients had TFRs. An SSc-RA overlap syndrome was found in 6 (6%) SSc patients. The mean disease activity score 28 (DAS 28) in the group with an SSc-RA overlap syndrome was 4.46 ±1.29. The prevalence of IgM RF and a-CCP antibodies in SSc patients with and without joint manifestations is presented in Table 2.

In the SSc study group without overlapped RA, 28 patients had arthritis, 65 patients were positive for IgM RF and 7 patients were positive for a-CCP antibodies. In the group of 28 SSc patients with arthritis, IgM RF was present in 19 patients (68%), at a high value in 15 (54%) patients and

Table 2. The prevalence of IgM RF and a-CCP antibodies in SSc patients with and without joint manifestations

Prevalence of IgM RF and a-CCP antibodies	Total	Group with joint manifestations		Group without joint manifestations	p-value
		arthralgia	arthritis		
Number of patients	100	90/100 (90%)	34/100 (34%)	10/100 (10%)	–
IgM RF	71/100 (71%)	67/90 (74.4%)	25/34 (73.5%)	4/10 (40%)	0.023
			p = 0.049		
a-CCP antibodies	10/100 (10%)	9/90 (10%)	7/34 (20.6%)	1/10 (10%)	NS
			NS		

IgM RF – immunoglobulin M class rheumatoid factor; a-CCP – anti-citrullinated protein; SSc – systemic sclerosis; NS – nonsignificant. Data is presented as number and percentage; p-value of <0.05 was considered statistically significant.

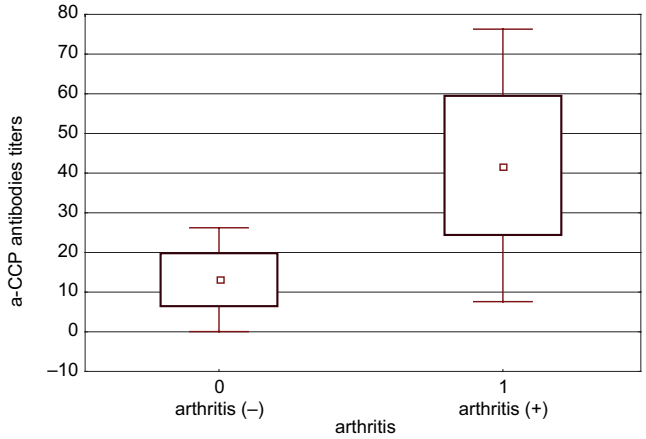

Fig. 1. Statistically significant differences in the titers of a-CCP antibodies in groups with and without arthritis

a-CCP – anti-citrullinated protein; probability value: p = 0.0119.

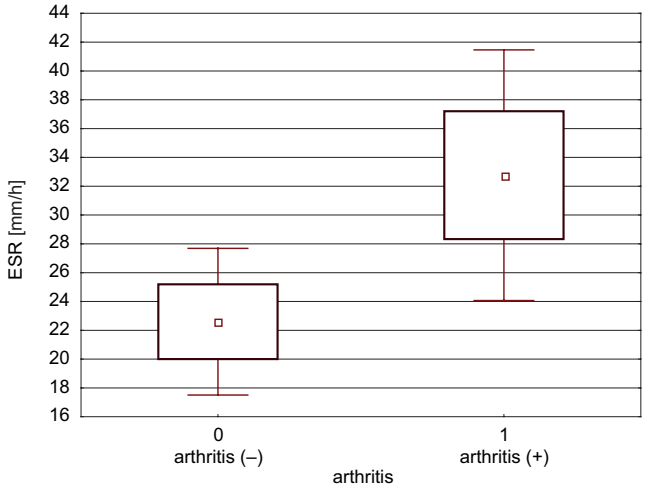

Fig. 2. Statistically significant differences in ESR in groups with and without arthritis

ESR – erythrocyte sedimentation rate; probability value: p = 0.0294.

at a low value in 4 (14%) patients. Moreover, a-CCP antibodies were present in 4 out of 28 patients (14%) with arthritis, 3 (11%) with a high value and 1 (3%) with low. In the group of 66 SSc patients without arthritis, 46 patients (70%) were positive for IgM RF, 32 (49%) at a high value, 8 (12%)

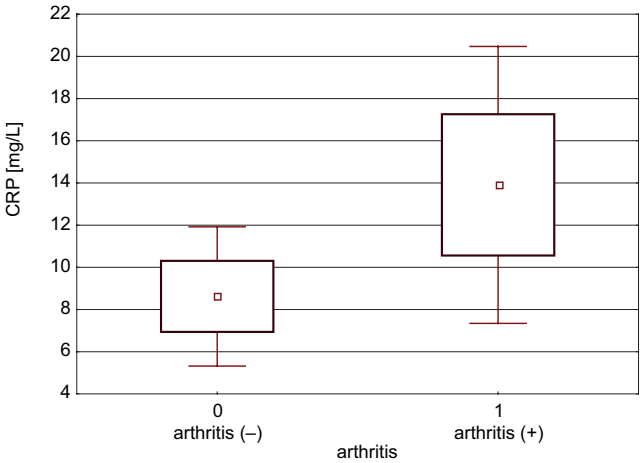

Fig. 3. Statistically significant differences in the titers of CRP in groups with and without arthritis

CRP – C-reactive protein; probability value: p = 0.0201.

at a medium value and 6 (9%) at a low value. Anti-citrullinated protein antibodies were found in 3 (5%) SSc patients without arthritis, 1 (2%) with a high value and 2 (3%) with low. However, in the group of 46 patients with positive IgM RF without overlapped RA and without arthritis, 42 (91%) patients had arthralgia. Our findings indicated that the prevalence of IgM RF was significantly higher in the group with joint manifestations compared to the group without it (p = 0.0230). However, no significant intergroup differences in the presence of a-CCP antibodies were determined (Table 2). Significantly higher concentrations of a-CCP antibodies (p = 0.0119) and CRP (p = 0.0201), as well as ESR (p = 0.0294) were observed in the SSc group with arthritis compared to the group without arthritis (Fig. 1–3). The titer of IgM RF was not significantly higher in the SSc group with arthritis (p = 0.0713) than in the group without arthritis. Interestingly, a significant correlation was determined between the SSc group with arthritis and the presence of a-CCP antibodies (p = 0.013; Φ = 0.263) and between the SSc group with arthralgia and the presence of IgM RF (p = 0.025; Φ = 0.238). Moreover, a significant correlation was noted between the SSc group with arthritis and the concentrations of inflammatory parameters (ESR and CRP) (Table 3).

Table 3. Correlations between IgM RF, a-CCP antibodies, inflammation parameters and joint involvement

Joint manifestations	ESR	CRP	IgM RF	a-CCP antibodies
Arthritis	p = 0.0158 Φ = 0.234	p = 0.050 Φ = 0.192	p = 0.481 Φ = 0.073	p = 0.013 Φ = 0.263
Arthralgia	p = 0.467 Φ = 0.070	p = 0.844 Φ = 0.025	p = 0.025 Φ = 0.238	p = 0.895 Φ = 0.012

ESR – erythrocyte sedimentation rate; CRP – C-reactive protein; IgM RF – immunoglobulin M class rheumatoid factor; a-CCP – anti-citrullinated protein; p-value of <0.05 was considered statistically significant.

Discussion

In the present study, we investigated the presence of serological parameters of joint involvement: a-CCP antibodies and IgM RF in SSc. According to our observations, a-CCP antibodies were found in 10% of SSc patients. Our findings are similar to those reported in the literature. Polimeni et al. demonstrated that in a SSc group, 7 of 78 (9%) patients were a-CCP positive.[2] According to Ingegnoli et al., the presence of a-CCP antibodies was detected in 8 of 75 (10.7%) patients with SSc.[1] Other studies showed that a-CCP antibodies were revealed in 18 out of 146 (12.3%), 3 out of 28 (10.7%), 11 out of 82 (13.4%), and 3 out of 114 (2.6%) SSc patients.[6,14–17] Moreover, Horimoto and Costa found a-CCP antibodies in 4 out of 24 patients (16.7%), but all patients had an SSc-RA overlap syndrome.[9] Based on literature data, we can suppose that a-CCP antibodies are a useful marker in identifying patients diagnosed with an SSc-RA overlap syndrome; however, these antibodies may also be positive in 7% of SSc patients without arthritis.[15] In our study, we also detected a-CCP antibodies in 10% of SSc patients without joint involvement. There are many data indicating a significant association between positive a-CCP antibodies and arthritis and bone erosions in SSc.[1,6,16,17] According to our findings, there was a significant correlation between the group of SSc patients with arthritis and the presence of a-CCP antibodies; higher titers of a-CCP antibodies were observed in the SSc group with arthritis compared to the group without arthritis. Additionally, the prevalence of IgM RF in SSc was evaluated; IgM RF was detected in 71% of patients, which seems to be higher than in other studies. According to our research, the prevalence of RF in SSc ranged from 12% to 35% and may be positive in SSc patients without joint manifestations.[1,6,9,15,18,19] Avouac et al. suggested that the RF test seems non-specific and does not distinguish SSc patients with musculoskeletal manifestations from those unaffected by them.[19] Rheumatoid factor may also be seen in patients with SSc associated with secondary Sjögren's syndrome, which is not uncommon in SSc patients.[19] However, our results revealed that the prevalence of IgM RF was significantly higher in the group with joint manifestations as compared to the group without joint manifestations. This observation seemed to be associated with the presence of a large number of SSc patients with joint manifestations in our study group. According to our study, 90% of SSc patients had joint manifestations and 71% were positive for IgM RF, but only 6% developed an SSc-RA overlap syndrome. The above results suggest that the presence of RF or a-CCP antibodies in SSc patients does not lead to a diagnosis of an SSc-RA overlap syndrome. According to literature data, the search for anti-CCP antibodies might be of great help in some infrequent cases of an SSc-RA overlap syndrome, but not in all situations.[19] Destructive joint disease in patients with SSc may suggest an overlap syndrome with RA.[6,10] Numerous studies have reported such results. According to Arslan Tas et al., such radiographic findings as erosions, joint space narrowing and arthritis were less frequent in the SSc group, but acro-osteolysis, flexion contracture and calcinosis were more frequent than in the RA group.[6] The abovementioned radiological findings can worsen the prognosis. Apart from hand radiography, the potential of USG in the assessment of joint and tendon involvement in the course of SSc was evaluated. Some studies revealed that SSc patients with a history of arthralgia without arthritis developed synovial inflammation, which could be observed during an USG examination, particularly in the wrist and small hand joints.[20,21] Another important finding was that TFRs were part of functional impairment in SSc.[22] Moreover, according to the largest worldwide database, joint and tendon involvement predict disease progression in SSc.[23] Using the latest data from the European League Against Rheumatism (EULAR) Scleroderma Trials and Research (EUSTAR) cohort, this prospective study investigating 1,301 patients with SSc demonstrated that joint synovitis and TFRs were strong independent predictors of skin progression and that positivity for a-Scl-70 antibodies and a history of digital ulcers were also predictive markers. Furthermore, joint synovitis was predictive of the occurrence of decreased left ventricular ejection fraction and the occurrence of new digital ulcers.[23] To sum up, according to literature data, hand arthropathy in SSc should alert one to functional damage, severe skin progression and serious internal organ involvement, particularly cardiopulmonary complications, which was the main cause of death in SSc.[24–27] In conclusion, serological parameters which could predict severe articular involvement are needed. According to Generini et al., antibodies such as heterogeneous nuclear ribonucleoprotein isoform A1

and A2 antibodies (anti-hnRNP-A1 and anti-hnRNP-A2) may have some diagnostic value for joint involvement and the risk of developing erosive arthritis in SSc.[28]

Conclusions

Immunoglobulin M class rheumatoid factor and a-CCP antibodies seem to be a helpful tool to differentiate cases with joint manifestations, although not in all patients. In our study, arthralgia was a common manifestation in SSc patients and the prevalence of RF was high in this group. Furthermore, RF correlated with arthralgia and a-CCP antibodies correlated with arthritis in SSc patients. Our study requires further analysis with the results based on clinical picture, USG and radiological joint examinations.

References

1. Ingegnoli F, Galbiati V, Zeni S, et al. Use of antibodies recognizing cyclic citrullinated peptide in the differential diagnosis of joint involvement in systemic sclerosis. *Clin Rheumatol*. 2007;26:510–514.
2. Polimeni M, Feniman D, Skare TS, Nisihara RM. Anti-cyclic citrullinated peptide antibodies in scleroderma patients. *Clin Rheumatol*. 2012;31:877–880.
3. Schmeiser T, Pons-Kühnemann J, Özden F, Müller-Ladner U, Dinser R. Arthritis in patients with systemic sclerosis. *Eur J Intern Med*. 2012; 23:25–29.
4. Lima TR, Guimarães FS, Silva LA, Silva DP, Menezes SL, Lopes AJ. Relationship between functional capacity, joint mobility and pulmonary function in patients with systemic sclerosis. *J Bodyw Mov Ther*. 2015;19:17–24.
5. Chevreul K, Brigham KB, Gandré C, Mouthon L; BURQOL-RD Research Network. The economic burden and health-related quality of life associated with systemic sclerosis in France. *Scand J Rheumatol*. 2014; 18:1–9.
6. Arslan Tas D, Erken E, Sakalli H, Yucel AE. Evaluating hand in systemic sclerosis. *Rheumatol Int*. 2012;32:3581–3586.
7. Mouthon L. Hand involvement in systemic sclerosis. *Presse Med*. 2013; 42:1616–1626.
8. Marrone M, Chialà A, Tampoia M, et al. Prevalence of anti-CCP antibodies in systemic sclerosis. *Reumatismo*. 2007;59:20–24.
9. Horimoto AM, Costa IP. Overlap between systemic sclerosis and rheumatoid arthritis: A distinct clinical entity? *Rev Bras Reumatol*. 2015;4: 482–504.
10. Chung L, Lin J, Furst DE, Fiorentino D. Systemic and localized scleroderma. *Clin Dermatol*. 2006;24:374–392.
11. Arslan Tas D; Subcommittee for scleroderma criteria of the American Rheumatism Association Diagnostic and Therapeutic Criteria Committee. Preliminary criteria for the classification of systemic sclerosis (scleroderma). *Arthritis Rheum*. 1980;23:581–590.
12. McHugh NJ, Distler O, Giacomelli R, Riemekasten G. Non organ based laboratory markers in systemic sclerosis. *Clin Exp Rheumatol*. 2003;21: 32–38.
13. Arnett FC, Edworthy SM, Bloch DA, et al. The American Rheumatism Association 1987 revised criteria for the classification of rheumatoid arthritis. *Arthritis Rheum*. 1988;31:315–324.
14. Payet J, Goulvestre C, Bialé L, et al. Anticyclic citrullinated peptide antibodies in rheumatoid and nonrheumatoid rheumatic disorders: Experience with 1162 patients. *J Rheumatol*. 2014;41:2395–2402.
15. Ueda-Hayakawa I, Hasegawa M, Kumada S, et al. Usefulness of anticyclic citrullinated peptide antibody and rheumatoid factor to detect rheumatoid arthritis in patients with systemic sclerosis. *Rheumatology (Oxford)*. 2010;49:2135–2139.
16. Stamenković B, Stanković A, Dimić A, et al. The clinical significance of antibody determination to cyclic citrullinated peptides in systemic sclerosis. *Srp Arh Celok Lek*. 2012;140:350–354.
17. Morita Y, Muro Y, Sugiura K, Tomita Y. Anti-cyclic citrullinated peptide antibody in systemic sclerosis. *Clin Exp Rheumatol*. 2008;26:542–547.
18. Allali F, Tahiri L, Senjari A, Abouqal R, Hajjaj-Hassouni N. Erosive arthropathy in systemic sclerosis. *BMC Public Health*. 2007;7:260–266.
19. Avouac J, Clements PJ, Khanna D, Furst DE, Allanore Y. Articular involvement in systemic sclerosis. *Rheumatology (Oxford)*. 2012;51: 1347–1356.
20. Iagnocco A, Vavala C, Vasile M, Stefanantoni K, Valesini G, Riccieri V. Power Doppler ultrasound of the hand and wrist joints in systemic sclerosis. *Clin Exp Rheumatol*. 2013;31:89–95.
21. Gutierrez M, Pineda C, Cazenave T, et al. Ultrasound in systemic sclerosis. A multi-target approach from joint to lung. *Clin Rheumatol*. 2014;33:1039–1047.
22. Stoenoiu MS, Houssiau FA, Lecouvet FE. Tendon friction rubs in systemic sclerosis: A possible explanation – an ultrasound and magnetic resonance imaging study. *Rheumatology (Oxford)*. 2013;52:529–533.
23. Avouac J, Walker UA, Hachulla E, et al; EUSTAR collaborators. Joint and tendon involvement predict disease progression in systemic sclerosis: A EUSTAR prospective study. *Ann Rheum Dis*. 2016;75: 103–109.
24. Bálint Z, Farkas H, Farkas N, et al. A three-year follow-up study of the development of joint contractures in 131 patients with systemic sclerosis. *Clin Exp Rheumatol*. 2014;32:68–74.
25. Ingegnoli F, Boracchi P, Ambrogi F, Gualtierotti R, Galbiati V, Meroni PL. Hand impairment in systemic sclerosis: Association of different hand indices with organ involvement. *Scand J Rheumatol*. 2010;39: 393–397.
26. Fett N. Scleroderma: Nomenclature, etiology, pathogenesis, prognosis, and treatments: Facts and controversies. *Clin Dermatol*. 2013;31: 432–437.
27. Grant-Kels JM, Rothe MJ, Mease P. Rheumatology and dermatology: Part 1. *Clin Dermatol*. 2006;24:347.
28. Generini S, Steiner G, Miniati I, et al. Anti-hnRNP and other autoantibodies in systemic sclerosis with joint involvement. *Rheumatology (Oxford)*. 2009;48:920–925.

Experience with thoracic endovascular aortic repair applied in treating Stanford type B aortic dissection: An analysis of 98 cases

Lei Chen[1,C,D], Sheng-Jia Yang[2,B,E], Feng-Ling Guo[3,B,C], Qing-Yun Zhang[1,B], Zhi Yang[1,A,F]

[1] Department of Vascular Surgery, Chengde Medical University Affiliated Hospital, China
[2] Department of Vascular Surgery, Xuan Wu Hospital, Capital Medical University, Beijing, China
[3] Department of Nephrology, Chengde Medical University Affiliated Hospital, China

A – research concept and design; B – collection and/or assembly of data; C – data analysis and interpretation; D – writing the article; E – critical revision of the article; F – final approval of the article

Advances in Clinical and Experimental Medicine, ISSN 1899-5276 (print), ISSN 2451-2680 (online) *Adv Clin Exp Med*. 2018;27(9):1259–1262

Address for correspondence
Zhi Yang
E-mail: yangzhi_chg6@sina.com

Funding sources
None declared

Conflict of interest
None declared

Received on March 29, 2016
Reviewed on June 16, 2016
Accepted on April 13, 2017

Abstract

Background. Thoracic endovascular aortic repair (TEVAR) has been frequently applied in Stanford type B aortic dissection since thoracic aortic diseases were first treated with artificial vessels.

Objectives. The aim of this study was to analyze the clinical value of TEVAR applied in treating Stanford type B aortic dissection.

Material and methods. Between January 2007 and April 2014, 167 consecutive Stanford type B aortic dissection patients were treated with TEVAR and retrospectively analyzed.

Results. All patients had a successful operation. A total of 98 patients were followed-up and the duration of the follow-up ranged from 3 to 63 months with a mean of 25.6 ±8.4 months. Proximal type I endoleak occurred in 18 patients with an incidence rate of 18.37% and a cuff was deployed in 7 patients, in whom the endoleak disappeared after 3 months. Two patients died in the perioperative period: one died from aortic dissection rupture, while the other died from infectious shock. One patient died from acute myocardial infarction during the follow-up period. Tears occurred in the end piece of stent grafts in 12 patients, and additional TEVAR was performed. One patient had a proximal retrograde type A dissection; the patient was in an acceptable state of health apart from persistent chest and back pain, and is still in follow-up. Spinal cord ischemia, stent displacement and collapse did not occur.

Conclusions. TEVAR is reliable and safe, and it can be widely applied in treating Stanford type B aortic dissection.

Key words: thoracic endovascular aortic repair, Stanford type B aortic dissection, clinical value

DOI
10.17219/acem/70453

Introduction

Thoracic endovascular aortic repair (TEVAR) has been frequently applied in Stanford type B aortic dissection since thoracic aortic diseases were first treated with artificial vessels.[1–3] The indications for TEVAR have been broadened continuously with the development of endovascular techniques. In our study, 167 consecutive patients with Stanford type B aortic dissection were treated with TEVAR. Among them, 68 patients completed follow-up, and the therapeutic effect was then analyzed.

Material and methods

General data

A total of 167 patients with Stanford type B aortic dissection, including 112 males and 55 females (aged 32–82 years), were treated with TEVAR in the Department of Vascular Surgery in Chengde Medical University Affiliated Hospital (China) from January 2007 to April 2014. All 167 patients were admitted for sudden chest and back pain; 96 patients were complicated with hypertension, 15 patients with diabetes mellitus, 6 patients with coronary artery disease, and 2 patients with renal failure. Among them, 3 patients had a rupture of aortic dissection or rupture aura, 2 patients had a rapid augmentation of dissecting aneurysm, 1 patient had severe pleural effusion, 2 patients had severe ischemia of the internal organs, 2 patients had acute lower limb ischemia and acute spinal cord ischemia, and 6 patients had persistent pain and unmanageable hypertension. Other patients were in stable condition. Blood pressure control and analgesia were administered in all patients. Preoperatively, aortic computed tomography angiography (CTA) was performed to make a definite diagnosis and to evaluate the site of tears, the length of the proximal landing zone and the status of the access vessels in all patients. All 167 patients had no tear/dissection of the aortic arch and were classified with Stanford type B aortic dissection. In addition, all patients had acute dissection. Dissection of the abdominal aorta was found only in 1 patient, but the tear extended to the abdominal aorta and even to the iliac artery in 117 patients.

Operative techniques

A hybrid operation was performed in 20 patients. The site of aortic tears was located between the left subclavian artery and the left common carotid artery in 12 patients, and they underwent a right common carotid–left common carotid–left subclavian artery bypass. The site of aortic tears was located between the left common carotid artery and the brachiocephalic trunk in 5 patients, who underwent an ascending aorta–right common carotid–left common carotid–left subclavian artery bypass. One patient was complicated with innominate aneurysm and underwent an innominate aneurysm resection and an ascending aorta–right common carotid–left common carotid–left subclavian artery bypass. One patient showed the left vertebral artery dominance, as revealed by preoperative angiography, and underwent a left vertebral–left common carotid artery anastomosis. Thoracic endovascular aortic repair was then performed after 1 week. One patient still had a malperfusion of the right lower extremity after TEVAR, so a femoral–femoral artery bypass was then performed with artificial blood vessels.

In the study conducted by Nienaber et al., all patients received TEVAR.[4] All stent grafts were deployed with the common femoral artery approach via unilateral femoral access. When the primary tear was close to the left subclavian artery and/or the left common carotid artery, a debranching of the common carotid artery was first performed by a right common carotid artery–left common carotid artery bypass, and the origin of the left subclavian artery and/or the left common carotid artery was then covered with the stent graft. A left common carotid artery–left subclavian artery bypass was performed either immediately before, or after TEVAR on the basis of a radiographic evaluation of vertebrobasilar circulation. Adjunctive stenting of the iliac arteries and the visceral branches should be performed for static malperfusion after the deployment of a thoracic stent graft when considered necessary on the basis of angiographic assessments.

Results

All patients had a successful operation. A total of 210 stent grafts were deployed; 7 were used for sealing proximal endoleaks and 35 for distal tears. Debranching was not performed, because all patients suffered from Stanford type B aortic dissection. In our study, we tried to follow-up with all 167 patients, but 47 patients refused to participate in follow-up, because they were far away from our hospital, and 20 patients could not be reached. A total of 98 patients were followed-up, and the rate of follow-up was 58%. The duration of follow-up ranged from 3 to 63 months and the mean was 25.6 ±8.4 months. Proximal type I endoleak occurred in 18 patients with an incidence rate of 18.37% and a cuff was deployed in 7 patients, in whom the endoleak disappeared after 3 months. Two patients died in the perioperative period: one died from a rupture of aortic dissection and the other died from infectious shock. One patient was admitted for sudden coma and died from acute myocardial infarction. A total of 12 patients had a tear in the end piece of a stent graft after TEVAR, and additional TEVAR was performed. One patient had a proximal retrograde type A dissection and a tear in the end piece of a stent graft. The tear in the end piece of the stent graft was sealed, but the proximal tear was not successfully sealed. Therefore, graft replacement of the ascending aorta

was recommended, but this procedure was not performed, because open surgery was not suitable for the patient – a senior in poor condition. The patient is in acceptable health at the present time, except for persistent chest and back pain, and is still in follow-up. The remaining patients had no complications during follow-up.

Discussion

Operation opportunity

Whether type B dissection in the acute phase should be treated with TEVAR or not is still controversial.[5] In this study, the 16 patients who were treated with TEVAR within 1 week of onset had no recurrent tears or dissection thrombosis after TEVAR. The indications for emergency TEVAR include: 1. dissection rupture or rupture aura, a rapid augmentation of dissecting aneurysm and severe pleural effusion; 2. severe ischemia of the internal organs; 3. acute lower limb ischemia and acute spinal cord ischemia; 4. persistent pain and unmanageable hypertension.[6] A selective operation might be performed on patients without the above-mentioned indications.

Extension of the proximal landing zone

The length of the proximal landing zones should be greater than 1.5 cm to seal off the primary tear and to avoid proximal type I endoleak, and the branch vessels should be sealed to achieve a sufficient length of the landing zones for the tears around the aortic arch.[7] In that study, a hybrid operation was frequently used for securing the blood supply of important vessels; 12 patients underwent a preventive right common carotid–left common carotid–left subclavian artery bypass and 5 patients underwent an ascending aorta–right common carotid–left common carotid–left subclavian artery bypass before TEVAR. The end piece of a stent graft with a length of 150 mm was usually located in the junctional zone between the aortic arch and the descending part of the aorta, because the stent graft shifted forward to the proximal part of the innominate artery. The intima of the artery can be torn because of the elastic stress of a stent graft (1 patient had this complication in our study) or a tear can occur in the end piece of a stent graft because of long-term elastic stress. According to our experience, the length of a stent graft should be greater than 200 mm, and the end piece of a stent graft should cross the aortic arch with a distance long enough to reduce the elastic stress of the end piece. The alternative method was deploying a stent graft into the descending part of the aorta before TEVAR in order to avoid the impact and shearing of blood flow against the intima of the aorta, which could reduce the risk of a recurrent rupture. Short stent grafts can only be used for tears in short and straight segments; long and tapered stent grafts should be used for tears around the aortic arch.[8,9] For tears in the left subclavian artery and with a distance shorter than 4 cm between the tears and the proximal part, the left subclavian artery was routinely sealed to achieve the greatest possible length of the landing zones. This method carries the potential risk of cerebral ischemia and left upper extremity ischemia, but ischemia can mostly be compensated for by the contralateral circle of Willis, the arteries in the chest wall and those around the shoulder. In our study, no patients had complications of cerebral ischemia or left upper extremity ischemia.

Treatment of multiple tears

The aorta dissection usually involves multiple tears. It is widely accepted that distal tears should be treated at the same time as proximal tears if they are large and are located above the renal artery, and that distal tears may be left untreated temporarily if they are far away from proximal tears and have a small regurgitation volume. In this study, distal proximal tears were sealed in 35 patients. Our experience demonstrated that distal tears should be selectively sealed after the first tear was sealed, and indications included the occurrence of distal ischemia and a luminal diameter at a tear exceeding 5 cm.

Complications of thoracic endovascular aortic repair

Proximal type I endoleak is the most frequent complication, which can induce an early dissection rupture following TEVAR.[10] In our study, proximal type I endoleak occurred in 18 patients. A cuff was deployed in 7 patients and the endoleak disappeared after 3 months. Our experience showed that: 1. the utmost extension of the landing zones via an artificial vessel bypass can effectively prevent type I endoleak; 2. the maximum length of the proximal landing zones can be achieved by sealing the left subclavian artery in order to prevent type I endoleak; 3. precise localization can be achieved with a secondary low dose and through low-pressure angiography via the brachial artery after 2 segments of proximal stent grafts were opened, which might help avoid the waste of the proximal anchoring length.

Retrograde type A dissection is a fatal complication after TEVAR, which can induce cerebrovascular ischemia, cardiac tamponade and coronary artery infarction with a mortality rate of up to 27.3%.[11] One patient had multiple serpentine tears and prominent edema in the aortic wall, and the stent graft used for sealing the first tear was oversized by less than 5% of the aortic diameter. The patient had a retrograde type A dissection and a recurrent tear in the distal end of the stent graft after 2 months. In order to avoid the occurrence of retrograde type A dissection, our experience showed that: 1. the status of the aorta should be carefully evaluated with CTA before TEVAR;

in patients with intramural hematoma of the ascending artery and aortic arch, edema in the aortic wall, a serpentine dissection of the aorta, and multiple tears in the aorta, TEVAR should be performed after edema has disappeared; 2. a stent graft should be oversized by less than 5% of the aortic diameter; 3. tapered stent grafts should be used.

Spinal cord ischemia is a severe neurological complication after TEVAR with an incidence rate of 0–15%.[12] Spinal cord ischemia did not occur in our study. Drainage of cerebrospinal fluid was not routinely adopted for all patients, but only for patients with a high risk of spinal cord ischemia before TEVAR and for patients with evidence of spinal cord ischemia after TEVAR.

Nowadays, the effectiveness of TEVAR in preventing the expansion and rupture of the aorta still needs to be confirmed by prospective, random and controlled studies. However, we believe that TEVAR will become widely applied in treating aortic dissection with the development of endovascular techniques and stent grafts.

Conclusions

TEVAR had a high success rate and a low rate of occurrence of complications when applied in treating Stanford type B aortic dissection. Therefore, it was reliable and safe, and it had immense potential for treating Stanford type B aortic dissection.

References

1. Mantas GK, Antonopoulos CN, Sfyroeras GS, et al. Factors predisposing to endograft limb occlusion after endovascular aortic repair. *Eur J Vasc Endovasc Surg*. 2015;49:39–44.
2. Faure EM, Becquemin JP, Cochennec F. Predictive factors for limb occlusions after endovascular aneurysm repair. *J Vasc Surg*. 2015;61(5):1138–1145.e2.
3. Dake MD, Kato N, Mitchell RS, et al. Endovascular stent-graft placement for the treatment of acute aortic dissection. *N Engl J Med*. 1999;340:1546–1552.
4. Nienaber CA, Rousseau H, Eggebrecht H, et al. Randomized comparison of strategies for type B aortic dissection: The Investigation of Stent Grafts in Aortic Dissection (INSTEAD) trial. *Circulation*. 2009;120(25):2519–2528.
5. Jing QM, Han YL, Wang XZ, et al. Endovascular stent-grafts for acute and chronic type B aortic dissection: Comparison of clinical outcomes. *Chin Med J*. 2008;121:2213–2217.
6. Si Y, Fu WG, Wang YQ, et al. Prospective study of coverage of left subclavian artery during thoracic endovascular aortic repair in a single center. *Chin J Surg*. 2009;47(24):1868–1872.
7. Nathanson DR, Rodriguez-Lopez JA, Ramaiah VG, et al. Endoluminal stent-graft stabilization for thoracic aortic dissection. *J Endovasc Ther*. 2005;12(3):354–359.
8. Neuhauser B, Czermak BV, Fish J, et al. Type A dissection following endovascular thoracic aortic stent-graft repair. *J Endovasc Ther*. 2005;12(1):74–81.
9. Xu SD, Huang FJ, Du JH, et al. A study of aortic dimension in type B aortic dissection. *Interact Cardiovasc Thorac Surg*. 2008;7(4):244–248.
10. Dong ZH, Fu WG, Wang YQ, et al. Retrograde type A aortic dissection after endovascular stent graft placement of type B dissection. *Circulation*. 2009;119:753–741.
11. Tang DG, Dake MD. TEVR for acute uncomplicated aortic dissection. *Semin Vasc Surg*. 2009;22:145–151.
12. Swee W, Dake MD. Endovascular management of thoracic dissections. *Circulation*. 2008;117:1460–1473.

Comparison of the clinical and microbiological effects of antibiotic therapy in periodontal pockets following laser treatment: An in vivo study

Kinga Grzech-Leśniak[1,A–F], Jacek Matys[1,2,C,D], Marzena Dominiak[1,E,F]

[1] Department of Dental Surgery, Wroclaw Medical University, Poland
[2] Private Dental Practice, Wschowa, Poland

A – research concept and design; B – collection and/or assembly of data; C – data analysis and interpretation;
D – writing the article; E – critical revision of the article; F – final approval of the article

Advances in Clinical and Experimental Medicine, ISSN 1899-5276 (print), ISSN 2451-2680 (online) *Adv Clin Exp Med*. 2018;27(9):1263–1270

Address for correspondence
Jacek Matys
E-mail: jacek.matys@wp.pl

Funding sources
None declared

Conflict of interest
None declared

Received on December 29, 2016
Reviewed on February 5, 2017
Accepted on April 12, 2017

Abstract

Background. Laser technology in periodontal therapy could help in reducing total bacterial count.

Objectives. The aim of this study was to evaluate the effects of pocket debridement using an erbium-doped yttrium aluminium garnet laser (Er:YAG laser – ERL), scaling and root planing (SRP) with photodynamic therapy (PDT), or SRP alone. Teeth vitality and soft tissue carbonization were also assessed.

Material and methods. This study included 1,169 single-rooted teeth from 84 patients divided into 3 groups (n = 28). The G1 group had ERL with 40 mJ of energy, a frequency of 40 Hz and a fluence of 63.66 J/cm^2. The G2 group had SRP + PDT (635 nm diode laser, 12 J of energy and irradiation time of 30 s) and a Toluidine Blue photosensitizer (PS) (application time of 60 s). The G3 group was administered SRP alone. In the 42 subjects (G1: n = 11, G2: n = 14 and G3: n = 17) with high amounts of *Aggregatibacter actinomycetemcomitans* (*Aa*), *Porphyromonas gingivalis* (*Pg*), *Treponema denticola* (*Td*) and *Tannerella forsythia* (*Tf*), additional 1-week antibiotic treatments with clindamycin or amoxicillin + clavulanic acid – in doses of 600 mg/day or 1000 mg/day, respectively – were prescribed 3 months after the therapy. Microbiological and clinical analyses of the probing depth (PD), recession (RC), plaque index (PI), bleeding on probing (BOP), and attachment loss (AT) were performed at baseline and at the follow-up of 3 months, 3 months and 1 week, and 6 months.

Results. Plaque index decreased in G1 after 3 months, 3 months and 1 week, and 6 months ($p < 0.05$) and was lower in G1 vs G2 after 3 months ($p < 0.05$). The reduction in BOP in G1 after 3 months and 1 week was higher in comparison with G2 or G3 ($p < 0.02$). Probing depth decreased in all groups ($p < 0.05$). We found a reduction in the percentage of sites with some bacteria after 3 months – *Prevotella intermedia* (*Pi*) (G1 and G2), *Capnocytophaga gingivalis* (*Cg*) and *Eubacterium nucleatum* (*En*) (G3), and after 3 months and 1 week with *En*, *Td*, *Tf* (G1, G2 and G3), *Pi* (G1 and G2), *Aa*, *Peptostreptococcus micros* (*Pm*), and *Cg* (G3), and with *Pi* (G1 and G2), *Tf* (G2), *Pg*, *En* (G2 and G3), and *Pm* (G3) after 6 months ($p < 0.05$). We observed no signs of carbonization or teeth injury.

Conclusions. Scaling and root planing + PDT and ERL may be an alternative therapy for chronic periodontitis.

Key words: chronic periodontitis, photodynamic therapy, antibacterial therapy, scaling and root planning, Er:YAG laser

DOI
10.17219/acem/70413

Introduction

Recently, more and more bacterial strains have become resistant to antibiotics.[1] The excessive use of antibiotics and the development of several new ones by pharmaceutical companies are 2 reasons why some researchers describe the first decade of the 21st century as the antibiotic resistance crisis.[2–4] Anaerobic bacterial growth in the periodontal pocket leads to periodontal diseases, which are becoming more and more common in Poland; they also increase the risk of tooth loss or other medical complications, such as acute myocardial infarction or stroke.[5–7]

Clinical and microbiological analyses using traditional culture methods and the polymerase chain reaction (PCR) test provide general data about the severity of periodontitis, which are useful in designing treatment strategies.[8] Unfortunately, the basic PCR technique does not provide a quantitative assessment of the identified bacteria.[9] Due to its ability to generate both qualitative and quantitative results, the newer and more costly real-time polymerase chain reaction (rtPCR) analysis has provided scientific advancement.[9]

The gold standard in periodontal treatment is the proper eradication of pathological bacterial strains inside the infected pockets by means of mechanical debridement.[10,11] However, root architecture and its particular anatomical variations are an obstruction in establishing effective protocols for debridement in non-surgical periodontal therapy, which uses traditional tools, such as curettes or ultrasonic scalers.[12] Therefore, different devices (e.g., lasers) have been used in non-surgical periodontal treatment as alternative or adjunct methods to mechanical scaling and root planing (SRP). Many clinical studies have confirmed the effectiveness of the 2940 nm erbium-doped yttrium aluminium garnet laser (Er:YAG laser – ERL) in periodontal therapy, with or without additional SRP.[13–15] The combination of low-power lasers and different photosensitizers (PSs), known as antimicrobial photodynamic therapy (aPDT), enhanced the elimination of periopathogenic bacteria and the reduction of bone loss.[16–18] Furthermore, the ability of lasers to decontaminate the root surface with minimal (ERL) or no damage (PDT) could be of great value in periodontal therapy, because mechanical instruments may lead to excessive removal of root material.[19] However, in their study, Zach and Cohen reported that an intrapulpal temperature increase of 5.5°C caused pulpitis or pulp necrosis in 15% of the irradiated teeth.[20] Thus, particular attention should be paid to preventing thermal injury of periodontal tissues when high-powered lasers are applied during periodontal procedures.

Objectives

The aim of this randomized, controlled clinical trial was to compare the clinical and microbiological effects of antibiotic therapy following pocket debridement, using ERL and SRP + PDT as compared to SRP alone. Additionally, the objective was to assess the vitality of the teeth after periodontal procedures and the occurrence of soft tissue carbonization.

Material and methods

The trial was designed as a randomized and controlled test lasting 6 months. The study protocol was reviewed and approved by the Bioethics Commission of the Regional Chamber of Physicians and Dentists in Kraków (permission No.: 74/KBL/OIL/2014). Informed consent was obtained from all participating subjects.

Subjects

The study included 1,169 periodontally-involved single-rooted teeth in 84 patients (38 women and 46 men, aged 48.6 ±9.4 years). All patients were diagnosed with generalized chronic periodontitis according to the classification of periodontal diseases from the American Academy of Periodontology (AAP) classification from 1999.[21] The groups were treated at the private clinic PerioCare in Kraków, Poland. Selected patients in the study: 1. had all single-rooted teeth with a probing depth (PD) of ≥5 mm and no signs of apical pathology; 2. had no systemic diseases; 3. were not using anti-inflammatory drugs; 4. had not used antibiotics for the previous 24 months; 5. were non-smokers; 6. had not undergone periodontal treatment before the trial; 7. had undergone hygienist treatment before the clinical trial.

Treatment procedures

A total of 84 patients were randomly assigned by a computer to the 3 study groups according to the treatment procedure: G1 – ERL (n = 28); G2 – SRP + PDT (n = 28); and G3 – SRP alone (n = 28). For the 592 periodontally-involved single-rooted teeth in 42 subjects (G1: n = 11, G2: n = 14 and G3: n = 17) with high amounts of *Aggregatibacter actinomycetemcomitans* (*Aa*), *Porphyromonas gingivalis* (*Pg*), *Treponema denticola* (*Td*), and *Tannerella forsythia* (*Tf*), additional antibiotic treatments were prescribed after the therapy according to the antibiogram: clindamycin (Clindamycin-MIP®; MIP Pharma, Innsbruck, Austria) or amoxicillin + clavulanic acid (Amoksiklav; Sandoz, Warszawa, Poland), in dosages of 600 mg/day or 1000 mg/day for 1 week, respectively.

Clinical treatment

In each patient, non-surgical periodontal pocket debridement was performed by a specialist in the area of periodontal treatment, using different therapeutic methods.

Group 1 received periodontal debridement with the Er:YAG laser (LightWalker; Fotona, Ljubljana, Slovenia)

with the following fixed operation parameters: pulse mode – medium-short pulse (MSP), energy – 40 mJ, frequency – 40 Hz, fluence per point – 63.66 J/cm^2, perio tip (Varian) – 400 µm, and water spray – 100%. Laser therapy was performed by inserting the fiber into the periodontal pocket almost parallelly to the tooth and moving in a mesial to distal direction continuously on the buccal and lingual surface of the tooth, 10 to 30 s per tooth.

Group 2 received periodontal debridement with a combination of SRP and Photoactive Disinfection with a Diode laser (Smart M; Lasotronix, Piaseczno, Poland) with the following fixed operation parameters: continuous wave mode and 200 mW of energy. Photosensitizer (Toluidine Blue 0.1%) was applied into the pocket and left for 60 s; then, the tip of the Diode laser (PACT® Light Guides Universal; Cumdente GmbH, Tübingen, Germany) was inserted into the pocket subgingivally and the PS was irradiated for 30 s.

Group 3 (control) received SRP alone – periodontal debridement, using hand curettes (Double Gracey XP; American Eagle Instruments, Inc., Missoula, USA).

Clinical parameters

Clinical data was collected before treatment (baseline) and at follow-up examinations after 3 months, 3 months and 1 week, and 6 months. All recordings in each patient were taken with a fully automated periodontal probe (paon; Orangedental GmbH & Co.KG, Biberach an der Riss, Germany), which transfers the data onto a computer screen.

The following clinical parameters were evaluated:

– plaque index (PI): evaluation of the presence of plaque at the cervical margin of the tooth, using a periodontal probe, expressed as percentage;

– pocket depth (PD): the distance from the gingival margin to the bottom of the pocket, measured at 6 sites of the single-rooted teeth (mesiobuccal/midbuccal/distobuccal/mesiopalatal/midpalatal/distopalatal) with a constant probing force of 0.2 g of pressure;

– bleeding on probing (BOP): determined by the presence (+) or absence (–) of bleeding for 30 s after the first probe was inserted into the pocket, expressed as percentage;

– recession (RC): distance from the cemento-enamel junction (CEJ) to the gingival margin (and from the crown margin to the gingival margin);

– attachment loss (AT): the distance between the CEJ and the base of the sulcus; it includes both PD and RC measurements.

Microbiological analysis

The microbiological examination of every patient consisted of a biological-molecular test (PetPlus; MIP Pharma GmbH, Blieskastel-Niederwürzbach, Germany) which involves the detection of 9 periodontal pathogens, including red, orange, green, and yellow complexes (e.g., *Aa*, *Pg*, *Td*, *Tf*, *Prevotella intermedia* – *Pi*, *Peptostreptococcus micros* – *Pm*, *Fusobacterium nucleatum* – *Fn*, *Eubacterium nucleatum* – *En*, and *Capnocytophaga gingivalis* – *Cg*). The test was performed by means of the rtPCR method. The samples were taken according to the manual with enclosed sterile paper swabs, so the uniformity of the sampling was ensured. The paper swabs were inserted into the gingival pockets for 30 s.

Microbiological analysis by means of rtPCR was conducted: 1. at baseline; 2. 3 months after the treatment in all 3 groups; 3. 1 week after introducing the additional antibiotic therapy (Clindamycin-MIP or Amoksiklav, duration: 1 week); 4. 3 months after the antibiotic therapy (6 months since baseline).

Tissue injury test

The visual signs of soft tissue carbonization and the reaction of the teeth (+/–) to ethyl chloride after the treatment were evaluated.

Statistical analysis

All data was subjected to statistical analyses with STATISTICA 12 software (StatSoft, Kraków, Poland). The differences in the clinical parameters (PI, PD, BOP, RC, and AT) in the time periods and between the groups were analyzed according to the 2-way repeated analysis of variance (ANOVA) test. The Cochran's Q test and the χ^2 McNemar exact test were used to assess bacterial prevalence. Values of $p \leq 0.05$ were considered to be significant.

Results

A total of 1,169 periodontally-involved single-rooted teeth in 84 patients were included in this study.

Plaque index

In the comparison between the baseline and 3 months (8.4% to 4.6%), 3 months and 1 week (8.4% to 5.8%), and 6 months (8.4% to 4.0%) after the treatments, there was a significant reduction in PI ($p < 0.05$) in the G1 group (Fig. 1).

The difference among the groups revealed a significantly lower PI value after 3 months in the G1 group as compared to the G2 group ($p < 0.01$) (Fig. 2).

Bleeding on probing

A significant reduction in BOP after an additional antibiotic treatment at 3 months and 1 week, and 6 months, in both the G1 and G2 groups, was observed compared with the G3 group ($p < 0.01$) (Fig. 3).

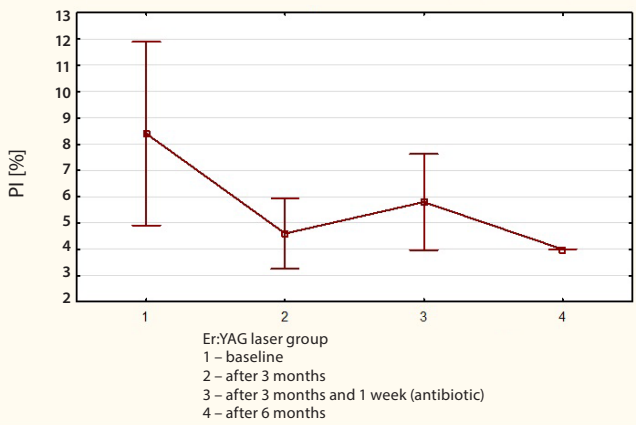

Fig. 1. The mean value of PI after periodontal pocket debridement with Er:YAG laser at 4 time points

PI – plaque index.

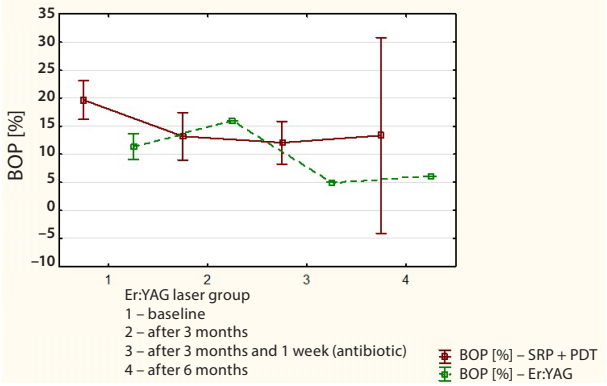

Fig. 3. The mean value of BOP after periodontal pocket debridement with Er:YAG laser or SRP + PDT at 4 time points

BOP – bleeding on probing; SRP – scaling and root planing; PDT – photodynamic therapy.

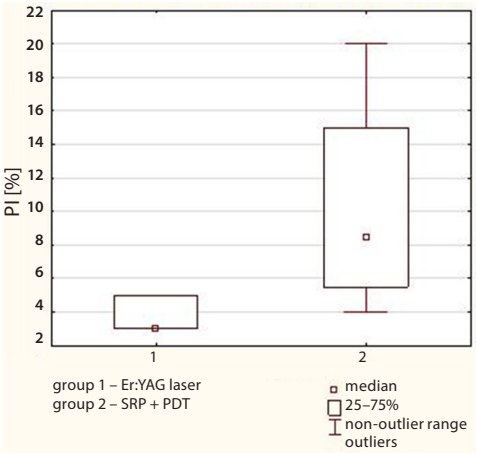

Fig. 2. The results of PI 3 months after periodontal pocket debridement with different treatment methods

PI – plaque index; SRP – scaling and root planing; PDT – photodynamic therapy.

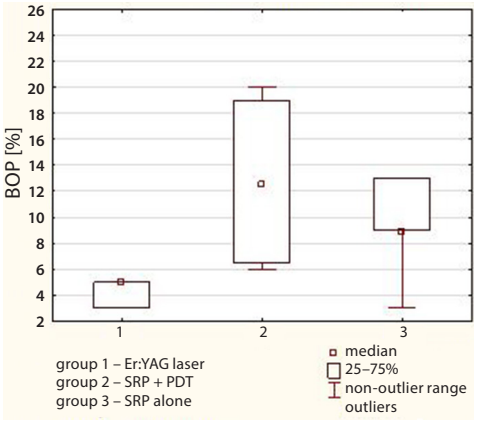

Fig. 4. The results of BOP after periodontal pocket debridement with Er:YAG laser, SRP + PDT or SRP alone 1 week after additional antibiotics delivery

BOP – bleeding on probing; SRP – scaling and root planing; PDT – photodynamic therapy.

Table 1. The mean reduction in PD [mm] for all 3 patient groups after 3 months, 3 months and 1 week, and 6 months

Study groups	Baseline	3 months	3 months 1 week	6 months	p-value
G1	6.12 ±1.95	2.88 ±0.75	2.72 ±0.65	2.95 ±0.67	<0.05
G2	6.7 ±1.73	2.76 ±0.61	2.5 ±0.53	2.6 ±0.49	<0.05
G3	6.03 ±1.41	2.55 ±0.58	2.66 ±0.53	2.89 ±0.58	<0.05
p-value	NS	NS	NS	NS	–

G1 – group with ERL; G2 – group with SRP + PDT; G3 – group with SRP alone; PD – pocket depth; ERL – Er:YAG laser; SRP – scaling and root planing; PDT – photodynamic therapy; NS – not significant. Data is presented as mean ± standard deviation (SD).

The additional delivery of antibiotics resulted in a decrease in the BOP level in the G1 group as compared with the G2 and G3 groups ($p < 0.02$) (Fig. 4).

Pocket depth

There was a significant difference in the reduction of PD in all 3 patient groups after 3 months, 3 months and 1 week, and 6 months as compared with the baseline ($p < 0.05$) (Table 1).

Recession and attachment loss

The comparison of RC and AT showed insignificant results among all groups and between all study periods ($p > 0.05$) (Tables 2, 3).

Microbiological results

After 3 months, we observed a reduction of *Pi* in the laser-treated groups G1 and G2, of *Cg* and *En* in the G3

Table 2. The mean RC size [mm] for all 3 patient groups after 3 months, 3 months and 1 week, and 6 months

Study groups	Baseline	3 months	3 months 1 week	6 months	p-value
G1	1.1 ±0.75	1.19 ±0.78	1.22 ±0.73	1.11 ±0.72	NS
G2	0.8 ±0.62	0.96 ±0.52	0.99 ±0.38	0.97 ±0.49	NS
G3	1.13 ±0.75	1.19 ±0.79	1.1 ±0.8	1.13 ±0.81	NS
p-value	NS	NS	NS	NS	–

G1 – group with ERL; G2 – group with SRP + PDT; G3 – group with SRP alone; RC – recession; ERL – Er:YAG laser; SRP – scaling and root planing; PDT – photodynamic therapy; NS – not significant. Data is presented as mean ± standard deviation (SD).

Table 3. The mean AT [mm] for all 3 patient groups after 3 months, 3 months and 1 week, and 6 months

Study groups	Baseline	3 months	3 months 1 week	6 months	p-value
G1	3.22 ±0.77	3.03 ±0.92	2.93 ±1.03	4.02 ±1.73	NS
G2	3.25 ±1.09	3.13 ±0.98	3.09 ±0.67	3.26 ±0.91	NS
G3	3.15 ±0.77	3.04 ±0.97	2.76 ±1.29	2.99 ±1.32	NS
p-value	NS	NS	NS	NS	–

G1 – group with ERL; G2 – group with SRP + PDT; G3 – group with SRP alone; AT – attachment loss; ERL – Er:YAG laser; SRP – scaling and root planing; PDT – photodynamic therapy; NS – not significant. Data is presented as mean ± standard deviation (SD).

group, and a significant increase in *Aa* (G2 and G3), *Pi* (G3), and *Pg* (in all 3 study groups) ($p < 0.05$).

After 3 months and 1 week, we noted a reduction of *Td*, *Tf* and *En* in all 3 groups, of *Pi* in the G1 and G2 groups, *Aa*, *Pm*, *Cg* in the G3 group, and a significant increase in *Aa* in the G2 group ($p < 0.05$).

After 6 months, a reduction in the percentage of sites with bacterial prevalence of *Pi* (G1 and G2), *Tf* (G2), *Pg*, *En* (G2 and G3), and *Pm* (G3) was reported as compared to the baseline ($p < 0.05$) (Fig. 5).

Additionally, we observed no signs of carbonization during periodontal pocket debridement with the Er:YAG laser with the fixed operation parameters used in this study (energy – 40 mJ, frequency – 40 Hz, fluence per point –63.66 J/cm^2). The pulp vitality test in all the teeth indicated a positive reaction to ethyl chloride following treatment.

Discussion

A review of the literature to date provides no record of a comparison of in vivo studies which evaluated the clinical and microbiological effects of antibiotic therapy following pocket debridement, using ERL and SRP + PDT in the same study. Furthermore, the impact of additional antibiotic therapy on bacterial counts in periodontal pockets, assessed by means of the rtPCR test has not been analyzed in relation to previous laser applications. The main objective of this study was to determine the effects of different periodontal pocket debridement methods (ERL and SRP + PDT) on clinical parameters, such as PI, PD, BOP, AT, RC, and bacterial count in the rtPCR test (PetPlus test).

The results of our study show a significant reduction in PD of 6.12 mm to 2.95 mm, 6.7 mm to 2.6 mm and 6.03 mm to 2.89 mm in the groups G1, G2 and G3 after 6 months, respectively. Our findings were consistent with the results presented by other authors for different laser wavelengths, e.g., 2940 nm,[14] 2780 nm,[22] 940 nm,[22] and for aPDT[23,24] and SRP alone.[14] All the methods of treating chronic periodontitis discussed in the present study were efficient and resulted in a reduction of PD; however, there were no significant differences identified between the treatment groups, which was confirmed in another study.[25]

The second tested outcome parameter was the BOP score. Several authors indicated significant improvements in BOP after erbium laser irradiation[13–15,22] or PDT.[23] We found an insignificant increase in BOP after the application of the Er:YAG laser. Ciurescu et al. also reported a lower reduction in the BOP score, but only when the Er:YAG laser and SRP were compared at 2 months' follow-up (32% vs 38%).[22]

Surprisingly, we found no significant differences among all treatment methods with respect to AT and RC size at each time point. Rotundo et al. in their study also showed that there was no significant difference between ERL + SRP and SRP alone in the clinical attachment level in a group of 27 patients who underwent non-surgical periodontal therapy. These results were confirmed by Tomasi et al., comparing the Er:YAG laser and the ultrasonic scaler at a 4-month follow-up examination.[25,26] On the other hand, Moreira et al. demonstrated different results, as they found clinical attachment gain to be significantly higher after the application of 4 sessions of aPDT than in the control group (SRP).[27]

Particular attention in our study was paid to the influence of additional antibiotic therapy on the pathogenic bacteria which colonize the periodontal pockets. Regardless of the reduction in PD and the BOP index after Er:YAG laser debridement and the combination of SRP + PDT therapy, bacteria in the periodontal pocket were not completely eliminated. While laser application helped reduce bacterial counts without any side effects for the

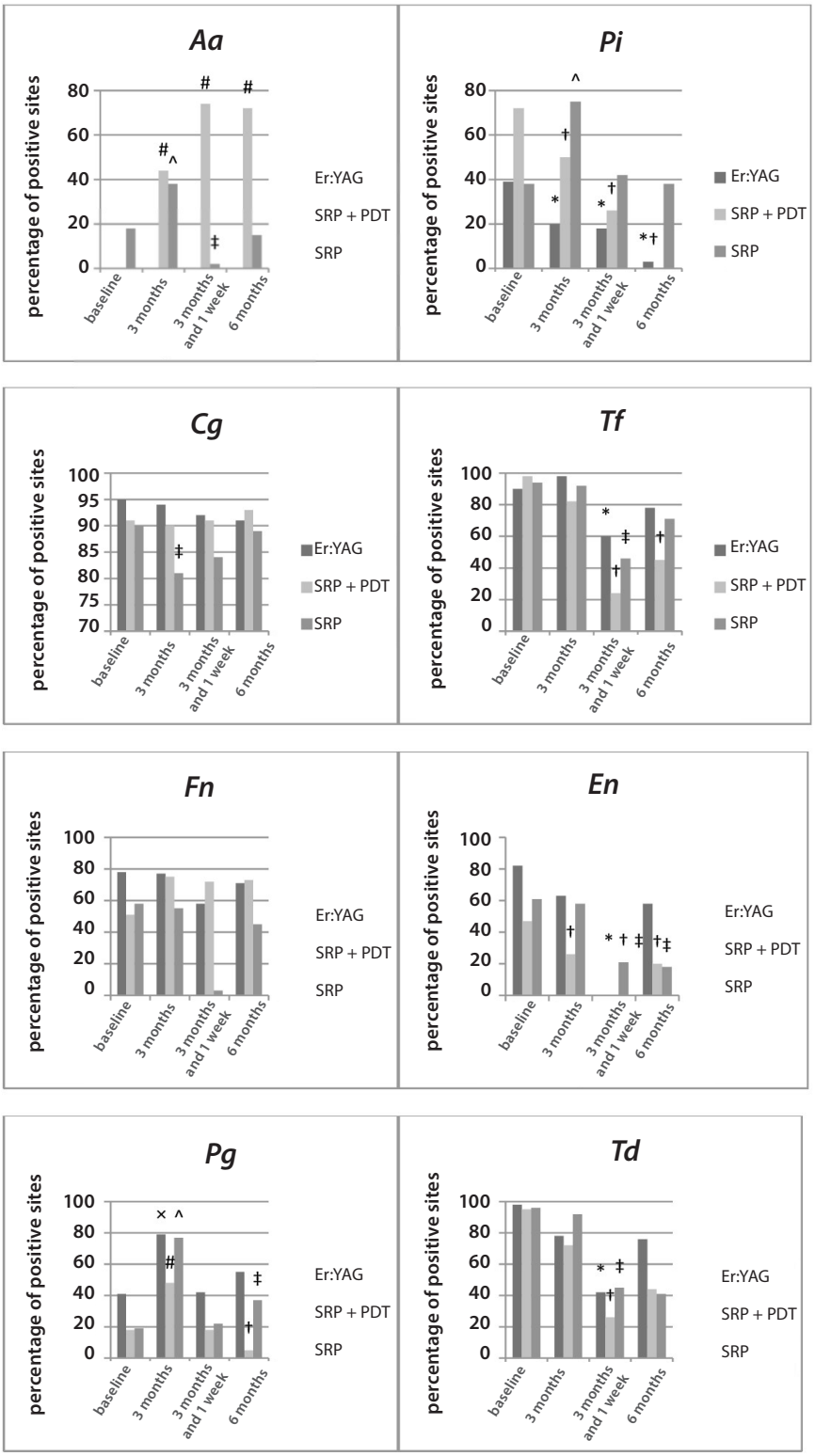

Fig. 5. The microbiological examination of different periodontal pathogens, using the rtPCR test at baseline, 3 months, 3 months and 1 week, and 6 months

rtPCR – real-time polymerase chain reaction; SRP – scaling and root planing; PDT – photodynamic therapy; *Aa – Aggregatibacter actinomycetemcomitans*; *Pi – Prevotella intermedia*; *Cg – Capnocytophaga gingivalis*; *Tf – Tannerella forsythia*; *Fn – Fusobacterium nucleatum*; *En – Eubacterium nucleatum*; *Pg – Porphyromonas gingivalis*; *Td – Treponema denticola*. Significant reduction in the percentage of sites positive to microbial testing in comparison with the baseline for: * Er:YAG laser (G1); † SRP + PDT (G2); ‡ SRP (G3); × Er:YAG laser (G1); # SRP + PDT (G2); ^ SRP (G3).

patient, the goal was to eradicate any bacterial strains from the periodontal pocket. Our study design involved only 1 application of the laser, which resulted in incomplete elimination of bacteria. The remaining bacteria may be eradicated by additional antibiotic treatment, as suggested by the American Academy of Periodontology and the European Federation of Periodontology.[28] However, to date there have been no established protocols or guidelines on the optimal additional antibiotic therapy recommended in such cases. It remains a challenge for the dental community to design protocols that will reduce the use of systemic antibiotics in favor of local ones. Generally speaking, we should aim at a minimally invasive treatment, and laser therapy is exactly that.

We conducted a microbiological analysis of the bacterial strains in the periodontal pockets after the use of the

erbium laser and PDT. The success of these treatments can be attributed to the efficient removal of the subgingival biofilm and the eradication of bacteria from the root surface.[12] Similarly to the findings of Lopes et al., our trial showed a significant reduction in the percentage of sites with *Pi* and *Pg* after erbium laser irradiation.[14] However, there is a fundamental difference in the response to PDT between Gram-positive and Gram-negative bacteria. Gram-negative bacteria consist of an inner cytoplasmic membrane and an outer membrane, while Gram-positive bacteria are composed of only a cytoplasmic membrane surrounded by a relatively porous cell wall composed of lipoteichoic acid and peptidoglycan. The differences in their composition result in different susceptibility and permeability to chemicals.[24] It was found that neutral, anionic and cationic PS molecules efficiently kill Gram-positive bacteria, whereas only cationic PS molecules are able to kill Gram-negative strands.[24] However, some modified non-cationic PS, such as chlorin (e6), have the ability of anchoring to the negatively charged lipopolysaccharide molecules. Unfortunately, studies using this dye in aPDT in periodontal research are scarce. Hence, additional alternatives to antibiotic therapy with different non-cationic PS during periodontal therapy should be researched.

We also evaluated the influence of additional antibiotic treatment on bacterial counts. The levels of bacteria strains such as *Aa*, *Pg*, *Td*, and *Tf* remained high after periodontal treatment using the tested therapeutic methods (ERL, SRP + PDT and SRP alone). We confirmed that antibiotics caused a decrease in the number of *Pg*, *Td* and *Tf* bacteria. Unfortunately, the overuse of antibiotics contributes to the development of bacterial resistance, thus careful patient selection, proper antibiotic treatment protocols and guidelines, the use of antibiograms, and – most of all – new non-antibiotic treatment methods require rigorous research and development.[29,30]

In comprehensive periodontal treatment, lasers offer a non-invasive alternative or complementary therapy method. The use of lasers in repeated therapy could help decrease the number of periopathogenic bacteria and keep their counts at a stable, low level. Hence, we are of the opinion that laser therapy constitutes a promising alternative and calls for more research to be conducted for the repeated therapy of periodontal diseases by means of the Er:YAG laser and PDT.

Conclusions

The current study failed to confirm significant differences in many compared clinical outcome parameters for non-surgical periodontal treatments with Er:YAG laser debridement, SRP + PDT therapy and the conventional SRP procedure alone. It did, however, show that additional systemic antibiotic administration significantly decreased BOP in the G1 group. The microbiological analysis in the present study revealed somewhat better results after non-surgical periodontal treatment with the Er:YAG laser than after a combination of SRP with PDT, which had little clinical effect on the eradication of red complex bacteria. Additional antibiotic therapy with clindamycin or amoxicillin+clavulanic acid had a positive effect on the reduction of *Td* and *Tf* after periodontal pocket debridement with ERL, SRP + PDT and SRP alone.

The use of combined antibiotic therapy and Er:YAG laser treatment may be a valuable therapeutic option in the treatment of periodontal diseases and it demands further research.

References

1. Wright GD. Something new: Revisiting natural products in antibiotic drug discovery. *Can J Microbiol*. 2014;60(3):147–154.
2. Ventola CL. The antibiotic resistance crisis: Part 1: Causes and threats. *P&T*. 2015;40(4):277–283.
3. Piddock LJ. The crisis of no new antibiotics – what is the way forward? *Lancet Infect Dis*. 2012;12(3):249–253.
4. Michael CA, Dominey-Howes D, Labbate M. The antibiotic resistance crisis: Causes, consequences, and management. *Front Public Health*. 2014;2:145.
5. Górska R, Pietruska M, Dembowska E, Wysokińska-Miszczuk J, Włosowicz M, Konopka T. Prevalence of periodontal diseases in 35–44 year-olds in the large urban agglomerations. *Dent Med Probl*. 2012;49:19–27.
6. Górski B, Nargiełło E, Grabowska E, Opolski G, Górska R. The association between dental status and risk of acute myocardial infarction among poles: Case-control study. *Adv Clin Exp Med*. 2016;25(5):861–870.
7. Slowik J, Wnuk MA, Grzech K, et al. Periodontitis affects neurological deficit in acute stroke. *J Neurol Sci*. 2010;15:297(1):82–84.
8. Yoshida A, Ansai T. Microbiological diagnosis for periodontal diseases. In: Manakil J, ed. *Periodontal Diseases – A Clinician's Guide*. Rijeka, Croatia: InTech; 2012:55.
9. Valones MA, Guimarães RL, Brandão LA, Souza PR, Carvalho AD, Crovela S. Principles and applications of polymerase chain reaction in medical diagnostic fields: A review. *Braz J Microbiol*. 2009;40(1):1–11.
10. Sanz I, Alonso B, Carasol M, Herrera D, Sanz M. Nonsurgical treatment of periodontitis. *J Evid Base Dent Pract*. 2012;12(3):76–86.
11. Graetz C, Plaumann A, Wittich R, et al. Removal of simulated biofilm: An evaluation of the effect on root surfaces roughness after scaling. *Clin Oral Invest*. 2016;27:1–8.
12. Graetz C, Plaumann A, Bielfeldt J, Tillner A, Sälzer S, Dörfer CE. Efficacy versus health risks: An in vitro evaluation of power-driven scalers. *J Indian Soc Periodontol*. 2015;19(1):18.
13. Gutknecht N, Van Betteray C, Ozturan S, Vanweersch L, Franzen R. Laser supported reduction of specific microorganisms in the periodontal pocket with the aid of an Er,Cr:YSGG laser: A pilot study. *Sci World J*. 2015;2015:450258. doi:10.1155/2015/450258
14. Lopes BM, Theodoro LH, Melo RF, Thompson GM, Marcantonio RA. Clinical and microbiologic follow-up evaluations after non-surgical periodontal treatment with erbium: YAG laser and scaling and root planing. *J Periodontol*. 2010;81(5):682–691.
15. Sgolastra F, Petrucci A, Gatto R, Monaco A. Efficacy of Er:YAG laser in the treatment of chronic periodontitis: Systematic review and meta-analysis. *Laser Med Sci*. 2012;27(3):661–673.
16. Talebi M, Taliee R, Mojahedi M, Meymandi M, Torshabi M. Microbiological efficacy of photodynamic therapy as an adjunct to non-surgical periodontal treatment: A clinical trial. *J Lasers Med Sci*. 2016;(2):126–130.
17. Nielsen HK, Garcia J, Væth M, Schlafer S. Comparison of riboflavin and toluidine blue O as photosensitizers for photoactivated disinfection on endodontic and periodontal pathogens in vitro. *PloS ONE*. 2015;10(10):e0140720.

18. Prates RA, Yamada AM, Suzuki LC, et al. Histomorphometric and microbiological assessment of photodynamic therapy as an adjuvant treatment for periodontitis: A short-term evaluation of inflammatory periodontal conditions and bacterial reduction in a rat model. *Photomed Laser Surg*. 2011;29:835–844.
19. de Oliveira GJ, Cominotte MA, Beraldo TP, Sampaio JE, Marcantonio RA. A microscopic analysis of the effects of root surface scaling with different power parameters of Er, Cr: YSGG laser. *Microsc Res Techniq*. 2015;78(6):529–535.
20. Zach L, Cohen G. Pulp response to externally applied heat. *Oral Surg Oral Med Oral Pathol*. 1965;19:515–530.
21. Armitage GC. Development of a classification system for periodontal diseases and conditions. *Ann Periodontol*. 1999:4:1–6.
22. Ciurescu C, Teslaru S, Zetu L, Ciurescu D. Laser assisted periodontal treatment: From bactericidal effect to local modification of the host response. Paper presented at: Sixth International Conference on Lasers in Medicine; May 7–9, 2015; Bucharest, Romania. doi:10.1117/12.2189324
23. Polansky R, Haas M, Heschl A, Wimmer G. Clinical effectiveness of photodynamic therapy in the treatment of periodontitis. *J Clin Periodontol*. 2009;36:575–580.
24. Dai T, Huang YY, Hamblin MR. Photodynamic therapy for localized infections – state of the art. *Photodiagnosis Photodyn Ther*. 2009;6(3):170–188.
25. Tomasi C, Schander K, Dahlén G, Wennström JL. Short-term clinical and microbiologic effects of pocket debridement with an Er:YAG laser during periodontal maintenance. *J Periodontol*. 2006;77(1):111–118.
26. Rotundo R, Nieri M, Cairo F, et al. Lack of adjunctive benefit of Er:YAG laser in non-surgical periodontal treatment: A randomized split-mouth clinical trial. *J Clin Periodontol*. 2010;37:526–533.
27. Moreira AL, Novaes Jr AB, Grisi MF, et al. Antimicrobial photodynamic therapy as an adjunct to non-surgical treatment of aggressive periodontitis: A split-mouth randomized controlled trial. *J Periodont*. 2015;86(3):376–386.
28. Deas DE, Mealey BL. Response of chronic and aggressive periodontitis to treatment. *Periodontol 2000*. 2010;53(1):154–166.
29. Bizzarro S, Laine ML, Buijs MJ, et al. Microbial profiles at baseline and not the use of antibiotics determine the clinical outcome of the treatment of chronic periodontitis. *Sci Rep*. 2016;6:20205. doi:10.1038/srep20205
30. Walters J, Lai PC. Should antibiotics be prescribed to treat chronic periodontitis? *Dent Clin North Am*. 2015;59(4):919–933.

A need for intervention: Childhood adversities are a significant determinant of health-harming behavior and poor self-efficacy in patients with alcohol dependence. An observational, cross-sectional study on the population of Central Poland

Dominika Berent[1,A–D,F], Michał Podgórski[2,C,F], Andrzej Kokoszka[1,E,F]

[1] Department of Psychiatry II, Medical University of Warsaw, Poland
[2] Department of Diagnostic Imaging, Polish Mother's Memorial Hospital Research Institute, Łódź, Poland

A – research concept and design; B – collection and/or assembly of data; C – data analysis and interpretation; D – writing the article; E – critical revision of the article; F – final approval of the article

Advances in Clinical and Experimental Medicine, ISSN 1899-5276 (print), ISSN 2451-2680 (online) *Adv Clin Exp Med*. 2018;27(9):1271–1277

Address for correspondence
Dominika Berent
E-mail: dominikaberent@poczta.fm

Funding sources
None declared

Conflict of interest
None declared

Received on November 4, 2016
Reviewed on April 11, 2017
Accepted on April 27, 2017

Abstract

Background. Adverse childhood experiences (ACEs) are known to be associated with a lasting effect on physical and psychological well-being in adulthood. Patients with alcohol dependence (AD) are a particular clinical subgroup who report a higher number of ACE categories than the general population and who develop several health-harming behaviors and poor social skills.

Objectives. To our knowledge, this is the first study on patients with AD that aimed to assess whether ACEs correlate with health habits and general self-efficacy in adulthood.

Material and methods. The study comprised 196 patients with AD (F = 50) with a mean age of 43.8 years. The following research tools were used: the Health Behavior Inventory (HBI), the Generalized Self-Efficacy Scale (GSES) and the ACE Study score, expanded with 3 more questions about exposure to sudden stress and violence outside the family. Additionally, the patients' sociodemographic and clinical characteristics were assessed and included in the multiple stepwise regression analysis for variation in health habits and general self-efficacy.

Results. The mean scores of the patients were 64.4 ±16.6 points on the HBI and 28.4 ±6.2 points on the GSES. The study revealed a mean number of 3.3 ±2.7 ACEs. The multiple regression analysis showed that the ACEs were significantly and inversely associated with self-efficacy assessed by the GSES and with health habits evaluated by the HBI ($\beta = -0.377$; $p = 0.026$ and $\beta = -1.210$; $p = 0.007$, respectively). The ACEs accounted for 3.2% of the GSES model variability and 3.9% of the HBI variability.

Conclusions. Adverse childhood experiences might promote the development of health-harming behaviors and inferior general self-efficacy in adult patients with AD. The study suggests the need for primary and secondary preventive strategies targeted at ACEs and at general self-efficacy impaired by childhood adversities for further better well-being. However, although the influence of the ACEs was significant, there are many other factors that were not included in the analysis, which explain the remaining variability of health behaviors and general self-efficacy.

Key words: health, alcoholism, child abuse, adult survivors, self-efficacy

DOI
10.17219/acem/70792

Introduction

Emotional and interpersonal impairments continue to be studied in the area of alcohol dependence (AD) because of their role in treatment outcomes and general well-being in patients with AD. The literature states that social disabilities in patients with AD may be either primary or secondary to alcohol misuse and may be produced by both social and biological factors.[1–3] Patients with AD were found to present a loss of behavioral flexibility, significant impairment in facial emotion recognition and a generally impaired ability to recognize one's own and others' mental states.[1,2] Patients with AD and impairment in facial emotion recognition were found to consider alcohol misuse as a tool for improving social abilities.[3] However, alcohol misuse, especially in adolescence, was found in animal studies to result in lifelong neurobiological changes and a permanent loss of hippocampal neurogenesis with the further phenotype result of impairment in behavioral flexibility.[1]

General self-efficacy, which is an important measure of social ability, is referred to as global confidence in one's coping ability in demanding or new situations, which require a variety of stressful experiences to be dealt with and which characterize one's social skills.[4] As was noted by Bandura, patients who have strong self-efficacy are likely to mobilize the effort needed to successfully resist situations which put them at a high risk for using alcohol.[5] Skill-oriented self-efficacy, i.e., the ability to not drink in high-risk situations, is associated with the effective use of coping strategies and lower relapse rates.[6,7] General self-efficacy may be influenced by adverse childhood experiences (ACEs), understood as physical, emotional and sexual abuse, loss of attachment figures, and sudden potentially traumatic events, i.e., witnessing someone's death. Bandura et al. pointed out that there is a bimodal association between life adversities and self-efficacy.[8] Strong self-efficacy supports recovery from traumatic experiences, but self-efficacy may be impaired by previously experienced life adversities.[8] Reports in the literature indicate that ACEs may trigger adverse adaptation following traumatic experiences, and impair self-efficacy.[9–11]

Individuals with AD were found to report a higher number of ACEs than the general population.[12,13] As compared with people with an ACE Study score of 0, those with an ACE Study score of 4 or more were 7 times more likely to suffer from AD.[12] It was postulated that this may be due to having been raised in a dysfunctional household; however, the correlation is obviously not absolute.[14,15] Nevertheless, a national study in Great Britain on ACEs found that individuals with ≥4 ACEs (vs 0 ACEs) were at an approx. 3 times higher risk of developing any disease before 70 years of age, e.g., cancer, diabetes or stroke.[16] This may be due to the fact that patients with AD, apart from drinking alcohol, develop multiple health-harming behaviors, e.g., poor diet, low physical activity or cigarette smoking.[17] The results of studies on the association between ACEs and general health in adulthood based on the ACE Study score have been widely published.[12,13,18,19] However, exposure to sudden stress and violence outside the family is also considered to be an important predictor of health in adulthood.[20] Thus, we posed 3 more questions to our participants concerning them potentially witnessing a family member's attempted suicide, a family member's death from any cause or a stranger's death from any cause (e.g., a traffic accident).

Both health habits and general self-efficacy are contributors to individual mental and physical well-being; therefore, searching for the factors that may trigger them is still necessary in order to propose possible preventive strategies for better overall health.[8,21] To our knowledge, this is the first study to assess the possible influence of childhood adversities on health habits and general self-efficacy in patients with AD. Here, we hypothesize that ACEs may promote the adoption of health-harming behaviors and may impair general self-efficacy in patients with AD.

Material and methods

Study participants

This is an observational, cross-sectional study that was performed in Poland between 2013 and 2015. A total of 209 consecutive patients with AD who were admitted to psychiatric wards for a course of AD psychotherapy or treatment of alcohol withdrawal syndrome and who gave informed consent were involved in the study. Of these patients, 13 did not undergo further analysis because of incomplete data or the withdrawal of their consent during the study. The study analyzed 196 patients with AD (F = 50) aged 43.8 ±10.7 years (mean ±SD). Each patient received a consensus diagnosis of AD by 2 psychiatrists according to the 10th revision of the International Statistical Classification of Diseases and Related Health Problems (ICD-10).[22] The most recent alcohol intake was at least 1 week priorly. The exclusion criteria were: age of <18 years, a history of a significant psychiatric comorbidity according to the ICD-10.[22]

Data collection

This study used a structured self-reported questionnaire that was designed to measure the sociodemographic and clinical characteristics of the study participants (gender, age, education, employment status, marital status, place of living, and cigarette smoking). The study participants were assured of the confidentiality of the data obtained. The researcher remained present during the completion of the questionnaires in order to address the participants' questions and to make sure the respondents understood all of the items. Patients who answered "yes" to the following question: "Have you smoked at least 100 cigarettes during your lifetime?" were considered smokers.

The current severity of drinking was measured using the Alcohol Use Disorders Identification Test (AUDIT) with a Cronbach's alpha index of 0.85.[23]

The ACEs were measured with a tool designed for this study, named the ACE (13) Score. The first 10 questions, developed by Kaiser Permanente and the Centers for Disease Control and Prevention, evaluated exposure to abuse and family dysfunction occurring during the first 18 years of one's life (the ACE Study score).[18] These 10 questions focused on chronic physical, verbal and sexual abuse, neglect, the loss of one or both parents for any reason (i.e., divorce, separation or death), exposure to domestic violence, and growing up in a household with mental illness, alcohol abuse, drug abuse, or incarceration. The 3 additional questions concerned events that also took place in one's life before the age of 18 and included the following: witnessing a family member's attempted suicide, witnessing a family member's death due to any cause and witnessing a stranger's death due to any cause (e.g., traffic accident). The details of our statistical analysis allow for our results to still be comparable with the studies based on the ACE Study score.

Health behaviors were assessed with the Health Behavior Inventory (HBI) designed by Juczyński.[24] Internal reliability for the total HBI measured by Cronbach's alpha was estimated at 0.85 and ranged between 0.6 and 0.65 for its 4 subscales.[24] The HBI comprises 24 statements used to assess health behaviors on 4 subscales: positive attitude (PA), proper dietary habits (PDH), health-related practices (HP), and preventive behaviors (PB). Total HBI scoring falls in the range of 24–120 points, i.e., the respondent must specify on a 5-point scale how often he/she performed a certain action over the previous year (1 = almost never, 2 = rarely, 3 = sometimes, 4 = often, and 5 = almost always). The higher the score, the higher the level of health-oriented behaviors. For further interpretation, HBI scoring may be converted into standardized units on a sten scale, which is a sectional scale with an average sten score of 5.5 and a standard deviation of 2, ranging from 1 to 10. It was proposed to adopt the following sten ranges: results 1–4 (low score), 5–6 (average score) and 7–10 (high score).[24]

Self-efficacy was measured with the Polish version of the Generalized Self-Efficacy Scale (GSES) by Schwarzer, Jerusalem and Juczyński. A 10-point psychometric scale was used to assess optimistic self-beliefs in coping with a variety of difficult demands in life.[24] The GSES, with a Cronbach's alpha index of 0.85 for internal reliability, was created to assess a general sense of perceived self-efficacy and to predict the ability to cope with daily struggles and adaptation after experiencing all kinds of stressful life events.[24] Responses are marked on a 4-point scale for each item and total scoring ranges from 10 to 40 points. The higher the score, the greater the individual's generalized sense of self-efficacy. Scoring ≤24 points is interpreted as a low outcome, between 25 and 29 points as medium outcome, and ≥30 points as high outcome.[24]

In order to address a possible bias connected with participants' intentional attempts to present themselves in either a better or worse mental and general condition, the researcher who remained present during the completion of the questionnaires was not involved in the patients' therapy. Recall bias was still possible during the ACE (13) Score completion, which is listed among the limitations of the study.

Ethics

All of the participants gave written informed consent for their participation in the study. The study was approved by the Local Bioethics Committee (No. RNN/467/13/KB and KB/843/13/P). The study was carried out in accordance with the ethical standards laid down in the 1964 Declaration of Helsinki and its later amendments.

Statistical analysis

Statistical analysis was performed using STATISTICA v. 12.0 (StatSoft Polska, Kraków, Poland). Generally, a p-value of <0.05 was considered significant. The normality of data distribution was evaluated with the Shapiro-Wilk test. Parameters with normal distribution (age and HBI) are presented as the mean and standard deviation (SD). If the distribution was other than normal, the median and range (min–max) were provided.

The multiple stepwise regression analysis was employed to evaluate the influence of continuous and categorical variables on the GSES and HBI. Variables included in the analysis were selected based on a literature review as possibly associated with self-efficacy and health habits, and were as follows: age, gender, educational level, marital status, occupational status, and place of living.[25–27] Additionally, for both the GSES and the HBI model, we included the number of ACEs determined by the ACE (13) Score.

In both analyses, the automatic forward selection of variables included in the model was applied. Thus, at the beginning there were no variables in the model, so in the process of testing the algorithm, the variables which improved the model the most were added. This procedure was repeated until no additional variable improved the model.

Results

Characteristics of patients with alcohol dependence

The sociodemographic characteristics of 196 patients with AD (F = 50) are presented in Table 1. The mean age of the patients was 43.8 ±10.7 years. Approximately 40% of the patients with AD were high school graduates (38.8%) and over half were unemployed (60.2%). Over 30% of the patients with AD were divorced (31.2%). The severity of drinking, measured by the AUDIT interview, was 27.2 ±7.6 out of possible 40 points (Table 1).

Table 1. Socio-demographic and clinical characteristics among patients with AD

Characteristic		Patients with AD (n = 196)
Age [years], mean ±SD		43.8 ±10.7
AUDIT score, median (range)		28.0 (6.0–40.0)
Smokers[1], n (%)		180 (91.8)
Educational level, n (%)	basic vocational secondary higher	50 (25.5) 49 (25.0) 76 (38.8) 21 (10.7)
Marital status, n (%)	single married divorced widowed	77 (39.3) 42 (21.4) 63 (32.1) 14 (7.1)
Occupational status, n (%)	employed unemployed retired or survivor sickness	44 (22.4) 118 (60.2) 34 (17.3)
Place of living, n (%)	village town[2] city[3]	12 (6.1) 20 (10.2) 164 (83.7)

AD – alcohol dependence; AUDIT – Alcohol Use Disorders Identification Test; [1] smoker – respondent who smoked at least 100 cigarettes during their lifetime; [2] town – place of living of <50,000 citizens; [3] city – place of living of >50,000 citizens.

ACE (13) Score, HBI and GSES

The patients reported from 3 to 10 ACEs (median: 3). Figure 1 presents the reporting frequency of each ACE in both females and males.

On the HBI scale, the patients' mean score was 64.4 ±16.6 out of 120 points. Within this scale, scores on the subscales for PDH ranged from 6 to 30 points (median: 14); for PB they also ranged from 6 to 30 points (median: 17); for PA they varied between 6 and 29 points (median: 18); and for HP, between 6 and 28 points (median: 15.5).

On the GSES scale, patients scored from 10 to 40 points (median: 30) out of 40 possible points.

Multiple stepwise regression analysis for variation in health habits assessed by the HBI and self-efficacy assessed by the GSES

The model for the GSES explained 6.8% of its variability (Table 2). Gender (β = –2.176; p = 0.036) and the number of ACEs (β = –0.377; p = 0.026) were significant determinants. Although marital status, educational level and place of living were not significant determinants in the stepwise method, they entered the final model. The ACEs explained 3.2% of the variability of general self-efficacy assessed by the GSES.

The model for the HBI explained 11.2% of its variability (Table 2). Age (β = 0.336; p = 0.008), place of living (β = 7.481; p < 0.001) and the number of ACEs (β = –1.210; p = 0.007) were significant determinants; however, marital status also entered the model. Here, the ACEs explained 3.9% of the variability of health behaviors assessed by the HBI.

Table 2. The multiple stepwise regression analysis for variation in health habits assessed by the HBI and general self-efficacy assessed by the GSES in patients with AD

Variable	GSES		HBI	
	β coefficient	p-value	β coefficient	p-value
Gender	–2.178	0.036*	–0.406	0.883
Age	–0.025	0.703	0.368	0.004*
Occupational status	0.117	0.879	1.809	0.371
Marital status	–0.676	0.128	–1.817	0.176
Educational level	0.651	0.150	1.253	0.294
Place of living	1.065	0.195	7.481	<0.001*
ACE (13) Score	–0.377	0.026*	–1.21	0.007*

AD – alcohol dependence; GSES – General Self-Efficacy Scale; HBI – Health Behavior Inventory; * statistical significance.

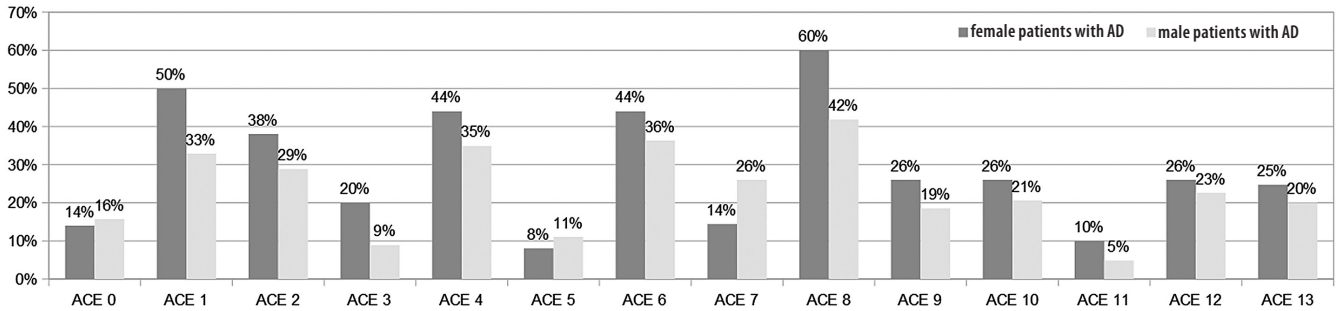

Fig. 1. Prevalence of ACEs in patients with AD (n = 196)

The categories with an ACE (13) Score are as follows: ACE1 – psychological abuse; ACE2 – physical abuse; ACE3 – sexual abuse; ACE4 – emotional neglect; ACE5 – physical neglect; ACE6 – loss of contact with parents; ACE7 – witnessing physical abuse toward one's mother or stepmother; ACE8 – drinking/alcohol/drug use by a household member; ACE9 – mental illness/suicide attempt of a household member; ACE10 – incarceration of a household member; ACE11 – witnessing a family member's suicide attempt; ACE12 – witnessing a family member's death; ACE13 – witnessing a stranger's death.
ACE – adverse childhood experience; AD – alcohol dependence.

Discussion

This study examined health behaviors, general self-efficacy and self-reported childhood adversities in patients with AD. We found the ACEs to be among the factors that significantly and adversely influenced general self-efficacy and promoted health-harming behaviors in adulthood in patients with AD.

The explanatory power of the model of health behaviors for patients with AD as used in this study was found to be 11.2%. The ACEs, current age and place of living were variables with a significant association with health habits (Table 2). Out of all of these variables, the ACEs explained 3.9% of the HBI variability.

The literature on health harm associated with alcohol drinking states that there is no obvious positive association between alcohol intake and health harm, as health harm is already a final result associated at least partially with alcohol misuse and other health-harming behaviors, such as cigarette smoking, poor diet and poor voluntary exercise.[17,28] Cross-sectional studies relying on self-reporting may provide underestimated data on the duration and severity of drinking, or show less severe alcohol drinking in patients with existing alcohol-related health harm, i.e., head and neck cancer or esophageal cancer, without a lifetime drinking history and previous drinking patterns.[29,30] Health-harming behaviors also decreased with age of our patients, which may suggest that they improved their health behaviors because of alarming health costs, or as a result of support from family or healthcare providers. Our study did not aim to assess current health harm that was potentially associated with alcohol misuse, but current health habits in patients with AD. Our results are in line with other studies that show a parallel coexistence of alcohol misuse and other health-harming behaviors. Approximately 92% of our patients with AD were also cigarette smokers. Bellis et al. confirmed strong associations between alcohol misuse or smoking and low levels of exercise or poor diet.[16] A meta-analysis by Probst et al. confirmed the accumulation of health-harming behaviors in individuals with alcohol misuse.[31] However, they stated that this accumulation was predominantly reserved for communities living in socioeconomic deprivation and they considered healthcare provision, dietary habits and smoking behaviors as putative main factors underlying this phenomenon.[31] According to their analysis, low socioeconomic status was related to malnutrition, i.e., to purchasing foods that are high in fat, salt and sugar, processed food and fast food consumption, and low fruit and vegetable consumption, which may interact with alcohol consumption to alter protein and vitamin absorption and increase the risk of vitamin and mineral deficiencies.[31] In our study, occupational status and educational level did not enter the model of variability in health behaviors, as there were probably factors other than education, i.e., factors related to the place of living, which implicated health habits. There might have been better availability of healthcare and health education, and better promotion of voluntary exercise and a healthy diet in cities than in towns and villages. Health habits were more health-oriented in the city-dwelling patients, less health-oriented among the inhabitants of towns, and the least among village inhabitants. However, the ACEs were found to correlate with them adversely, i.e., the higher the number of ACEs, the more health-harming habits were present in the patients.

The ACEs were also considered a measure of social inequities and were more frequent in communities of poor socioeconomic status.[32] A USA national study that applied the ACE Study score in a sample of the general population found that the rate of premature death (<65 years of age) rose along with the number of self-reported ACEs.[18,19] Respondents who had experienced at least 4 ACEs of any type were about twice as likely to have an elevated prevalence of premature death relative to the respondents with no such experience. The highest risk occurred among those who reported having been physically neglected and living with substance-abusing or criminal family members during their childhood.[17]

The explanatory power of the model of general self-efficacy for our patients was found to be 6.8% (Table 2). Only the ACEs and gender of the study participants were found to be significantly associated with general self-efficacy; the ACEs explained 3.2% of GSES variability.

In our model of general self-efficacy variability, being a female patient and reporting a higher number of ACEs was significantly associated with lower general self-efficacy. As pointed out by Bandura et al., general self-efficacy may be impaired by previously experienced life adversities.[8] The kind of ACE category and individual susceptibility to ACEs may also be meaningful for future general self-efficacy. The female patients with AD were more likely to report both psychological and sexual abuse, and a household member's alcohol or drug misuse. General self-efficacy was referred to as global confidence in one's coping with demanding or novel situations. It warrants dealing with a variety of stressful situations and characterizes one's social skills.[4] Lower general self-efficacy was found to be related with a higher risk of suicide ideation.[33,34] The majority of studies on self-efficacy in substance abuse disorders have focused on skill-oriented self-efficacy as an important factor which influences treatment outcome. Skill-oriented self-efficacy, i.e., the ability to not drink in high-risk situations, is associated with an effective use of coping strategies and with lower relapse rates.[6] As reviewed by Trucco et al., there has been a growing number of studies which indicate that individuals with higher skill-oriented self-efficacy scores are less likely to relapse and more likely to remain abstinent up to 6 months following treatment, and, similarly, that low skill-oriented self-efficacy was predictive of a relapse during 12 months following inpatient alcohol detoxification.[7] As assessed by Czyz et al., lower self-efficacy was reported by subjects with substance abuse disorders who had more severe suicidal ideation and by those with more

suicide attempts.[33] The explanatory power of our model of general self-efficacy for our patients was found to be only 6.8%. Alcohol consumption is a known factor which promotes a phenotype of loss of behavioral flexibility; thus, alcohol misuse may be primary to social impairment and may promote social anxiety, altered adult synapses, altered cognition, reduced adult neurogenesis, and increased neuroimmune gene expression and the epigenetic modifiers of gene expression.[1] Since the adolescent brain is uniquely sensitive to alcohol neurotoxicity, decreased adult neurogenesis might contribute to an increased risk of adult psychopathology and cognitive dysfunction.[1] As reviewed by Crews et al., ethanol exposure in early adolescence adversely affected social skills of rats, particularly males, in terms of social inhibition, although it occurred in a lesser degree in adolescents than in adult rats.[1] A meta-analysis by Bora and Zorlu showed that patients with alcohol abuse disorders presented significantly impaired facial emotion recognition, particularly for disgust and anger.[2] Further studies on general self-efficacy and its relationship to ACEs should utilize more psychometric analyses and functional neuroimaging.

The World Health Organization pointed to ACEs as an important target for primary preventive strategies of chronic ill health during one's lifetime.[35] Our study found ACEs to be one of the factors that significantly correlate with general self-efficacy and health habits in patients with AD and indicate that they should be targeted with primary preventive strategies for better overall health in adulthood. However, in case it is already too late for primary preventive strategies, secondary prevention to improve general self-efficacy impaired by childhood adversity should be introduced. The cognitive-behavioral theory posits that higher confidence in the ability to not drink in a high-risk situation is associated with the effective use of coping strategies and lower relapse rates.[6]

Limitations

The main limitation of studies on childhood adversities, including ours, is that the analyzed data is retrospective and self-reported, and that recall bias is still possible; for example, the respondent may recall more negative autobiographical adversity when he or she is answering the questions regarding poor mental and physical health conditions in adulthood.[36] Thus, it is possible that variables identified in later life as factors possibly influencing general well-being in adulthood would not prove to be predictive of ultimate health outcomes when assessed in earlier stages of life.[20] Moreover, the paucity of factors that might have been either supportive or harming to the respondent and were not included in the study (i.e., a parent's hidden emotional problems or receiving professional help) could influence the respondent's current health. The cross-sectional design of the study precludes both causal inference (as event-reporting may be confounded by the current psychological condition and age) and a longitudinal analysis of adjustment methods.[37] Finkelhor et al. also considered another important limitation of studies analyzing retrospectively-recalled ACEs.[20] Between older and younger respondents, there may be a difference in pointing to childhood experiences as adversities or not, which mirrors social changes regarding the norms and awareness of childhood experiences. Thus, in the younger cohort of respondents, due to the increased availability of professional support (i.e., a psychotherapist at school) and more cultural awareness, parental divorce may be non-predictive of a worse health outcome in adulthood than may be the case in an older cohort.[20]

Conclusions

We confirmed that childhood adversities, understood as neglect, trauma, physical and psychological abuse, and witnessing someone's death, are one of the factors significantly associated with the development of health-harming behaviors and worse general self-efficacy in adult patients with AD. Even though these were among many other factors influencing health habits and general self-efficacy, and explained only approx. 4% of the variability of health habits and about 3.5% of the variability of general self-efficacy, the study suggests the need for psychotherapy to focus on childhood trauma while strengthening general self-efficacy, targeted to improve alcohol abstinence.

References

1. Crews FT, Vetreno RP, Broadwater MA, et al. Adolescent alcohol exposure persistently impacts adult neurobiology and behavior. *Pharmacol Rev*. 2016;68(4):1074–1109.
2. Bora E, Zorlu N. Social cognition in alcohol use disorder: A meta-analysis. *Addiction*. 2017;112(1):40–48. doi:10.1111/add.13486
3. Thorberg FA, Young RM, Lyvers M, et al. Alexithymia in relation to alcohol expectancies in alcohol-dependent outpatients. *Psychiatry Res*. 2016;236:186–188. doi:10.1016/j.psychres.2016.01.016
4. Schwarzer R, Mueller I, Greenglass E. Assessment of perceived general self-efficacy on the internet: Data collection in cyberspace. *Anxiety Stress Coping*. 1999;12:145–161.
5. Bandura A. *Social Foundations of Thought and Action: A Social Cognitive Theory*. Englewood Cliffs, NY: Prentice-Hall; 1986.
6. Greenfield SF, Hufford MR, Vagge LM, et al. The relationship of self-efficacy expectancies to relapse among alcohol dependent men and women: A prospective study. *J Stud Alcohol*. 2000;61(2):345–351.
7. Trucco EM, Connery HS, Griffin ML, et al. The relationship of self-esteem and self-efficacy to treatment outcomes of alcohol-dependent men and women. *Am J Addict*. 2007;16(2):85–92.
8. Bandura A, Reese L, Adams NE. Microanalysis of action and fear arousal as a function of differential levels of perceived self-efficacy. *J Pers Soc Psychol*. 1982;43:5–21.
9. Benight C, Bandura A. Social cognitive theory of posttraumatic recovery: The role of perceived self-efficacy. *Behav Res Ther*. 2004;42(10):1129–1148. doi:10.1016/j.brat.2003.08.008
10. Hinnen C, Sanderman R, Sprangers MAG. Adult attachment as mediator between recollections of childhood and satisfaction with life. *Clin Psychol Psychother*. 2009;16:10–21. doi:10.1002/cpp.600
11. Suzuki H, Tomoda A. Roles of attachment and self-esteem: Impact of early life stress on depressive symptoms among Japanese institutionalized children. *BMC Psychiatry*. 2015;15:8. doi:10.1186/s12888-015-0385-1

12. Felitti VJ. The relationship of adverse childhood experiences to adult health: Turning gold into lead [in German]. *Z Psychosom Med Psychother*. 2002;48(4):359–369.
13. Anda RF, Whitfield CL, Felitti VJ, et al. Adverse childhood experiences, alcoholic parents, and later risk of alcoholism and depression. *Psychiatr Serv*. 2002;53:1001–1009.
14. Shin SH, Pelucchi C, Bagnardi V, et al. Child abuse and neglect: Relations to adolescent binge drinking in the national longitudinal study of adolescent health (AddHealth) study. *Addict Behav*. 2009;34: 277–280.
15. Latendresse SJ, Rose RJ, Viken RJ, et al. Parenting mechanisms in links between parents' and adolescents' alcohol use behaviors. *Alcoholism Clin Exp Res*. 2008;32:322–330. doi:10.1111/j.1530-0277.2007.00583.x
16. Bellis MA, Hughes K, Leckenby N, et al. Measuring mortality and the burden of adult disease associated with adverse childhood experiences in England: A national survey. *J Public Health (Oxf)*. 2015;37(3): 445–454.
17. Bellis MA, Hughes K, Nicholls J, et al. The alcohol harm paradox: Using a national survey to explore how alcohol may disproportionately impact health in deprived individuals. *BMC Public Health*. 2016;16:111. doi:10.1186/s12889-016-2766-x
18. Felitti VJ, Anda RF, Nordenberg D, et al. Relationship of childhood abuse and household dysfunction to many of the leading causes of death in adults: The Adverse Childhood Experiences (ACE) Study. *Am J Prev Med*. 1998;14:245–258.
19. Anda RF, Dong M, Brown DW, et al. The relationship of adverse childhood experiences to a history of premature death of family members. *BMC Public Health*. 2009;9:106. doi:10.1186/1471-2458-9-106
20. Finkelhor D, Shattuck A, Turner H, et al. Improving the adverse childhood experiences study scale. *JAMA Pediatr*. 2013;167(1):70–75. doi:10.1001/jamapediatrics.2013.420
21. Stathopoulou G, Powers M, Berry A, et al. Exercise interventions for mental health: A quantitative and qualitative review. *Clin Psychol Sci Pract*. 2006;13:180–193.
22. World Health Organization. *The ICD-10 Classification of Mental and Behavioral Disorders: Clinical Description and Diagnostic Guidelines*. Geneva, Switzerland: WHO; 1992.
23. Daeppen JB, Yersin B, Landry U, et al. Reliability and validity of the Alcohol Use Disorders Identification Test (AUDIT) imbedded within a general health risk screening questionnaire: Results of a survey in 332 primary care patients. *Alcohol Clin Exp Res*. 2000;24(5):659–665.
24. Juczyński Z. Instruments for Measurement in Health Promotion and Health Psychology [in Polish]. 2nd ed. Warsaw, Poland: Pracownia Testów Psychologicznych; 2012.
25. Schieman S, Taylor J. Statuses, roles, and the sense of mattering. *Sociol Perspect*. 2001;44(4):469–484. doi:10.1525/sop.2001.44.4.469
26. McCormack L, Haun J, Sørensen K, Valerio M. Recommendations for advancing health literacy measurement. *J Health Commun*. 2013;18(1): 9–14.
27. Weaver NL, Wray RJ, Zellin S, et al. Advancing organizational health literacy in health care organizations serving high-needs populations: A case study. *J Health Commun*. 2012;17(3):55–66.
28. Dawson DA, Li TK, Grant BF. A prospective study of risk drinking: At risk for what? *Drug Alcohol Depend*. 2008;95:62–72.
29. Roerecke M, Rehm J. Irregular heavy drinking occasions and risk of ischemic heart disease: A systematic review and meta-analysis. *Am J Epidemiol*. 2010;171:633–644.
30. Rehm J, Patra J, Popova S. Alcohol drinking cessation and its effect on esophageal and head and neck cancers: A pooled analysis. *Int J Cancer*. 2007;121:1132–1137.
31. Probst C, Roerecke M, Behrendt S, et al. Socioeconomic differences in alcohol-attributable mortality compared with all-cause mortality: A systematic review and meta-analysis. *Int J Epidemiol*. 2014;43(4): 1314–1327. doi:10.1093/ije/dyu043
32. Marmot M, Allen J, Bell R, et al.; Consortium for the European Review of Social Determinants of Health and the Health Divide. WHO European review of social determinants of health and the health divide. *Lancet*. 2012;380(9846):1011–1029.
33. Czyz EK, Bohnert ASB, King CA, et al. Self-efficacy to avoid suicidal action: Factor structure and concurrent validity among adults in substance use disorder treatment. *Suicide Life Threat Behav*. 2014;44(6): 698–709. doi:10.1111/sltb.12101
34. Kobayashi Y, Fujita K, KanekoY, et al. Self-efficacy as a suicidal ideation predictor: A population cohort study in rural Japan. *Open Journal Prev Med*. 2015;5:61–71.
35. World Health Organization. Global Action Plan for the Prevention and Control of Noncommunicable Diseases 2013–2020. http:/www.who.int/nmh/publications/ncd_action_plan/en/. Published 2013. Accessed December 16, 2015.
36. Hardt J, Rutter M. Validity of adult retrospective reports of adverse childhood experiences: Review of the evidence. *J Child Psychol Psychiatry*. 2004;45(2):260–273.
37. Layne CM, Warren JS, Hilton S, et al. Measuring Adolescent Perceived Support Amidst War and Disaster: The Multi-Sector Social Support Inventory. In: Baker BK, ed. *Adolescents and War: How Youth Deal With Political Violence*. New York, NY: Oxford University Press; 2009:145–176.

Elevated beta-thromboglobulin and mean platelet volume levels may show persistent platelet activation in systemic lupus erythematosus patients

Seyit Uyar[1,A,B,D–F], Gül Babacan Abanonu[2,C,E], Seval Masatlıoğlu Pehlevan[3,A,E], Cumali Karatoprak[4,A,C], Meral Uluköylü Mengüç[2,B,C], Alper Daşkin[2,4,A,B], Süleyman Dolu[1,A,C], Refik Demirtunç[2,A,E]

[1] Department of Internal Medicine, University of Health Science, Antalya Training and Research Hospital, Turkey
[2] Department of Internal Medicine, University of Health Science, Haydarpaşa Numune Training and Research Hospital, Istanbul, Turkey
[3] Department of Rheumatology, University of Health Science, Haydarpaşa Numune Training and Research Hospital, Istanbul, Turkey
[4] Bezmialem Vakıf University Faculty of Medicine, Internal Medicine Clinic, Istanbul, Turkey

A – research concept and design; B – collection and/or assembly of data; C – data analysis and interpretation; D – writing the article; E – critical revision of the article; F – final approval of the article

Advances in Clinical and Experimental Medicine, ISSN 1899-5276 (print), ISSN 2451-2680 (online) *Adv Clin Exp Med*. 2018;27(9):1279–1283

Address for correspondence
Seyit Uyar
E-mail: seyituyar79@hotmail.com

Funding sources
None declared

Conflict of interest
None declared

Received on March 9, 2017
Reviewed on April 17, 2017
Accepted on June 3, 2017

Abstract

Background. Patients with systemic lupus erythematosus (SLE) have an increased risk of thrombotic events. Platelets become more active and they enlarge to release proteins from alpha granules for aggregation during the plaque formation period. Beta-thromboglobulin is one of the proteins released from alpha-granules when platelets are activated and used as a marker of platelet activation in vivo.

Objectives. The aim of this study was to evaluate the plasma levels of beta-thromoglobulin and mean platelet volume as markers of the presence of platelet activation in systemic lupus erythematosus patients compared with healthy controls.

Material and methods. Thirty-seven SLE patients with a mean disease duration of 4.96 years and without any organ involvement as well as 30 healthy volunteers were included in the study. All patients were in remission of SLE.

Results. The mean beta-thromboglobulin level was 97.36 ±55.8 ng/mL in the SLE group and 72.67 ±33.5 ng/mL in the control group ($p = 0.029$). The mean platelet volume level was 8.27 ±1.68 fL in the SLE group and 9.16 ±1.52 fL ($p = 0.031$) in the controls.

Conclusions. Elevated beta-thromboglobulin levels in systemic lupus erythematosus patients may be associated with platelet activation in the early stages of disease, whereas lower mean platelet volume levels in the same population may be due to the effects of hydroxychloroquine and the inactivity of SLE.

Key words: systemic lupus erythematosus, mean platelet volume, β-thromboglobulin

DOI
10.17219/acem/74389

Introduction

Systemic lupus erythematosus (SLE) is an autoimmune disease with an increased risk of thrombosis.[1] Thrombotic events are becoming more of a factor on morbidity and mortality than inflammation due to developing effective anti-inflammatory treatments.[2] For these reasons, SLE patients experience thrombotic events at younger ages than the general population.[3] According to a study by Mok et al., women with SLE are hospitalized with myocardial infarction and stroke almost 9 times more often than the normal population.[4] Longer disease duration, older age at SLE diagnosis, disease activity, smoking, and the presence of antiphospholipid antibodies have all been established as risk factors for thrombosis in SLE patients.[5] Several blood parameters have been proposed to predict the occurrence of thrombosis, including the presence of lupus anticoagulant, anticardiolipin antibodies, and anti-2-glycoprotein I antibodies. However, these well-known risk factors do not explain thrombosis formation exactly. For example, approximately 40% of SLE patients with thrombosis tested negative for antiphospholipid antibodies in 2005.[1] Therefore, better predictors of thrombosis are needed for the early prevention of this potentially fatal disease complication.

The activation and aggregation of platelets during hemostasis is essential for plug formation and for preventing excessive blood loss. However, if this process occurs in an uncontrolled manner it may lead to thrombotic events. During the formation of plaque, platelets become more active and they enlarge to release proteins from alpha granules for aggregation. Platelet factor 4 and β-thromboglobulin (β-TG) are proteins released from alpha-granules when platelets become activated and can be used as a marker of platelet activation in vivo.[6] An elevation in mean platelet volume (MPV) may also be an indicator for platelet activation, as demonstrated in studies of many different diseases.[7–11] There have also been many studies investigating β-TG levels in different autoimmune diseases.[12–15] A review of the literature, however, shows that there are few studies evaluating β-TG levels and MPV levels in SLE patients as a platelet activator.[16–19]

Many studies suggest that there is persistent platelet activation in SLE patients.[16,20,21] In this study, we aimed to show platelet activation in the early stages of the disease and during the remission period in SLE patients by evaluating β-TG and MPV levels and comparing them with healthy controls. We can hypothesize that there is a risk of thrombosis in the early stages of SLE.

Material and methods

Study design

This study was designed as a prospective, cross-sectional clinical trial with a control group. It was performed in the outpatient clinics of the internal medicine and rheumatology departments of Haydarpasa Numune Training and Research Hospital. The study protocol was performed in accordance with the Declaration of Helsinki and approved by the ethic committees of our hospital. Written informed consent was obtained from each participant before the commencement of the study.

Thirty-seven patients who were followed in the outpatient clinics of the rheumatology and internal medicine departments of our hospital with a diagnosis of SLE as well as 30 healthy volunteers without any systemic disease were included in the study. All patients were in the remission period of SLE and were not on any medication apart from hydroxychloroquine phosphate. The diagnosis of SLE was based on the diagnostic criteria revised by the American Rheumatism Association in 1987.[22] Patients were excluded from the study if they had any disease affecting platelet function, diabetes mellitus, renal failure, liver failure, any kind of malignancy, peripheral vascular disease, any thrombotic events, cerebrovascular disease, chronic thyroid disease, hypertension, coronary artery disease, congestive heart failure, idiopathic thrombocytopenic purpura, iron deficiency anemia, or pregnancy, or if they were using any medications which affect platelet functions (for example, aspirin, clopidogrel, non-steroidal anti-inflammatory drugs, anti-coagulants, or corticosteroids) within the previous 15 days, their body mass index (BMI) was ≥30, or they had active SLE. None of the patients had kidney involvement of SLE. For each individual participating in the study, a questionnaire consisting of physical examination and medical history was completed.

After the approval of informed consent from all patients, the patients were physically examined by an internist and checked for inclusion and exclusion criteria. All patients had no organ involvement according to ACR criteria and none of them had any active complaints. All patients were using only hydroxychloroquine phosphate for SLE.[23] None of the patients were receiving corticosteroids and/or immune suppressant agents. After 12 h of fasting and half an hour of rest, venous blood samples were taken for biochemical tests between 8:00 and 8:30 am. The total cholesterol, low-density lipoprotein cholesterol (LDL-C), high-density lipoprotein cholesterol (HDL-C), and triglyceride levels, the sedimentation rate, and C-reactive protein levels of all patients were measured in the Biochemistry Laboratory with "Beckman Coulter" device (Beckman Coulter Diagnostics, Fullerton, USA).

Measurement of MPV and β-TG

The measurement of MPV and β-TG levels was performed in the Ozel Gelisim Tip Laboratory (Istanbul, Turkey). Blood samples were taken as stated above and sodium citrate was used for the anticoagulation of the blood samples taken for MPV and β-TG. All samples were meticulously studied within half an hour. The first 2 mL of blood was drained out and the remaining amount was put into a special tube containing a mixture for β-TG level

platelet markers. The tubes were kept for 15 min in ice water and were then centrifuged at 2–8°C at the 2,500 cycle for 20 min. The middle 1/3 part of the plasma of the centrifuged blood was isolated from the rest with a pipette. The samples were stored at –20°C and β-TG levels were measured with an ELISA kit for human beta thromboglobulin (Elabscience Biotechnology, Wuhan, China).

Statistical analysis

Statistical analysis was performed using v. 16.0 of SPSS (Statistical Package for Social Sciences) for Windows (SPSS Inc., Chicago, USA). Besides descriptive statistical methods (mean, median, standard deviation, and range), Student's t-test was used for the comparison of the parameters showing normal distribution. The χ^2 test or Fisher's exact test was used to compare qualitative data. The distribution of the continuous variables was tested with the One-Sample Kolmogorov-Smirnov Test. A p-value of <0.05 was considered significant.

Results

Thirty-seven patients (SLE group) and 30 healthy volunteers (control group) who were similar to the patient group in terms of age and gender distribution were included in the study. The SLE group consisted of 34 females and 3 males, and the mean age was 35.78 ±8.93 years. The healthy control group consisted of 26 females and 4 males and the mean age was 34.76 ±9.84 years. There was no significant difference between the groups in terms of age or gender distribution ($p > 0.05$). The mean age of diagnosis was 33.05 ±9.05 years and the mean disease duration was 4.96 ±4.97 years for SLE patients (Table 1).

The demographic characteristics, cholesterol levels, acute phase reactants, and complement levels of the SLE and control groups are presented in Table 1. There was no statistical difference between the groups with respect to these parameters ($p > 0.05$).

The number of patients who smoked in the SLE group was 13 and in the control group it was 9. The difference between the groups was not statistically significant ($p = 0.656$) (Table 1). There was no difference between the groups in terms of platelet count ($p > 0.05$). The mean β-TG levels in the SLE group was 97.36 ±55.85 ng/mL and 72.67 ±33.55 ng/mL in the healthy controls. The difference between the groups in terms of β-TG levels was found to be significant ($p = 0.029$) (Table 2).

The mean MPV value of the SLE group was 8.27 ±1.68 fL and in the control group it was 9.16 ±1.52 fL. The difference between these groups in terms of MPV levels was significant ($p = 0.031$) (Table 2).

Table 1. Demographic characteristics, cholesterol levels, acute phase reactants, and complement levels of the groups

Parameters	SLE patients (n = 37)	Healthy controls (n = 30)	p-value
Age [years], mean ±SD	35.78 ±8.93	34.76 ±9.84	0.66*
Female, n	34	26	0.692**
Smoking status, n	13	9	0.656**
Total cholesterol [mg/dL], mean ±SD	178.46 ±38.41	185.0 ±31.21	0.455*
High-density lipoproteins [mg/dL], mean ±SD	59.37 ±17.33	53.96 ±9.02	0.106*
Low-density lipoproteins [mg/dL], mean ±SD	95.62 ±32.26	110.33 ±27.91	0.053*
Triglycerides [mg/dL], mean ±SD	117.81 ±63.61	101.20 ±50.21	0.248*
Age of diagnosis [years], mean ±SD	33.05 ±9.05	–	–
Disease duration [years], mean ±SD	4.96 ±4.97	–	–
Sedimentation rate [mm/h], median (min–max)	11 (3–73)	–	–
C-reactive protein [mg/dL], median (min–max)	0.10 (0.06–2.7)	–	–
White blood cell [$\times 10^3$/uL], mean ±SD	6.84 ±2.35	–	–
Complement C3 [mg/dL], mean ±SD	87.46 ±2.26	–	–
Complement C4 [mg/dL], mean ±SD	16.69 ±6.51	–	–

* Student's t-test; ** χ^2 test; SLE – systemic lupus erythematosus.

Table 2. Comparison of the groups in terms of β-thromboglobulin, MPV, and platelet count levels

Parameters	SLE patients (n = 37)	Healthy controls (n = 30)	p-value*
β-thromboglobulin [ng/mL], mean ±SD	97.36 ±55.85	72.67 ±33.55	0.029
MPV [fL], mean ±SD	8.27 ±1.68	9.16 ±1.52	0.031
Platelet count, mean ±SD	211,406.25 ±81,476.63	209,041.66 ±70,825.86	0.910

* Student's t-test; SLE – systemic lupus erythematosus; MPV – mean platelet volume.

Discussion

The β-TG levels were significantly higher and the MPV levels were significantly lower in the SLE group than in the healthy controls in this study. The SLE group and the healthy controls were similar demographically and in terms of cardiac risk factors (e.g., age, sex, smoking, and lipid levels). All patients were in remission for SLE because the sedimentation rate and the C-reactive protein, white blood cell, and complement levels of patients were within normal range. The mean age of diagnosis was 33.05 years and the mean disease duration of the patients was 4.96 years. Due to the increased levels of β-TG, it can be assumed that platelet activation occurs in the early course of the disease and during the remission period, according to our findings. Ekdahl et al. studied β-TG, phosphorylated fibrinogen, and activated factor IX-antithrombin complexes in SLE patients with and without deep vein thrombosis (DVT) and compared these levels to patients with DVT and to healthy individuals. They reported that high levels of β-TG and phosphorylated fibrinogen in the samples from patients with SLE were strongly associated with thrombosis. β-TG levels of SLE patients without thrombosis were also higher than the normal range in their study.[16] When we evaluate our results together with the Ekdahl study, we may conclude that SLE patients may be prone to thrombosis in the early course of the disease. This hypothesis is compatible with a study done by Chang et al.[24] They concluded that thrombovascular events occur throughout the course of lupus with the highest risk in the first year after diagnosis.[24]

β-TG levels were higher and MPV values were significantly lower in SLE patients, though these results may seem contradictory. There are a few studies investigating MPV levels in SLE patients and their results are also contradictory. In one of the earliest laboratory investigations, Turner-Stokes et al. reported that the platelet count and volume were significantly lower in SLE patients according to 2 different hematology analyzers.[18] In a recent study, MPV levels were found to be lower in adult patients with active SLE as compared to inactive patients. In that study, there was no healthy control group and MPV values were 7.16 fL and 8.16 fL in active and inactive SLE patients, respectively.[19] Safak et al. also found that the MPV levels in active SLE patients were significantly lower than in SLE patients in remission and in healthy controls, which is consistent with our results.[25] Lower MPV levels correlated with active inflammatory states in that study. In another study, Yolbas et al. reported that MPV levels were higher (but not statistically significantly higher) in SLE patients than in healthy controls.[26] Although the findings of this study seem to be the opposite of our findings, the mean SLEDAI score of SLE patients was 12.1 in that study. Our study population had no complaints of SLE and were in remission; this may be the reason for the lower MPV levels in this study.

This discordance of MPV levels between studies may be explained by the different methodologies and designs of the studies. The blood sample anticoagulation type (ethylenediaminetetraacetic acid [EDTA] used as an anticoagulant), a delay in the processing of blood samples, anti-inflammatory therapies, and smoking are a few such differences. We processed samples quickly (in under 1 h) and used tubes with sodium citrate to minimize technical mistakes. We did not exclude smokers, but there was no difference in the smoking status between patients and controls in our study.

All patients in our study were taking only hydroxychloroquine for SLE. Although not fully understood, hydroxychloroquine may have potential anti-thrombotic effects through several mechanisms.[27] The inhibition of platelet aggregation, the inhibition of the intravascular aggregation of red blood cells, and the inhibition of the binding of antiphospholipid antibodies to phospholipid surfaces are the mechanisms of the potential anti-thrombotic actions of hydroxychloroquine.[27] In the literature, there is not a single study precisely investigating the effects of drugs, including hydroxycholoroquine, used for SLE on the platelets.[28] The effect of hydroxychloroquine may be another reason for the lower MPV levels in our study, but this contrasts with higher β-TG levels in same group. Further studies that include more patients are needed for more precise elucidation of this issue.

We have included in the study patients with no organ involvement and whose disease duration was less than 10 years. We may include some of the exclusion criteria and the small sample size as limitations of this study.

Conclusions

Elevated β-TG levels in SLE patients who were in the early stages of disease and in remission may support the hypothesis that there is platelet activation throughout the course of SLE. In contrast, lower MPV levels in the same population may be associated with the hydroxychloroquine effect and the inactivity of SLE. Clinicians should also watch out for thrombosis in the early stages of SLE, even if the patients have no organ involvement. However, further prospective, controlled studies with larger populations are needed in this area.

References

1. Afeltra A, Vadacca M, Conti L, et al. Thrombosis in systemic lupus erythematosus: Congenital and acquired risk factors. *Arthritis Rheum.* 2005;53(3):452–459.
2. Nowak B, Szmyrka-Kaczmarek M, Durazińska A, et al. Anti-ox-LDL antibodies and anti-ox-LDL-B2GPI antibodies in patients with systemic lupus erythematosus. *Adv Clin Exp Med*. 2012;21(3):331–335.
3. Cervera R, Khamashta MA, Font J, et al. Morbidity and mortality in systemic lupus erythematosus during a 10-year period: A comparison of early and late manifestations in a cohort of 1,000 patients. *Medicine (Baltimore).* 2003;82(5):299–308.

4. Mok CC, Tang SS, To CH, et al. Incidence and risk factors of thromboembolism in systemic lupus erythematosus: A comparison of three ethnic groups. *Arthritis Rheum*. 2005;52(9):2774–2782.
5. Kaiser R, Li Y, Chang M, et al. Genetic risk factors for thrombosis in systemic lupus erythematosus. *J Rheumatol.* 2012;39(8):1603–1610.
6. Kaplan KL, Owen J. Plasma levels of beta-thromboglobulin and platelet factor 4 as indices of platelet activation in vivo. *Blood.* 1981;57(2): 199–202.
7. Endler G, Klimesch A, Sunder-Plassmann H, et al. Mean platelet volume is an independent risk factor for myocardial infarction but for coronary artery disease. *Br J Haematol*. 2002;117(2):399–404.
8. Yazici S, Yazici M, Erer B, et al. The platelet indices in patients with rheumatoid arthritis: Mean platelet volume reflects disease activity. *Platelets*. 2010;21(2):122–125.
9. Bai M, Xing L, Feng J, et al. Mean platelet volume as a possible marker for monitoring the disease activity in ulcerative colitis. *Int J Lab Hematol*. 2016. https://doi.org/10.1111/ijlh.12495
10. Pyo JS, Sohn JH, Kang G. Diagnostic and prognostic roles of the mean platelet volume in malignant tumors: A systematic review and meta-analysis. *Platelets*. 2016;9:1–7.
11. Lippi G, Danese E, Montagnana M, et al. Mean platelet volume is significantly associated with serum levels of thyroid-stimulating hormone in a cohort of older euthyroid subjects. *Endocr Res*. 2015;40(4): 227–230.
12. Karatoprak C, Uyar S, Abanonu GB, et al. The levels of β-thromboglobulin in femalerheumatoid arthritis patients as activation criteria. *Rheumatol Int.* 2013;33(5):1229–1232.
13. Abanonu GB, Daskin A, Akdogan MF, et al. Mean platelet volume and β-thromboglobulin levels in familial Mediterranean fever: Effect of colchicine use? *Eur J Intern Med.* 2012;23(7):661–664.
14. Yamamoto T, Chikugo T, Tanaka Y. Elevated plasma levels of beta-thromboglobulin and platelet factor 4 in patients with rheumatic disorders and cutaneous vasculitis. *Clin Rheumatol*. 2002;21(6):501–504.
15. Vrij AA, Rijken J, Van Wersch JW, et al. Platelet factor 4 and beta-thromboglobulin in inflammatory bowel disease and giant cell arteritis. *Eur J Clin Invest.* 2000;30(3):188–194.
16. Ekdahl KN, Bengtsson AA, Andersson J, et al. Thrombotic disease in systemic lupus erythematosus is associated with a maintained systemic platelet activation. *Br J Haematol.* 2004;125(1):74–78.
17. Tam LS, Fan B, Li EK, et al. Patients with systemic lupus erythematosus show increased platelet activation and endothelial dysfunction induced by acute hyperhomocysteinemia. *J Rheumatol.* 2003;30(7): 1479–1484.
18. Turner-Stokes L, Jones D, Patterson KG, et al. Measurement of haematological indices of chronic rheumatic disease with two newer generation automated systems, the H1 and H6000 (Technicon). *Ann Rheum Dis*. 1991;50:583–587.
19. Delgado-García G, Galarza-Delgado DÁ, Colunga-Pedraza I, et al. Mean platelet volume is decreased in adults with active lupus disease. *Rev Bras Reumatol.* 2016;56(6):504–508.
20. Joseph JE, Harrison P, Mackie IJ, et al. Increased circulating platelet––leucocyte complexes and platelet activation in patients with antiphospholipid syndrome, systemic lupus erythematosus and rheumatoid arthritis. *Br J Haematol.* 2001;115(2):451–459.
21. Bäck J, Lood C, Bengtsson AA, et al. Contact activation products are new potential biomarkers to evaluate the risk of thrombotic events in systemic lupus erythematosus. *Arthritis Res Ther.* 2013. doi: 10.1186/ar4399
22. Tan E, Cohen A, Fries J, et al. The 1982 revised criteria for the classification of systemic lupus erythematosis. *Arthritis Rheum.* 1982;25: 1271–1277.
23. Hochberg MC. Updating the American College of Rheumatology revised criteria for the classification of systemic lupus erythematosus. *Arthritis Rheum*. 1997;40(9):1725.
24. Chang ER, Pineau CA, Bernatsky S, et al. Risk for incident arterial or venous vascular events varies over the course of systemic lupus erythematosus. *J Rheumatol.* 2006;33(9):1780–1784.
25. Safak S, Uslu AU, Serdal K, et al. Association between mean platelet volume levels and inflammation in SLE patients presented with arthritis. *Afr Health Sci.* 2014;14(4):919–924.
26. Yolbas S, Yildirim A, Gozel N, et al. Hematological indices may be useful in the diagnosis of systemic lupus erythematosus and in determining disease activity in Behçet's disease. *Med Princ Pract.* 2016; 25(6):510–516.
27. Belizna C. Hydroxychloroquine as an anti-thrombotic in antiphospholipid syndrome. *Autoimmun Rev.* 2015;14(4):358–362.
28. Gasparyan AY, Ayvazyan L, Pretorius E, et al. Platelets in rheumatic diseases: Friend or foe? *Curr Pharm Des*. 2014;20(4):552–566.

Extremely low frequency electromagnetic field reduces oxidative stress during the rehabilitation of post-acute stroke patients

Natalia Cichoń[1,A–D,F], Paulina Rzeźnicka[1,B], Michał Bijak[1,A,C,D,F], Elżbieta Miller[2,3,A,D–F], Sergiusz Miller[4,E,F], Joanna Saluk[1,A,C–F]

[1] Department of General Biochemistry, Faculty of Biology and Environmental Protection, University of Lodz, Poland
[2] Department of Physical Medicine, Medical University of Lodz, Poland
[3] Neurorehabilitation Ward, III General Hospital in Lodz, Poland
[4] Department of Orthodontics, Medical University of Lodz, Poland

A – research concept and design; B – collection and/or assembly of data; C – data analysis and interpretation; D – writing the article; E – critical revision of the article; F – final approval of the article

Advances in Clinical and Experimental Medicine, ISSN 1899-5276 (print), ISSN 2451-2680 (online) *Adv Clin Exp Med*. 2018;27(9):1285–1293

Address for correspondence
Natalia Cichoń
E-mail: natalia.cichon@biol.uni.lodz.pl

Funding sources
This study was supported by the University of Lodz (grant No. 506/1136).

Conflict of interest
None declared

Received on February 17, 2017
Reviewed on March 27, 2017
Accepted on May 11, 2017

Abstract

Background. One of the therapeutic methods used in stroke rehabilitation is magnetotherapy using extremely low frequency and variable pulse shape electromagnetic field (ELF-EMF).

Objectives. The aim of our study was to investigate the effect of magnetotherapy on the condition of post-acute stroke patients, as measured by plasma oxidative stress markers and clinical parameters which show the progress of rehabilitation.

Material and methods. The selected 57 post-stroke patients were divided into 2 groups, those with ELF-EMF therapy and those without. The level of oxidative stress in the plasma was estimated by typical markers: thiobarbituric acid reactive substances (TBARS), thiol groups, and carbonyl groups. The effect of ELF-EMF on the course of the patients' rehabilitation following ischemic stroke was evaluated with the use of scales of physical activity and mental state: Activities of Daily Living (ADL), Mini-Mental State Examination (MMSE) and Geriatric Depression Scale (GDS).

Results. Our comparative analysis showed that all parameters of oxidative stress are significantly reduced during rehabilitation using ELF-EMF, compared to the control group rehabilitated only by kinesiotherapy. We also recorded much higher therapeutic benefits using magnetotherapy, which revealed a significant improvement of clinimetric parameters.

Conclusions. The ELF-EMF therapy meaningfully improves the overall condition of patients through a decrease of oxidative stress markers and it significantly affects the psychophysical abilities of patients after stroke. The change in carbonyl group level correlates with the change in the degree of physical and mental disability; therefore, it could be a marker for the effectiveness of rehabilitation.

Key words: stroke, rehabilitation, oxidative stress, extremely low frequency electromagnetic field therapy

DOI
10.17219/acem/73699

Introduction

A large body of evidence confirms a relationship between oxidative stress and the development of neurological diseases, including cerebrovascular disorders such as stroke.[1] Epidemiological studies clearly indicate that ischemic stroke is characterized by high levels of oxidative stress biomarkers and by the insufficient activity of antioxidant defense mechanisms in the brain and peripheral tissues. The excessive neuronal production of reactive species and the accumulation of oxidative damage has been proposed as one of the major factors of brain stroke pathogenesis.[2]

Brain damage following stroke is irreversible, but immediate and long-term rehabilitation helps improve neurotransmission and affects the mental and physical functions of the patients. One of the therapeutic methods used in stroke rehabilitation is magnetotherapy, which uses extremely low frequency and an electromagnetic field with various pulse shape quantities (ELF-EMF). This procedure is supplementary to the treatment for physical post-stroke rehabilitation.[3] Magnetotherapy is one of the physical methods characterized by non-invasiveness and a broad spectrum of applications, especially in osteoarticular diseases. Moreover, variable ELF-EMF reduces muscle tension and spasticity, increases muscle strength, and exhibits an analgesic effect. The therapeutic effect of ELF-EMF is associated with improving neurotransmission. It increases blood flow, which contributes to an increase of nervous tissue metabolism and has beneficial effects on regeneration.[4]

There is little data on the effect of ELF-EMF on the level of oxidative stress, which is an important destructive factor in ischemic stroke.[5]

Ischemic stroke is the result of the obstruction of cerebral vessels: a clot is formed and blocks an artery, which causes an interruption in the blood flow to a portion of the brain. After ischemia, the subsequent reperfusion is associated with a massive production of reactive oxygen species (ROS). An uncontrolled rise in ROS concentration leads to a series of radical reactions which increase the scope of damage to biological molecules. These highly reactive compounds readily react with lipids, proteins, carbohydrates, and nucleic acids. They induce changes in the structure and function of cell membranes, and they are responsible for the modifications of proteins, lipoproteins, enzymes, hormones, and genetic material.[6] In particular, cell membranes are the main target for ROS. The highly reactive products of lipid peroxidation lead to the decomposition of polyunsaturated fatty acids and the formation of the final products, including reactive aldehydes, such as malondialdehyde (MDA). MDA is one of the most popular and reliable markers that determine oxidative stress in the clinical stage.[7] Lipid peroxidation is accompanied by the inactivation of membrane enzymes and the disintegration of structural proteins. Reactive oxygen species are responsible for the oxidation of the polypeptide chain. As a result of their oxidation, proteins undergo irreversible changes that rely on the creation of carbonyl or hydroxyl groups. These modifications lead to a fragmentation of the polypeptide chain, and an aggregation or formation of cross-links. The oxidative modifications of proteins are responsible for irreversible functional changes which are significant in both tissue damage and the impairment of the regeneration process.[8]

Our study aimed to investigate the ELF-EMF treatment effects on the reduction of the oxidative damage of biomolecules after a stroke. To this effect, the changes in the level of oxidative stress markers were correlated with the clinimetric parameters of the patients. The impact of a standard series of ELF-EMF treatments on protein oxidative damage was evaluated based on the level of protein carbonylation and thiol groups. Furthermore, we examined the potential antioxidative effect of magnetotherapy on plasma lipid peroxidation by measuring the level of MDA and other thiobarbituric acid reacting substances (TBARS). The effect of ELF-EMF on the course of the patients' rehabilitation following ischemic stroke was evaluated with the use of the Activities of Daily Living scale (ADL), the Mini-Mental State Examination (MMSE), and the Geriatric Depression Scale (GDS). The differences in the values of clinimetric scale parameters before and after rehabilitation reflect the effectiveness of treatments by evaluating the motor ability and cognitive ability of patients.

Material and methods

Subject presentation

Fifty-seven patients following ischemic stroke were enrolled in the study. The patients were randomly divided into 2 groups: the ELF-EMF group (n = 23) and the non-ELF-EMF one (n = 34). From the ELF-EMF group, we excluded participants with metal or electronic implants. The ELF-EMF patients were exposed to ELF-EMF for 15 min with the following parameters: frequency – 40 Hz, magnetic induction – 5 mT, and waveform – bipolar, rectangular. The tests on the non-ELF-EMF patients were conducted only with placebo exposure. The area of operation of ELF-EMF was the pelvic girdle. Magnetotherapy was conducted according to the accepted guidelines using a Magnetronic MF10 (EiE Elektronika i Elektromedycyna, Otwock, Poland). Both groups of patients had the same rehabilitation program consisting of aerobic exercise for 30 min, neurophysiological methods for 60 min, and psychological therapy for 15 min. A total of 57 patients (study group age: 68.0 ±15.8; control group age: 70.9 ±15.3) with moderate stroke severity (study group National Institutes of Health Stroke Scale scores: 5.8 ±3.8; control group scores: 6.2 ±2.7) who agreed to participate were included in this analysis. Their clinical demographic characteristics are shown in Table 1. The patients were

Table 1. Clinical and demographic characteristics

Clinical and demographic properties		Control n = 34	Study group n = 23	p-value
Demographics	age (mean ±SD)	70.9 ±15.3	68.0 ±15.6	0.05
	sex (female, %)	65.6	64.8	0.64
	living alone [%]	48.1	51.9	0.14
Vascular risk	hypertension [%]	95.7	94.7	0.08
	diabetes [%]	24.8	21.7	0.36
	dyslipidemia [%]	74.9	67.9	0.14
	BMI ≥30 [%]	32	22	0.82
Concomitant medications	antidepressants [%]	32	23	0.47
	ASA [%]	72	67	0.39
	NSAIDs [%]	21	24	0.72
Stroke characteristics	weeks since stroke (mean ±SD)	2.1 ±3.7	1.8 ±3.5	0.61
	NIHSS score (mean ±SD)	6.2 ±2.7	5.8 ±3.8	0.81
	ADL score (mean ±SD)	9.77 ±2.87	8.80 ±2.35	0.22
Lesion location	anterior [%]	13	14	0.88
	posterior [%]	39	49	0.53
	intermediate [%]	48	33	0.12
Lesion side	left [%]	58	54	0.75
	right [%]	42	46	0.62

BMI – body mass index; ASA – acetylsalicylic acid; NSAIDs – nonsteroidal anti-inflammatory drugs; NIHSS – National Institutes of Health Stroke Scale; ADL – Activities of Daily Living scale.

followed-up with at Neurorehabilitation Ward III of the General Hospital in Łódź. They were undergoing neurorehabilitation for 4 weeks, and in that time they received no immunomodulators, immunostimulators, hormones, vitamins, minerals, or any other substances with antioxidative properties. Prior to the study, all the subjects had undergone medical check-ups including neurological and internist examinations. Blood samples were collected 3 times at an interval of 20 days: before treatment, after 10, and after 20 rehabilitation treatments using magnetotherapy and/or aerobic training. All blood samples were taken in the morning (between 7 am and 9 am) after fasting, and stored according to the same protocol. The Ethics Committee of University of Łódź, Poland approved the protocol (No. 28/2015). All participants provided written informed consent prior to participation. Depression was screened using the Geriatric Depression Scale (GDS), which is a reliable and sensitive indicator of post-stroke depression.[9] A trained psychologist researcher administered the GDS scale. The GDS, ADL, and MMSE were administered either on the same day as the blood draw or on the afternoon before.

Blood sample collection

Blood samples were collected in tubes containing Citrate Phosphate Dextrose Adenine Solution (CPDA1) and immediately centrifuged to isolate the plasma (15 min, 1500 g) at 25°C and stored in –32°C until further processing.

Determination of protein carbonyl groups

The protein carbonyl groups in the human blood plasma were detected using the ELISA method described by Alamdari et al.[10] The linearity of the ELISA method was confirmed by the construction of a standard curve ranging from 0.1 to 10 nmol carbonyl groups/mg of fibrinogen. Albumin is known to be a powerful antioxidant and its concentration in the plasma is significant. But the increase of acute phase proteins with high molecular weights, such as fibrinogen, requires important protein antioxidants to counteract the high amounts of reactive oxygen species under oxidative stress conditions. The high-molecular-weight antioxidant proteins are more suitable to prevent oxidation than albumin.[11] For this reason, in our study we used fibrinogen as the standard plasma oxidation protein. Moreover, fibrinogen exhibits higher adhesion to the plate than albumin. The amount of carbonyl groups present in fibrinogen was determined spectrophotometrically as described by Levine et al. The molar extinction coefficient of 2,3-diaminophenazine (OPD with horseradish peroxidase reaction product) at a wavelength of 490 nm is $\varepsilon = 16170\ M^{-1}\ cm^{-1}$; its specific absorption value is $a = 79.437\ dm^3\ g^{-1}\ cm^{-1}$.[12]

Estimation of thiol groups

Thiol groups in plasma proteins were determined using 5,5'-dithio-bis(2-nitro-benzoic acid) (Ellman's reagent, DTNB).[13] The thiol-disulfide interchange reaction between

DTNB and a thiol compound is the basis of this spectrophotometric assay. The reaction results in a mixture of disulphides, accompanied by the release of 5-thio-2-nitrobenzoic acid (TNB), which is colorimetrically determined. The mixture of samples with DTNB was incubated (1 h, 37°C) and then the absorbance was measured at 412 nm. The concentration was calculated by using the molar extinction coefficient for TNB (Í = 13600 M^{-1} cm^{-1}) and based on a specific absorption of a = 68.297 dm^3 g^{-1} cm^{-1}.

Detection of thiobarbituric acid reactive substances

Lipid peroxidation was determined by the reaction with TBA following the method described by Placer et al.[14] The level of peroxidation was calculated on the basis of the molar extinction coefficient of malondialdehyde (MDA), a reliable marker of lipid peroxidation, which is condensed with TBA ($\varepsilon = 1.56 \times 10^5$ M^{-1} cm^{-1}) and is based on a specific absorption of a = 2.273 dm^3 g^{-1} cm^{-1} and expressed in nmoles of MDA/mL of plasma.

Statistical analysis

All the experiments were performed in duplicate and results were calculated as mean values. For all the subjects, the values of experimental parameters before treatments were used as the output values (100%). The data obtained from the same subjects after appropriate treatment were expressed as a percentage of the output value. Values obtained in this way were expressed as a mean ±SD. All the statistical analyses were performed using the StatsDirect statistical software v. 2.7.2. The obtained results were analyzed for normality with the Shapiro-Wilk test.[15,16] The significance of the differences between the values obtained for the patients before and after treatments was analyzed by the paired Student's t-test or Wilcoxon signed rank tests, depending on the normality; the significance of the differences between the ELF-EMF group and the control group, however, was analyzed using the unpaired Student's t-test or U Mann-Whitney test. To compare the clinical parameters in the ELF-EMF study group and the non-ELF-EMF control group, we assessed the changes in the GDS, ADL, and MMSE values after the appropriate treatment. These results were also analyzed for normality with the Shapiro-Wilk test. Depending on the result of this test, an unpaired Student's t-test or U Mann-Whitney test was used. We also performed correlation analysis between changes in both the biochemical and clinical parameters. For this analysis, we used Spearman's rank correlation and Spearman's rank correlation coefficient; moreover, we designated the probability of correlation.[17] For all analyses, the level of $p < 0.05$ was accepted as statistically significant.

Results

In our study, we determined plasma oxidative stress parameters in acute stroke patients. It is well-estimated that oxidative stress is significantly higher in stroke patients than in healthy people (data not shown).

We observed statistically significant differences in the decreased level of carbonyl groups ($p < 0.001$) (Fig. 1) and the increased level of thiol groups ($p < 0.01$) (Fig. 2) in plasma proteins of the patients who were rehabilitated using magnetotherapy. The reduction of oxidative stress markers was significantly greater with an increasing number of treatments (Fig. 1, 2). The antioxidant effect of rehabilitation in the non-ELF-EMF control group undergoing only aerobic exercise was clearly weaker and not statistically significant (Fig. 1, 2). Furthermore, our comparative analysis showed that all the measured parameters of oxidative stress are significantly reduced during rehabilitation with the use of both ELF-EMF and aerobic exercise, compared to the control group rehabilitated only by kinesiotherapy. We observed that the level of protein carbonylation was lower in the ELF-EMF group than in the non-ELF-EMF group, both after 10 treatments (18% vs 7%; $p < 0.05$) and after 20 sessions (36% vs 1%; $p < 0.001$). Similarly, in the study group, the level of thiol groups increased more

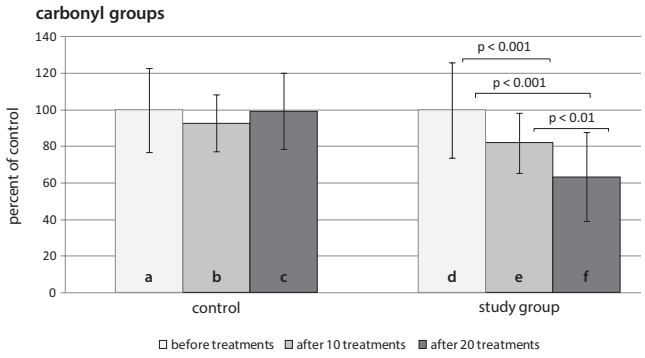

Fig. 1. The comparison of carbonyl group levels in plasma proteins obtained from the ELF-EMF group vs the non-ELF-EMF group. Statistical significance between the ELF-EMF and the non-ELF-EMF groups: b vs e = $p < 0.05$; c vs f = $p < 0.001$

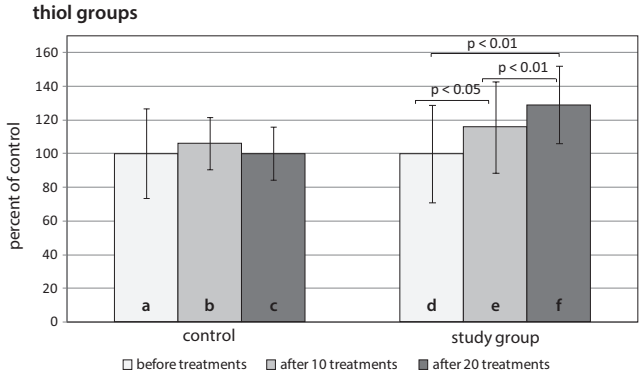

Fig. 2. The comparison of thiol group levels in plasma proteins obtained from the ELF-EMF group vs the non-ELF-EMF group. Statistical significance between the ELF-EMF and the non-ELF-EMF groups: b vs e = $p < 0.05$; c vs f = $p < 0.01$

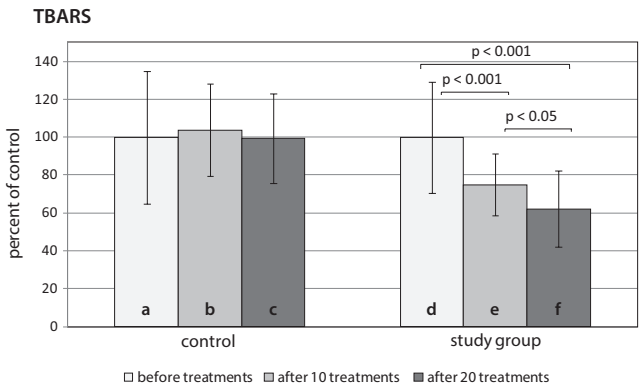

Fig. 3. The comparison of TBARS concentrations in plasma obtained from the ELF-EMF group vs the non-ELF-EMF group. Statistical significance between the ELF-EMF and the non-ELF-EMF groups: b vs e = $p < 0.001$; c vs f = $p < 0.001$

than in the control group: after 10 treatments (16% vs 6%; $p < 0.05$) and after 20 (29% vs 0%; $p < 0.01$).

Next, we determined the effect of magnetotherapy on lipid oxidative damage. The amount of TBARS produced in the plasma of patients after ELF-EMF therapy was significantly lower when compared to that in the plasma of patients without ELF-EMF treatments, both after 10 sessions ($p < 0.001$) and 20 ($p < 0.001$). The level of TBARS decreased significantly (up to 30%) with an increasing number of rehabilitation sessions in the ELF-EMF group, but did not change significantly in the non-ELF-EMF group (Fig. 3).

In addition, we evaluated the impact of rehabilitation methods on the clinical effects, expressed in such clinimetric scales as the ADL, the MMSE, and the GDS. The ADL value in patients treated with ELF-EMF increased by about 25% compared with the control group ($p < 0.01$). For the MMSE, the increase in parameters between the ELF-EMF group and the non-ELF-EMF group reached about 35% ($p < 0.05$); the level of depression determined by the GDS was significantly lower in the group with magnetotherapy than in the group without it (the difference was up to 65%) ($p < 0.001$) (Table 2).

The distribution of the results of the ADL, the MMSE, and the GDS deviated from the norm in the ELF-EMF group, so the method of Spearman correlation was used for analysis. The obtained correlation parameters (Table 3) indicated a significant positive correlation between thiol group concentration and ADL value. On the other hand, we observed a significant negative correlation between carbonyl group level and ADL value. Table 3 shows the statistically significant negative correlation between carbonyl group level and the MMSE score. Moreover, the correlation parameters indicated a significant positive correlation between carbonyl group level and GDS value. The detailed course of carbonyl group correlations are shown in Fig. 4.

Discussion

It has been observed that during a stroke there is an increase in ROS production. Ischemia of brain tissue leads to depletion of the chemicals necessary for ATP synthesis, including glucose and oxygen.[18] This results in an inhibition of the activity of the membrane's sodium–potassium pump, membrane depolarization, and an influx of Ca^{2+} into the cell.[19] Accumulated cellular calcium leads to the

Table 2. The clinical parameters of ADL, MMSE, and GDS measured in the ELF-EMF group and the non-ELF-EMF group. Data are presented as the delta of the clinimetric scale before and after the standard series of treatments (ΔADL – the increase of ADL; ΔMMSE – the increase of MMSE; and ΔGDS – the decrease of GDS)

Clinical scale	non-ELF-EMF group n = 34			ELF-EMF group n = 23		
	before treatment	after treatment	Δ	before treatment	after treatment	Δ
ADL	9.77	14.73	4.97	8.80	15.35	6.55
MMSE	22.28	25.41	3.08	20.94	25.61	4.67
GDS	12.41	9.37	3.04	17.43	9.57	7.86

ELF-EMF – extremely low frequency and variable pulse shape electromagnetic field; ADL – Activities of Daily Living scale; MMSE – Mini-Mental State Examination; GDS – Geriatric Depression Scale.

Table 3. Correlation coefficient values obtained in the ELF-EMF group for oxidative stress markers and the parameters of clinimetric scales (the ADL, the MMSE, and the GDS)

Carbonyl groups			Thiol groups			TBARS		
ADL	MMSE	GDS	ADL	MMSE	GDS	ADL	MMSE	GDS
Rho = –0.683	Rho = –0.678	Rho = 0.613	Rho = 0.506	Rho = 0.392	Rho = 0.041	Rho = –0.353	Rho = –0.381	Rho = –0.189
p = 0.001	p = 0.002	p = 0.007	p = 0.023	p = 0.392	p = 0.433	p = 0.090	p = 0.054	p = 0.512
H1: negative correlation	H1: negative correlation	H1: positive correlation	H1: positive correlation	H0: no correlation	H0: no correlation	H0: no correlation	H0: no correlation	H0: no correlation

Rho – Spearman's rank correlation coefficient; p – probability for correlation; H1 – hypothesis verification; ADL – Activities of Daily Living scale; MMSE – Mini-Mental State Examination; GDS – Geriatric Depression Scale.

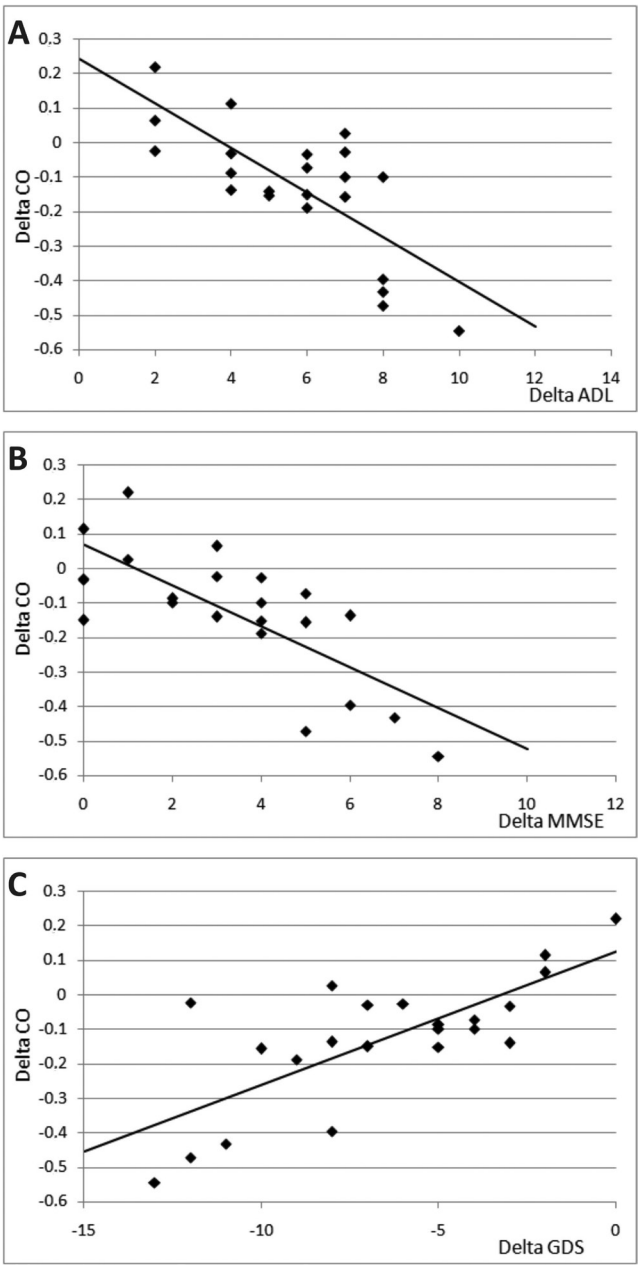

Fig. 4. Regression plots for the delta of carbonyl group levels in the ELF-EMF group (the changes of concentrations before and after a standard series of treatments) and the delta of clinical parameters established on the basis of clinimetric scales read before and after therapy. A – carbonyl group levels and ΔADL; B – carbonyl group levels and ΔMMSE; C – carbonyl group levels and ΔGDS

activation of many Ca^{2+}-dependent enzymes (including proteases, nucleases, and NO synthase). This process is the basic mechanism of cell damage. On the other hand, it is the phospholipase A2 and cyclooxygenase that generate the production of free radicals.[20]

During hypoxia/reperfusion, ROS are generated in the reaction of xanthine oxidase, which catalyzes the oxidation of hypoxanthine and xanthine to uric acid, leading to the generation of enzymes of superoxide anions and, consequently, hydrogen peroxide and the highly toxic hydroxyl radical.[21] Moreover, the mitochondrial electron chain associated with reductase and NADH cytochrome b5 plays an important role in the production of ROS. The auto-oxidation of adrenaline, noradrenaline, and thiol compounds also leads to superoxide anion generation.[22]

The high metabolic and oxygen activity of the brain is particularly dangerous for proteins. ROS damage strategic amino acids, thus modifying the properties of proteins. What may occur under the action of ROS is oxidation of the polypeptide chain, as well as alteration of amino acid residues. This variation could lead to a fragmentation of the polypeptide, a formation of cross-linking, and changes in the structure of the amino acids, causing a loss of the most common biological function of the protein; it may also fulfill a regulatory function.[23]

Ischemic stroke is one of the diseases which are directly life-threatening. It is caused by an obstruction of the brain or carotid arteries with embolic or thrombotic etiology, which leads to deficits in neurological function. The disablement and quality of life of patients is associated with motor disabilities. The neuromuscular dysfunctions responsible for such disabilities include apraxia, pain syndrome, limb spasticity, and urinary incontinence.[24] The cognitive problems causing disabilities include memory loss, speech impairment, poor problem-solving skills, and disorganized thoughts. Furthermore, a stroke is often accompanied by psychosomatic complications such as anxiety, depression, emotional instability, and fatigue.[25]

All post-stroke patients should receive rehabilitation at an early stage of the disease. Active rehabilitation should be initiated immediately after the patient is stabilized. Although irreversible damage to the neurons occurs during a stroke, rehabilitation must be performed in order to restore the patient's fitness and return him or her to their pre-illness functional state or to adapt and achieve an optimal level of independence. The rehabilitation should deliver an improvement in practical activities and should include an improvement in cognitive impairment and changes in behavior. A preferred aspect of the rehabilitation process can be the inclusion of physical treatments such as magnetotherapy.[3] The application of extremely low frequency ELF-EMF is widely used in rehabilitation primarily because of its extensive therapeutic possibilities. There are well-documented applications of ELF-EMF in rehabilitation, which reduces muscle tension and spasticity, increases muscle strength, and demonstrates an analgesic effect. The therapeutic influence of ELF-EMF is associated with its effect on nerve transduction. ELF-EMF increases blood flow, which improves the metabolism of the nervous tissue and its regeneration. In many medical centers, the use of ELF-EMF remains at the experimental stage and is not a routine method for post-stroke treatment. However, there are reports that acknowledge the use of this method as a physical treatment in improving the condition of stroke patients.[26] In the literature, there are a few studies evaluating the effect of ELF-EMF on the redox system.[27,28] Kurzeja et al.

found a positive effect of ELF-EMF on the functioning of connective tissue in mice. They noted a decrease in the level of oxidative stress markers, with a simultaneous normalization of antioxidant enzyme activities.[27] Similarly, Sosnowski et al. showed a reduction in hydrogen peroxide concentration after the exposure of laboratory animals to ELF-EMF, as well as a normalization of antioxidant enzyme activities.[28] However, there are no data describing the in vivo ability of ELF-EMF to change the redox status of rehabilitated patients.

The aim of our study was to monitor the parameters of oxidative stress as well as the parameters assessing the patients' physical and mental improvement during rehabilitation with ELF-EMF. This study was designed to investigate the impact of ELF-EMF in comparison with classical rehabilitation using only kinesiotherapy.

The most common free radical process in the cell is a chain lipid peroxidation involving the oxidation of polyunsaturated fatty acid residues, which are part of membrane phospholipids and lipoproteins.[29] Peroxidation products undergo further transformations into fragments of different lengths.

The end products of the degradation of polyunsaturated fatty acids react with other lipids, thiol groups, amino groups of proteins, and nitrogenous bases of nucleic acids causing various effects, such as a change of antigenic protein properties, enzyme inactivation, and the inhibition of replication and transcription.[30]

The human brain is composed of more than 60% lipids, and is particularly rich in membrane phospholipids with unsaturated fatty acid residues. Especially arachidonic acid and docosahexaenoic acid (DHA), which are the main source of polyunsaturated fatty acids in the brain, readily undergo peroxidation. In addition, the concentration of iron in some brain structures also accelerates the oxidation of lipids. The aldehyde products of lipid peroxidation may be covalently bound to a Michael reaction with the sulfhydryl groups of proteins or glutathione, reducing their concentration in the cell.[31] The effect of ELF-EMF on the level of oxidative stress in vivo was examined by Rauš Balind et al.[32] They noted positive consequences of applying ELF-EMF in gerbils with induced cerebral ischemia. In this study, the index of lipid peroxidation was examined in the forebrain cortex, striatum, and hippocampus. The results indicate a decrease of oxidative stress induced by global cerebral ischemia, and thereby a beneficial effect of ELF-EMF through the reduction of negative consequences which free radical species could have in the brain.[33]

In our study, we investigated the change of lipid peroxidation level in the plasma of post stroke patients, after the application of ELF-EMF. Because plasma is a less invasive diagnostic material, we were able to monitor the levels of markers of oxidative stress in patients during stroke rehabilitation. The results presented here indicate that the level of plasma lipid peroxidation significantly decreases with an increasing number of magnetotherapy treatments and is over 40% lower than in patients rehabilitated by exercise alone (Fig. 4).

In the present study, it was also first demonstrated that oxidative damage of plasma proteins in patients after post-stroke rehabilitation was inhibited, as evidenced by a reduction in the level of carbonyl groups (Fig. 2) and an increase in thiol group concentration (Fig. 3). The antioxidant effects of ELF-EMF used in stroke rehabilitation can provide extremely important benefits due to major implications caused by ROS in the activity of regulatory proteins, which are especially dangerous in the metabolism of neurons. Highly reactive oxygen species impair the functioning of cascades of intracellular signals and modify responses to oxidative stress gene transcription factors by changing the conformation and/or oxidation of strategic amino acids. Proteins which are particularly sensitive to oxidative stress are thioredoxin and glutathione S-transferase.[34,35] The damaged oxidative proteins in general lose their biological activity; they may form aggregates because they do not undergo ubiquitination, so they are not recognized by the proteasome.[36]

In our previous studies, we showed that the potential ELF-EMF antioxidant mechanism is associated with a rise in the activity of the antioxidant enzyme. The ELF-EMF increases SOD and CAT activities and improves the effectiveness of post-stroke rehabilitation. Elevated SOD and CAT activities after surgery correlate with improved degrees of physical and mental disability based on the clinical scales used in research (the ADL, the MMSE, and the GDS).[37]

A high level of oxidative stress is the cause of complications after stroke and, according to our research as well, it significantly affects the progress of the patient's rehabilitation process.[36,37] In our study, we determined the correlation between the level of markers of protein damage and the degree of clinical effects in patients rehabilitated by EMF. In order to define clinical effects, we used clinimetric scales: the ADL, the MMSE, and the GDS. The ADL is a scale which indicates the patient's independence during basic and complex activities of daily living as well as his or her gait efficiency. ADL allows for a reliable assessment of the patient's situation, his or her nursing requirements and the need to adapt the environment according to the degree of his or her impairment.[38] We noted a positive correlation between increased levels of thiol groups and ΔADL (Table 3) and a negative correlation between the reduction of carbonyl groups and ΔADL (Fig. 5, Table 3). Our results suggest that under the action of ELF-EMF, the concentration of oxidative damage markers in plasma proteins is reduced, and thereby the independence of stroke patients is improved. The MMSE is used to evaluate abnormalities in the cognitive functioning of the patient and it determines the degree of dementia. Dementia is a serious problem after a stroke, characterized by numerous disorders of higher cortical functions (memory, thinking, orientation, comprehension, and learning ability).[39] We found a negative

correlation between the changes in the level of carbonyl groups and ΔMMSE using magnetotherapy (Fig. 5, Table 3). The size of the concentration gradient of carbonyl groups caused by magnetotherapy was negatively correlated with the growth of MMSE scores. This indicates that the level of oxidative protein damage is referenced not only in the physical functioning of the patients, but also in his or her cognitive functions. On the other hand, the GDS scale determines the level of post-stroke depression. It is the most common psychogenic disorder occurring after a stroke. There are some reports about the somatic cause of this disease, specifying the location of ischemia and changes in biochemical parameters, among other things. In our previous studies we identified the existence of a relationship between the level of oxidative stress and the occurrence of post-stroke depression.[40] We demonstrated a positive correlation between a reduction in the level of plasma protein carbonyl groups and in the degree of depression under treatment with ELF-EMF (Fig. 4, Table 3). Our results strongly support the hypothesis that rehabilitation using ELF-EMF has a positive impact on the improvement of the psychophysical condition of post-stroke patients, which is associated with a decrease in the level of protein oxidative stress parameters in vivo.

Conclusions

We emphasize that ELF-EMF significantly decreases the parameters of oxidative stress and improves the effectiveness of stroke rehabilitation. The level of changes in the concentration of plasma protein carbonyl groups correlates with the revised degrees of physical and mental disability determined by the 3 clinimetric scales used. Therefore, the plasma level of the carbonyl groups could be a marker for non-invasive evaluation of oxidative stress in vivo in the course of stroke rehabilitation, as well as a marker of the progress of the patient's recovery.

References

1. Zundorf IC, Karnath HO, Lewald J. The effect of brain lesions on sound localization in complex acoustic environments. *Brain*. 2014;137: 1410–1418.
2. Zhao J, Zhang X, Dong L, et al. The many roles of statins in ischemic stroke. *Curr Neuropharmacol*. 2014;12:564–574.
3. Sureshkumar K, Murthy GV, Munuswamy S, et al. 'Care for Stroke', a web-based, smartphone-enabled educational intervention for management of physical disabilities following stroke: Feasibility in the Indian context. *BMJ Innov*. 2015;1:127–136.
4. Galace de FD, Marcondes FB, Monteiro RL, et al. Pulsed electromagnetic field and exercises in patients with shoulder impingement syndrome: A randomized, double-blind, placebo-controlled clinical trial. *Arch Phys Med Rehabil*. 2014;95:345–352.
5. Hall ED. The contributing role of lipid peroxidation and protein oxidation in the course of CNS injury neurodegeneration and neuroprotection: An overview. In: Kobeissy FH, ed. *Source Brain Neurotrauma: Molecular, Neuropsychological, and Rehabilitation Aspects*. Boca Raton, FL: CRC Press, 2015:49–60.
6. Liu J, Wang Z. Increased oxidative stress as a selective anticancer therapy. *Oxid Med Cell Longev*. 2015;2015:294303. doi: 10.1155/2015/ /294303
7. Metta S, Basalingappa DR, Uppala S, et al. Erythrocyte antioxidant defenses against cigarette smoking in ischemic heart disease. *J Clin Diagn Res*. 2015;9:8–11.
8. Costantini D, Goutte A, Barbraud C, et al. Demographic responses to oxidative stress and inflammation in the wandering albatross (*Diomedea exulans*). *PLoS One*. 2015;10(8):e0133967. https://doi.org/10.1371/journal.pone.0133967
9. Nabavi SF, Dean OM, Turner A, et al. Oxidative stress and post-stroke depression: Possible therapeutic role of polyphenols? *Curr Med Chem*. 2015;22:343–351.
10. Alamdari DH, Kostidou E, Paletas K, et al. High sensitivity enzyme-linked immunosorbent assay (ELISA) method for measuring protein carbonyl in samples with low amounts of protein. *Free Radic Biol Med*. 2005;39:1362–1367.
11. Olinescu RM, Kummerow FA. Fibrinogen is an efficient antioxidant. *J Nutr Biochem* 2001;12:162–169.
12. Levine RL, Garland D, Oliver CN, et al. Determination of carbonyl content in oxidatively modified proteins. *Methods Enzymol*. 1990;186: 464–478.
13. Ellman GL. Tissue sulfhydryl groups. *Arch Biochem Biophys*. 1959;82: 70–77.
14. Placer ZA, Cushman LL, Johnson BC. Estimation of product of lipid peroxidation (malonyl dialdehyde) in biochemical systems. *Anal Biochem*. 1966;16:359–364.
15. Bijak M, Kolodziejczyk-Czepas J, Ponczek MB, et al. Protective effects of grape seed extract against oxidative and nitrative damage of plasma proteins. *Int J Biol Macromol*. 2012;51:183–187.
16. Saluk J, Bijak M, Nowak P, et al. Evaluating the antioxidative activity of diselenide containing compounds in human blood. *Bioorg Chem*. 2013;50:26–33.
17. Hauke J, Kossowski T. Comparison of values of pearson's and spearman's correlation coefficients on the same sets of data. *Quaestiones Geographicae*. 2011;30:87–93.
18. Liu LF, Qin Q, Qian ZH, et al. Protective effects of melatonin on ischemia-reperfusion induced myocardial damage and hemodynamic recovery in rats. *Eur Rev Med Pharmacol Sci*. 2014;18:3681–3686.
19. Tano JY, Gollasch M. Calcium-activated potassium channels in ischemia reperfusion: A brief update. *Front Physiol*. 2014;5:381. doi: 10.3389/fphys.2014.00381
20. Yano T, Fujioka D, Saito Y. Group V secretory phospholipase A2 plays a pathogenic role in myocardial ischaemia-reperfusion injury. *Cardiovasc Res*. 2011;90:335–343.
21. Yamaguchi M, Okamoto K, Kusano T. The effects of xanthine oxidoreductase inhibitors on oxidative stress markers following global brain ischemia reperfusion injury in C57BL/6 mice. *PLoS One*. 2015;10(7):e0133980. https://doi.org/10.1371/journal.pone.0133980
22. Gutowicz M. The influence of reactive oxygen species on the central nervous system. *Postepy Hig Med Dosw*. 2011;65:104–113.
23. Voskou S, Aslan M, Fanis P, et al. Oxidative stress in beta-thalassaemia and sickle cell disease. *Redox Biol*. 2015;6:226–239.
24. Young JA, Tolentino M. Stroke evaluation and treatment. *Top Stroke Rehabil*. 2009;16:389–410.
25. Annoni JM, Staub F, Bruggimann L, et al. Emotional disturbances after stroke. *Clin Exp Hypertens*. 2006;28:243–249.
26. Bassett CA. Beneficial effects of electromagnetic fields. *J Cell Biochem*. 1993;51:387–393.
27. Kurzeja E, Synowiec-Wojtarowicz A, Stec M, et al. Effect of a static magnetic fields and fluoride ions on the antioxidant defense system of mice fibroblasts. *Int J Mol Sci*. 2013;4:15017–15028.
28. Sosnowski P, Mikrut K, Paluszak J, et al. The antioxidative enzymes activity in blood of rats exposed to long-term magnetic field. *Baln Pol*. 1990;41,18–24.
29. Shibata T, Shimizu K, Hirano K et al. Adductome-based identification of biomarkers for lipid peroxidation. *J Biol Chem*. 2017. doi: 10.1074/ jbc.M116.762609
30. Coimbra-Costa D, Alva N, Duran M, et al. Oxidative stress and apoptosis after acute respiratory hypoxia and reoxygenation in rat brain. *Redox Biol*. 2017;12:216–225.
31. Ionescu N, de Freitas C, Bueno AA. Perturbations in blood phosphatidylcholine and sphingomyelin fatty acid composition in a sample population of cigarette smokers. *Indian J Clin Biochem*. 2013;28(4): 361–367.

32. Rauš Balind S,, Selakovic V, Radenovic L, et al. Extremely low frequency magnetic field (50 Hz, 0.5 mT) reduces oxidative stress in the brain of gerbils submitted to global cerebral ischemia. *PLoS One.* 2014; 9(2):e88921. https://doi.org/10.1371/journal.pone.0088921
33. Adler V, Yin Z, Tew KD, et al. Role of redox potential and reactive oxygen species in stress signaling. *Oncogene.* 1999;18:6104–6111.
34. Chakraborti S, Chakraborti T. Oxidant-mediated activation of mitogen-activated protein kinases and nuclear transcription factors in the cardiovascular system: A brief overview. *Cell Signal.* 1998;10: 675–683.
35. Paspalj D, Nikic P, Savic M, et al. Redox status in acute ischemic stroke: Correlation with clinical outcome. *Mol Cell Biochem*. 2015;406:75–81.
36. Eyre H, Baune BT. Neuroimmunological effects of physical exercise in depression. *Brain Behav Immun.* 2012;26:251–266.
37. Cichon N, Bijak M, Miller E, et al. Extremely low-frequency electromagnetic field (ELF-EMF) reduces oxidative stress and improves functional and psychological status in ischemic stroke patients. *Bioeletromagtetics*. 2017. doi. 10.1002/bem.22055
38. Heyman N, Nili F, Shahory R, et al. Prevalence of delirium in geriatric rehabilitation in Israel and its influence on rehabilitation outcomes in patients with hip fractures. *Int J Rehabil Res*. 2015;38:233–237.
39. Streit S, Limacher A, Zeller A, et al. Detecting dementia in patients with normal neuropsychological screening by Short Smell Test and Palmo-Mental Reflex Test: An observational study. *BMC Geriatr.* 2015; 15:90. doi: 10.1186/s12877-015-0094-0
40. Cichon N, Bijak M, Miller E, et al. Poststroke depression as a factor adversely affecting the level of oxidative damage to plasma proteins during a brain stroke. *Oxid Med Cell Longev.* 2015. http://dx.doi.org/10.1155/2015/408745

An evaluation of the effect on lower extremity fracture healing of collagen-based fusion material containing 2 different calcium phosphate salts: An experimental rat model

Atıf Mehmet Erol Aksekili[1,A–B,D,F], Yusuf Polat[2,A–C], Kaan Yüksel[3,A–C], Mehmet Asiltürk[4,B,D,F], Mahmut Uğurlu[1,E,F], Halil Kara[1,B,C], Evrim Öztürk Önder[5,A,B], Nihat Tosun[1,E,F]

[1] Department of Orthopedics and Traumatology, Faculty of Medicine, Ankara Yıldırım Beyazıt University, Turkey
[2] Department of Orthopedics and Traumatology, Çankırı Public Hospital, Turkey
[3] Department of Orthopedics and Traumatology, Dr. Nafiz Korez Sincan Public Hospital, Turkey
[4] Department of Orthopedics and Traumatology, Ankara Atatürk Training and Research Hospital, Turkey
[5] Department of Pathology, Ankara Dışkapı Yıldırım Beyazıt Traning and Research Hospital, Turkey

A – research concept and design; B – collection and/or assembly of data; C – data analysis and interpretation; D – writing the article; E – critical revision of the article; F – final approval of the article

Advances in Clinical and Experimental Medicine, ISSN 1899-5276 (print), ISSN 2451-2680 (online) *Adv Clin Exp Med*. 2018;27(9):1295–1301

Address for correspondence
Mehmet Asiltürk
E-mail: mehmetasilturk@gmail.com

Funding sources
None declared

Conflict of interest
None declared

Received on December 19, 2017
Reviewed on January 14, 2018
Accepted on May 5, 2018

Abstract

Background. Collagen-based synthetic bone grafts which contain tricalcium phosphate (TCP) and hydroxyapatite (HA), and collagen-based synthetic bone grafts containing only TCP have some advantages compared to autografts. Therefore, these grafts are frequently used to fill bone defects and pseudoarthrosis.

Objectives. The aim of this study was to evaluate and compare the clinical, radiological and histopathological effects of TCP-HA and TCP alone + Type-1 collagen in healing lower extremity fractures in a pseudoarthrosis model in rat femurs.

Material and methods. A total of 36 female Wistar rats were randomly separated into 4 groups. Group 1 (n = 10) was the control group. A femur pseudoarthrosis model was created in Groups 2, 3 and 4. On the 90th day after the 1st surgery in Group 2 (n = 10), TCP-HA + Type-1 collagen was applied, in Group 3 (n = 10), TCP alone + type-1 collagen was applied, and in Group 4 (n = 6, the placebo group), saline solution was applied. Fixation was performed with an intramedullar pin. After 60 days and clinical and radiological scoring, all animals were sacrificed and a histopathological evaluation of the pseudoarthrosis areas was conducted.

Results. In all the clinical, radiological and histopathological measurements used in the evaluations of the differences between the groups, a higher rate of union was determined in Group 2 (TCP-HA). No significant difference was determined between Group 3 and Group 4 in terms of union rates.

Conclusions. The clinical, radiological and histopathological results of this study showed that TCP alone was less effective than TCP-HA in the union of a femur pseudoarthrosis model in rats. The reason for this difference was considered to be hydroxyapatite (HA).

Keywords: rats, collagen, synthetic bone graft, bone healing, pseudoarthrosis

DOI
10.17219/acem/90766

Introduction

As an increasing number of fractures and non-union cases are encountered in orthopedic practice, along with developments in the implants and biomaterials used, there is ongoing research into achieving more rapid union with less surgical damage. In the treatment of bone defects which occur during reconstructive procedures such as trauma, osteomyelitis and arthroplasty revision surgery, increasingly frequent use of bone grafts and substances that can be used instead of bone is observed.[1] Of the grafts used, autografts taken from the iliac wing are the gold standard, with osteoinductive, osteogenesis and osteoconductive properties. However, this procedure has disadvantages, including increased morbidity in the patient, prolonged operating time, limitations to the extent it can be used, and pain in the donor site. Great care is necessary in the use of allograft because of a possibility of infection and immunological reactions.[2,3]

Bone tissue engineering has presented solutions for the production of new bone tissue that has all the necessary functional and mechanical properties at a sufficient level, considering the costs and the risks involved in the use of autografts and allografts. As most of the products that have been developed are at the experimental stage, their clinical use is still limited. Scientific studies contribute to the effective and safe use of these products in practice.[4]

From the spongeous structure of collagen, which is a natural protein in the body, a membrane form is obtained by physically attaching calcium phosphate salts and/or hydroxyapatite (HA) crystals in nano dimensions to this structure, resulting in synthetic grafts for use in bone defects and fracture healing. MasterGraft Putty® (Medtronic Sofamor Danek, Memphis, USA) is a biomaterial designed for filling bone defects; it is highly porous and bioabsorbable; it contains cruciate ligament type-1 collagen, tricalcium phosphate and HA. Debone® (Desu Medical, Ankara, Turkey) is another biomaterial designed for filling bone defects; it contains cruciate ligament type-1 collagen and only tricalcium phosphate.

The aim of this study was to evaluate with clinical, radiological and histopathological measurements the effects on lower extremity fracture healing of MasterGraft Putty and Debone by creating a pseudoarthrosis model in rat femurs, and to compare the efficacy of these products with each other and with a placebo.

Material and methods

Prior to starting the study, approval was granted by the Local Ethics Committee (decision dated June 3, 2014). All procedures were carried out in accordance with the Research Animal Laboratory Local Ethics Committee regulations. The rats were obtained from the Experimental Animals Laboratory, Ankara, Turkey, where they had been bred.

Animals

The study included 36 outbred, conventional female Wistar rats, aged 8–10 weeks, each weighing 300 g (±10%). The rats were housed in cages constructed of plastic in the lower half and wire in the upper, with easy access to food and water. The cages were lined with sawdust and cleaned 4 times a week. All the rats were housed in single cages at room temperature (23°C), 60% humidity and a 12-hour light-dark cycle with 100% air change 12 times per hour. Throughout the study the animals had free access to a pellet diet and refined tap water provided in an autoclavable Makrolon bottle (Optima, Balıkesir, Turkey).

The 36 rats were randomly separated into 4 groups. Group 1 (n = 10) was the control group with no surgical procedure applied; in Group 2 (n = 10) MasterGraft Putty was applied to the femur pseudoarthrosis model; in Group 3 (n = 10) Debone was applied to the femur pseudoarthrosis model; and Group 4 (n = 6) was the placebo group, with saline solution applied.

Surgical procedure

First surgical intervention

The surgical pseudoarthrosis model was created as described in previous studies.[5] With the exception of the rats in Group 1, anesthesia of 10 mg/kg of 10% ketamine + 100 mg/kg of 2% xylazine was administered intraperitoneally to all rats. After the preparation of the rats in a lateral position, the left lower extremity was shaved. Following disinfection with a 10% polyvinylpyrrolidone-iodine complex (Batticon®; Adeka, Samsun, Turkey), a femoral diaphyseal osteotomy was performed, a fascia lata flap was taken and fixed to the proximal and distal fracture lines with 3-0 nylon sutures, and then all the layers were closed in order. Oxytetracycline hydrochloride aerosol (Neo-CafSpray®; Intervet, Aprilia, Italy) was applied to the suture line (Fig. 1).

In the postoperative follow-up, analgesia of 0.05 mL/day of meloxicam (Maxicam®; Sanovel, Istanbul, Turkey; 5 mg/ml) was applied subcutaneously with a 25 G syringe for 3 days. As a prophylactic antibiotic, 50 mg/kg of amoxicillin (Amoxycure LA®; Provet Veteriner Ürünleri A.Ş., Istanbul, Turkey; 150 mg) was applied intramuscularly with a 21 G syringe for 3 days.

The rats were checked daily by a veterinarian experienced in the field of laboratory animals and the cages were cleaned 4 times per week. In the 1st week after the 1st surgical procedure, 2 rats from Group 2 and 2 rats from Group 3 died; thus, the study continued with 10 animals in Group 1, 8 in Group 2, 8 in Group 3, and 6 in Group 4. At this stage the 32 rats were labeled C, M, D, and P + number, corresponding to Groups 1, 2, 3, and 4.

On the 90th day after the 1st surgical procedure, all the rats underwent claudication scoring and direct radiographs to check whether union had occurred. Two rats

were selected at random from each of Groups 2, 3 and 4 (M-4, M-5, D-1, D-2, P-2, P-5), and were euthanized with an anesthesia overdose (4 mL of 2.5% sodium pentothal, intraperitoneally) and the lower left extremity was amputated. A sample was taken from the pseudoarthrosis tissue and histopathological evaluation of the tissue confirmed the pseudoarthrosis model.

Second surgical intervention

With the exception of the control group, the 2nd surgical procedure was applied to the remaining 16 rats 90 days after the 1st surgery. With a longitudinal entry incision from the lateral femur, fibrotic tissues around the fracture were cleaned. The proximal and distal bone medulla was opened by rotating a 27 mm × 8 G hypodermic needle. In Group 2, MasterGraft Putty was prepared by wetting with sterile water, and then applied to encircle the pseudoarthrosis line 360°, according to the anatomy of the femur. Following the same steps, Debone was applied to Group 3 (Fig. 2). Saline solution only was applied to Group 4. Then the femur fractures of all rats were fixed with an intramedullar pin including 50–60% of the medulla. Finally, the layers were closed in order.

At 3 days before and 60 days after the 2nd procedure, clinical evaluations of all rats were conducted using a claudication scoring system that was developed for use in dogs and later adapted for other animals (Table 1).[6]

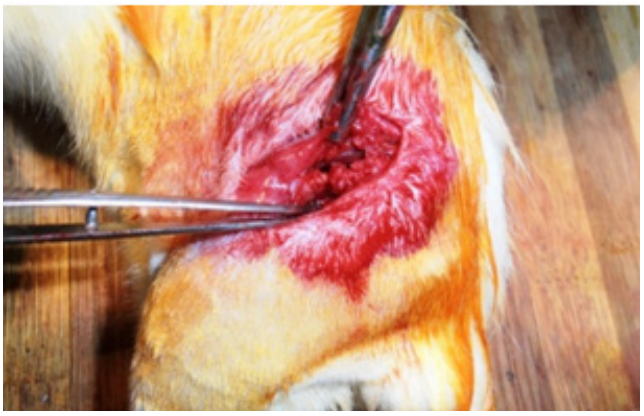

Fig. 1. First surgical procedure

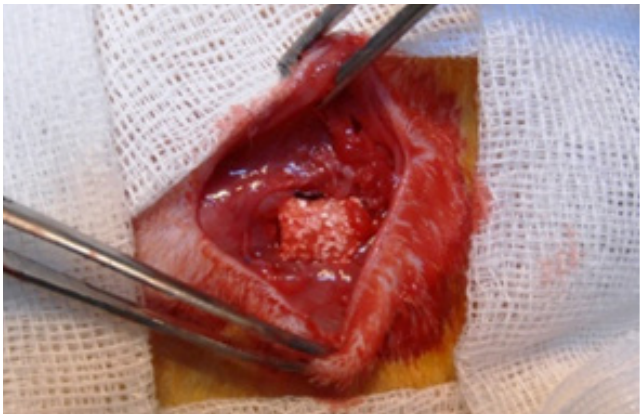

Fig. 2. Application of the graft during the 2nd surgical procedure

Table 1. Claudication scoring system

Degree	Criterion
1	absence of claudication, full limb support when the animal was in a standing position or during physical activities
2	mild claudication after exercise or prolonged decumbency
3	sporadic claudication when walking or running and weight relief on the operated limb, even in a standing position
4	constant claudication when walking and lack of limb support when running; incomplete support in the orthostatic position
5	full or absent support during physical activities or in a standing position

At 3 days before and 30 and 60 days after the 2nd surgical procedure, radiological evaluations of all rats were performed using x-rays, with modifications of a radiological scoring system that had previously been used on rat tibias.[7] For each rat the number of cortices showing union on anteroposterior and lateral radiographs was noted. The number of cortices showing union was defined as 0 = no union, 1 or 2 = partial union, and 3 or 4 = full union (Table 2).

Table 2. Radiological scoring system

Degree of union	Number of cortices showing union
Nonunion	0
Partial union	1 or 2
Union	3 or 4

Sixty days after the 2nd surgery, all the remaining rats were sacrificed using high-dose anesthesia, the lower left extremity was amputated and the intramedullar pins were removed. Samples were taken for histopathological examination from the osteotomized femur and the pseudoarthrosis tissue. The prepared materials were fixed in 10% formalin and then embedded in paraffin blocks. Sections 4 µm in thickness were cut from the blocks and stained with hematoxylin and eosin (HE). The sections were examined under a microscope and photomicrographs were obtained. The healing tissue in the fracture region was evaluated histopathologically using the scale recommended by Huo et al. (Table 3).[8]

Table 3. Histopathological evaluation scale recommended by Huo et al.[8]

Score	Histopathological features of healing tissue
1	fibrous tissue
2	fibrous tissue containing a small amount of cartilage
3	equal ratio of fibrous and cartilage tissue
4	cartilage tissue containing a small amount of fibrous tissue
5	cartilage tissue only
6	cartilage tissue containing a small amount of immature bone
7	equal ratios of cartilage and immature bone tissue
8	immature bone tissue containing a small amount of cartilage
9	immature bone tissue combined with fragments
10	mature bone tissue combined with fragments

Statistical analysis

The statistical analyses and calculations were carried out using SPSS v. 21.0 software (IBM Corp., Armonk, USA). The claudication and histopathological results obtained were stated as median (minimum–maximum) values and the radiology results were stated as numbers. The comparisons of the claudication and histopathological results of the 3 groups apart from the control group were made with the Kruskall-Wallis test. Paired comparisons of the groups were made with the Mann-Whitney U test with Bonferroni correction. The difference between the preoperative claudication results and the claudication results 60 days after the 2nd surgery within the groups was determined with the Wilcoxon test. For the radiology results, 10,000 repetitions of a Monte Carlo simulation of the Pearson's χ^2 test provided the result. To determine the origin of the difference, paired groups were compared using the same test. A value of $p < 0.05$ was considered statistically significant.

Results

After the 1st surgical procedure, a total of 4 rats – 2 from Group 2 and 2 from Group 3 – died because of anesthesia-related complications. These complications were consistent with the type and rate of complications published in previous studies by other laboratories.[9]

In Group 1, all the claudication results were evaluated as Grade 1. When the claudication results before the 2nd surgery were examined, all 22 rats in Groups 2, 3 and 4 were evaluated as median grade 3 (range: 2–5). No statistically significant differences were determined between these 3 groups in terms of the claudication scores before the 2nd surgical procedure ($\chi^2 = 0.095$, $p = 0.953$). The claudication results of 16 rats in all the groups 60 days after the 2nd surgical procedure were similar ($\chi^2 = 4.562$, $p = 0.102$).

In the radiological evaluation 90 days after the 1st operation, it was confirmed that pseudoarthrosis had occurred in the model used in the Group 2, 3 and 4 rats.

Radiological evaluations were performed on a total of 16 rats 30 and 60 days after the 2nd surgical procedure. No difference was observed between the groups in the 30-day postoperative results ($p = 0.116$). On the 60th postoperative day, in Group 2 full union was observed in 5 rats and partial union in 1 rat; in Group 3, full union was seen in 1 rat and partial union in 5 rats; in Group 4, full union was seen in 1 rat, partial union in 1 rat and non-union in 2 rats (Fig. 3). The rate of union in Group 2 was determined to be significantly higher than in Groups 3 and 4 ($p = 0.004$). Group 3 showed no superiority over Group 4.

The fact that bone union had not occurred was confirmed with histopathological evaluations of 6 rats – 2 each from Groups 2, 3 and 4 – sacrificed 90 days after the 1st surgery.

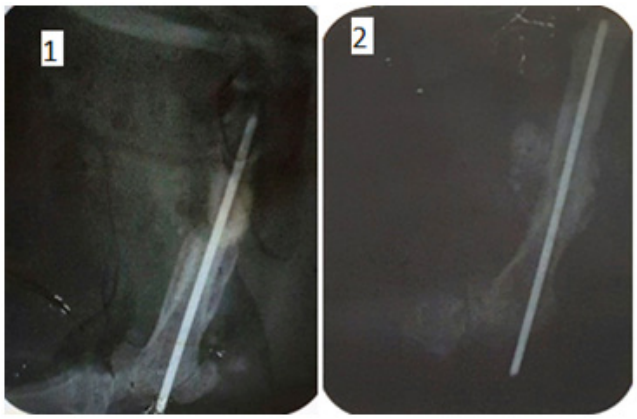

Fig. 3. 1 – the pseudoarthrosis line seen immediately after the 2nd surgical procedure; 2 – union of the fracture line using MasterGraft Putty seen at 60 days after the 2nd surgical procedure

On the 60th postoperative day, the histopathology results were determined as median 5.5 (range: 4–7) in Group 2, median 4.5 (range: 3–7) in Group 3 and median 3 (range: 1–4) in Group 4 (Fig. 4).

In the comparison of the groups according to the histopathological results, a significantly higher rate of union was found in Group 2 compared to Group 4 ($p < 0.05$). No statistically significant difference was determined between Group 3 and Groups 2 and 4 ($p > 0.05$).

Discussion

Although there is no consensus on which method is the best in the current surgical treatment of pseudoarthrosis, there are many treatment options. Various methods, such as vascularized bone graft, cancellous autograft, bone morphogenetic protein (BMP), transforming growth factor (TGF), ultrasound, shock waves, and electromagnetic fields are used to provide union.[10] Of these, composite synthetic grafts offer an alternative combining osteogenesis, osteoconduction and osteoinduction as potentially effective and controlled combinations without the disadvantages created by autograft, and many ceramic composites have been developed for this purpose.[11,12]

Wistar rats were selected for this study because their hind extremities contain a bone structure covered with a large muscle mass comparable to that in humans, which is resistant to infection and can be easily used because of its small size. Furthermore, the hypertrophic pseudoarthrosis model formed following femoral diaphyseal osteotomy has been observed to mimic human conditions at an appropriate level and rats have been proven to create a useful model for examination of the in vivo effects of locally placed osteoinductive agents in addition to intramedullary nailing.[13]

In studies of fracture healing in rats, different techniques have been used, such as internal fixation, external fixation and intramedullary nailing.[14,15] Although nailing is accepted as the gold standard treatment method in long bone

diaphyseal fractures, it is the callus formation resulting from micromovement in the osteotomy area that leads to fracture healing.[16] With the placement of osteoinductive agents, fracture healing in the osteotomy site can be misinterpreted as the presence of callus. In addition, the application of rigid fixation with plating is very difficult in rats.[13] Furthermore, the application of HA and tricalcium phosphate-based ceramics along with fixed plates or external fixators for segmentary losses in the long bones has been shown to prevent mechanical stimuli, which are necessary for healing of the defective area.[17,18]

In cases of bone defects or nonunion, successful results have been obtained with the use of osteoconductive scaffolds designed to support osteointegration with osteogenic substances.[19] When designing the ideal scaffold, the aim is to obtain the mechanical properties needed to support the fracture line with a particular 3-dimensional structure, an osteoconductive matrix suitable for osteogenic cells, and (instead of fusion) a rate of matrix resorption that will be compatible with progressive bone replacement. If the scaffold is not sufficiently robust, it cannot undertake the skeletal function in the defective area and the success of the graft will be reduced, with early or late resorption of the scaffold.[20]

Synthetic materials used to fill bone defects are HA, beta-tricalcium phosphate (β-TCP) or HA/β-TCP biphasic composite. As the resorption of HA takes 10 years, it is accepted as a non-resorbable substance. The solubility of β-TCP is very close to the mineral part of bone, is eroded with osteoclastic activity as in necrotic bones and is resorbed within 1 to 2 years in vivo. Biphasic calcium phosphate (BCP) is between HA and β-TCP in terms of the resorption rate. If there is a high ratio of β-TCP, then BCP is resorbed more quickly.[21]

The biocompatibility of ceramics used as grafts is very important to minimize complications that may develop in the future. Particles that emerge after the erosion of the biomaterials create inflammation and bone resorption as negative effects on the long-term success. Material debris <2 mm in size create osteolysis as a result of erosion, and these debris lead to a cellular reaction in the surrounding cytokines as a result of phagocytosis.[22] In the current study, although large and small HA and TCP particles that had broken off the ceramic wear were encountered, especially in the areas close to the K-wire and in sections close to the contact surface with the femur, no phagocytes were found in the examined sections. This shows the low capacity of the HA and TCP materials to form an inflammatory response.

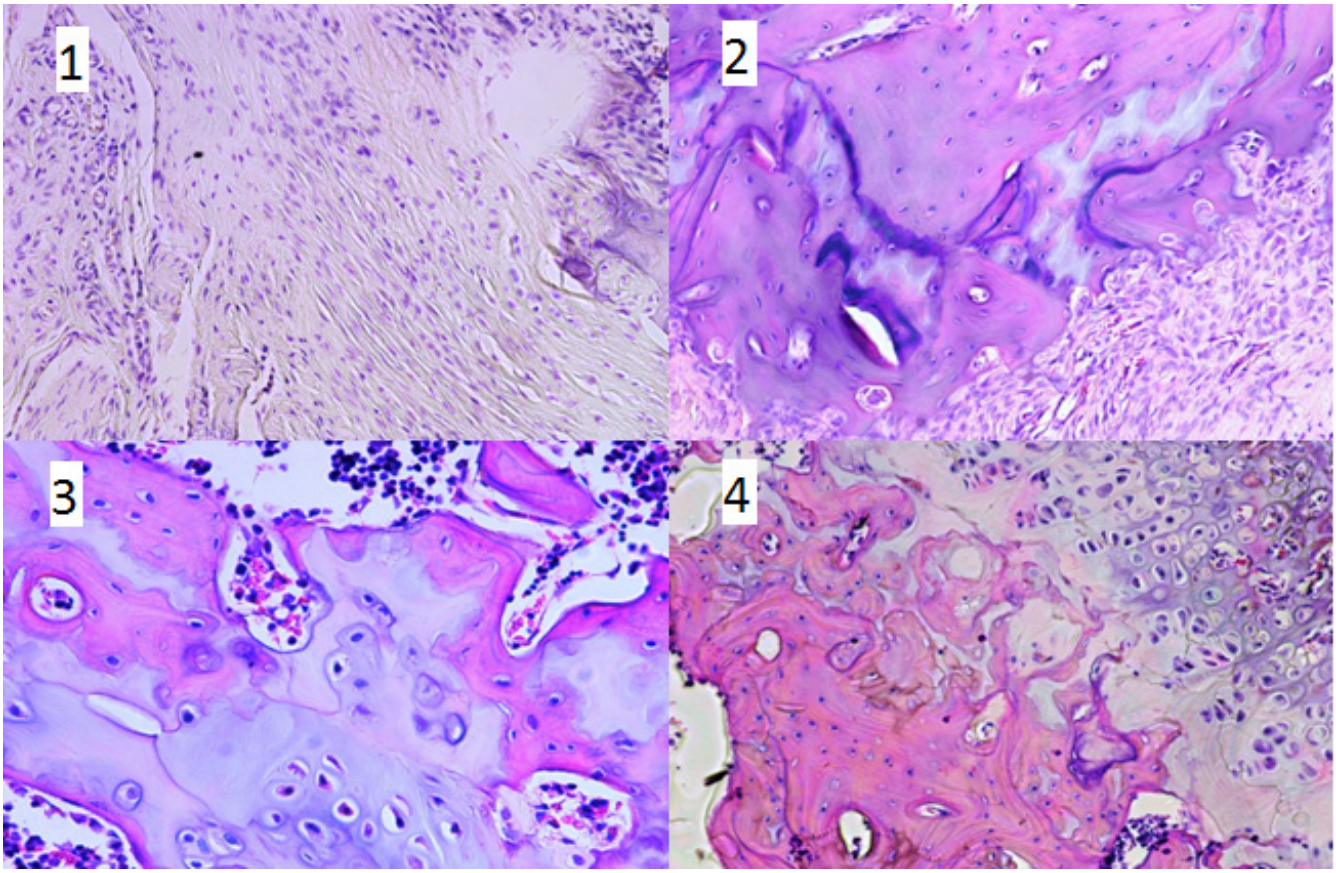

Fig. 4. 1 – photomicrograph of the femur pseudoarthrosis region (light microscope), fibrous tissue filling the healing line (histological score 1), hematoxylin and eosin (HE) staining, magnification ×400; 2 – photomicrograph of the femur pseudoarthrosis region (light microscope), cartilage tissue containing a small amount of fibrous tissue in the healing line (histological score 4), HE staining, magnification ×200; 3 – photomicrograph of the femur pseudoarthrosis region (light microscope), cartilage tissue containing a small amount of immature bone (histological score 6), HE staining, magnification ×200; 4 – photomicrograph of the femur pseudoarthrosis region (light microscope), bone and cartilage tissue filling the healing line (histological score 7), HE staining, magnification ×200

Type-1 collagen is an appropriate structure for the support, growth and matrix accumulation of several cell types and has been seen to have high biocompatibility with weak antigenicity. In addition, in bioreactors applied with moderate perfusion or hydrostatic fluid pressure, type-1 collagen has been shown to increase the histogenicity of cells in collagen sponges. Collagen-based biomaterials with calcium phosphate and HA as basic components have a long history in multiple clinical applications before they were used as bone graft materials.[23,24]

MasterGraft Putty is a biomaterial containing 85% β-TCP and 15% HA with type-1 collagen, the efficacy of which has been shown in spinal fusion in previous studies.[25] The biphasic structure provides a completely osteoconductive graft with a structure similar to that found naturally within the bone.[21,26] Debone is a biomaterial containing β-TCP with type-1 collagen that does not contain HA.

When the claudication results were evaluated in the current study, no difference was determined between the groups before the 2nd surgical procedure. In the evaluation conducted 60 days after the 2nd surgical procedure, although the claudication results of Group 2 were at a lower grade, the difference was not statistically significant. However, a statistically significant difference was determined between the preoperative and postoperative claudication scores in Group 2. In the other 2 groups, the differences between the preoperative and postoperative scores were not found to be statistically significant. As a result of this difference, the efficacy in Group 2 can be considered greater. In the radiological evaluation, no significant difference was determined between the groups 30 days after the 2nd surgical procedure, but in the evaluation on the 60th day, the rate of union in Group 2 was determined to be significantly higher than that of Groups 3 and 4. In the histopathological evaluation, the results in Group 2 were observed to be better than those in Group 3, and Group 3 was better than Group 4. However, statistically, only Group 2 was superior over Group 4.

When all these results were evaluated, the bone union in Group 2 was seen to be superior over that in Group 3. It was concluded that as Group 2 contained HA, unlike Group 3, this had an effect on the results. It was thought that the reason that there was no significant difference between the results in Group 3 and Group 4 was that Group 3 contained only β-TCP, which was quickly resorbed by the body.

In a study by Smucker et al. of a rabbit posterolateral fusion model with 3 groups – autograft, MasterGraft Putty 25/75 autograft and MasterGraft Putty 50/50 autograft – the results of the MasterGraft Putty 50/50 autograft group were no worse than those of the group where autograft only was used, and by some criteria obtained better results. It was recommended that the use of autograft could be reduced in this way.[25] In contrast, in a rabbit study by Miller et al. using 2 different ceramic grafts, it was reported that they made no significant contribution to the fusion rates compared to the use of autograft alone.[19]

Oryan et al. examined the effect on healing of a chitosan/gelatin/platelet gel enriched with TCP alone, HA alone or a TCP-HA mixture, in a radial bone defect created in rats. The best result was obtained in the graft enriched with the TCP-HA mixture, and it was reported that it could be used in place of autograft.[27]

There were some limitations to the current study. To examine the effects of collagen and bioceramics on fracture healing in more detail, a greater number of subjects are needed, and biomechanical and biochemical examinations should be added. Although animal models shed a significant amount of light on the subject, there is a need for further investigation of the biotechnology of these products in a clinical setting.

Conclusions

The results of this study showed that in a rat femur pseudoarthrosis model, MasterGraft Putty was effective in bone healing according to clinical, radiological and histopathological criteria, while Debone was not effective to the same degree. The ceramics used were seen to be biocompatible with bone cells. The application of long-term implants containing HA and β-TCP is promising. It can be concluded that with the support of bioelements which will provide an osteogenic contribution and by optimizing the resolution time with HA, ceramic composites have the potential to be used safely in the future for the healing of segmentary bone losses in place of autografts and allografts.

References

1. Greenwald AS, Boden SD, Goldberg VM, et al.Khan Y, Laurencin CT, Rosier RN; American Academy of Orthopaedic Surgeons; The Committee on Biological Implants. Bone-graft substitutes: fFacts, fictions, and applications. *JBJS. J Bone Joint Surg Am*. 2001;83-A(Suppl 2 Pt 2):S98–S103.
2. Gupta AR, Shah NR, Patel TC, et al. Perioperative and long-term complications of iliac crest bone graft harvesting for spinal surgery: A quantitative review of the literature. *Int Med J.* 2001;8(3):163–166.
3. Szpalski M, Gunzburg R. Applications of calcium phosphate-based cancellous bone void fillers in trauma surgery. *Orthopedics*. 2002;25(5 Suppl):S601–S609.
4. Shadjou N, Hasanzadeh M. Bone tissue engineering using silica-based mesoporous nanobiomaterials: Recent progress. *Mater Sci Eng C Mater Biol Appl*. 2015;55:401–409.
5. Ferreira ML, Silva PC, Pereira LdPM, et al. Experimental model in rats for the development of pseudoarthrosis [in Portuguese]. *Rev Col Bras Cir*. 2009;36(6):514–518.
6. Muzzi L, Rezende C, Muzzi R, et al. Ruptura do ligamento cruzado cranial em cães: fisiopatologia e diagnóstico. *Clin Vet*. 2003;46(1):32–42.
7. Schmidmaier G, Wildemann B, Melis B, et al. Development and characterization of a standard closed tibial fracture model in the rat. *European Journal of Trauma*. 2004;30(1):35–42.
8. Huo MH, Troiano NW, Pelker RR, Gundberg CM, Friedlaender GE. The influence of ibuprofen on fracture repair: Biomechanical, biochemical, histologic, and histomorphometric parameters in rats. *J Orthop Res*. 1991;9(3):383–390.
9. Green C, Knight J, Precious S, Simpkin S. Ketamine alone and combined with diazepam or xylazine in laboratory animals: a 10 year experience. *Lab Anim*. 1981;15(2):163–170.
10. Ferreira ML, Silva PC, Silva LHA, et al. Heterologous mesenchymal stem cells successfully treat femoral pseudarthrosis in rats. *J Transl Med*. 2012;10:51.

11. Friedenstein A, Piatetzky-Shapiro I, Petrakova K. Osteogenesis in transplants of bone marrow cells. *J Embryol Exp Morphol*. 1966;16(3):381–390.
12. Hoffmeister BK, Johnson DP, Janeski JA, et al. Ultrasonic characterization of human cancellous bone in vitro using three different apparent backscatter parameters in the frequency range 0.6–15.0 MHz. *IEEE Trans Ultrason Ferroelectr Freq Control*. 2008;55(7):1442–1452.
13. Russell G, Tucci M, Conflitti J, et al. Characterization of a femoral segmental nonunion model in laboratory rats: Report of a novel surgical technique. *J Invest Surg*. 2007;20(4):249–255.
14. Hietaniemi K, Peltonen J, Paavolainen P. An experimental model for non-union in rats. *Injury*. 1995;26(10):681–686.
15. Kokubu T, Hak DJ, Hazelwood SJ, Reddi AH. Development of an atrophic nonunion model and comparison to a closed healing fracture in rat femur. *J Orthop Res*. 2003;21(3):503–510.
16. Grundnes O, Reikerås O. Mechanical effects of function on bone healing: Nonweight bearing and exercise in osteotomized rats. *Acta Orthop Scand*. 1991;62(2):163–165.
17. Petite H, Viateau V, Bensaid W, et al. Tissue-engineered bone regeneration. *Nat Biotechnol*. 2000;18(9):959–963.
18. Tiedeman JJ, Connolly JF, Strates BS Lippiello L. Treatment of nonunion by percutaneous injection of bone marrow and demineralized bone matrix: An experimental study in dogs. *Clin Orthop Relat Res*.1991;268:294–302.
19. Miller CP, Jegede K, Essig D, et al. The efficacies of 2 ceramic bone graft extenders for promoting spinal fusion in a rabbit bone paucity model. *Spine (Phila Pa 1976)*. 2012;37(8):642–647.
20. Tang ZB, Cao JK, Wen N, et al. Posterolateral spinal fusion with nanohydroxyapatite–collagen/PLA composite and autologous adipose-derived mesenchymal stem cells in a rabbit model. *J Tissue Eng Regen Med*. 2012;6(4):325–336.
21. LeGeros RZ. Properties of osteoconductive biomaterials: Calcium phosphates. *Clin Orthop Relat Res*. 2002;395:81–98.
22. LeGeros RZ. Biodegradation and bioresorption of calcium phosphate ceramics. *Clin Mater*. 1993;14(1):65–88.
23. Glowacki J, Mizuno S. Collagen scaffolds for tissue engineering. *Biopolymers*. 2008;89(5):338–344.
24. Lee CH, Singla A, Lee Y. Biomedical applications of collagen. *Int J Pharm*. 2001;221(1–2):1–22.
25. Smucker JD, Petersen EB, Fredericks DC. Assessment of MASTERGRAFT PUTTY as a graft extender in a rabbit posterolateral fusion model. *Spine (Phila Pa 1976)*. 2012;37(12):1017–1021.
26. Kalfas IH. Principles of bone healing. *Neurosurg Focus*. 2001;10(4):E1.
27. Oryan A, Alidadi S, Bigham-Sadegh A, Meimandi-Parizi A. Chitosan/gelatin/platelet gel enriched by a combination of hydroxyapatite and beta-tricalcium phosphate in healing of a radial bone defect model in rat. *Int J Biol Macromol*. 2017;101:630–637.

The role of ultrasonography in the diagnostic criteria for rheumatoid arthritis and monitoring its therapeutic efficacy

Sławomir Jeka[1,A,D–F], Marta Dura[3,5,A,B], Paweł Zuchowski[2,A–D], Beata Zwierko[3,B], Marzena Waszczak-Jeka[4,B]

[1] Clinic of Rheumatology and Systemic Connective Tissue Disorders, Jan Biziel University Hospital No. 2, Ludwik Rydygier Collegium Medicum in Bydgoszcz, UMK in Toruń, Poland
[2] Clinic of Rheumatology and Systemic Connective Tissue Disorders, Jan Biziel University Hospital No. 2, Bydgoszcz, Poland
[3] Department of Radiology, Jan Biziel University Hospital No. 2, Bydgoszcz, Poland
[4] Centre for Clinical Trials, Warszawa, Poland
[5] Ludwik Rydygier Collegium Medicum in Bydgoszcz, Nicolaus Copernicus University, Toruń, Poland

A – research concept and design; B – collection and/or assembly of data; C – data analysis and interpretation;
D – writing the article; E – critical revision of the article; F – final approval of the article

Advances in Clinical and Experimental Medicine, ISSN 1899-5276 (print), ISSN 2451-2680 (online) *Adv Clin Exp Med*. 2018;27(9):1303–1307

Address for correspondence
Paweł Zuchowski
E-mail: p.zuchowski81@gmail.com

Funding sources
None declared

Conflict of interest
None declared

Received on December 28, 2016
Reviewed on January 25, 2017
Accepted on February 23, 2017

Abstract

Rheumatoid arthritis (RA) is a chronic systemic disease of connective tissue. It is characterized by symmetrical multiple joint involvement and extra-articular symptoms. Modern RA treatment methods place a particular emphasis on the earliest possible diagnosis and initiation of appropriate treatment. Currently, ultrasonography (US) is the key imaging test performed in RA patients. However, despite the general acknowledgement of its role in the assessment of disease activity, US was not included in the applicable ACR/EULAR criteria. This is due to the lack of strictly defined criteria for US evaluation and the interpretation of test results. In addition, the absence of a correlation between the common DAS/DAS28 disease activity score and ultrasound assessment of joints makes developing new diagnostic criteria difficult. The objective of this article is to review recent scientific reports on the use of ultrasonography in the diagnosis and monitoring of RA and to indicate current problems associated with the interpretation of test results and the comparison with applicable scores of disease activity.

Key words: rheumatoid arthritis, ultrasonography, synovitis

DOI
10.17219/acem/69133

Introduction

Rheumatoid arthritis (RA) is a chronic systemic disease of connective tissue. The most characteristic symptom of RA is non-specific inflammation of symmetric joints. In early rheumatoid arthritis (ERA), inflammatory lesions usually affect the joints of the hands and feet. Currently, it is believed that inflammation of the joint synovial membrane is the most valid indicator of the course of the disease.

Nowadays, RA treatment methods focus on the earliest possible diagnosis and initiation of appropriate treatment. Treatment is aimed at reducing pain and improving the patient's quality of life by minimizing or completely blocking inflammatory processes in the joint synovium. Such therapy delays radiological progression, i.e., joint damage, and thus prevents the patient's disability level from worsening.

The earlier effective treatment is initiated, the better the prognosis. Unfortunately, early RA diagnosis is challenging due to its non-specific onset.

The 2010 American College of Rheumatology/European League Against Rheumatism criteria (ACR/EULAR) for RA currently in use are much more sensitive and specific than the previous 1987 version. However, they still cannot be considered complete as further amendments may be anticipated. The sensitivity of the current classification criteria is between 58% and 91% in patients with RA lasting for less than 2 years.[1] However, the detectability of RA in cases of shorter disease duration is much lower. In patients with RA lasting for less than 3 months (which can be considered ERA), the sensitivity is 62–74%.[1] Consequently, 1 in 4 ERA patients remains undiagnosed during the 1st few weeks of the disease. As a result, treatment initiation is delayed, and the patient's chances for maintaining full physical function and achieving sustained remission are lower.

Delayed treatment is also associated with poorer prognosis and a higher risk of complications. The most common consequences of delaying therapy include joint damage, a higher risk of orthopedic surgery at a further stage of the disease, multiple organ complications, and increased mortality.

Although it is hard to prove that there is indeed such a window of opportunity, it is certain that early RA diagnosis and administration of appropriate treatment with synthetic disease-modifying antirheumatic drugs (sDMARDs) and biological DMARDs (bDMARDs) increase the chances of remission.[2,3]

Consequently, the improvement of the current RA classification criteria to increase diagnostic sensitivity to early RA is crucial.

Imaging diagnostics

According to many rheumatologists and radiologists, modern imaging diagnostic tests, i.e., ultrasonography (US) and magnetic resonance imaging (MRI), are particularly significant for RA diagnostics. In the case of ERA, the diagnostic applicability of X-rays is much lower.

Of course, X-rays were included in the RA classification criteria as early as the Rome 1961 criteria.[4] Obviously, this should be considered in the historical context, as until the 1990s, US and MRI tests were relatively novel imaging techniques and the image quality they offered was inferior to that obtained today. For the same reason, the revised 1987 RA classification criteria did not take the methods into account either.[4]

Only during the last 20 years has a remarkable change taken place in the recognition of imaging tests as a diagnostic tool. Significant developments with respect to US, MRI, and computed tomography (CT) have granted imaging diagnostics a prominent position in rheumatology.

Computed tomography is not commonly used despite the fact that it is especially useful for bone lesion imaging.[5] This is due to the high amount of ionizing radiation the patients are exposed to during the test.

Magnetic resonance imaging, because of its long duration and high costs, has not become a basic RA diagnostic tool either. However, it is performed much more frequently than CT and its spectrum of applicability to RA diagnostics is broad.[6,7]

Ultrasonography is the basic imaging test used in RA diagnostics. In contrast to MRI, it is easily accessible and cost-effective.

Ultrasonography: The current status

Over the last few decades, US has gradually become more and more significant in RA diagnostics, which resulted in the establishment of the OMERACT initiative in 2004.[5,8] The objective of this group is to define RA diagnostic criteria in US tests. Although the initiative has existed for many years, no consensus or consistent principles on assessing US results in RA patients have been developed, and no decision on which joints should be evaluated has been made.[5,8]

Discrepancies in the evaluation of US findings resulted in the technique being omitted from the latest 2010 ACR/EULAR criteria. However, it should be emphasized that both ACR and EULAR recognize the significance of US in ERA and RA diagnosis and that neither of the organizations question its applicability. They established expert teams in order to work on introducing US to future RA classification criteria.

Despite the fact that US is not currently included either in the classification criteria or in standard disease activity scores or therapeutic efficacy measures – such as DAS/DAS28 – it is commonly performed by rheumatologists.[9]

Ultrasonography with a high-frequency (15–18 MHz) linear array transducer probe enables the assessment of early lesions in small joints and the detection of inflammatory changes in the synovial membrane.

Table 1. Joint inflammation assessment based on PDUS[10]

Grade	Description
0	normal (no PD signal)
1	mild hyperaemia (PD signal covers up to 25% of the synovium)
2	moderate hyperaemia (PD signal covers from >25% up to 50% of the synovium)
3	marked hyperaemia (PD signal covers more than 50% of the synovium)

PDUS – power Doppler ultrasonography.

Where power Doppler ultrasonography (PDUS) is used, blood flow within the joint synovium can be assessed, and consequently, inflammatory processes can be observed and evaluated (Table 1).[10]

Ultrasonography: Diagnostic challenges

Despite its broad use in RA diagnosis and monitoring, US poses a number of problems. Apart from the lack of consensus on which joints should be evaluated, the subjectivity inherent in US interpretation cannot be disregarded.

Erosions are one of the most common symptoms associated with RA, apart from synovitis, which can be observed in US. The prevention of erosions is one of the aims of RA treatment. Their development in RA patients is considered an indicator of poor prognosis for the further course of the disease. Consequently, their detection and on-treatment assessment may have a significant impact on decisions concerning therapy.

The correct assessment of erosions in US is not always unambiguous. The minimum size of an erosion is currently a topic of debate.[5] Along with the higher frequencies provided by transducers, images of increasingly higher resolutions can be obtained. This means that smaller structures can be visualized, which may lead to an overdiagnosis of erosions. Recent studies demonstrate that erosion-like lesions may also be detected in healthy individuals.[11] As a result, a minimum erosion size would be an essential criterion in the diagnostic process. Currently, it is believed that the minimum size should be at least 2 mm.[5]

The monitoring of erosion changes over the course of the disease is also a problem. Unfortunately, the simplest solution in this case, i.e., counting the erosions, is not a valid criterion for the assessment of disease progression.[5] With such an approach, cases involving the merging of 2 erosions can be challenging. In addition, the assessment of erosion activity by PDUS is necessary.

Researchers agree as to which joints should be included in erosion assessment. The metacarpophalangeal joints (MCP) and the metatarsophalangeal joints (MTP) have been suggested for assessment.[5]

Apart from erosions, synovitis is the most characteristic sign of RA. Its assessability through US/PDUS is one of the main reasons for the common use of ultrasonography in monitoring disease progression.

Many scientific and clinical studies have evaluated the efficacy of methotrexate monotherapy (MTX) or a combination therapy with MTX + anti-TNF inhibitors or biologics with a different mechanism of action, based not only on the activity scores (DAS/DAS28) but also on synovitis.

One of the reasons why such an emphasis is put on introducing US/PDUS to treatment efficacy assessment is the fact that remission with respect to DAS/DAS28 has been observed in patients despite the presence of synovitis and the resulting progression of radiological changes.[12,13]

Power Doppler ultrasonography enables the blood flow in the synovium of small joints in the hands and feet to be assessed. There is a correlation between PDUS results and laboratory test findings.[14] In addition, the sensitivity of PDUS is higher than that of physical examination.[14]

Novel treatment options, i.e., biologics, entail modifications not only in the modality of therapy, but also in the monitoring of its effects. Targeted treatment (treat-to-target, T2T) and recent EULAR guidelines recommend changing the treatment strategy after 3 months if the therapy proves ineffective or after 6 months if the treatment target has not been reached.[15–17] Such an approach to treatment also requires adopting a new approach to the assessment of its efficacy. In line with the current knowledge of the essence of RA as a disease causing inflammation of the synovial membrane, its assessment in PDUS should be best suited to reflect the efficacy of the therapy.

RA activity assessment on the basis of PDUS and DAS: Differences

DAS was developed with a view to assessing ERA patients.[18] At present, it is a standard score used in patients with RA lasting for many years. At the time of its development, imaging tests (US, CT and MRI) did not provide images of such a high quality as the ones available today. For this reason, DAS authors did not even consider including imaging diagnostics in the score.

Most commonly, over the course of RA, irreversible destructive joint lesions develop. In such cases, joint pain is no longer associated with disease activity. In this situation, despite improvements in the patient's health and the absence of synovitis in US/PDUS results, according to DAS still no remission occurs. This is connected with the significant impact of the number of tender joints on the total DAS result.[18] On the other hand, situations have been reported where US/PDUS scores indicate the presence of inflammation in joints which presents no symptoms in the physical examination, i.e., the patient does not feel pain and the assessing physician does not find any evidence of joint swelling.

Owing to the above situations, US/PDUS tests are not an appropriate representation of changes in DAS, which has been confirmed in scientific and clinical studies.

In a study conducted with the participation of 102 patients in remission (DAS28 <2.6), a 1-year progression in radiological changes detected in PDUS and MRI was confirmed in 19 patients (19%).[13]

In another study with 149 subjects, no positive correlation between the currently applicable remission criteria (ACR/EULAR 2010) and PDUS results was demonstrated.[19] In almost every other patient who met the remission criteria, PDUS scores confirmed the presence of synovitis.[19] A group of patients with no synovitis revealed in PDUS was also large despite the fact that they were not in remission according to the currently applicable criteria.[19] From among the parameters taken into consideration in the 2010 ACR/EULAR remission criteria, only C-reactive protein (CRP) and morning stiffness duration were correlated with the US/PDUS findings.[19] According to the authors, the parameters included in the assessment criteria for disease activity are often very subjective, which makes it difficult to achieve a correlation with US/PDUS results characterized by higher objectivity and repeatability.[19]

Saleem et al. suggest that currently DAS28 is not the best measure of remission assessment.[20] A DAS28 of <2.6 does not exclude the presence of tender and swollen joints or increased CRP and erythrocyte sedimentation rate (ESR) values, although it represents remission. Their study enrolled 128 patients in remission (DAS28 < 2.6) in whom no flare-ups had been observed during 6 months preceding the study enrolment and treatment had not been modified during that period. The patients received DMARDs (n = 66) or MTX + anti-TNF (n = 62). In 40 patients (31%), physical examination revealed the swelling of at least one joint although these patients were in DAS28 remission.[20] Based on PDUS scores, these patients were diagnosed with synovitis. PDUS results were much better correlated with the clinical assessment based on the Simplified Disease Activity Score (SDAI).[20] The authors suggest that the current remission criteria are more indicative of low disease activity than actual remission, and would better correlate with a US/PDUS test if the criteria were more restrictive.[20]

An interesting analysis of US applicability in remission assessment in RA patients was performed by Balsa et al.[21] They studied a group of 97 patients who received treatment with DMARDs or biologics. Remission was assessed using the 2 most common scores: the DAS28 and the SDAI. In addition, US/PDUS of 42 joints (proximal interphalangeal joints, MCPs, radiocarpal joints, radioulnar joints, glenohumeral joints, knee joints, ankle joints, metatarsal joints and MTPs) was performed. The joints' ultrasound evaluation was performed on the basis of the OMERACT score. In the study group, synovial overgrowth was found in 92 patients (95%), whereas a PD signal was observed in the case of 41 individuals (42%). DAS28 remission was confirmed in 74 subjects (76%), while according to SDAI criteria, remission was confirmed in 54 patients (56%). As compared with US findings, SDAI remission assessment is more accurate than that based on the DAS28. The study demonstrated that both SDAI and DAS28 scores render similar results in patients with active disease, whereas in the case of remission, significant discrepancies between the 2 measures can be observed.[21]

The APPRAISE study conclusions completely undermine the reasonability of comparing the results of US/PDUS with the DAS28.[15] This study enrolled biologic-naive patients with insufficient improvement from MTX therapy. During this 24-week study, abatacept was administered to all patients. During the study, PDUS tests of 44 joints and DAS28 assessment were performed in patients on a regular basis. PDUS results were assessed using the Global OMERACT-EULAR Synovitis Score (GLOESS). At the completion of the study, a total absence of correlation between disease activity assessments with PDUS and the DAS28 was demonstrated.[15]

These observations are consistent with previously presented studies, and they also suggest a higher correlation between PDUS and SDAI findings.[15]

The authors explain the lack of consistency between PDUS and the DAS28 by the fact that PDUS enables the detection of much smaller lesions than is possible with joint physical examination.[15]

The thesis seems to be confirmed by another study in which PDUS results were compared with the Clinical Disease Activity Index (CDAI) scores. A strong correlation was revealed only with respect to grade 3 synovitis on the basis of PDUS and CDAI evaluations.[22]

PDUS-assessed joints

In clinical practice, PDUS with multiple joints assessment is rarely performed due to timing considerations.[23] Usually, even 6-joint evaluation may pose a significant challenge due to the duration of the patients' visits. Consequently, doctors search for joints in which inflammatory lesions would be most reflective of the course of RA. Grassi et al. suggest that assessing a single joint may be sufficient for the assessment of disease activity and therapeutic efficacy.[23] According to them, MCP lesions are most indicative of the disease status.

Considering the discrepancies with regard to the number of joints assessed by individual researchers, attention should be paid to the results of the study conducted by Yoshimi et al.[24] They demonstrated that changing the number of assessed joints (24 or 8) did not have a significant impact on the assessment of RA activity.

It suggests that RA activity assessment does not, in fact, require a comprehensive US/PDUS test and that assessing only a few joints provides accurate disease status results.

Conclusions and future considerations

The results of recent studies show that both US/PDUS and the DAS/DAS28 are valid indicators of the patient's health improvements. However, looking for a correlation between them is wrong, as they reflect different aspects of the disease.[15] SDAI and CDAI scores are much better correlated with US/PDUS than DAS28 due to their higher objectivity, since the health status is assessed by the physician.

PDUS signal assessment depends on the operator. If the pressure of the transducer probe on the evaluated joint is excessive, the values can be easily distorted.[18] For this reason, training courses for operators need to be introduced in order to improve the quality of the testing.[25] Certainly, skilful test performance should not be particularly difficult; therefore, the issue is not likely to be an obstacle in the introduction of PDUS to the classification criteria.[19]

The advances in imaging diagnostics seen over the last 2 decades have had a significant impact on RA patient management. Currently, treatment without CT, MRI, or US is hard to imagine. Among these tests, US has become the most popular one because of its low costs and short duration of testing.

At present, the value of US/PDUS, both in diagnostics and in the monitoring of therapeutic efficacy, is indisputable. There is a shared conviction that the test should be introduced to the classification criteria. However, despite the publication of the results of many studies, the number of joints which need to be assessed is still being discussed. Comparing PDUS scores with the DAS, which was developed almost 40 years ago and has not changed much since then, can also be challenging. Recently, authors have been indicating that according to the current knowledge, DAS is not a correct measure of the disease and that juxtaposing it with US/PDUS synovial assessment is pointless.[15]

Potentially, US/PDUS and DAS/DAS28 scores should be no longer compared. Applicability of US is generally acknowledged, and discrepancies between the test results and the DAS/DAS28 assessment are well documented. At present, more attention should be paid to selecting joints for assessment as part of routine rheumatologic examinations and to developing clear criteria for the evaluation of joints.

References

1. Migliore A, Bizzi E, Petrella L, et al. The challenge of treating early-stage rheumatoid arthritis: The contribution of mixed treatment comparison to choosing appropriate biologic agents. *BioDrugs*. 2016; 30:105–115.
2. van Nies JA, Tsonaka R, Gaujoux-Viala C, et al. Evaluating relationships between symptom duration and persistence of rheumatoid arthritis: Does a window of opportunity exist? Results on the Leiden early arthritis clinic and ESPOIR cohorts. *Ann Rheum Dis*. 2015;74:806–812.
3. Świerkot J, Batko B, ed. *Reumatoidalne zapalenie stawów: praktyczne aspekty leczenia.* 1st ed. Poznań, Poland: Termedia Wydawnictwa Medyczne; 2016.
4. Arnett FC, Edworthy SM, Bloch DA, et al. The American Rheumatism Association 1987 revised criteria for the classification of rheumatoid arthritis. *Arthritis Rheum*. 1988;31:315–324.
5. Szkudlarek M, Terslev L, Wakefield RJ, et al. Summary findings of a systematic literature review of the ultrasound assessment of bone erosions in rheumatoid arthritis. *J Rheumatol*. 2016;43:12–21.
6. Boutry N, Morel M, Flipo RM, et al. Early rheumatoid arthritis: A review of MRI and sonographic findings. *Am J Roentgenol*. 2007;189: 1502–1509.
7. Piotto DG, Correa MJ, Miotto e Silva VB, et al. Laser Doppler imaging for assessment of microcirculation in juvenile systemic sclerosis. *Rheumatology (Oxford)*. 2014;53:72–75.
8. Naredo E, Wakefield RJ, Iagnocco A, et al. The OMERACT ultrasound task force-status and perspectives. *J Rheumatol*. 2011;38:2063–2067.
9. Naredo E, Iagnocco A. Why use ultrasound in rheumatology? *Rheumatology (Oxford)*. 2012;51(Suppl 7):vii1.
10. Fiocco U, Ferro F, Vezzù M, et al. Rheumatoid and psoriatic knee synovitis: Clinical, grey scale, and power Doppler ultrasound assessment of the response to etanercept. *Ann Rheum Dis*. 2005;64:899–905.
11. Finzel S, Ohrndorf S, Englbrecht M, et al. A detailed comparative study of high-resolution ultrasound and micro-computed tomography for detection of arthritic bone erosions. *Arthritis Rheum*. 2011;63: 1231–1236.
12. Brown AK, Quinn MA, Karim Z, et al. Presence of significant synovitis in rheumatoid arthritis patients with disease modifying antirheumatic drug-induced clinical remission: Evidence from an imaging study may explain structural progression. *Arthritis Rheum*. 2006;54: 3761–3773.
13. Brown AK, Conaghan PG, Karim Z, et al. An explanation for the apparent dissociation between clinical remission and continued structural deterioration in rheumatoid arthritis. *Arthritis Rheum*. 2008;58: 2958–2967.
14. Sreerangaiah D, Grayer M, Fisher BA, et al. Quantitative power Doppler ultrasound measures of peripheral joint synovitis in poor prognosis early rheumatoid arthritis predict radiographic progression. *Rheumatology (Oxford)*. 2016;55:89–93.
15. D'Agostino MA, Boers M, Wakefield RJ, et al. Exploring a new ultrasound score as a clinical predictive tool in patients with rheumatoid arthritis starting abatacept: Results from the APPRAISE study. *RMD Open*. 2016;5,2:e000237.
16. Smolen JS, Aletaha D, Bijlsma JW, et al. Treating rheumatoid arthritis to target: Recommendations of an international task force. *Ann Rheum Dis*. 2010;69:631–637.
17. Smolen JS, Breedveld FC, Burmester GR, et al. Treating rheumatoid arthritis to target: 2014 update of the recommendations of an international task force. *Ann Rheum Dis*. 2016;75:3–15.
18. Barczyńska TA, Dura M, Blumfield E, et al. DAS28 score vs ultrasound examination for assessment of rheumatoid arthritis disease activity: Comparison and discussion of pros and cons. *Reumatologia*. 2015; 4:213–218.
19. Dejaco C, Duftner C, Wipfler-Freissmuth E, et al. Ultrasound-defined remission and active disease in rheumatoid arthritis: Association with clinical and serologic parameters. *Semin Arthritis Rheum*. 2012;41: 761–767.
20. Saleem B, Brown AK, Keen H, et al. Should imaging be a component of rheumatoid arthritis remission criteria? A comparison between traditional and modified composite remission scores and imaging assessments. *Ann Rheum Dis*. 2011;70:792–798.
21. Balsa A, de Miguel E, Castillo C, et al. Superiority of SDAI over DAS-28 in assessment of remission in rheumatoid arthritis patients using power Doppler ultrasonography as a gold standard. *Rheumatology (Oxford)*. 2010;49:683–690.
22. Gärtner M, Mandl P, Radner H, et al. Sonographic joint assessment in rheumatoid arthritis: Associations with clinical joint assessment during a state of remission. *Arthritis Rheum*. 2013;65:2005–2014.
23. Grassi W, Gaywood I, Pande I, et al. From DAS 28 to SAS 1. *Clin Exp Rheumatol*. 2012;30:649–651.
24. Yoshimi R, Ihata A, Kunishita Y, et al. A novel 8-joint ultrasound score is useful in daily practice for rheumatoid arthritis. *Mod Rheumatol*. 2015;25:379–385.

Increasing beta cell mass to treat diabetes mellitus

Shakila Sabir[1,A,B,D,F], Ammara Saleem[1,A,E,F], Muhammad Furqan Akhtar[1,A,B,D,F], Muhammad Saleem[1,A,E,F], Moosa Raza[2,A,E,F]

[1] Faculty of Pharmaceutical Sciences, Government College University Faisalabad, Pakistan
[2] Faculty of Pharmacy, University of Lahore, Pakistan

A – research concept and design; B – collection and/or assembly of data; C – data analysis and interpretation; D – writing the article; E – critical revision of the article; F – final approval of the article

Advances in Clinical and Experimental Medicine, ISSN 1899-5276 (print), ISSN 2451-2680 (online) *Adv Clin Exp Med*. 2018;27(9):1309–1315

Address for correspondence
Muhammad Furqan Akhtar
E-mail: furqan.pharmacist@gmail.com

Funding sources
None declared

Conflict of interest
None declared

Received on March 8, 2017
Reviewed on May 17, 2017
Accepted on June 6, 2017

Abstract

Finding a radical cure for diabetes has reached paramount importance in medicine due to the widespread prevalence of the disease. A substantial reduction in insulin-secreting beta cells is evident in diabetes. The failure of cyclin-dependent kinases (CDKs) and cyclins to access the nucleus is responsible for quiescence or senescence in human and rodent beta cells. The augmentation of beta cell proliferation is supposed to reverse diabetes. This concept has inspired the discovery of newer drugs that encourage the proliferation of beta cells. Although it is a rational step towards a cure for diabetes, the differences in biochemical pathways in rodents and human beta cells pose difficulty in promoting the proliferation of human beta cells. Primarily, it is mandatory to clearly understand the intracellular pathways involved in the proliferation of beta cells so as to pave the way for therapeutic interventions. There are several intrinsic factors that trigger the proliferation of beta cells. Furthermore, it is also obvious that the early death of beta cells due to oxidative stress-related upregulation of pro-apoptotic genes also predisposes individuals to diabetes mellitus. Polyphenols, exendin 4, histone deacetylase inhibitors, glucagon-like peptide 1, phenyl pyruvic acid glucoside, and several flavonoids reduce the early apoptosis of beta cells partly through their role in the reduction of oxidative stress. A better understanding of intracellular pathways, the identification of specific mitogens, the induction of beta cell proliferation, and the inhibition of apoptosis may help us treat diabetes mellitus through an increase in beta cell mass.

Key words: diabetes mellitus, apoptosis, cell proliferation, rodent beta cells, human beta cells

DOI
10.17219/acem/74452

Introduction

There is a pronounced rise in the prevalence of diabetes mellitus around the world. The number of diabetic patients is expected to rise to 300 million globally by 2030.[1] Diabetes mellitus is a chronic metabolic abnormality characterized by persistent hyperglycemia. There are 2 main types of this disease: type 1 diabetes mellitus (DMT1) and type 2 diabetes mellitus (DMT2). DMT1 emerges from autoimmune reactions that result in the destruction of beta cells.[2] DMT2 is a chronic ailment. An unhealthy diet and a sedentary lifestyle are the prime risk factors for DMT2. Other risk factors include obesity, reduced physical activity, and a genetic predisposition.[3] DMT2 results from either a reduction in the secretion of and/or an emergence of resistance to insulin in the body.[4] The autoimmune destruction of beta cells is accountable for the decline in insulin secretion. Beta cells are mostly found in the islet; however, they make up only about 2% of the pancreas. Beta cells are highly susceptible to hyperglycemia and become dysfunctional or even damaged by glucotoxicity.[5]

The damage to beta cells is further aggravated by a high-fat diet, resulting in lipotoxicity. An autopsied pancreas model from DMT2 subjects revealed a 30% decline in the number of beta cells in DMT2 individuals compared to healthy adults.[6] The decrease in beta cells contributes to an increased death rate. Transplantation of the pancreas and beta cell replacement therapy have been investigated for the cure of DMT2. Although very promising, these procedures pose some serious obstacles and offer a limited scope of implementation.[7] Another promising approach for the treatment of diabetes is to enhance the proliferation of beta cells through drugs. Table 1 shows the advantages and disadvantages of pancreas transplantation and beta cell replacement therapy.

Another approach in treating diabetes is to increase beta cell mass. However, the induction of beta cell proliferation was not possible in the past. Several studies have been carried out in the past decade, making it feasible thanks to an improved understanding of intracellular pathways.[8] Adult human beta cells have an incredibly low rate of proliferation (about 1%). There is a lack of specific mitogens that induce the proliferation of only beta cells without inducing generalized proliferation. The proliferation of certain growth factors may pose a risk of oncogenesis through the stimulation of undesired proliferation.[9] In this review, we discuss the advancements and hindrances in the proliferation of beta cells. This review also highlights several factors that trigger the proliferation and inhibit the apoptosis of beta cells.

Table 1. Comparison of modern curative approaches to treating diabetes

Pancreatic islets transplant	Replacement of beta cell
Advantages: – independence of insulin – decrease in secondary complications – prevention of hypoglycemia	Advantages: – independent of insulin – less invasive – abundant supply of beta cells – simple therapy
Disadvantages: – shortage of donors – auto-immunity – allo-immunity – toxicity of immunosuppressive drugs	Disadvantages: – functionally immature beta cells – poor response to glucose – risk of cancer – ethical considerations – autoimmunity – poor quality control

Cell cycle cascade

Human beta cells contain cyclin-dependent kinases (CDKs) and transcription factors (E2F). These molecules, like most adult cells, direct the entry of beta cells into the cell cycle. On the other hand, beta cells also exhibit several factors that resist the entry of beta cells into the cell cycle, such as CDK inhibitors and pocket proteins (i.e., p107, p130, and pRb).[10,11] Mitogenic stimuli do not result in the proliferation of beta cells due to the inhibitory factors of the cell cycle. However, the overexpression of the positive factors directs the progression of beta cells in the cell cycle.[12] The reversal of diabetes in diabetic mice was more pronounced in mice transplanted with human islets overexpressing cyclins and CDKs than those transplanted with normal human islets.[13] It has also been found that the shRNA system of lentivirus silences cell cycle inhibitor p57KIP2, and thus allows entry into the cell cycle.[8] Moreover, mutations in cell cycle inhibitor and tumor suppressor genes may render them inoperative and may culminate in the hyperplasia of endocrine cells.[14]

Cell cycle-associated molecules are usually located in the nucleus of cells. However, human beta cells, contain more G1 and S molecules in the cytoplasm rather than the nucleus, as observed by subcellular fractionation and immunocytochemistry studies. The overexpression and movement of cyclins, CDKs, and cell cycle inhibitors – and their movement inside and outside the nucleus – contribute to the induction of beta cell replication, as confirmed by static immunocytochemistry and CDK-tagged live cells. Beta cells in rats also exhibit similar processes. For instance, CDK2 is abundantly found in the cytoplasm of non-proliferating rodent beta cells; however, it is located in the nucleus of proliferating insulinoma cells.[10] Therefore, it can be inferred that the failure of CDKs and cyclins to access the nucleus is responsible for the quiescence or senescence in human and rodent beta cells.

Intracellular signaling pathways

Pancreatic beta cells have all the necessary cell cycle molecules that play a pivotal role in the proliferation of beta cells. However, the response of cell cycle machinery to mitogens is yet unclear. There is a need to further explore the exact cell signaling pathways so as to assess the reason for

the nonproliferation of beta cells in response to growth factors and to some particular nutrients capable of inducing proliferation.[15] This knowledge gap may be attributed to the complexity of methods of isolating and refining human beta cells and difficulties in their long-term preservation. The activation of protein kinase B, protein kinase C, or intracellular Ca^{2+} by gamma-aminobutyric acid or glucose induces the proliferation of human beta cells.[16] The inhibition of glycogen synthase kinase 3 (GSK3) also induces proliferation.[17] Some studies have revealed other signaling pathways involved in the proliferation of beta cells, such as the PI3K and IRS2 signaling pathways, activated by insulin or IGFs, and the MAP-kinase signaling pathway, activated by PDGF.[18] Several efforts have been made to manipulate the signaling molecules for the induction of beta cell proliferation. However, the ultimate rate of proliferation was insignificant. For instance, lithium-induced inhibition of GSK3β increased the rate of proliferation up to threefold; however, the ultimate changes were insignificant, increasing from 0.17% to 0.71%.[17] On the whole, it can be assumed that the mitogenic signaling pathways are difficult to ameliorate and the currently-known mitogens exhibit only a weak effect on the activation of the cell cycle.

Human and rodent beta cells

Rodent and mammalian beta cells share the broad principles of beta cell biology. Rodent beta cells, therefore, have been extensively investigated.[19] Human and rodent beta cells show marked differences in cell function and patterns of gene expression owing to diverse metabolic and nutritional demands. For instance, GLUT-2 is a chief glucose transporter in rodent beta cells; however, GLUT-1 performs this function in humans.[20] Rodents exhibit 2 insulin genes – *Ins1* and *Ins2* – whereas humans have only one insulin gene (*INS*). An absolute congenital loss of beta cells and, ultimately, neonatal diabetes arises due to mutations in *NEUROG3* (which encodes the transcription factor neurogenin 3) in rodents. In humans, these mutations are linked to malabsorption and diarrhea due to damaged enteroendocrine cells.[21] These mutations have variable effects on beta cell function and contribute to congenital diabetes and an altered response to hyperglycemia in adults. It is further revealed that NEUROG3 is not critical for the proliferation of human beta cells.[22] MAFB (a transcription factor) is present in human beta cells and absent in rodents.[23] Table 2 shows the differences in rodent and human beta cells due to which both species respond differently to different mitogens.

The islets of Langerhans house 80% of the beta cells in rodents and make up the islet core. However, these islets in humans contain only 50% beta cells scattered throughout the islets. There is also a significant difference in beta cell proliferation in both species. Beta cells proliferate at a maximum rate of 2% at any point throughout human life.[24,25]

Table 2. Differences in human and rodent beta cells

Parameter	Human	Rodent
Major glucose transporter	GLUT-1	GLUT-2
Insulin gene	INS	Ins1, Ins2
NEUROG3	non-essential	essential
MAFB (transcription factor)	present	absent
β cells in islets	50%	80%
Position of β cells in islets	scattered	make up the core
Proliferation at any point during life	2%	10–30%

GLUT-1 – glucose transporter type 1; GLUT-2 – glucose transporter type 2; INS – insulin gene; Ins1 – insulin 1 rodent gene; Ins2 – insulin 2 rodent gene; NEUROG 3 – encoding the transcription factor neurogenin-3; MAFB – musculoaponeurotic fibrosarcoma oncogene homolog b.

However, the peak rate of proliferation is considerably higher in rats and ranges from 10% to 30%.[26] Most studies employed beta cell originating from juvenile rodents 2 to 3 months of age for regeneration experiments. However, regeneration experiments in humans employed beta cells that were mainly obtained from individuals 40–50 years old.

A large number of the interventions made in rats (such as obesity, high-fat diets, partial pancreatectomy, genetic models of insulin resistance, pregnancy, growth factors, mitogenic agents [such as placental lactogen, prolactin, glucose, hepatocyte growth factor, betatrophin, exendin 4, glucagon-like peptide (GLP1), epidermal growth factor (EGF), insulin-like growth factors (IGFs), osteocalcins, gastrin, and platelet-derived growth factor (PDGR)] and some other molecules, such as purinergic agonists, glucokinase activators, adenosine kinase inhibitors, and dihydropyridines) have been proven to be capable as strong proliferation activators.[27] However, these interventions were ineffective in humans in inducing proliferation owing to the differences in age and other intrinsic factors.[28] Consequently, there is a clear need to comprehend the biological differences in both species so that the findings in rat models may be implemented in the treatment of humans.

Hindrances in the proliferation of beta cells

The primary feature of human pancreatic beta cells is an incredibly small basal proliferation index (0.1–0.2%) and a poor response to almost all mitogenic stimuli (0.3–0.5%). Studies revealed that 99.9% of pancreatic beta cells are quiescent. However, the number of quiescent beta cells is reduced to 99.5% during mitogenic stimulation. Adult human beta cells exhibit resistance to mitogenic stimuli. Nevertheless, the proliferation rate during the early years of life is incredibly low (about 2%) even when there is a maximum proliferation of beta cells. The reason behind the low proliferation rate of the beta cells is unclear.

It has been speculated that the adult beta cells were replicatively senescent (a condition in which cells cannot enter the cell cycle due to a high activity of cell cycle inhibitory molecules like p16INK4a, p18INK4c, p27KIP1, p53, p57KIP2 p21CIP1, and others).[29] This explanation is not satisfactory, as the cell cycle can be induced by an increased expression of cyclins and CDKs or by the activation of other positive signaling pathways. These cyclins and CDKs cannot get entry into the nucleus of these pancreatic beta cells, which keeps them in quiescence.[10]

An age-related alteration in the epigenetic makeup of the replicative machinery culminates in senescence. The loss of *EZH2* (enhancer of zeste homolog 2) and BMI1 (a polycomb complex protein) results in an increased expression of p16INK4a and other CDK inhibitors. Age-related depletion of the receptors for mitogenic and platelet-derived growth factor may also render adult beta cells gradually unresponsive to mitogenic stimuli.[30] However, the presence of GLP 1 and HGF receptors involved in the stimulation of mitogenic signaling pathways of rodent and adult human beta cells suggests the need to further investigate the age-related and species-specific deviations in intracellular signaling pathways.[31]

Mitogens for proliferation

A rational therapeutic approach to treating diabetes is the promotion of insulin secretion through encouraging the proliferation of beta cells. A key challenge in promoting the proliferation of beta cells is to enhance their proliferation without increasing the generalized proliferation rate.[19] It is evident from the previous studies that glucose has the potential to promote human and rodent beta cell proliferation under both in vitro and in vivo conditions.[32] Glucokinase (GK) metabolizes glucose after its uptake into beta cells. It is the rate-limiting step of glycolysis. Glycolysis increases ATP concentration, which results in the closure of ATP-sensitive potassium channels (KATP) and causes a depolarization of the cell membrane. This depolarization results in the opening of voltage gated Ca^{2+} channels, and an ultimate increase in intracellular Ca^{2+} level triggers the exocytosis of insulin. Several studies have demonstrated that glucose-induced proliferation also occurs through this glucose-triggered insulin secretion pathway. Several studies have shown the link between glucokinase activation and beta cell proliferation. This renders glucokinase an appealing target for interventions to promote proliferation.[33] Glucokinase activators exhibit a conservation of beta cell mass in rat models.[34] Intracellular Ca^{2+} functions as a physiological regulator of the glucose-triggered insulin secretion pathway. It is also evident that dihydropyridine derivatives activate L-type Ca^{2+} channels to promote the proliferation of beta cells.[35] Beta cells also proliferate due to calcium-dependent phosphatase calcineurin, the nuclear factor of the activated T cell (NFAT) pathway. Table 3 lists the molecules involved in the conservation of beta cell mass through an enhancement of the proliferation rate and a reduction in the apoptosis of beta cells.

Table 3. List of the chemicals that enhance the proliferation rate and reduce beta cell apoptosis resulting in the conservation of beta cell mass

Nature of chemicals	Proliferation enhancer	Apoptosis inhibitors
Small molecules	GKA	N/A
	calcium signaling	
	adenosine signaling	
	WS6	
Hormones	insulin	insulin
	lactogen signaling	estrogen
	incretin	incretin
	betatrophin	triiodothyronine
Phytochemicals	N/A	resveratrol
		PPAG
		flavonoids
		glutathione peroxidase mimetics

GKA – glucokinase activator; N/A – not applicable; WS6 – compound name with molecular formula C29H31F3N6O3; PPAG – phenylpropenoic acid.

A nonspecific adenosine receptor agonist (NECA) was identified as a potent enhancer of beta cell proliferation through a zebra fish whole-body screen in regenerating conditions. NECA acts through the beta cell surface adenosine receptor A2α and its proliferative and hypoglycemic action has been demonstrated in diabetic mice. These observations suggest a possible link between glucose metabolism and adenosine signaling via a glucose-induced increase in intracellular ATP concentration that, in turn, enhances beta cell proliferation in a paracrine fashion.[36] ATP depletion in dying cells exhibits adenosine as a stress signal. This signal enhances beta cell proliferation following tissue damage.[37] It is also evident from the studies that the inhibition of nuclear adenosine kinase activity may induce beta cell proliferation selectively in rodent diabetic models.[38] WS6 effectively stimulates beta cell proliferation in both rodent and human islets dose-dependently. Additionally, there is a variety of growth factors and hormones that increase proliferation, such as incretins, insulin, parathyroid hormone related protein (PTHRP), PDGF, IGFs, EGF, and hepatocyte growth factor (HGF).[39] Gastric inhibitory polypeptide (GIP) and GLP1 are secreted from the gut and reduce the blood glucose level efficiently through multiple signaling pathways, including beta cell proliferation. GLP1 receptor agonists are extensively used for the management of diabetes and increase the secretion of insulin by binding to their receptors on beta cells.[40]

GLP1 receptor agonists and DPP4 inhibitors exhibit beta cell proliferation in rodent models. However, there is no evidence that either of these would be effective in diabetic patients. Moreover, it has also been found that incretin

therapy may induce pathological lesions with a high risk of oncogenicity.[41] Beta cells proliferate as a result of increased insulin demand in conditions such as pregnancy, obesity, and insulin resistance. These conditions are helpful in the identification of several hormones involved in beta cell mass expansion. The concentration of placental lactogen and prolactin increases during pregnancy and these hormones are involved in the proliferation of beta cells.[42] It has been established that the lactogen-induced proliferation of beta cells is accomplished through the production of the neurotransmitter serotonin in the islet tissues.[43] Consequently, modulation in serotonin signaling may be helpful in controlling hyperglycemia. In addition, prolactin stimulates the proliferation of beta cells by suppressing menin levels.[44] Menin inhibitors have also been developed and evaluated for their potential to induce proliferation. It is further necessary to identify and investigate the related drugs to enhance the proliferation of beta cells.

Inhibition of beta cell apoptosis

Apoptosis is the hallmark of beta cell loss and plays a pivotal role in the progression of DMT2.[45] A high fat diet contributes mainly to beta cell apoptosis owing to oxidative stress associated with glucotoxicity and lipotoxicity. Studies have revealed the upregulation of pro-apoptotic genes in response to oxidative stress resulting in cell death.[46] Several compounds causing elevated glucose uptake by the muscle and fat tissues also exerted positive effects on beta cell survival. Likewise, some compounds with antioxidant potential also proved helpful in the prevention of apoptosis.[47]

Polyphenols present in natural products may be used as anti-apoptotic agents due to their high antioxidant potential. Flavonoids (genistein, anthocyanins, and epigallocatechin gallate) and other polyphenolic compounds (like stilbene and resveratrol) prevent the apoptosis of beta cells through a reduction of oxidative stress. These compounds also exhibit a potential to modulate anti-apoptotic and pro-apoptotic proteins present in the beta cells.[48] It has been found that phenyl pyruvic acid glucoside (PPAG) protects patients from hyperglycemia and increases the beta cell mass in rodents.[49]

PPAG and several flavonoids have antioxidant potential. These compounds also cause an upregulation of Bcl-2 which prevents apoptosis.[50] Inflammation, along with gluco-lipotoxicity, plays a vital role in beta cell death in DMT2. Interleukin 1 (IL-1) signaling is found to be involved in the pathogenesis of DMT2.[51] Resveratrol prevents the IL-1ß-induced dysfunction of pancreatic beta cells.[52]

Histone deacetylase inhibitors (HDACi) can be utilized in the management of diabetes as these chemicals suppress IL-1ß signaling. HDACi also block cytokine-induced apoptosis in streptozotocin-induced diabetes.[53] Likewise, exendin-4 protects cytokine-induced beta cell apoptosis.[54] Additionally, exendin-4 also diminishes gene expression in response to stress in the endoplasmic reticulum of partially pancreatectomized rats.[55] GLP1 may expand beta cell mass in leptin receptor-deficient mice through a reduction of oxidative stress.[56]

GLP1 also exhibits an anti-apoptotic effect in isolated human islets.[57] Numerous rodent models reported a higher susceptibility to developing diabetes in male animals than in their female counterparts.[58] Therefore, it is suggested that gonadal hormones also play a significant role in the development of the disease. Estrogen-receptors (ERs) expressed in human and rodent beta cells include ERα, ERß, and G protein-coupled ERs. These receptors also contribute to beta cell survival. It is evident that estrogen reduces oxidative stress and lipotoxicity-associated loss of beta cells.[58,59] Additionally, estrogen also protects beta cells against pro-inflammatory cytokines. Triiodothyronine (T3), a thyroid hormone, also exhibits an anti-apoptotic effect through the modulation of pro- and anti-apoptotic factors like Bcl-XL, Bcl-2, Bad, Bax, and caspase 3.[60]

Conclusions

On the basis of this discussion, it can be concluded that physiological stimuli may enhance the proliferation of beta cells in order to conserve beta cell mass. Several small molecules have shown the potential to induce proliferation, which warrants further investigation in order to explore their exact mechanism of action and to optimize them. Numerous phytochemicals that are capable of reducing the apoptosis of beta cells to conserve beta cell function have also been introduced. Several mitogens increase the proliferation of beta cells in rodents; they are, however, unable to induce proliferation in human beta cells due to various intrinsic and nutritional factors. It is necessary to further develop and select more appropriate experimental models to test mitogens for beta cell proliferation. Likewise, it is also necessary to develop an appropriate non-invasive method to assess beta cell mass.

References

1. Kahn SE, Cooper ME, Del Prato S. Pathophysiology and treatment of type 2 diabetes: Perspectives on the past, present, and future. *Lancet*. 2014;383(9922):1068–1083.
2. Roizen JD, Bradfield JP, Hakonarson H. Progress in understanding type 1 diabetes through its genetic overlap with other autoimmune diseases. *Curr Diabetes Rep*. 2015;15(11):1–7.
3. Dupuis J, Langenberg C, Prokopenko I, et al. New genetic loci implicated in fasting glucose homeostasis and their impact on type 2 diabetes risk. *Nature Genet*. 2010;42(2):105–116.
4. Marques-Vidal P, Bastardot F, Kanel R, et al. Association between circulating cytokine levels, diabetes and insulin resistance in a population-based sample (CoLaus study). *J Clin Endocrinol*. 2013;78(2): 232–241.
5. Weir GC, Bonner-Weir S. Islet β cell mass in diabetes and how it relates to function, birth, and death. *Ann NY Acad Sci*. 2013;1281(1):92–105.

6. Rahier J, Guiot Y, Goebbels R, et al. Pancreatic β-cell mass in European subjects with type 2 diabetes. *Diabet Obes Metab*. 2008;10(s4): 32–42.
7. Niclauss N, Meier R, Bedat B, et al. Beta-cell replacement: Pancreas and islet cell transplantation. In: *Novelties in Diabetes*. Switzerland: Karger Publishers; 2016:146–162.
8. Avrahami D, Li C, Yu M, et al. Targeting the cell cycle inhibitor p57 Kip2 promotes adult human β cell replication. *J Clin Invest*. 2014;124(2): 660–664.
9. Bernal-Mizrachi E, Kulkarni RN, Scott DK, et al. Human β-cell proliferation and intracellular signaling part 2: Still driving in the dark without a road map. *Diabetes*. 2014;63(3):819–831.
10. Fiaschi-Taesch NM, Kleinberger JW, Salim FG, et al. Human pancreatic β-cell G1/S molecule cell cycle atlas. *Diabetes*. 2013;62(7):2450–2459.
11. Fiaschi-Taesch NM, Kleinberger JW, Salim FG, et al. Cytoplasmic-nuclear trafficking of G1/S cell cycle molecules and adult human β-cell replication a revised model of human β-cell G1/S control. *Diabetes*. 2013;62(7):2460–2470.
12. Lavine JA, Raess PW, Davis DB, et al. Overexpression of pre-pro-cholecystokinin stimulates β-cell proliferation in mouse and human islets with retention of islet function. *Mol Endocrinol*. 2008;22(12):2716–2728.
13. Fiaschi-Taesch NM, Salim F, Kleinberger J, et al. Induction of human β-cell proliferation and engraftment using a single G1/S regulatory molecule, CDK6. *Diabetes*. 2010;59(8):1926–1936.
14. Agarwal SK, Mateo CM, Marx SJ. Rare germline mutations in cyclin-dependent kinase inhibitor genes in multiple endocrine neoplasia type 1 and related states. *J Clin Endocrinol Metabol*. 2009;94(5): 1826–1834.
15. Kulkarni RN, Mizrachi EB, Ocana AG, et al. Human β-cell proliferation and intracellular signaling. *Diabetes*. 2012;61(9):2205–2213.
16. Demozay D, Tsunekawa S, Briaud I, et al. Specific glucose-induced control of insulin receptor substrate-2 expression is mediated via Ca^{2+}-dependent calcineurin/NFAT signaling in primary pancreatic islet β-cells. *Diabetes*. 2011;60(11):2892–2902.
17. Liu H, Remedi MS, Pappan KL, et al. Glycogen synthase kinase-3 and mammalian target of rapamycin pathways contribute to DNA synthesis, cell cycle progression, and proliferation in human islets. *Diabetes*. 2009;58(3):663–672.
18. Rhodes CJ, White MF, Leahy JL, et al. Direct autocrine action of insulin on β-cells: Does it make physiological sense? *Diabetes*. 2013;62(7): 2157–2163.
19. Conrad E, Stein R, Hunter CS. Revealing transcription factors during human pancreatic β cell development. *Trend Endocrinol Metab*. 2014;25(8):407–414.
20. De Vos A, Heimberg H, Quartier E, et al. Human and rat beta cells differ in glucose transporter but not in glucokinase gene expression. *J Clin Invest*. 1995;96(5):2489.
21. Gradwohl G, Dierich A, LeMeur M, et al. Neurogenin 3 is required for the development of the four endocrine cell lineages of the pancreas. *Proceed Nat Acad of Sci*. 2000;97(4):1607–1611.
22. Rubio-Cabezas O, Codner E, Flanagan SE, et al. Neurogenin 3 is important but not essential for pancreatic islet development in humans. *Diabetologia*. 2014;57(11):2421–2424.
23. Dai C, Brissova M, Hang Y, et al. Islet-enriched gene expression and glucose-induced insulin secretion in human and mouse islets. *Diabetologia*. 2012;55(3):707–718.
24. Gregg BE, Moore PC, Demozay D, et al. Formation of a human β-cell population within pancreatic islets is set early in life. *J Clin Endocrinol Met*. 2012;97(9):3197–3206.
25. Mezza T, Muscogiuri G, Sorice GP, et al. Insulin resistance alters islet morphology in nondiabetic humans. *Diabetes*. 2014;63(3):994–1007.
26. Teta M, Long SY, Wartschow LM, et al. Very slow turnover of β-cells in aged adult mice. *Diabetes*. 2005;54(9):2557–2567.
27. Campbell JE, Drucker DJ. Pharmacology, physiology, and mechanisms of incretin hormone action. *Cell Metabol*. 2013;17(6):819–837.
28. Griffin KJ, Thompson PA, Gottschalk M, et al. Combination therapy with sitagliptin and lansoprazole in patients with recent-onset type 1 diabetes (REPAIR-T1D): 12-month results of a multicentre, randomised, placebo-controlled, phase 2 trial. *Lancet Diabetes Endocrinol*. 2014;2(9):710–718.
29. Tchkonia T, Zhu Y, Van Deursen J, et al. Cellular senescence and the senescent secretory phenotype: Therapeutic opportunities. *J Clin Invest*. 2013;123(3):966–972.
30. Chen H, Gu X, Liu Y, et al. PDGF signaling controls age-dependent proliferation in pancreatic [bgr]-cells. *Nature*. 2011;478(7369): 349–355.
31. Baggio LL, Drucker DJ. Biology of incretins: GLP-1 and GIP. *Gastroenterology*. 2007;132(6):2131–2157.
32. Alonso LC, Yokoe T, Zhang P, et al. Glucose infusion in mice a new model to induce β-cell replication. *Diabetes*. 2007;56(7):1792–1801.
33. Porat S, Weinberg-Corem N, Tornovsky-Babaey S, et al. Control of pancreatic β cell regeneration by glucose metabolism. *Cell Metab*. 2011;13(4):440–449.
34. Futamura M, Yao J, Li X, et al. Chronic treatment with a glucokinase activator delays the onset of hyperglycaemia and preserves beta cell mass in the Zucker diabetic fatty rat. *Diabetologia*. 2012;55(4):1071–1080.
35. Wang W, Walker JR, Wang X, et al. Identification of small-molecule inducers of pancreatic β-cell expansion. *Proceed Nat Acad Sci*. 2009; 106(5):1427–1432.
36. Andersson O, Adams BA, Yoo D, et al. Adenosine signaling promotes regeneration of pancreatic β cells in vivo. *Cell Metab*. 2012;15(6):885–894.
37. Xu X, D'Hoker J, Stange G, et al. β cells can be generated from endogenous progenitors in injured adult mouse pancreas. *Cell*. 2008;132(2): 197–207.
38. Annes JP, Ryu JH, Lam K, et al. Adenosine kinase inhibition selectively promotes rodent and porcine islet β-cell replication. *Proceed Nat Acad Sci*. 2012;109(10):3915–3920.
39. Vasavada RC, Gonzalez-Pertusa JA, Fujinaka Y, et al. Growth factors and beta cell replication. *Int J Biochem Cell Biol*. 2006;38(5):931–950.
40. Ding L, Gysemans C, Mathieu C. β-cell differentiation and regeneration in type 1 diabetes. *Diabetes Obes Metab*. 2013;15(3):98–104.
41. Butler AE, Campbell-Thompson M, Gurlo T, et al. Marked expansion of exocrine and endocrine pancreas with incretin therapy in humans with increased exocrine pancreas dysplasia and the potential for glucagon-producing neuroendocrine tumors. *Diabetes*. 2013;62(7): 2595–2604.
42. Brelje TC, Bhagroo NV, Stout LE, et al. Beneficial effects of lipids and prolactin on insulin secretion and β-cell proliferation: A role for lipids in the adaptation of islets to pregnancy. *J Endocrinol*. 2008;197(2): 265–276.
43. Kim H, Toyofuku Y, Lynn FC, et al. Serotonin regulates pancreatic beta cell mass during pregnancy. *Nat Med*. 2010;16(7):804–808.
44. Karnik SK, Chen H, McLean GW, et al. Menin controls growth of pancreatic ß-cells in pregnant mice and promotes gestational diabetes mellitus. *Science*. 2007;318(5851):806–809.
45. Donath MY, Ehses JA, Maedler K, et al. Mechanisms of β-cell death in type 2 diabetes. *Diabetes*. 2005;54(Suppl 2):108–113.
46. Cunha DA, Igoillo-Esteve M, Gurzov EN, et al. Death protein 5 and p53-upregulated modulator of apoptosis mediate the endoplasmic reticulum stress-mitochondrial dialog triggering lipotoxic rodent and human β-cell apoptosis. *Diabetes*. 2012;61(11):2763–2775.
47. Mahadevan J, Parazzoli S, Oseid E, et al. Ebselen treatment prevents islet apoptosis, maintains intranuclear Pdx-1 and MafA levels, and preserves β-cell mass and function in ZDF rats. *Diabetes*. 2013;62(10): 3582–3588.
48. Gilbert ER, Liu D. Anti-diabetic functions of soy isoflavone genistein: Mechanisms underlying its effects on pancreatic β-cell function. *Food Funct*. 2013;4(2):200–212.
49. Mathijs I, Cunha DA, Himpe E, et al. Phenylpropenoic acid glucoside augments pancreatic beta cell mass in high-fat diet-fed mice and protects beta cells from ER stress-induced apoptosis. *Mol Nutr Food Res*. 2014;58(10):1980–1990.
50. Wang C, Guan Y, Yang J. Cytokines in the progression of pancreatic β-cell dysfunction. *Int J Endocrinol*. 2010;13:34–42
51. Banerjee M, Saxena M. Interleukin-1 (IL-1) family of cytokines: Role in type 2 diabetes. *Clini Chim Acta*. 2012;413(15):1163–1170.
52. Ku CR, Lee HJ, Kim SK, et al. Resveratrol prevents streptozotocin-induced diabetes by inhibiting the apoptosis of pancreatic β-cell and the cleavage of poly (ADP-ribose) polymerase. *Endocr J*. 2012;59(2): 103–109.
53. Lewis EC, Blaabjerg L, Storling J, et al. The oral histone deacetylase inhibitor ITF2357 reduces cytokines and protects islet beta cells in vivo and in vitro. *Mol Med*. 2011;17:369–377.
54. Liu X-H, Remedi MS, Pappan KL, et al. Exendin-4 protects murine MIN6 pancreatic β-cells from interleukin-1β-induced apoptosis via the NF-κB pathway. *J Endocrinol Invest*. 2013;36(10):803–811.

55. Kwon DY, Kim YS, Ahn IS, et al. Exendin-4 potentiates insulinotropic action partly via increasing beta-cell proliferation and neogenesis and decreasing apoptosis in association with the attenuation of endoplasmic reticulum stress in islets of diabetic rats. *J Pharmacol Sci*. 2009;111(4):361–371.
56. Shimoda M, Kanda Y, Hamamoto S, et al. The human glucagon-like peptide-1 analogue liraglutide preserves pancreatic beta cells via regulation of cell kinetics and suppression of oxidative and endoplasmic reticulum stress in a mouse model of diabetes. *Diabetologia*. 2011;54(5):1098–1108.
57. Farilla L, Bulotta A, Hirshberg B, et al. Glucagon-like peptide 1 inhibits cell apoptosis and improves glucose responsiveness of freshly isolated human islets. *Endocrinol*. 2003;144(12):5149–5158.
58. Tiano JP, Mauvais-Jarvis F. Importance of oestrogen receptors to preserve functional β-cell mass in diabetes. *Nat Rev Endocrinol*. 2012; 8(6):342–351.
59. Le-May C, Chu K, Hu M, et al. Estrogens protect pancreatic β-cells from apoptosis and prevent insulin-deficient diabetes mellitus in mice. *Proc Nat Acad Sci*. 2006;103(24):9232–9237.
60. Verga FC, Panacchia L, Bucci B, et al. 3,5,3′-triiodothyronine (T3) is a survival factor for pancreatic β-cells undergoing apoptosis. *J Cell Physiol*. 2006;206(2):309–321.

Advances in antibody therapeutics targeting small-cell lung cancer

Hongyang Lu[1,2,A–F], Zhiming Jiang[1,B,D]

[1] Zhejiang Key Laboratory of Diagnosis and Treatment Technology on Thoracic Oncology (Lung and Esophagus), Zhejiang Cancer Hospital, Hangzhou, China
[2] Department of Thoracic Medical Oncology, Zhejiang Cancer Hospital, Hangzhou, China

A – research concept and design; B – collection and/or assembly of data; C – data analysis and interpretation;
D – writing the article; E – critical revision of the article; F – final approval of the article

Advances in Clinical and Experimental Medicine, ISSN 1899-5276 (print), ISSN 2451-2680 (online) *Adv Clin Exp Med*. 2018;27(9):1317–1323

Address for correspondence
Hongyang Lu
E-mail: luhy@zjcc.org.cn

Funding sources
This work was supported by the Zhejiang Provincial Natural Science Foundation of China (No. LY15H290001), Public Welfare Technology Application Studies Program of the Zhejiang Province (No. 2016C33118) and the 1022 Talent Training Program of Zhejiang Cancer Hospital.

Conflict of interest
None declared

Received on July 13, 2016
Reviewed on November 17, 2017
Accepted on April 3, 2017

Abstract

The proportion of small-cell lung cancer (SCLC) among all lung cancers decreased from 17.26% in 1986 to 12.95% in 2002. Chemotherapy is the key mode of treatment. However, novel therapeutic strategies and drugs are imperative, as the prognosis remains poor. In recent years, antibody therapies have shown promising prospects against malignancy. This review focuses on the advances in antibody therapies in SCLC. Although the results of pembrolizumab, nivolumab, ipilimumab, and rovalpituzumab tesirine are inspiring, all of the clinical trials on these drugs are phase I/II and have been verified for further phase III clinical trials. It was demonstrated that chemotherapy in combination with bevacizumab can improve the progression-free survival (PFS) in phase III trials. The insulin-like growth factor-1 receptor (IGF-1R) is associated with a poor prognosis in SCLC, while the anti-IGF-1R monoclonal antibody figitumumab has a potential therapeutic value. Tarextumab, an antibody that blocks both Notch2 and Notch3 signaling, in combination with etoposide and platinum (EP) in patients with untreated extensive-stage SCLC, proved to be well-tolerated and showed dose-dependent anti-tumor activity. The therapeutic effect of sacituzumab govitecan, BW-2 and lorvotuzumab mertansine in SCLC warranted further evaluation. Bec2/BCG as an adjuvant vaccination in patients with limited-disease SCLC could not improve the survival, PFS, or quality of life. Thus, clinical studies are essential to confirm the anti-tumor efficacy of trastuzumab in SCLC.

Key words: small-cell lung cancer, antibody therapeutics, antibody-drug conjugate

DOI
10.17219/acem/70159

Lung cancer, including small-cell lung cancer (SCLC) and non-small-cell lung cancer (NSCLC), is the leading cause of cancer-related mortality and the most common malignancy in China as well as around the world.[1,2] The proportion of SCLC among all lung cancers decreased from 17.26% in 1986 to 12.95% in 2002.[3] Chemotherapy is the primary mode of treatment of SCLC; however, the prognosis still remains poor. To date, no targeted drugs for SCLC have been approved by the US Food and Drug Administration (FDA). Thus, novel therapeutic strategies and drugs are imperative. In recent years, antibody therapies have shown promising anti-tumor prospects in a variety of human cancers. The present review focuses on the advances in antibody therapies in SCLC, which include pembrolizumab, nivolumab, ipilimumab, bevacizumab, rovalpituzumab tesirine, sacituzumab govitecan, and lorvotuzumab mertansine (IMGN901).

Immune checkpoint inhibitors

Cytotoxic T-lymphocyte-associated protein 4 (CTLA-4) and programmed cell death-1 (PD-1) are typical immune checkpoint molecules that suppress anti-tumor immunity. Antibodies that keep the PD-1 and CTLA-4 immune checkpoint pathways as targets display superior clinical efficacy. It was assumed that pembrolizumab and nivolumab (anti-PD-1 antibody), as well as ipilimumab (anti-CTLA-4 antibody), act with the most promising immunotherapies under investigation in SCLC patients.[4] Pembrolizumab is a humanized immunoglobulin G4 (IgG4) monoclonal antibody against PD-1 designed to block the interaction between PD-1 and its ligands, programmed cell death ligand-1 (PD-L1) and programmed cell death ligand-2 (PD-L2). Pembrolizumab has demonstrated robust anti-tumor activity and a manageable toxicity profile in NSCLC. The safety and efficacy of pembrolizumab was assessed in PD-L1-positive SCLC patients in a multicohort, phase 1b KEYNOTE-028 study.[5] The results of this study demonstrated that the SCLC patients either did not respond to or were unable to receive the standard therapy. The authors observed the PD-L1 expression in ≥1% of cells in tumor nests or PD-L1-positive bands in stroma, as assessed by immunohistochemistry (IHC), using 22C3 anti-PD-L1 antibody. Pembrolizumab (10 mg/kg) was administered every 2 weeks for up to 2 years or until confirmed progression or unacceptable toxicity. Of the 147 SCLC patients with evaluable tumor samples screened for the PD-L1 expression, 42 patients (29%) showed PD-L1-positive tumors. Overall, 24 patients with SCLC were enrolled in the study and received at least 1 pembrolizumab dose. All 24 experienced drug-related adverse events (AEs) and only 2 patients showed grade 3 or higher drug-related AEs. On the other hand, 1 patient had a complete response (CR), and 7 patients had partial response (PR). The median progression-free survival rate (PFS) was 1.9 months, with a 6-month PFS rate of 28.6%.[5] This study was only a phase 1b trial with a limited sample size, so further investigation in randomized, controlled clinical trials is needed. Pembrolizumab is well-tolerated and promising in SCLC patients.

The safety and activity of nivolumab and nivolumab plus ipilimumab in patients with SCLC who progressed after 1 or more previous regimens were assessed in a multicenter, multi-arm, open-label phase 1/2 trial. A total of 216 patients were enrolled and received nivolumab (3 mg/kg) every 2 weeks (until disease progression or unacceptable toxicity) or nivolumab plus ipilimumab (1 mg/kg plus 1 mg/kg, 1 mg/kg plus 3 mg/kg, or 3 mg/kg plus 1 mg/kg, intravenously) every 3 weeks for 4 cycles, followed by 3 mg/kg of nivolumab every 2 weeks. The primary endpoint was an objective response rate (ORR). An objective response was achieved in 10 of 98 patients (10%) receiving 3 mg/kg of nivolumab, in 1 of 3 patients (33%) receiving 1 mg/kg of nivolumab plus 1 mg/kg of ipilimumab, in 14 of 61 patients (23%) receiving 1 mg/kg of nivolumab plus 3 mg/kg of ipilimumab, and in 10 of 54 patients (19%) receiving 3 mg/kg of nivolumab plus 1 mg/kg of ipilimumab. Grade 3 or 4 treatment-related AEs occurred in 13 patients (13%) in the 3 mg/kg nivolumab cohort, in 18 (30%) in the 1 mg/kg nivolumab plus 3 mg/kg ipilimumab cohort and in 10 (19%) in the 3 mg/kg nivolumab plus 1 mg/kg ipilimumab cohort. The most commonly reported grade 3 or 4 treatment-related AEs were increased lipase and diarrhea. Two patients who received 1 mg/kg of nivolumab plus 3 mg/kg of ipilimumab died due to treatment-related AEs, such as myasthenia gravis and aggravated renal failure, and 1 patient who received 3 mg/kg of nivolumab plus 1 mg/kg of ipilimumab died from treatment-related pneumonitis. Toxicity and efficacy, as well as safety profiles, should be carefully weighed. These results demonstrated a similar response to pembrolizumab.[5,6] This data supports the evaluation of nivolumab and nivolumab plus ipilimumab in another phase 3 randomized, controlled trials in SCLC after first-line platinum-based chemotherapy or maintenance therapy.[6] These results demonstrated a similar response to pembrolizumab as in the case of nivolumab plus ipilimumab in relapsed SCLC patients; the question which therapy is superior remains unanswered.

Tumor-infiltrating lymphocytes and the PD-L1 expression are frequently observed in brain metastases of SCLC. The presence of CD45RO+ memory T cells in SCLC brain metastases seems to be associated with favorable survival times. SCLC brain metastases exhibit an active immune microenvironment which might be targetable by immune-modulating drugs.[7] PD-L1 protein was infrequently expressed in SCLC (7.3%) and correlated with the limited disease stage that might serve as a prognostic marker for enhanced overall survival (OS).[8,9] The PD-L1 expression in 40 surgically resected SCLC specimens was evaluated by IHC with 3 different antibodies – E1L3N, 28-8 and SP142 clones – and using 3 different evaluations: all red score, 1% cut-off and 5% cut-off. The IHC evaluations with

the 5% cut-off showed similar rates of expression, using the 3 different antibodies.[10] The reagents and methods of PDL-1 detection require further standardization, and the cut-off value still needs to be consolidated.

Bevacizumab

Tumor growth and nutrition for angiogenesis is mediated primarily via the vascular endothelial growth factor (VEGF) family. The inhibition of angiogenesis has been the subject of research and clinical investigation. Bevacizumab is an anti-VEGF monoclonal antibody that inhibits angiogenesis and has been approved as the first-line treatment for advanced NSCLC.[11] According to the study by Ustuner et al., low serum VEGF concentration is a significant and independent prognostic factor in SCLC patients; however, the surveillance of VEGF and its receptors was not useful in predicting chemotherapy response.[12] A randomized phase 2/3 trial, which evaluated the efficacy and safety of bevacizumab added following the induction of chemotherapy in extensive-stage SCLC, demonstrated no difference in the response or PFS after randomization. Furthermore, serum VEGF and soluble VEGF receptor titrations failed to identify predictive biomarkers.[13] An Italian multicenter, randomized phase 3 study of cisplatin-etoposide (EP) with or without bevacizumab as the first-line treatment in extensive-stage SCLC showed that the addition of bevacizumab led to a statistically significant improvement in PFS (5.7 vs 6.7 months, hazard ratio (HR): 0.72; 95% confidence interval (CI): 0.54–0.97; p = 0.030) and an acceptable toxicity profile. However, a statistically insignificant increase in the primary endpoint of OS was observed. In this trial, patients were randomized to receive either 100 mg/m^2 of etoposide intravenously (iv.) and 25 mg/m^2 of cisplatin on days 1–3 (or carboplatin AUC 5 on day 1) (group A), or the same chemotherapy combined with 7.5 mg/kg of bevacizumab iv. on day 1 (group B) every 3 weeks for a maximum of 6 courses. In the absence of progression after 6 cycles, patients in group B continued bevacizumab alone until progression or for a maximum of 18 courses.[14] An EP combined with bevacizumab regimen followed by oral etoposide and bevacizumab maintenance treatment appeared to be feasible and efficient in terms of the 9-month disease control rate (36.3%) in patients with extensive-stage SCLC; severe AEs were rarely observed during the maintenance treatment. Since this data comes from a single institution with only 22 patients in the study, further clinical trials are essential to confirm the result.[15] Another study which involved the addition of bevacizumab to paclitaxel showed no improvement in the outcomes of 34 relapsed chemosensitive SCLC patients. The median PFS was recorded as 14.7 weeks.[16] This combination was feasible and active in chemoresistant relapsed SCLC as a salvage treatment in 30 patients with a median PFS of 2.7 months, which represented a valid therapeutic alternative. However, further evaluation is imperative.[17] The predictive factors for the therapeutic effect of bevacizumab are unclear, and which types of patients can benefit from the use of bevacizumab is still unknown. The US FDA has not approved bevacizumab for the treatment of SCLC. The selection of appropriate SCLC patients for a bevacizumab therapy is an important area of research.

Anti-insulin-like growth factor-1 receptor monoclonal antibody

The activation of the insulin-like growth factor-1 receptor (IGF-1R) – an autocrine growth factor – by IGF-1 and IGF-2 plays a key role in the growth of malignant tumors and the inhibition of apoptosis. The IGF-1R pathway is generally upregulated, and the IGF-1R inhibition is a plausible therapeutic strategy in SCLC. The prognosis of SCLC patients is poor, as assessed by 3+ immunostaining of IGF-1R.[18] The addition of R1 507 – a monoclonal antibody against IGF-1R to the current standard cisplatin-ionizing radiation doublet revealed remarkable chemo- and radiosensitizing effects in selected SCLC models, and warrants further investigations in clinical settings.[19] Cao et al. showed that the IGF-1R expression was significantly associated with tumor size, node (N) status, stage, and Ki-67, and the multivariate Cox analysis demonstrated that only the IGF-1R expression was found to be an independent predictor for OS. The study suggested that the IGF-1R expression was negatively correlated with the survival of patients. Additionally, anti-IGF-1R monoclonal antibody figitumumab exhibited a potential therapeutic effect through the IGF-1R blockage and downregulation.[20] The anti-IGF-1R monoclonal antibody exhibits anti-tumor activity in SCLC. The anti-IGF-1R therapeutic approach needs to be further investigated in clinical trials.

Tarextumab and MEDI0639

The canonical Notch pathway with 4 Notch receptors (Notch1–4) and 5 ligands (DLL1, 3–4, Jagged1–2) is an evolutionarily conserved cell signaling pathway that plays a prominent role in the determination of cell fate, differentiation, proliferation, and death. Several drugs that targeted the Notch pathway for various malignant tumors have been developed.[21] Tarextumab is an antibody which blocks both Notch2 and Notch3 signaling pathways and has been confirmed to inhibit tumor growth in patient-derived xenograft tumors.[22] A phase 1b study of tarextumab in combination with EP in untreated extensive-stage SCLC patients showed that this combination was well-tolerated with dose-dependent anti-tumor activity. Twenty-seven patients were treated with tarextumab doses ranging from 5 to 15 mg/kg. However, the maximum tolerated dose (MTD) was not reached and it was determined that

15 mg/kg of tarextumab was a phase 2 dose. The results showed that the ORR was 73% and that the median OS was 10.3 months with a median follow-up of 9.8 months; 16.0 months for patients receiving ≥12.5 mg/kg of tarextumab and 7.6 months for patients with a dosage <12 mg/kg.[23] Frequently reported (≥15%) tarextumab-related AEs were mostly grade 1 or 2, they were also reversible. A randomized, placebo-controlled phase 2 study with this regimen is ongoing. The appropriate dosage of tarextumab requires further exploration.

MEDI0639 is a human monoclonal antibody that selectively binds to DLL4 and inhibits DLL4-Notch receptor signaling. Preclinical studies demonstrated that the DLL4 blockade can reduce tumor cell proliferation and cancer stem cell frequency. A single-agent phase 1 study of MEDI0639 on 9 SCLC patients suggested that MEDI0639 may suppress cancer stem cell counts and activities.[24] However, further studies are required to evaluate the effect of MEDI0639 in a significant number of patients in a phase 1 study.

Tucotuzumab

Tucotuzumab – a humanized KS-interleukin-2 and an EpCAM-specific immune cytokine – combined with cyclophosphamide showed immunological activity. A randomized, open-label phase 2 study compared tucotuzumab/cyclophosphamide as maintenance therapy with the best supportive care in extensive-disease SCLC patients who responded to the first-line platinum-based chemotherapy, but the results showed no PFS or OS benefits.[25] The role of tucotuzumab has not been proven and its effects are still uncertain. Further studies involving a larger population may be appropriate in specific subtypes of patients receiving prior cranial irradiation for prophylaxis.

Trastuzumab

Human epidermal growth factor receptor 2 (HER2), a member of the HER family, is known to be involved in the signaling pathways which control cell proliferation, differentiation and apoptosis. Trastuzumab, a HER2-targeted agent, exerts an anti-tumor effect by blocking constitutive HER2 signaling, suppressing angiogenesis and by antibody-dependent cell-mediated cytotoxicity. The HER2 overexpression was detected in 17.9% of SCLC patients using IHC, which served as a marker for poor prognosis in extensive-stage SCLC.[26,27] The chemotherapy-regulated microRNA-125-HER2 pathway as a novel therapeutic target for trastuzumab-mediated cellular cytotoxicity in SCLC seemed to be feasible.[28] HER2 is upregulated when HER2-expressing SCLC cells acquire chemoresistance. A stepwise treatment of these positive cells with trastuzumab and bevacizumab is promising in terms of chemoresistance in SCLC patients.[29] A study by Kinehara et al. reported on 2 relapsed HER2-positive SCLC patients treated with trastuzumab plus irinotecan, wherein 1 patient achieved PR after the 1st cycle and underwent 6 cycles without disease progression for 4.5 months, and the other patient received 4 cycles and maintained SD for 3.5 months.[30] Therefore, this drug combination is considered promising and further clinical studies are encouraged in order to confirm the anti-tumor efficacy of trastuzumab in SCLC.

Bec2

Ganglioside GD3, a cell surface glycosphingolipid antigen, is expressed on the surface of most SCLC tumors, with a limited expression in normal tissues. Ganglioside GD3 may be an appropriate antigenic target for active immunization to eliminate microscopic residual tumors and to enhance survival. Bec2 is an anti-idiotypic antibody that mimics GD3. Fifteen SCLC patients who had completed the standard therapy received a series of 5 intradermal immunizations consisting of 2.5 mg Bec2 plus Bacillus Calmette-Guérin (BCG) over 10 weeks. The median relapse-free survival for patients with extensive-stage disease was 11 months, whereas for patients with limited-stage disease it was >47 months. The immunization of SCLC patients using Bec2 plus BCG was considered safe.[31] Bec2/BCG was further evaluated in a phase 3 study of adjuvant vaccination in responding patients with limited-disease SCLC. A study conducted by Horn et al. in 515 patients demonstrated no improvement in the survival rate, PFS or quality of life in the vaccinated group. One-third of the vaccinated patients developed a humoral response, and hence showed a significant trend toward prolonged survival ($p = 0.085$).[4] In 2005, Giaccone et al. demonstrated that the primary toxicities of vaccination were transient skin ulcerations and mild flu-like symptoms.[32] In the study by Bottomley et al., patients in both groups demonstrated significantly impaired scores on the scale of global quality of life at baseline. However, the symptom scores and health-related quality of life showed no statistical difference between the 2 groups.[33] Therefore, Bec2/BCG may be suitable for certain SCLC patients, though the patient selection for this treatment requires further study.

Antibody-drug conjugate

Antibody-drug conjugate is a type of human or humanized monoclonal antibody conjugated with cytotoxic small molecules using chemical linkers. It represents a paradigm shift in chemotherapy. Delta-like protein 3 (DLL3) is highly expressed in approx. 80% of SCLC cases, but not in normal adult tissues. DLL3 might be associated with the neuroendocrine phenotype and plays an important role in tumorigenesis. Rovalpituzumab tesirine is an antibody-drug

conjugate comprised of a humanized monoclonal antibody against DLL3, a dipeptide linker and a pyrrolobenzodiazepine dimer toxin. Rudin et al. showed that rovalpituzumab tesirine exhibited single-agent anti-tumor activity and durability in recurrent or refractory SCLC. A dosage ranging from 0.05 to 0.8 mg/kg of either q3w or q6w was administered to eligible cases among the 74 patients enrolled. Among the 60 eligible patients treated with an active dose, 11 (18%) patients had a confirmed objective response. The proportion of patients with a response was higher among assessable DLL3-high patients (10 [38%] of 26 patients had a confirmed objective response and 23 [88%] achieved disease control) than among assessable DLL3-low patients (no confirmed objective responses and 4 [50%] of 8 patients achieved disease control). The most common grade 3+ toxicities associated with rovalpituzumab tesirine treatment included pleural effusions (8%), increased lipase (7%) and thrombocytopenia (11%).[34] Rovalpituzumab tesirine treatment shed new light on SCLC and may represent a major therapeutic breakthrough. The toxicity and safety of rovalpituzumab tesirine are a cause for concern, though, warranting further clinical trials.

Trop-2 is a new target for an antibody-drug conjugate due to its elevated expression in solid cancers, including SCLC. Sacituzumab govitecan is a novel antibody-drug conjugate comprised of 7-ethyl-10-hydroxy-camptothecin – the active metabolite of irinotecan – conjugated to an anti-Trop-2 humanized antibody. A phase 1/2 clinical trial is underway in previously-treated metastatic SCLC patients. The trial involves the administration of sacituzumab govitecan 8 or 10 mg/kg iv. on days 1 and 8 during a 21-day treatment cycle. On an intention-to-treat basis (n = 50), the ORR was 14%, the median response duration 5.7 months, median PFS 3.7 months, and median OS 7.5 months. Grade 3+ drug-related toxicities with an incidence rate greater than 5% included diarrhea (9%), fatigue (13%), anemia (6%), and neutropenia (34%).[35] The side effects of sacituzumab govitecan treatment, such as neutropenia, require further study in patients with previously-treated SCLC.

All SCLC tumor cells express HuD-antigen, a neuronal RNA-binding protein. BW-2 is a novel antibody-toxin compound derived via the assembly of a mouse anti-human-HuD monoclonal antibody onto streptavidin/saporin complexes. A previous study showed that BW-2 was lethal to SCLC at very low concentrations in vitro. Furthermore, it significantly reduced local tumor progression without causing toxicity in a nude mouse model of human SCLC.[36] Thus, an anti-HuD-based immunotoxin may be an effective alternative for patients with SCLC, prompting the need for further investigation in controlled clinical trials.

Most SCLC tumors expressing CD56 exhibit a poor 5-year survival rate of only 5–10%. CD56 provides a promising therapeutic target for SCLC. Lorvotuzumab mertansine is an antibody-drug conjugate comprised of a humanized monoclonal antibody against CD56, a cleavable disulfide linker and a tubulin-binding maytansinoid DM1.[37] Lorvotuzumab mertansine was evaluated in a phase 1 study in patients with CD56-positive solid tumors, including SCLC and others; 52 patients were treated with doses of 4–94 mg/m^2 per day. The MTD was 75 mg/m^2 and the recommended phase 2 dose was 60 mg/m^2. The most common grade 3 or 4 treatment-emergent AEs were dyspnea and hyponatremia (8.2% each). Responses included 1 CR, 1 clinical CR and 1 unconfirmed PR in Merkel cell carcinoma, and 1 unconfirmed PR in SCLC. Stable disease was recorded in 25% of the patients who received doses of ≥60 mg/m^2.[38] The limited number of patients enrolled in this study warrants further evaluation.

Others

ROBO1 is a membrane protein that contributes to tumor angiogenesis and metastasis. The 90Y-labeled anti-ROBO1 monoclonal antibody (90Y-anti-ROBO1 IgG) shows an anti-tumor effect against ROBO1-positive tumors. A biodistribution study was conducted by injecting the 111In-labeled anti-ROBO1 monoclonal antibody (111In-anti-ROBO1 IgG) into ROBO1-positive SCLC xenograft mice. A radioimmunotherapy study was conducted to evaluate the anti-tumor effects. The livers, spleens, kidneys, and lungs displayed a high accumulation of 111In-labeled anti-ROBO1, whereas 90Y-anti-ROBO1 IgG significantly reduced the tumor volume.[39] Radioimmunotherapy with 90Y-anti-ROBO1 IgG is a promising approach against SCLC, and clinical trials are needed.

Tumor necrosis treatment (TNT) involves the use of degenerating tumor cells and necrotic regions of tumors as targets for radioimmunotherapy. (131)I-chTNT, a chimeric monoclonal antibody labeled with the radionuclide iodine-131, has been approved for advanced lung cancer treatment in China. Eligible patients (n = 107) included those with advanced lung cancer refractory to radiotherapy or chemotherapy, and treated with asystemic or intra-tumoral injection of (131)I-chTNT. The results showed an ORR of 34.6% for all patients and for 50% of the 10 patients with SCLC.[40] The adverse side effects were mild and reversible. Despite the high ORR, the limited sample size warrants the need for a clinical trial with a larger SCLC population in order to validate the therapeutic effect and toxicities.

Lewis Y, CD174, is a blood group antigen robustly expressed on the surface of SCLC, and is a potential target for antibody-based immunotherapy. Hu3S193 is an anti-Lewis Y antibody with superior specificity, affinity and cytotoxicity. Hu3S193 was used to treat 10 progressive SCLC patients – 5 with 10 mg/m^2 and the remainder with 20 mg/m^2. Nine out of the 10 patients completed the course of 4 injections. All fluorodeoxyglucose (FDG)-avid lesions measuring over 2 cm were visualized using antibody single-photon emission computed tomography. Toxicities included grade 2 urticaria (n = 1), grade 1 vomiting (n = 2)

Table 1. Clinical studies antibody therapeutics in small-cell lung cancer with promising results

Author	Phase of clinical trial	Study population	Number of patients	Treatment
Ott et al.[5]	phase 1b	failed or were unable to receive standard therapy for SCLC patients	147	pembrolizumab
Antonia et al.[6]	phase 1/2	recurrent SCLC	216	nivolumab VS nivolumab plus ipilimumab
Tiseo et al.[14]	phase 3	first-line treatment in extensive-stage SCLC	204	cisplatin-etoposide vs cisplatin-etoposide plus bevacizumab
Petrioli et al.[15]	single institution experience	first-line treatment in extensive-stage SCLC	22	cisplatin-etoposide and bevacizumab followed by oral etoposide and bevacizumab maintenance
Mountzios et al.[17]	phase 2	chemoresistant relapsed SCLC	30	paclitaxel plus bevacizumab
Chiang et al.[23]	phase 1b	untreated extensive-stage SCLC	27	tarextumab in combination with cisplatin and etoposide
Bao et al.[24]	phase 1	SCLC patients	9	MEDI0639
Rudin et al.[34]	phase 1	recurrent or refractory SCLC	74	rovalpituzumab tesirine
Gray et al.[35]	phase 1/2	previously treated metastatic SCLC	31	sacituzumab govitecan
Shah et al.[38]	phase 1	CD56-positive solid tumors, including SCLC, Merkel cell carcinoma and ovarian cancer	52	lorvotuzumab mertansine
Chen et al.[40]	pivotal study	lung cancer failure prior to radiotherapy or chemotherapy, including SCLC	107	(131)I-chTNT
Krug et al.[41]	pilot trial	progressive SCLC	10	Lewis Y

and grade 2 hypertension (n = 1) after the high-dose infusion.[41] The strong tumor targeting of all FDG-avid lesions measuring over 2 cm using hu3S193 and visualized under antibody single-photon emission computed tomography warrants further clinical study of SCLC.

Table 2. Drugs with targeted proteins and genes

Drugs	Targeted proteins and genes
Pembrolizumab	PD-1
Nivolumab	PD-1
Ipilimumab	CTLA-4
Bevacizumab	VEGF
R1507	IGF-1R
Tarextumab	Notch2 and Notch3
MEDI0639	DLL4
Tucotuzumab	EpCAM
Trastuzumab	HER2
Bec2	GD3
Rovalpituzumab tesirine	DLL-3
Sacituzumab govitecan	Trop-2
BW-2	HuD-antigen
Lorvotuzumab mertansine	CD56
90Y-anti-ROBO1 IgG	ROBO1
(131)I-chTNT	tumor proliferating cell nuclear antigen
hu3S193	Lewis Y
111In-hu3S193	Lewis Y

Conclusions

All the studies to date support the following findings:

– the clinical efficacy of pembrolizumab, nivolumab, ipilimumab, and rovalpituzumab tesirine in SCLC showed promising results and called for further verification through phase 3 clinical trials;

– chemotherapy combined with bevacizumab in SCLC can improve PFS;

– the therapeutic effect of tarextumab, sacituzumab govitecan, BW-2, and lorvotuzumab mertansine in SCLC requires further evaluation;

– clinical studies are encouraged to confirm the anti-tumor efficacy of figitumumab and trastuzumab in SCLC;

– Bec2/BCG as adjuvant vaccination in responding patients with limited-disease SCLC showed no improvement in the survival, PFS or quality of life.

Clinical studies regarding antibody therapeutics in SCLC with promising results are presented in Table 1. The drugs investigated in SCLC with targeted proteins and genes are shown in Table 2.

References

1. Siegel R, Naishadham D, Jemal A. Cancer statistics, 2013. *CA Cancer J Clin*. 2013;63:11–30.
2. Chen W, Zheng R, Baade PD, et al. Cancer statistics in China, 2015. *CA Cancer J Clin*. 2016;66:115–132.
3. Govindan R, Page N, Morgensztern D, et al. Changing epidemiology of small-cell lung cancer in the United States over the last 30 years: Analysis of the surveillance, epidemiologic, and end results database. *J Clin Oncol*. 2006;24:4539–4544.
4. Horn L, Reck M, Spigel DR. The future of immunotherapy in the treatment of small cell lung cancer. *Oncologist*. 2016;21:910–921.

5. Ott PA, Elez E, Hiret S, et al. Pembrolizumab in patients with extensive-stage small-cell lung cancer: Results from the phase Ib KEYNOTE-028 study. *J Clin Oncol*. 2017;35:3823–3829.
6. Antonia SJ, López-Martin JA, Bendell J, et al. Nivolumab alone and nivolumab plus ipilimumab in recurrent small-cell lung cancer (CheckMate 032): A multicentre, open-label, phase 1/2 trial. *Lancet Oncol*. 2016;17:883–895.
7. Berghoff AS, Ricken G, Wilhelm D, et al. Tumor infiltrating lymphocytes and PD-L1 expression in brain metastases of small cell lung cancer (SCLC). *J Neurooncol*. 2016;130:19–29.
8. Schalper KA, Carvajal-Hausdorf DE, McLaughlin JF, et al. Objective measurement and significance of PD-L1, B7-H3, B7-H4 and TILs in small cell lung cancer (SCLC). *J Clin Oncol*. 2016;34(Suppl abstr):8566.
9. Miao L, Lu Y, Xu Y, et al. PD-L1 and c-MET expression and survival in patients with small cell lung cancer. *Oncotarget*. 2017;8:53978–53988.
10. Takada K, Toyokawa G, Okamoto T, et al. An immunohistochemical analysis of PD-L1 protein expression in surgically resected small cell lung cancer using different antibodies and criteria. *Anticancer Res*. 2016;36:3409–3412.
11. Roviello G, Generali D. Is there a place for bevacizumab in patients with extensive-stage small cell lung cancer? *Curr Cancer Drug Targets*. 2016;16:209–214.
12. Ustuner Z, Saip P, Yasasever V, et al. Prognostic and predictive value of vascular endothelial growth factor and its soluble receptors, VEGFR-1 and VEGFR-2 levels in the sera of small cell lung cancer patients. *Med Oncol*. 2008;25:394–399.
13. Pujol JL, Lavole A, Quoix E; French Cooperative Thoracic Intergroup IFCT: Randomized phase II–III study of bevacizumab in combination with chemotherapy in previously untreated extensive small-cell lung cancer: Results from the IFCT-0802 trial. *Ann Oncol*. 2015;26:908–914.
14. Tiseo M, Boni L, Ambrosio F, et al. Italian, multicenter, phase III, randomized study of cisplatin plus etoposide with or without bevacizumab as first-line treatment in extensive-disease small-cell lung cancer: The GOIRC-AIFA FARM6PMFJM trial. *J Clin Oncol*. 2017;35:1281–1287.
15. Petrioli R, Roviello G, Laera L, et al. Cisplatin, etoposide, and bevacizumab regimen followed by oral etoposide and bevacizumab maintenance treatment in patients with extensive-stage small cell lung cancer: A single-institution experience. *Clin Lung Cancer*. 2015;16:229–234.
16. Jalal S, Bedano P, Einhorn L, et al. Paclitaxel plus bevacizumab in patients with chemosensitive relapsed small cell lung cancer: A safety, feasibility, and efficacy study from the Hoosier Oncology Group. *J Thorac Oncol*. 2010;5:2008–2011.
17. Mountzios G, Emmanouilidis C, Vardakis N, et al. Paclitaxel plus bevacizumab in patients with chemoresistant relapsed small cell lung cancer as salvage treatment: A phase II multicenter study of the Hellenic Oncology Research Group. *Lung Cancer*. 2012;77:146–150.
18. Gately K, Collins I, Forde L, et al. A role for IGF-1R-targeted therapies in small-cell lung cancer? *Clin Lung Cancer*. 2011;12:38–42.
19. Ferté C, Loriot Y, Clémenson C, et al. IGF-1R targeting increases the antitumor effects of DNA-damaging agents in SCLC model: An opportunity to increase the efficacy of standard therapy. *Mol Cancer Ther*. 2013;12:1213–1222.
20. Cao H, Dong W, Shen H, et al. Combinational therapy enhances the effects of anti-IGF-1R mAb figitumumab to target small cell lung cancer. *PLoS One*. 2015;10:0135844.
21. Previs RA, Coleman RL, Harris AL, Sood AK. Molecular pathways: Translational and therapeutic implications of the Notch signaling pathway in cancer. *Clin Cancer Res*. 2015; 21:955–961.
22. Yen WC, Fischer MM, Axelrod F, et al. Targeting Notch signaling with a Notch2/Notch3 antagonist (tarextumab) inhibits tumor growth and decreases tumor-initiating cell frequency. *Clin Cancer Res*. 2015;21:2084–2095.
23. Chiang AC, Rudin CM, Spira AI, et al. Updated results of phase 1b study of tarextumab (TRXT, anti-Notch2/3) in combination with etoposide and platinum (EP) in patients (pts) with untreated extensive-stage small-cell lung cancer (ED-SCLC). *J Clin Oncol*. 2016;34(Suppl abstr):8564.
24. Bao H, Chen X, Thomas S, et al. Evaluation of anti-cancer stem cell activity of the anti-DLL4 antibody MEDI0639 in a phase I clinical trial of SCLC. *J Clin Oncol*. 2016;34(Suppl abstr):20093.
25. Gladkov O, Ramlau R, Serwatowski P, et al. Cyclophosphamide and tucotuzumab (huKS-IL2) following first-line chemotherapy in responding patients with extensive-disease small-cell lung cancer. *Anticancer Drugs*. 2015;26:1061–1068.
26. Potti A, Willardson J, Forseen C, et al. Predictive role of HER-2/neu overexpression and clinical features at initial presentation in patients with extensive stage small cell lung carcinoma. *Lung Cancer*. 2002;36:257–261.
27. Canoz O, Ozkan M, Arsav V, et al. The role of c-erbB-2 expression on the survival of patients with small-cell lung cancer. *Lung*. 2006;184:267–272.
28. Yagishita S, Fujita Y, Kitazono S, et al. Chemotherapy-regulated microRNA-125-HER2 pathway as a novel therapeutic target for trastuzumab-mediated cellular cytotoxicity in small cell lung cancer. *Mol Cancer Ther*. 2015;14:1414–1423.
29. Minami T, Kijima T, Kohmo S, et al. Overcoming chemoresistance of small-cell lung cancer through stepwise HER2-targeted antibody-dependent cell-mediated cytotoxicity and VEGF-targeted antiangiogenesis. *Sci Rep*. 2013;3:2669.
30. Kinehara Y, Minami T, Kijima T, et al. Favorable response to trastuzumab plus irinotecan combination therapy in two patients with HER2-positive relapsed small-cell lung cancer. *Lung Cancer*. 2015;87:321–325.
31. Grant SC, Kris MG, Houghton AN, Chapman PB. Long survival of patients with small cell lung cancer after adjuvant treatment with the anti-idiotypic antibody BEC2 plus Bacillus Calmette-Guérin. *Clin Cancer Res*. 1999;5:1319–1323.
32. Giaccone G, Debruyne C, Felip E, et al. Phase III study of adjuvant vaccination with Bec2/bacille Calmette-Guerin in responding patients with limited-disease small-cell lung cancer (European Organisation for Research and Treatment of Cancer 08971-08971B; Silva Study). *J Clin Oncol*. 2005;23:6854–6864.
33. Bottomley A, Debruyne C, Felip E, et al. Symptom and quality of life results of an international randomised phase III study of adjuvant vaccination with Bec2/BCG in responding patients with limited disease small-cell lung cancer. *Eur J Cancer*. 2008;44:2178–2184.
34. Rudin CM, Pietanza MC, Bauer TM, et al. Rovalpituzumab tesirine, a DLL3-targeted antibody-drug conjugate, in recurrent small-cell lung cancer: A first-in-human, first-in-class, open-label, phase 1 study. *Lancet Oncol*. 2017;18(1):42–51.
35. Gray JE, Heist RS, Starodub AN, et al. Therapy of small cell lung cancer (SCLC) with a topoisomerase-I-inhibiting antibody-drug conjugate (ADC) targeting Trop-2, sacituzumab govitecan. *Clin Cancer Res*. 2017;23:5711–5719.
36. Ehrlich D, Wang B, Lu W, Dowling P, Yuan R. Intratumoral anti-HuD immunotoxin therapy for small cell lung cancer and neuroblastoma. *J Hematol Oncol*. 2014;7:91.
37. Whiteman KR, Johnson HA, Mayo MF, et al. Lorvotuzumab mertansine, a CD56-targeting antibody-drug conjugate with potent antitumor activity against small cell lung cancer in human xenograft models. *Mabs*. 2014;6:556–566.
38. Shah MH, Lorigan P, O'Brien ME, et al. Phase I study of IMGN901, a CD56-targeting antibody-drug conjugate, in patients with CD56-positive solid tumors. *Invest New Drugs*. 2016;34:290–299.
39. Fujiwara K, Koyama K, Suga K, et al. 90Y-labeled anti-ROBO1 monoclonal antibody exhibits antitumor activity against small cell lung cancer xenografts. *PLoS One*. 2015;10:e0125468.
40. Chen S, Yu L, Jiang C, et al. Pivotal study of iodine-131-labeled chimeric tumor necrosis treatment radioimmunotherapy in patients with advanced lung cancer. *J Clin Oncol*. 2005;23:1538–1547.
41. Krug LM, Milton DT, Jungbluth AA, et al. Targeting Lewis Y (Le(y)) in small cell lung cancer with a humanized monoclonal antibody, hu3S193: A pilot trial testing two dose levels. *J Thorac Oncol*. 2007;2:947–952.

Advances
in Clinical and Experimental
Medicine